Role of Cancer Stem Cells in Breast and Prostate Cancer

Nicola Evelyn Wright

A Thesis submitted in partial fulfilment of the requirements of Sheffield Hallam University for the degree of Doctor of Philosophy

December 2016

Dedication

For my beautiful daughters,

Asha and Sienna

Abstract

Cancer stem cells (CSC) are thought to be responsible for the initiation, propagation and tumour re-occurrence. CSC have been identified in most solid and haematological cancers and account for ~1% of the total cell population. Culturing cancer cell lines in monolayers enriches for the most dominant subpopulation which in most cases does not represent the slow dividing CSC population.

We investigated the expression of CSC markers in 2D vs. 3D cell culture with the aim of identifying CSC-like cells via a nanog-reporter cell line and enable the subsequent targeting of these cells with CSC-targeting agents.

SUM159 and MCF7 cell lines cultured in 3D cell culture significantly enriched for the $CD44^{+}/CD24^{-}$ breast cancer stem cell phenotype when compared against 2D cell culture ($p<0.05$ and 0.001 respectively) and also enriched for expression of CD181 ($p<0.05$ and 0.001 respectively). However, this method did not enrich for the prostate CSC with the $CD44^{+}/CD133^{+}$ phenotype in PC3, DU145 and LNCAP cells. Using reporter cell lines to further identify the CSC population in SUM159 cell line that express GFP in response to Nanog (NRE-GFP), found that these cells were GFP^{+ve} in the absence of Nanog protein. As these reporters were selected based on GFP that was supposedly Nanog driven other mechanistic studies were examined to determine how GFP is expressed in the NRE-GFP and control cell line. It was found that GFP could be induced in apoptosis, CSC enriching medium, hypoxia and by inhibiting the proteasome in the absence of Nanog protein. It was concluded that reporter cell lines that respond to a response element may not identify the CSC population as other factors can induce GFP expression.

Compounds related to Withaferin A have been proposed to specifically target CSCs. Prostate and breast cancer cell lines cultured in 2D and 3D were treated with a novel withanolide derivative (LG-02) and Withanilode E to determine if these compounds were more effective at inducing cell cycle arrest and apoptosis using flow cytometry and microscopy. It was determined that LG-02 and WE primary mode of action is cell cycle inhibition and both compounds are more potent cell cycle inhibitors than Withaferin A. G1 phase accumulation was observed in the SUM159, PC3 and LNCAP cell lines and G2/M phase accumulation in the DU145 cell line. Cell cycle arrest was inconclusive in the MCF7 cell line. An apoptotic morphology was only significantly induced at higher concentrations in MCF7, PC3, DU145 and LNCAP. Withanolide derivatives also target the androgen response pathway, demonstrated by a decrease in PSA and androgen receptor in prostate cancer cell lines. LG-02 slowed growth of breast cancer cell lines cultured in 3D and inhibited spheroid formation of prostate cancer cell lines, however the androgen-dependent cell line LNCAP was consistently able to form 3D colonies, most likely via pAkt activation.

We conclude that 3D cell culture does enrich for the CSC population in breast cancer cell lines but using a reporter cell line expressing GFP under the control of a NRE is not a suitable model for identifying the CSC population for subsequent drug treatment. In addition, Withanolide derivatives have potential anti-tumour activity and may represent a novel class of anti-androgenic agents.

Contents

List of Figures

List of Tables

Abbreviations

Apoptotic peptidase factor 1	Apaf-1
ATP-binding cassette	ABC
Breast cancer susceptibility gene 1	BRAC1
Cancer stem cells	CSC
Castrate resistant prostate cancer	CRPC
Cyclin dependent kinases	Cdks
Death inducing signalling complex	DISC
Dihydrotestosterone	DHT
Embryonic stem cells	ESC
Estrogen receptor	ER
Extracellular matrix	ECM
Follicle stimulating hormone	FSH
Forward scatter	FSC
Green Fluorescent Protein	GFP
Human epidermal growth factor receptor 2	HER2
Hypoxia inducing factors	HIFs
Hypoxia-inducible factor 1α	HIF-1α
Induced pluripotent stem	IPS
Leutenising hormone releasing hormone	LHRH
Mammalian target of rampamycin	Mtor
Microtubule-associated protein light chain 3	LC3
Nanog response element	NRE
Phosphatase and Tensin	PTEN

Phosphate buffered saline	PBS
Polymerase chain reaction	PCR
Programmed cell death	PCD
Prostate specific antigen	PSA
Protein kinase B	Akt
RET Receptor Tyrosine Kinase	RET
Retinoblastoma associated	RB
Serum free medium	SFM
Severe combined immune deficient mice	SCID
Side scatter	SSC
Sodium dodecyl sulfate polyacrylamide gel electrophoresis	SDS-PAGE
Standard error of the mean	SEM
Three dimensional	3D
Transcription response element	TRE
Transforming growth factor beta	TGFβ
Tumour necrosis factor	TNF
Tumour suppressor genes	TSG
Two dimensional	2D
Two dimensional gel electrophoresis	2DGE
Vascular endothelial growth factor	VEGF
Withaferin A	WFA

Dissemination of this work

Manuscript in progress

Wright N.E, Brookes A, Cross N and Sayers T (2016). Anti-tumour activities of withanolides in hormone-sensitive prostate cancer cells are via androgen signalling and resistance emerges via pAKT. To be submitted to Biochemical and Biophysical Research Communications.

Conference presentations

North of England Cell Biology Forum- Sep 2013, Foresight Centre, The University of Liverpool, Liverpool UK. **Wright N.E**, Doherty R.E, Smith D, Sayers T and Cross N. Nanog as a functional marker of CSC.

BMRC/MERI annual poster event- December 2013, Sheffield Hallam University, Sheffield, UK. **Wright N.E**, Doherty R.E, Smith D, Sayers T and Cross N. Nanog as a functional marker of CSC.

NCRI Cancer Conference- November 2014, The BT convention centre, Liverpool UK. **Wright N.E**, Walker C, Smith D, Sayers T and Cross N Studies of Nanog expression in SUM159 breast cancer cells using a Nanog-response-GFP reporter in 2D vs. 3D cell culture

BMRC/MERI annual poster event- December 2015, Sheffield Hallam University, Sheffield, UK. **Wright N.E**, Smith D, Sayers T and Cross N. Low proteasome activity as a CSC marker using Nanog response driven-GFP reporter cell lines.

Acknowledgements

There are a number of people I am indebted to for contributing their time, knowledge resources and support towards this thesis.

Firstly, I am extremely grateful to my Director of Studies Dr Neil Cross for his constant support both in and out of the lab. I would also like to thank Tom Sayers for allowing me to come and work at your side at the NCI, USA and showing me such kindness whilst I was there.

I have been privileged to work with a great group of people, my colleagues at the Biomolecular Research centre. In particular: Kate, Rebecca, Jodie, Aimee, Karl, Mootaz and Rachel. You have endured many years of my constant moaning and complaining, thank you for always being at my side.

To my wonderful parents who have made this all possible, and have always supported and encouraged me. Everything I have achieved is all because of you. Words cannot express how grateful I am to have such great parents. I love you both dearly.
I am most thankful to my lovely, wonderful and thoughtful children who have willingly sacrificed time spent together to allow me to complete my PhD.

A special thanks to Chris Smith and Laura Mulcahy for providing figures 3.18, 3.19 and 3.21 on pages 136, 137 and 141. I would also like to thank the BMRC for funding my PhD.

1 General Introduction

1.1 Introduction into cancer

Cancer is a disease that can affect any proliferative cell within the body (Cancer Research UK, 2015) and it is characterised based on the ability to overcome stringent biological factors that are normally in place to monitor cell growth, tissue architecture and homeostasis (Bissell, Rizki and Mian 2003). When these stringent biological factors fail, a highly proliferative neoplasm (new growth) develops putting a huge burden on local tissues and nutritional supplies (Evan and Vousden 2001). Neoplasms are benign as these have not yet acquired the ability to invade local or distant tissue although these can also be aggressive. As they progress benign tumours become more aggressive, invasive and metastatic and are reclassified as malignant as these are able to invade and recolonise at local or distant tissues (Tward et al. 2007). Cancer is considered to be the leading cause of death worldwide and in 2013 there were 352,000 new cases, equalling to 960 cases of cancer diagnosed every day in the UK (Cancer Research UK, 2015). In 2014 alone, there were 55,222 new cases of breast cancer and 46,690 new cases of prostate cancer in the UK (Cancer Research UK, 2015).

There are 6 different classifications of cancers based on the tissue types that they originate from. Carcinoma is the most prevalent type of cancer as it originates from epithelial cells and is found in 80-90% of cancers diagnosed. Other types of cancers include Sarcoma, Myeloma, Leukaemia, Lymphoma and mixed type (two or more components of the cancer). The most prevalent carcinomas in the UK are breast followed by prostate, lung and bowel (Cancer Research UK, 2015).

Cancer is caused by external carcinogens such as tobacco smoke, alcohol, UV and ionising radiation and certain viruses (Tonini et al. 2013, Boffetta and Hashibe 2006, Granstein and Matsui 2004), or internal factors such as inherited mutations, hormones

or immune conditions (Anand et al. 2008). Cancer develops due to the acquisition of a series of mutations in which the cell acquires the ability to evade growth suppression. In 1971, Alfred Knudson outlined a concept known as the 'two-hit hypothesis' to explain the acquisition of genetic mutations and the development of cancer (Knudson 1971). Knudson demonstrated in retinoblastoma, individuals with a germline mutation in a tumour suppressor gene (TSG) only required a second mutation within the other homologue in order for loss of function of that gene (Knudson 1971). Other germline mutations have been identified in various cancers such as breast, ovarian and colon (Hall et al. 1990, Miki et al. 1994, Bronner et al. 1994) and in individuals with Li-Fraumeni Syndrome in which multiple tumours may occur (Srivastava et al. 1990). Hereditary cancers are rare and develop early on in life and are commonly associated with more than one primary tumour whereas sporadic cancers generally occur later and usually form a single tumour due to the number of genetic changes required to transform cells. The two hit hypothesis is applicable for non-hereditary cancers (sporadic cancers) in which the second somatic mutation of a tumour suppressor gene initiates tumourigenesis.

Figure 1.1 Knudson 2 hit hypothesis.

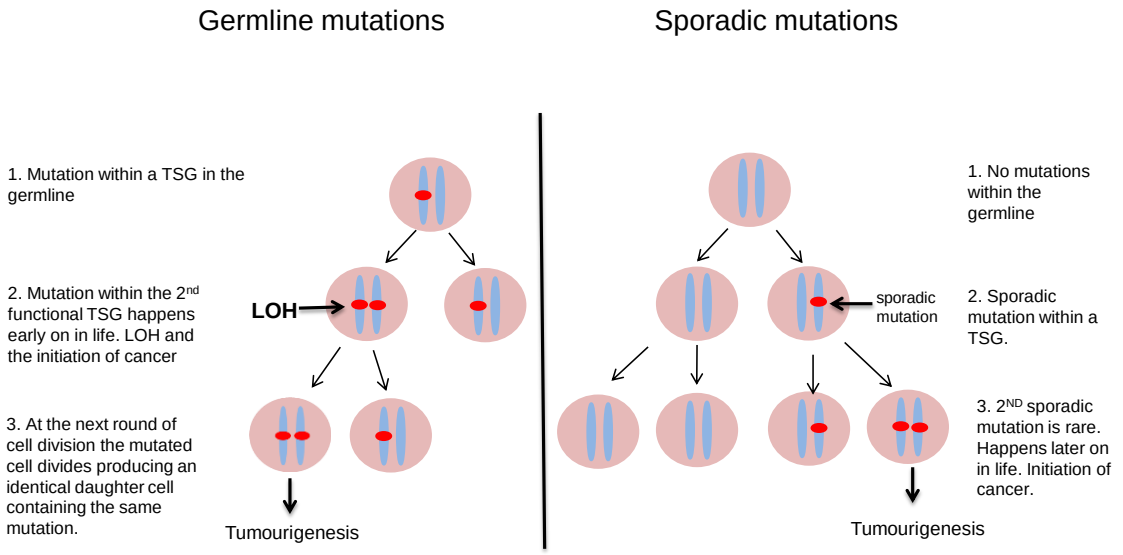

Figure 1.1 Knudson 2 hit hypothesis. In germline mutations an offspring is born with an inherited mutation in a TSG derived from either parent. Germline mutations and the corresponding phenotype are not expressed in the host as the other TSG compensates for the germline mutation and can function efficiently. A second mutation in the corresponding TSG results in loss of heterozygosity and the onset of tumourigenesis. Germline mutations of TSG induce tumourigenesis earlier on in life than that of sporadic mutations. In sporadic mutations, a mutation occurs in a TSG at random, and requires an additional mutation for inactivation of TSG. Cancers derived from sporadic mutations occur later on in life due to the length of time required to acquire inactivation of both TSG genes.

Genetic mutation of genes that are responsible for cell growth, cell death and DNA repair are common targets in the evolution of a normal cell to their neoplastic counterparts (Hall et al. 1990, Li et al. 1997, Hainaut et al. 1998). These genes can be classified into two groups which are 1) TSG where loss of function mutations, needing inactivation of both copies of gene or 2) proto-oncogenes where a gain of function mutation occurs in only one copy of the gene (Vogelstein and Kinzler 2004). As the name states TSG are involved in inhibiting tumourigenesis by preventing cell proliferation, inducing cell death or are part of the DNA repair mechanisms. Loss of

function of TSG such as p53, pRb or PTEN results in uncontrolled cell proliferation and the development of cancer (Hainaut et al. 1998, Li et al. 1997, Knudson 1971).

In contrast to TSG, proto-oncogene when activated drives cell proliferation and inhibits cell death (Vogelstein and Kinzler 2004). GTPases such as the Ras family of proto-oncogenes are involved in signal transduction, proliferation and apoptosis and are a common target for mutation. Activation of Ras induces uncontrolled cell proliferation and the development of cancer (Fromowitz et al. 1987, Rodenhuis and Slebos 1992). In various cancers, particularly breast cancer overexpression of an oncogene known as the Human epidermal growth factor receptor 2 (HER2) has been identified, and is responsible for the downstream signalling cascades that drives cell proliferation (Hynes and Stern 1994, Slamon et al. 1989, Lei et al. 1995, Beckhardt et al. 1995). Another growth factor receptor known as the epidermal growth factor receptor (EGFR) is also frequently mutated in solid cancers (Nicholson, Gee and Harper 2001).

1.2 Mutator phenotype hypothesis

Although inactivation of TSG's or oncogene activation could lead to defective mechanisms that control DNA repair, apoptosis or cell proliferation, a single cell needs to acquire multiple mutations before becoming malignant (Tanooka 2004). The mutator phenotype hypothesis was proposed to explain how cancer cells exhibit a mutator phenotype in which mutations that are often observed in cancer must induce subsequent mutations as normal cells do not acquire the vast amount of mutations that would facilitate tumourigenesis (Loeb, Springgate and Battula 1974). Mutations in genes that control and regulate DNA replication and repair (Paulovich, Toczyski and Hartwell 1997), chromosome segregation, damage surveillance (checkpoints) and cellular responses (apoptosis) drive the mutator phenotype. Multifaceted

manifestations are observed in cells that have point mutations, microsatellite instability and LOH in genetic stability genes (Loeb, Loeb and Anderson 2003) resulting in a heterogeneous tumour population with phenotypically different progeny (Loeb 2011).

1.3 The hallmarks of cancer

In 2000, Hanahan and Weinberg identified that there are six biological capabilities that are acquired during the multistep development of human tumours and these have been categorised to explain the complexities of neoplastic disease (Hanahan and Weinberg 2000). The six hallmarks of cancer originally identified are sustaining proliferative signalling, evading growth suppressors, resisting cell death, enabling replicative immortality, inducing angiogenesis, and activating invasion and metastasis (Hanahan and Weinberg 2000). Since then another four proposed hallmarks of cancer have been identified and these are genome instability, inflammation, reprogramming of energy metabolism and evading immune destruction (Hanahan and Weinberg 2011) (see figure 1.2).

Figure 1.2 The hallmarks of cancer

Figure 1.2. The hallmarks of cancer adapted from Hanahan and Weinberg (2011). The 10 hallmarks of cancer are: proliferative signalling, evading growth suppressors, resisting cell death, enabling replicative immortality, inducing angiogenesis, and activating invasion and metastasis, genome instability, inflammation, reprogramming of energy metabolism and evading immune destruction.

1.3.1 Sustaining proliferative signalling

In normal tissues, cell proliferation is highly regulated for cell number homeostasis and tissue architecture maintenance and is orchestrated by the careful production and release of growth stimulating factors (Witsch, Sela and Yarden 2010). In cancer, these processes are deregulated to facilitate and maintain uncontrolled cell proliferation by the binding of growth factors to their reciprocal receptor, which in most cases contains an intracellular tyrosine kinase domain (Turner and Grose 2010). The binding of growth factors to its cell surface receptor induces an intracellular signalling network which activates genes required for cell cycle progression, growth and other pathways such as those for survival and metabolism (Baixeras et al. 2001, Vaughan et al. 2013). During

tumourigenesis mutations occur within the mitogen derived genes (Lemmon and Schlessinger 2010). Over 30 years ago it was first identified that cancer cells did not fully rely on exogenous supply of growth factors for proliferation as these produce a vast amount of peptide growth factors and participate in autocrine secretion (Sporn and Roberts 1985). In paracrine signalling a cancerous cell may signal to a nearby normal cell in the stroma that is associated with tumours which in turn reciprocates by releasing growth factors (Cheng et al. 2008). Another deregulated mechanism utilised in cancer is the upregulation of growth factor receptors in which cancer cells are extremely sensitive to low levels of mitogens (Brady et al. 2007, Rubin Grandis et al. 1998, Budillon et al. 1991). Constitutive activation of downstream effectors of mitogen signalling has been identified in ~40% human melanomas as mutations within the B-Raf locus alters the protein structure inducing signalling through RAF to mitogen-activated protein (MAP)-kinase pathway (M and Samuels 2010). Similarly, constitutive activation of the Akt/PKB pathway caused by mutations within the catalytic subunit of phosphoinositide 3-kinase (PI3-kinase) isoforms has been identified in many different tumour types (Jiang and Liu 2008). A negative feedback mechanism that reduces cell proliferation signalling is inhibited in some cancers as Phosphatase and Tensin (PTEN) phosphatase, an inhibitory protein of PI3-kinase signalling may be silenced due to promoter methylation (Jiang and Liu 2008, T and L 2008).

1.3.2 Evading growth suppressors

A mechanism that negatively regulates proliferation is the action of TSG, and as the name states expression of these genes can slow down and inhibit cell division, repair DNA mistakes or prime the cells for apoptosis (Sherr 2004). In cancer many of these TSG are mutated and inactivated resulting in a loss of function (Girod et al. 1998). Two of the prototypical types of TSG that encode for the Retinoblastoma associated (RB)

and p53 proteins are commonly found to be non-functional in many types of cancer (Hanahan and Weinberg 2011). The pRb responds to many intra and extracellular stimuli for G1 cell cycle arrest (Weinberg 1995), regulation of apoptosis (Hilgendorf et al. 2013), regulation of double strand DNA repair (Cook et al. 2015) and other maintenance/homeostatic roles (Burkhart and Sage 2008). Unlike pRb protein that receives both internal but predominantly external stimulus, p53 activation is initiated from intracellular stress and abnormality sensors (Hanahan and Weinberg 2011). The p53 TSG has been described by Lane 1992, and Levine 1997 as "guardian of the genome" and "cellular gate keeper" (Lane 1992, Levine 1997) due to its anti-proliferative cellular response. The p53 protein primarily functions as a transcription factor by inducing the expression of genes involved in cell cycle arrest (Brugarolas et al. 1995), senescence (Serrano et al. 1997) and apoptosis (Clarke et al. 1993). Loss of function of pRB and p53 protein ultimately results in tumour formation. Transforming growth factor beta (TGFβ) is an anti-proliferative signalling molecule that functions in many ways to prevent cell cycle progression (Hanahan and Weinberg 2011). TGFβ acts to prevent pRb inactivation, to halt the cell in G1 phase of the cell cycle (Laiho et al. 1990) primarily through the upregulation of $p15^{INK4B}$ and p21 (Hannon and Beach 1994, Yoo et al. 1999), and in some instances TGFβ can downregulate c-myc (oncogene) expression (Pietenpol et al. 1990). Loss of the TGFβ receptor and signalling is common in cancers such as ovarian and colon (Antony et al. 2010, Yu et al. 2014) and has been found to promote prostate cancer metastasis (Tu et al. 2003).

1.3.3 Resisting cell death

A normal cell undergoes a process known as programmed cell death by apoptosis (discussed later) as a mechanism for cancer evasion (Evan and Littlewood 1998) however it has been found in high grade malignancies and therapy resistance tumours

that these cells are resistant to apoptosis (Vaux, Cory and Adams 1988, Sentman et al. 1991). Apoptosis evasion is propagated by a number of factors such as: Loss of p53 (Nigro et al. 1989, Munroe et al. 1988), upregulation of anti-apoptotic proteins Bcl-2 (Vaux, Cory and Adams 1988) and survival growth factors (Hellawell et al. 2002), downregulation of pro-apoptotic proteins (Manoochehri et al. 2014) and death inducing ligands (Butler et al. 1998). Another type of programmed cell death known as autophagy (discussed later) can be anti- or pro-tumorigenic depending on the physiological state of the cell and stage of the tumour (Chen and Debnath 2010). Nutrient starvation, radiotherapy and some cytotoxic compounds induce autophagy in cancer as this impairs cellular function to a dormant state rather than killing the cell (Li, Chen and Gibson 2013a, Ito et al. 2005, Cheng et al. 2012). Necrosis is a form of programmed cell death unlike apoptosis in which a dying cell shrinks and is engulfed by neighbouring cells, necrotic cells expand and explode releasing their cellular contents into the tissue microenvironment (Hanahan and Weinberg 2011). The release of cellular components and pro-inflammatory signals recruit inflammatory cells that can propagate tumour growth, inducing angiogenesis and invasion (Murdoch et al. 2008, Lin et al. 2001).

1.3.4 Enabling Replicative Immortality

Normal cells within the body have a limited number of cell divisions before they become senescent in which cells are viable but no longer proliferative and go through a process known as crisis in which cells die (Hayflick and Moorhead 1961). In normal cells the ends of chromosomes are protected from end to end fusion by tandem hexonucleotide repeats known as telomeres (Muller 1938, McClintock 1941, McClintock 1942), however at each cell division the telomeres shorten, eventually resulting in senescence and or cell death (Zhang et al. 1999). On some rare occasion a

normal cell can overcome this barrier and have unlimited replicative potential, known as immortalisation, which is a phenomena present in most cultured cell lines and in ~90% of cancers (Hanahan and Weinberg 2011). Telomerase is a specialised type of DNA polymerase that is expressed in immortalised cells due to mutations within the genome and is virtually absent in normal cells and is responsible for adding on telomere repeats to the ends of the chromosome, to prevent chromosome shortening and enabling replicative immortality (Kim et al. 1994a). Recent literature has found that even in the absence of other tumour associated mutations, the proliferative barrier imposed by telomere shortening is overcome by mutations within the promoter of telomerase facilitating immortalisation and tumourigenesis (Chiba et al. 2015).

1.3.5 Inducing Angiogenesis

In normal tissue maintenance and tumour development the need for nutrients and oxygen and the removal of metabolic waste and carbon dioxide is vital to maintain homeostasis and facilitate growth of a tumour (Hanahan and Weinberg 2011). The vasculature system is fundamental in these processes. Normal adult vasculature is in a dormant quiescent state that transiently activates wound healing (Heimark, Twardzik and Schwartz 1986) and during the menstrual cycle (Hanahan and Folkman 1996) however, in tumour progression angiogenic signalling is switched on facilitating quiescent vasculature to become active and the sprouting of new blood vessels (Tsunoda et al. 2001). Angiogenesis is regulated by anti and pro-angiogenic factors that when bound to their reciprocal receptors can inhibit or promote angiogenesis (Peiris-Pages et al. 2010). A pro-angiogenic factor known as Vascular Endothelial Growth Factor (VEGF) is a ligand that is responsible for inducing angiogenesis in embryonic (Gogat et al. 2004) and postnatal development (Gerber et al. 1999), and in

physiological and pathological situations in the adult (Taichman et al. 1998). VEGF can be regulated by many factors such as hypoxia (Liu et al. 1995) and oncogene signalling in cancer (Goel and Mercurio 2013). The vasculature in chronic activated angiogenesis is often leaky, with micro-haemorrhaging and erratic blood flow, and there is also excessive vessel branching which are distorted and enlarged, even in premalignant neoplasms (Hanahan and Weinberg 2011).

1.3.6 Activating Invasion and Metastasis

Activating invasion and metastasis is the process in which a tumour cell leaves its primary site and invades local tissue and stroma, or migrates to distant sites and forms secondary tumours also referred to as a metastasis (Valastyan and Weinberg 2011). Within the tumour microenvironment carcinomas form adheren junctions for cell to cell contact with adjacent epithelial cells and this is facilitated by an adhesion molecule known as E-cadherin (Pecina-Slaus 2003). At the onset of invasion, premalignant tumour cells alter their morphology and interactions with neighbouring cells by the loss of E-cadherin (Onder et al. 2008). Conversely, an upregulation of adhesion molecule N-cadherin that is normally expressed in migratory cells such as migrating neurons or mesenchymal stem cells has been identified to be a key player in this process (Frixen et al. 1991, Ramis-Conde et al. 2009). Activating invasion and metastasis have similar traits to that found during embryonic morphogenesis and wound healing, in which cells have the ability to undergo a process known as epithelial to mesenchymal transition (EMT) (Baum, Settleman and Quinlan 2008, Lin et al. 2012, Shook and Keller 2003). Similarly, increasing evidence about invasive CSC's appear to utilise EMT by the acquisition of an ESC phenotype (Chaffer and Weinberg 2011, Dang et al. 2011, Gupta, Chaffer and Weinberg 2009, Mani et al. 2008, Santisteban et al. 2009).

During the switch from an epithelial to mesenchymal phenotype the upregulation of mesenchymal cell markers such as vimentin (Xu, Lamouille and Derynck 2009, Hay 2005), fibronectin and actin are observed although these proteins are not exclusive to mesenchymal cells (Hay 2005). Collagen and fibronectin are extracellular proteins that are increased in EMT and these stimulate signalling via integrin which in turn stimulates focal adhesion complexes to enable cell migration (Imamichi and Menke 2007). Focal adhesion complexes are also activated by the down regulation of E-cadherin, and down regulation of E-cadherin elevates expression of N-cadherin, making these cells more invasive and metastatic (Lim and Thiery 2012, Shirakihara, Saitoh and Miyazono 2007). In cancer, after acquisition of a mesenchymal phenotype a number of steps commence for the initiation of a secondary tumour. This begins with the detachment from neighbouring cells at the primary tumour and penetration into local stroma then into the lymphatic vessels or vascular, the cell can then adhere to distant endothelia before extravasation followed by the reversal of EMT by a process known as mesenchymal to epithelial transition (MET) where the cell recolonizes and expands (Geho et al. 2005, Thompson, Newgreen and Tarin 2005, Vergara et al. 2010).

EMT has been identified in many of the highly malignant cancers including breast (Hwang, et al. 2013, Lombaerts et al. 2006), prostate (Cao et al. 2008, Kong et al. 2010, Xie et al. 2010), ovarian (Rosanò et al. 2006, Tseng et al. 2011), colon and (Lin et al. 2012, Qi, et al. 2012, Jang, Jeon and Jung 2009), lung cancer (Shintani et al. 2008, Joëlle Roche et al. 2013).

1.4 Emerging hallmarks of cancer

1.4.1 Genome instability and mutation

The multiple hallmarks of cancer largely depend on a succession of mutations and alterations within the genome to facilitate the progression of a neoplastic cell to a malignant tumour, although some may be triggered by non-mutational epigenetic modifications such as DNA methylation (Feinberg and Vogelstein 1983, Jin and Robertson 2013) or histone modifications (Sharma, Kelly and Jones 2010). Spontaneous mutations are usually low during each cell division as genome maintenance and surveillance systems that monitor genome integrity often referred to as "caretakers" of the genome prevent tumourigenesis (Kinzler and Vogelstein 1997). However, early neoplastic cells increase the rate of mutation to facilitate tumourigenesis by inactivating genes required for: intercepting mutagens before DNA damage occurs, detection of DNA damage and DNA repair (Hanahan and Weinberg 2011). Another precursor in genome instability is the erosion of telomeres in premalignant, rapidly proliferating cells (Wong and DePinho 2003, Wright and Shay 2005). If telomere shortening reaches crisis point and a rare cell continues to proliferate, chromosome instability may occur leading to duplicated or deleted chromosome's (Davoli, Denchi and de Lange 2010, Rudolph et al. 2001). In transformed cells with chromosomal instability, selective pressure ensues for activation of telomerase (Kim et al. 1994b) or alternative lengthening of telomeres (Heaphy et al. 2011), further ensuing for tumour growth with immortalised cells. Centrosome amplification is another defect found in most solid and haematological cancers and has been implicated in multipolar mitoses, chromosome mis-segregation, and subsequent genome instability and mutation (Ferguson et al. 2015). Catastrophic aneuploidy would normally be tumour suppressive, however cancer cells have utilised

the abnormal amount of centrosomes by clustering them together for cancer cell survival (Kramer, Maier and Bartek 2011).

1.4.2 Tumour-promoting inflammation

In some benign and malignant tissues there are a number of immune cells that were initially thought to be anti-cancerous by disposing of and eradicating transformed mutant cells. However it has become apparent that the tumour associated inflammatory response promotes tumourigenesis by aiding neoplastic cells to acquire the hallmarks of cancer (Hanahan and Weinberg 2011).

Cells of predominantly the innate immune system promote carcinogenesis by supplying biological factors to facilitate proliferation, anti-apoptosis, angiogenesis, invasion and metastasis and EMT (Schoppmann et al. 2002, Fan et al. 2014, Liu et al. 2014b).

One of the most prevalent immune cell involved in tumour promoting inflammation is the tumour-associated macrophage as it produces cytokines and proteases to stimulate angiogenic and lymphangiogenic growth (Schoppmann et al. 2002). Neutrophils are another type of immune cell that propagates a mutagenic phenotype as when activated these release reactive oxygen species which increases genetic defects within tumours (Campregher, Luciani and Gasche 2008).

1.4.3 Deregulating cellular energetics: Reprogramming Energy Metabolism

Reprogramming energy metabolism in cancer was first identified by Warburg in which he found that cancer cells can reprogramme their glucose metabolism to glycolysis (Warburg 1956a, Warburg 1956b). In normal cellular metabolism and in the presence of oxygen, glucose is first processed to pyruvate in the cytosol and then into carbon dioxide in the mitochondria. In anaerobic conditions and in cancer, even when oxygen

is abundant, glucose is processed to pyruvate and then into lactate as a waste product (Pertega-Gomes et al. 2015). In cancer, aerobic glycolysis is increased due to the high demand of proliferating cells and this is facilitated by the up-regulation of glucose transporters (Macheda, Rogers and Best 2005). The lactate that is produced as a by-product to glycolysis is utilised by the tumour associated stroma as their main energy source (Sonveaux et al. 2008).

1.4.4 Avoiding immune destruction

The cells of the immune system play a vital role in immune surveillance for premalignant and incipient cancer cells as it has been shown that immunocompromised individuals are more susceptible to certain forms of cancer (Vajdic and van Leeuwen 2009). Also, in mice that are deficient in $CD8^+$ cytotoxic T lymphocytes, $CD4^+$ T_h1 helper T cells, or natural killer (NK) cells and assessed for carcinogen-induced tumours and it has been found that there was an increase in tumour formation in immune-deficient mice, signifying the role of the innate and adaptive immune system in surveillance and in eradicating tumours (Kim, Emi and Tanabe 2007, Vesely and Schreiber 2013). However a secondary tumour would not occur if cancer cells derived from an immunocompromised host were implanted into an immunocompetent host, but cancer cells derived from an immunocompetent host would recapitulate the tumour of origin in all hosts (Teng et al. 2008, Vesely and Schreiber 2013). Solid tumours have somehow evaded immune-surveillance and eradication, and it has been suggested that these cancer cells have a low immunogenic response and a process known as immune-editing takes place in which immune cells selectively target and eliminate highly immunogenic cancer cells (Teng et al. 2015).

Within a tumour microenvironment there are a number of different cell types that work symbiotically to propagate tumourigenesis. These cell types are cancer associated fibroblasts, endothelial cell, pericyte, immune inflammatory cells and CSC (Thoma et al. 2014).

1.5 Cancer stem cells

1.5.1 Stochastic vs hierarchy model for tumour formation

There are two theories that have been widely accepted for tumourigenesis which are the stochastic model and the hierarchy model (Odoux et al. 2008). The stochastic model was the first concept proposed and it states that cancers are made up of a predominantly homogeneous cell population, and that a few cells may acquire genetic mutations and gain the potential for extensive proliferation and tumour formation and that any cell within the tumour has the potential to be invasive and metastatic (Odoux et al. 2008). The hierarchy model states that tumours are made up of a heterogeneous cell population and that CSC's form a hierarchy in which these cells can proliferate extensively to generate identical or phenotypically different progeny that can initiate new tumours (Cabrera, Hollingsworth and Hurt 2015). CSC also known as tumour initiating cells are a small population of cells within a tumour that have a similar phenotype to embryonic stem cells as these are self-sustaining, and can maintain the bulk of the tumour by dividing symmetrically or asymmetrically. This is required to maintain the CSC population and the non-tumorigenic cancer cells which in most cases form the mass of the tumour (Ho 2005, Clarke et al. 2006).

Figure 1.3 Stochastic model vs Hierarchy model.

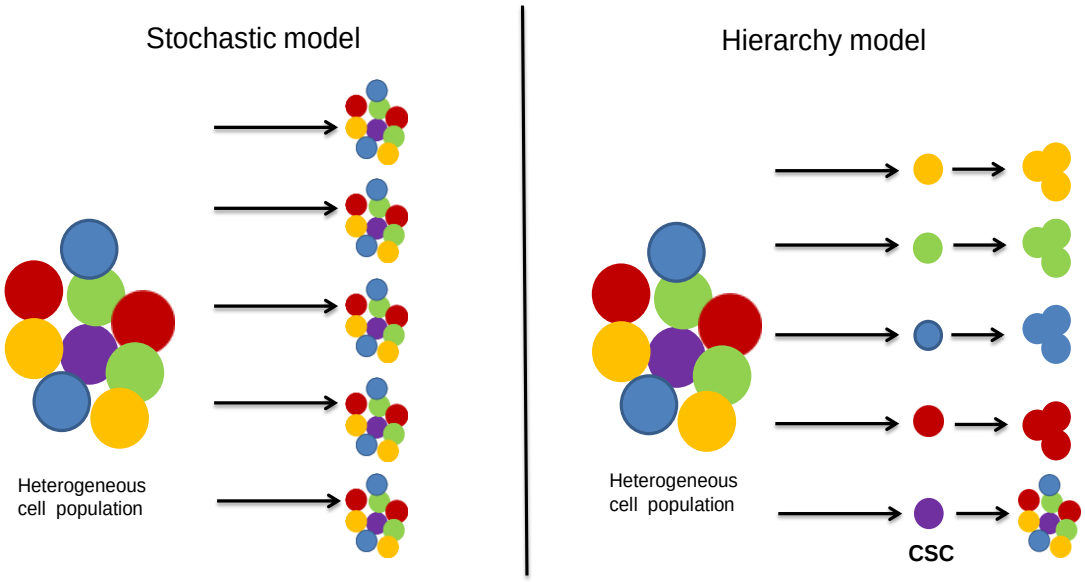

Figure 1.3 Stochastic model vs Hierarchy model. In the stochastic model it is thought that any cell within a heterogeneous cell population can give rise to a tumour consisting of a mixed population of cells. In the hierarchy model it is said that only the cancer stem cells can give rise to a heterogeneous cell population and the other, terminally differentiated cell types give rise to phenotypically identical cells.

Since the identification of CSC's the hierarchy model has been studied extensively *in vitro* using colony forming assays in soft agar and spleen colony assay in which cells that express 'stem cell markers' form more colonies when compared to the non-stem like cells (Hamburger and Salmon 1977), and *in vivo* using transplant injection in NON/SCID mice, in which transplantation of a small number of CSC resulted in tumour formation whereas using the same amount or more of the non-stem like cells failed to form tumours (Chiba et al. 2006). However using a more immunocompromised NOD/SCID interleukin-2 receptor gamma chain-null (IL-2) strain of mouse, this can significantly increase the efficiency for tumour formation from unsorted cells (CSC and non CSC) (Quintana et al. 2008).

1.5.2 Hierarchy in stem cells

Within the stem cell niche there is a cellular hierarchy based on the morphology, proliferation and differentiation potential of the cells and the clones of cells formed in the hierarchy are known as: holoclones, meroclones and paraclones (Barrandon and Green 1987). Holoclones are the least abundant colony forming cells within the hierarchy, but are the most proliferative and can differentiate into both meroclone and paraclone, whereas paraclones are terminally differentiated cells and can divide a limited number of times by symmetrical cell division. Meroclones are said to be in a transitional state between holoclones and paraclones and have some proliferative capacity although not as great as holoclones, and can differentiate into meroclones and paraclones (Barrandon and Green 1987). The hierarchy within stem cells has also been identified in many cancer cell lines including head and neck squamous carcinoma, oral squamous carcinoma and prostate cancer (Felthaus et al. 2011, Li et al. 2008, Locke et al. 2005, Doherty et al. 2011, Beaver, Ahmed and Masters 2014). It is apparent that holoclones may contain the CSC population, or the CSC form holoclones. Whichever concept it may be, holoclones have the ability to differentiate into meroclones and paraclones and upon terminal differentiation these colony forming cells lose the ability to transdifferentiate (Doherty et al. 2011), although in epithelial to mesenchymal transition phenotypic plasticity is observed (Baum, Settleman and Quinlan 2008, Lin et al. 2012) .

Embryonic stem cells and Cancer stem cells have many shared characteristics. They are distinctive from differentiated cells due to their properties and phenotype and they are also unique in stem cell markers, allowing positive identification within a heterogeneous cell population although stem cells from different lineages, tissues and tumours generally have different cell markers.

1.5.2.1 Enrichment of CSC population

The CSC population of cells grown *in vitro* remains low when these are cultured on a two dimensional (2D) flat substrate. This is due to the morphology (Knight & Przyborski, 2015) and gene expression being distorted and also restricts the three dimensional (3D) growth that would be found *in vivo* (C. H. Thomas, Collier, Sfeir, & Healy, 2002). Culturing cancer cells in a 3D matrix that is reflective of a tumour *in vivo* enriches for the CSC markers/phenotype and cell population (Chaturvedi et al., 2013b; Straussman et al., 2012).

1.5.3 Markers of stem cells and CSC

1.5.3.1 CD44

CD44 is a cell surface glycoprotein that modulates signal transduction through binding to the ligand hyaluronan (hyaluronic acid) or with interactions with extracellular matrix components, and growth factors to regulate adhesion, differentiation and migration (Williams et al. 2013). CD44 is expressed in embryonic, hematopoietic and mesenchymal stem cells and also in epithelial and cancer stem cells (Haegel, Dierich and Ceredig 1994, Campagnoli et al. 2001, Du et al. 2008, Al-Hajj et al. 2003). The highly conserved CD44 gene produces various forms of CD44 protein due to different posttranslational modifications dependent upon cell type and growth conditions and splice site variants (Screaton et al. 1992). The CD44 gene consists of 20 different exons that can be alternatively spliced resulting in ~20 different isoforms with tissue and differentiation-specific expression (Liu and Sy 1997). CD44 exons 1–5 and 16–18 translate to the smallest, constant and non-variant standard isoforms also denoted as CD44s and are the most abundantly expressed isoforms on the surface of most cells (Naor, Sionov and Ish-Shalom 1997). CD44 exons 6–15 and 19–20 are variants and inserted by alternative splicing (Screaton et al. 1992), resulting in larger isoforms that

lengthens the extracellular membrane domain that are subjected to alternative post-translational modifications and ligand binding sites (Ponta, Sherman and Herrlich 2003). Expressions of the variant isoforms of CD44 are regulated by oncogenic signalling pathways such as Ras-MAPK pathway and tissue and environmental specific factors (Hofmann et al. 1993, Weg-Remers, et al. 2001). In breast cancer cell lines the CD44 isoforms are heterogeneously expressed, however the variant isoforms are associated with other cancer stem cell phenotypes (Olsson et al. 2011). CD44 variants have also been implicated in breast cancer metastasis by binding to E-selectin (Shirure et al. 2015)

1.5.3.2 CD24

CD24 is a heavily glycosylated small cell surface protein that is anchored to the cell membrane by glycosyl-phosphotidyl-inositol, however due to variable glycosylation it has distinct physiological functions in different cell types with some functions still to be elucidated (Fang et al. 2010b). It is expressed in haematopoietic cells: B-cells and neutrophils but is not expressed in T-cells or monocytes. Its expression has also been identified in hematologic malignancies and solid tumours such as lung cancer, neuroblastoma, rhabdomyosarcoma, renal cell carcinoma breast and ovary (Akashi, Shirasawa and Hirokawa 1994, Jackson et al. 1992, Kristiansen et al. 2002, Kristiansen et al. 2003). CD24 is a ligand for adhesion molecule P-selectin that is expressed on activated endothelial cells and plays a role in leukocyte rolling or when attached to activated platelets (Aigner et al. 1997, Sammar et al. 1994). CD24 facilitates cell-cell and cell-extracellular matrix interactions. Cell surface mucin P-selectin glycoprotein ligand-1 is the major ligand for P-Selectin, however in its absence; CD24 has a similar affinity for P-Selectin and functions in the rolling of tumour cells and attachment of tumour cells to activated platelets (Aigner et al. 1998, Aigner et al. 1997). In bladder

carcinoma, CD24 has been found to induce proliferation and inhibit apoptosis and is regulated downstream of Ral GTPase signalling (downstream effectors of Ras oncoprotein) (Smith et al. 2006). However, breast cancers that express low level of CD24 are more tumorigenic, metastatic and invasive than their counterparts (Sun et al. 2013b, Sheridan et al. 2006).

1.5.3.3 CD133

CD133, like CD44 is a five transmembrane glycoprotein that localises to membrane protrusions and was first identified in hematopoietic stem and progenitor cells (Yin et al. 1997). Two isoforms of CD133 have been identified and named CD133-1 (Yin et al. 1997) and CD133-2 in which the latter has a 27 nucleotide deletion brought about due to alternative mRNA splicing (Yu et al. 2002). CD133-1 has been found to be expressed in human fetal liver, bone marrow and blood (Yin et al. 1997) whereas CD133-2 is mainly expressed in human foetal tissue, adult tissues and several carcinomas (Yu et al. 2002). Although CD133 function still needs to be elucidated, it has been suggested that it functions in cell-cell interaction and signal transduction (Ren, Sheng and Du 2013). In cancer $CD133^+$ cells are more tumorigenic (Ma et al. 2010, Fang et al. 2010a, Baba et al. 2009), and metastatic (Zhang et al. 2012) than $CD133^-$ cells and also show a higher degree of chemo-resistance (Damdinsuren et al. 2006) and radio-resistance (Piao et al. 2012).

1.5.3.4 ALDH1A

The aldehyde dehydrogenase (ALDH) family are a group of enzymes with oxidative capabilities as these oxidise aldehydes to carboxylic acid. In humans there are 19 different isoforms of ALDH and depending on the enzyme family can vary distribution in tissue and organs and also enzyme levels (Sladek 2003, Yanagawa et al. 1995). ALDH isoforms play a role in several physiological processes such as cell survival,

cell proliferation and early differentiation. In normal and cancer stem cells ALDH isoforms are found to be upregulated, in particular ALDH1A1 and ALDH3A1 (Muzio et al. 2012). ALDH1A1 is suggested to be a "stemness" marker as it is involved in the oxidation of aldehydes which is essential for early differentiation and survival, and has been used in the identification of normal hematopoietic, neural and mammary stem cells (Chute et al. 2006, Corti et al. 2006, Hess et al. 2004, Ma and Allan 2011, Yoshida et al. 1998). Aldehyde dehydrogenase may also be a potential CSC marker as it has been used to identify the most primitive, clonogenic cells in many malignant tissues (RW.ERROR - Unable to find reference:84, Emmanuelle Charafe-Jauffret et al. 2010, Croker et al. 2009, Huang et al. 2009, Burger et al. 2009, Wu et al. 2013, Doherty et al. 2011).

1.5.3.5 ABC transporters

The ATP-binding cassette (ABC) transporters are a superfamily of membrane bound protein transporters that use ATP to transport substrates across membranes (Vasiliou, Vasiliou and Nebert 2009). ABC transporters utilise energy from a pair of ATP molecules by binding to and/or hydrolysing this molecule to efflux or flip specific compounds across the membrane (Higgins 1992, Dean and Allikmets 1995). A subset of this superfamily known as the multidrug resistant (MDR) channels are important in stem cells as these remove intracellular cytotoxic agents, preventing cell death. The efflux transporter pumps have been identified in many stem cell types and in the cancer stem cell population offering resistance to anticancer drugs and increasing longevity. Hematopoietic stem cells express ABC transporters ABCB1 and ABCG2, and upon differentiation to progenitors or mature blood cells, expression of these genes are silenced (Gottesman, Fojo and Bates 2002, Kim et al. 2002, Scharenberg, Harkey and Torok-Storb 2002). In several tumour cell lines the first MDR superfamily, ABCB1

gene was the first ABC transporter identified and found to be amplified or overexpressed (Kartner et al. 1985, Riordan et al. 1985). Since then other ABC transporters have been found to be upregulated or amplified in cancer (Dean and Allikmets 1995, Kim et al. 2002, Cole et al. 1992, Chua et al. 2016). In Identifying the CSC population, cells stained with Hoechst dye can efflux this compound out of the cell and when analysed using flow cytometry appear as a side population of unstained cells (Moitra 2015). In cell lines derived from solid cancers, a small side population cells able to efflux Hoechst dye out of the cell have been identified, these representing the cancer stem cell population (Hiraga, Ito and Nakamura 2011, Jin et al. 2015, Boesch et al. 2016)

1.5.3.6 Nanog, Oct4 and Sox2

Nanog, Oct4 and Sox2 are transcription factors that are expressed in embryonic stem cells. Nanog, Oct4 and Sox2 form a core transcriptional regulatory circuit that play a crucial role in maintaining pluripotency and self-renewal by the transcriptional activation of target genes, and the repression of genes required for lineage specific cell differentiation (Loh et al. 2006, Boyer et al. 2005). In human ESC Nanog, Oct4 and Sox2 co-occupy many of the same loci but with different response element's to induce gene expression (Boyer et al. 2005), and Oct4 and Sox2 form a cooperative interaction to drive target gene expression (Rodda et al. 2005). Wang et al, (2012) found that not only are these transcription factors co repressors of differentiation but they each regulate specific cell fate (Wang et al. 2012b). Deficiency in Nanog or Oct4 in ESC by knock-out (Mitsui et al. 2003) or knock-down (Nichols et al. 1998, Zaehres et al. 2005) experiments resulted in loss of pluripotency, diminished self-renewal capabilities and differentiation and in mouse ESC apoptosis is induced (Chen, Du and Lu 2012). Alternatively, over-expression of Nanog resulted in proliferation (Zhang et al. 2005). In

ESC, p53 induces cell differentiation by the down-regulation of Oct4, KLF4, LIN28A, and Sox2 by p53 transcriptional activity of the microRNAs miR-34a and miR-145 (Jain et al. 2012, Qin et al. 2007). In addition, p53 inhibited Nanog expression in mouse ESC by directly binding to the promoter after DNA damage and there was a direct correlation to the down-regulation of Nanog transcription during differentiation and the induction of p53 (Lin et al. 2005). This activity of p53 is hypothesised to induce differentiation of ESCs in response to DNA damage and hence is potentially tumour suppressive. In cancer, the triad of transcription factors Oct4, Sox2 and Nanog have been implicated as the initiating factor and sustaining factors of tumour growth (Gangemi et al. 2009, Gidekel et al. 2003, Jeter et al. 2009, Niu et al. 2011, Piestun et al. 2006, Park et al. 2016).

1.5.4 Limitations of the cancer stem cell hypothesis

Increasing evidence validates the hierarchy model CSC model, however transformation of a somatic cell may also be responsible for tumourigenesis as addition of endogenous Oct3/4, Sox2, c-Myc, and Klf4 can reprogram mouse embryonic or adult fibroblasts to pluripotent stem cells with embryonic stem cell properties, morphology and are able to form all three germ layers of a developing blastocyst (Takahashi and Yamanaka 2006). In addition, oncogenic reprogramming of primary differentiated fibroblast *in vitro* induces multiple cell lineages, facilitating tumour growth (Scaffidi and Misteli 2011). In non-tumorigenic mammary epithelial cell line MCF-10A Oct3/4, Sox2, c-Myc, and Klf4 induced a breast CSC phenotype with increased malignancy and formed multiple tumours in immuno-compromised mice (Nishi et al. 2014). In severe injuries, normal epithelial cells can de-differentiate to a stem like state (Blanpain and Fuchs 2014). Inducing pluripotent stem cell may be a similar mechanism in which re-

expression of cancer stem cell markers arise corroborating the stochastic model, although both may play a part in tumourigenesis

1.6 Introduction into prostate cancer

Prostate cancer is the second most common cancer diagnosed in the UK affecting men with a peak age of 70 years. Over time there has been an increase in the number of men being diagnosed with prostate cancer (Cancer Research UK, 2015) due to improved diagnosis of asymptomatic patients (Chodak 2006).

The prostate is a highly organised glandular tissue comprised of epithelial cells in a fibromuscular stromal network (Packer and Maitland 2016). The basal layer is composed of four different cell types which are stem cells, transit amplifying cells, neuroendocrine cells and committed basal cells and there is also a layer of columnar luminal cells (Litvinov et al. 2006, Isaacs and Coffey 1989). The basal layer forms ~40% of the epithelium with the remaining being that of the luminal secretory cells (Packer and Maitland 2016). Identification of basal and luminal cells is based on cell marker expression, as basal cells have low expression of the androgen receptor (AR) and are positive for cytokeratin 5 and 14, p63, CD44, and GSTP1 whereas luminal cells are AR^{+}, and express cytokeratin 8 and 18, CD57, and NKX3 (Schrecengost and Knudsen 2013).

1.6.1 Prostate CSC phenotype

In the prostate epithelium there are a small population of ~1% of cells that make up the stem cell niche, and these have an increased expression of integrin $\alpha_2\beta_1$ (Collins et al. 2001) and these cells exclusively express CD133 (Richardson et al. 2004). Prostate cancer stem cells are reported to have a $CD44^{+}/\alpha_2\beta_1^{hi}/CD133^{+}$ phenotype as these cells that have been extracted from human prostate tumours are able to recapitulate the tumour of origin generating progeny of different cellular hierarchies (Collins et al.

2005). In addition, prostate CSC's are not eradicated by chemotherapy agents and radiotherapy but are induced in prostate cancer cell lines and are more tumorigenic and invasive (Wang et al. 2013a). $CD44^+$ cells have been classified as more proliferative, clonogenic, tumorigenic and metastatic than $CD44^-$ cells and are able to differentiate into both androgen receptor +ve and -ve cells (Patrawala et al. 2006). $CD44^+/CD133^+$ prostate CSC when cultured in 3D induce differential expression of Wnt related genes and increased expression of APC and downstream targets than CSC cultured in 2D (Goksei et al. 2013). Expression of CD44 and CD133 is upregulated when cells are cultured in a 3D environment and the $CD44^+/CD133^+$ cells have an increase in PI3K/Akt signalling (Dubrovska et al. 2009).

1.6.2 Development, progression and metastasis of prostate cancer

Prostatic intraepithelial neoplasia (PIN) is defined by the neoplastic growth of epithelial cells within the prostatic duct which can lead on to high grade PIN, which is the most common precursor to prostate cancer (Bostwick and Qian 2004). PIN is characterised by highly proliferative cells within ducts and acini with some cytogenic changes and nuclear enlargement (Bostwick 2000). Increasing grades of PIN is associated with progressive disruption of basal layer, and high grade PIN can be identified based on four main architectural patterns which are flat, tufting, micropapillary and cribriform, (Bostwick 2000). High grade PIN and prostate cancer share many genetic alterations however it is the activation or inactivation of specific genes that induces carcinoma (Table 1).

Initiation and progression to prostate cancer			
Gene	Product	Human phenotype	Reference
Rb	Cell-cycle regulator	Lost or silenced in early onset of prostate cancer.	(Steiner et al. 2000)
p27	Cell-cycle regulator	Lost or silenced in early onset of prostate cancer.	(Slingerland and Pagano 2000)
p16	Cell-cycle regulator	Lost or silenced in early onset of prostate cancer.	(Steiner et al. 2000)
Telomerase	Ribonucleoprotein	Reduced telomere lengths and increased expression of telomerase.	(Meeker 2006)
Myc	Transcription factor	Amplified in some tumours	(Koh et al. 2010)
PIN and carcinoma			
PTEN	Lipid phosphatase	Loss of TSG leads to PI3K/Akt signalling.	(Ferraldeschi et al. 2015)
TMPRSS2:ERG translocations	Transcription factor	Translocation of ERG to the TMPRSS2 promoter leads to a constitutively active ERG	(Tomlins et al. 2005)
E-cadherin	Cell adhesion	Reduced in PIN and lost in carcinoma.	(Fan et al. 2012a)
c-CAM	Cell adhesion	Reduced in PIN and lost in carcinoma.	(Hsieh et al. 1995)
Integrins	Cell interactions	Reduced expression of some family members in advancing prostate cancer.	(Goel et al. 2008).
c-Met	Tyrosine kinase receptor	Overexpressed in PIC, carcinoma and metastasis.	(Varkaris et al. 2011)
Advanced carcinoma and metastasis			
Androgen receptor	Hormone receptor	Expression maintained in androgen independent cancers. Often amplified or mutated.	(Kahn, Collazo and Kyprianou 2014)
p53	Transcription/apoptotic regulator	Frequently mutated in metastasis, overexpression correlates with a poor prognosis.	(Eastham et al. 1995)
NKX3.1	Homeodomain transcription factor and TSG	Down regulated in high grade carcinoma and lost in metastasis.	(Gurel et al. 2010)

Table 1. **Common genetic alterations that are acquired in the normal prostate gland that induces PIN and carcinoma formation**. During the progression from normal prostate to a neoplasm a number of successive mutations are acquired that facilitates cell proliferation. As an early neoplasm develops the number of mutations increases due to the loss of TSG and activation of oncogenes to form a PIN. Later stage and advanced carcinoma results in further genetic mutations and metastasis.

1.6.3 Cell of origin in prostate cancer

Identification of the type of cell involved in the origin of cancer is important as different cell types can give rise to a sub-population of cells, distinguishable only by their phenotype which has significant implications for patient outcome. In prostate cancer it was originally thought that cancers originated from luminal cells, however recent evidence suggest that prostate cancer may be of basal or luminal origin (Schrecengost and Knudsen 2013). Contrary to this Wang et al 2014, identified that luminal cells are the favoured cell type of origin as determined by lineage tracing experiment and that basal cells only formed tumours after differentiating into luminal cells (Wang et al. 2014b).

1.6.4 Grading and staging system in prostate cancer

In order to establish how aggressive a prostate cancer and the likelihood of metastases, a grading system is used known as the Gleason classification system (Byar 1973, Epstein et al. 2005). The Gleason classification system compares how reflective the tumour is to normal tissue and is put on a scale from 1-5 to generate a sum score. The two most common sum scores are then added together to form a Gleason sum-score from 2-10. The lowest sum score mediates a better prognosis as this is the most reflective of normal tissue and the higher the number, the least representative of normal tissue (Gleason 1992). Many carcinomas are diagnosed >6 indicating a poorer prognosis.

Figure 1.4. The Gleason Grading System as adapted from (Gleason 1992). Gleason grade 1 cells appear uniformed in shape and size with minimal nuclear changes. As you increase in stages the cells lose their cellular morphology with infiltration of neighbouring stroma and tissues. At pattern 5 there is a total loss of structure and is no longer representative of a normal prostate gland.

In addition to the Gleason grading system a complex Tumour Node Metastasis (TNM) staging system is employed to determine the stage of the cancer. The T category consists of T_1, T_2, T_3 and T_4 with the T_1 being the most desirable stage as this indicates that the tumour is too small to be identified using a scan or during examination. With increasing T stages there is a worse prognosis as identification of a T_4 stage prostate cancer details that the cancer has spread to nearby tissues (Cancer Research UK, 2015). T1 and T2 are potentially curative and may be suitable for radical prostatectomy or local radiotherapy, whereas most T3 and all T4 are not curative by surgery so systemic therapies are used (Caner Research UK, 2015).

The N stage can be subdivided into 3 stages consisting of NX, N0 and N1. NX stage means that the lymph nodes cannot be assessed, N0 is where there nearby lymph

nodes do not contain any cancer cells and the worse prognosis of N1 is where there are cancer cells in the nearby lymph nodes (Cancer Research UK, 2015).

The M stage which is subdivided into 5 categories describes if the cancer has spread to different parts of the body consisting of M0, M1, M1a, M1b and M1c. M0 is the better prognosis with increasing malignancy as you move through the stages. M1 means that the cancer has spread outside of the pelvis and is divided into a, b and c dependent upon the location of the metastasis. Staging a cancer at M1a signifies that there is presence of cancer cells within the lymph nodes outside of the pelvis, M1b means there are cancer cells within the bone whereas M1c means there are cancer cells within other locations within the body (Cancer Research UK, 2015).

Both the Gleason grading system and TNM staging are of particular importance as the outcome of these depicts which treatments options are available and determine survival rates for the patient.

1.7 Introduction into breast cancer

Breast tissue also referred to as the mammary gland is distinguishable from other organs as development does not fully occur until after birth (Russo and Russo 2004). The breast is made up of 12-20 lobes and within each lobe are many smaller lobules which make up the gland that produce milk in lactating women (Gusterson and Stein 2012). Milk ducts are tubes that are connected to the lobes and lobules to transport milk to the nipple (Russo and Russo 2004). The vast majority of cancers arise at the lobes, lobules or ducts (Cancer Research UK, 2015). Ductal carcinoma *in situ* (DCIS) is a pre-invasive lesion that is confined to the ducts of the breast and is the most common type of non-invasive breast cancer diagnosed, and in many cases it may progress to invasive ductal carcinoma (Silverstein et al. 1995). Invasive ductal carcinoma- no

special type represents up to 80% of cancers diagnosed (Makki 2015). The majority of cells have a luminal cell phenotype that express estrogen receptors (ER), epithelial membrane antigen and cytokeratins: CK8, CK18 and CK19 (Fulford et al. 2006). However in invasive ductal carcinoma- no special type (IDC-NST) there is a small population of cells with a basal phenotype that express cytokeratins: CK5/7, CK14 and CK17 and smooth muscle markers and are negative for estrogen, progesterone and herceptin receptor (Her-2) (Gusterson et al. 1982, Nagle et al. 1986, Gould et al. 1990, Wetzels et al. 1991, van de Rijn et al. 2002, Fulford et al. 2006) .

1.7.1 Breast CSC phenotype

Cancer stem cells are difficult to isolate within a heterogeneous cell population due to their lack of accepted cell markers and due to stem cell markers being tissue specific. In normal breast epithelial there are a proportion of cells that are proposed to be stem/progenitor cells and these have a $CD44^{+}/CD24^{-}$ phenotype and express other stem cell related genes (Bhat-Nakshatri et al. 2010, Ghebeh et al. 2013). Breast cancer stem cells are reported to have a $CD44^{+}/CD24^{-}$ phenotype (de Beça et al. 2013, Al-Hajj et al. 2003, Wei et al. 2012, Ricardo et al. 2011) and can induce angiogenesis, invasion and metastasis (Sun et al. 2013b, Sheridan et al. 2006), are resistant to radiation (Phillips, Mcbride and Pajonk 2006) and chemotherapy agents (Ji et al. 2016). The $CD44^{+}/CD24^{-}$ phenotype is largely expressed in tumours derived from basal cells that are negative for estrogen and progesterone receptors as well as HER2 (Honeth et al. 2008, Giatromanolaki et al. 2011, Idowu et al. 2012), and is found in majority of hereditary BRCA1 breast cancers (Honeth et al. 2008). Patients with the $CD44^{+}/CD24^{-}$ phenotype typically present with a 10 year lower median age than the $CD44^{+}/CD24^{+}$ expressing patients (Giatromanolaki et al. 2011). In addition lack of CD44 is associated with lymph node metastasis and dual negative for both markers appears to be the

worst phenotype, as this is associated with high histological grade (Giatromanolaki et al. 2011). The $CD44^+$ population of cells has been associated with stem cell characteristics and CD24 positivity is related to differentiated epithelia (Park et al. 2010). However these CSC markers are somewhat controversial (Ricardo et al. 2011) and the $CD44^+/CD24^-$ phenotype is not expressed in all breast CSC (Honeth et al. 2008).

Interleukin 8 (IL-8) is a chemokine that is expressed by many cell types and is chemotactic to leukocytes in inflammatory responses (Baggiolini and Clark-Lewis 1992, Harada et al. 1994). In normal tissues it is virtually undetected but can be rapidly induced by TNFα, and is upregulated in cancer (Ning and Lenz 2012). IL-8 binds to receptors CD181 and CD182, also known as CXCR1 and CXCR2 respectively, to induce its biological effects. In colorectal cancer, IL-8 induces proliferation, invasion, metastasis and angiogenesis by binding to CXCR2 (Ning and Lenz 2012). In breast cancer, CD181 is suggested to be a CSC marker as cells that are positive for both CD181 and Aldehyde dehydrogenase, a putative CSC marker can reconstitute a heterogeneous tumour with phenotypically different progeny, and the hierarchy within tumours is facilitated by IL-8/CD181 signalling (Ginestier et al. 2010). Additionally, the up-regulation of IL-8 in breast cancer is associated with a poorer prognosis and increases CSC self-renewal of cell lines (Brandolini et al. 2015).

1.7.2 Breast cancer grading and staging system

In breast cancer grading there are a number of grading systems employed to describe the aggressive potential of the tumour with low grade tending to be less aggressive than high grade cancers. The Nottingham histological score system takes into consideration of 3 aspects of the tumour which include the amount of gland formation in relation to differentiation, nuclear pleomorphism and mitotic activity with each

feature scoring from 1-3. Each score is then added to give a final score between 3-9. Grade 1 tumours have a score of 3-5 whereas Grade 2 and 3 tumours score between 6-7 and 8-9 respectively (Cancer Research UK, 2015).

Breast cancers are also staged using a TNM scoring system with subdivisions within each category. The T stage can be divided into T_X, T_{is}, T_1, T_2, T_3 and T_4 with further division within each T category. T_X means that the tumour cannot be scored whereas T_{is} is ductal carcinoma in situ. In stages T_1 to T_4 the increase in number reflects the increase in size of the tumour (Cancer Research UK, 2015).

The N stage is further divided into N1, N2 and N3 with further subdivision within each category with the higher category representing cancer cells being present in lymph nodes that are not directly next to the primary cancer (Cancer Research UK, 2015).

The M stage is divided into 3 categories to identify if the cancer has metastasised and where in the body these cells have been found. These sub-divisions are M0 which means that the tumour has not spread, cMo(i+) means that there is no sign of cancer during physical examination, scans or X-rays but are detected in blood, bone marrow or lymph nodes identified using laboratory testing. M1 means that the cancer cells have metastasised to another part of the body (Cancer Research UK, 2015).

As in prostate cancer, the grade and stage of the cancer helps determine treatment options for the patient in addition to determine chance of survival.

1.7.3 Cell of interest in breast cancer

In the vast majority of breast cancers it has been found that the cell of origin is derived from the luminal population and that basal cells may only contribute to the rarer forms of cancer (Keller, et al. 2012). In addition, basal-like breast cancers that

represents BRAC1 cancers were originally thought to have developed from a transformed basal stem cell, however it has been demonstrated that luminal progenitors can give rise to cells with basal like phenotypes, demonstrating phenotypic plasticity under selective conditions (Molyneux et al. 2010)

1.8 Genetics of cancer

1.8.1.1 p53

Tumour suppressor gene p53 is probably the most frequently mutated gene in cancer, and is usually subjected to point mutations (Hainaut et al. 1998). In normal cells p53 is rapidly degraded, however in cancer the mutated allele translates to an abnormally stable protein that accumulates within the nucleus. Mutated p53 is normally associated with a more aggressive form of cancer, typically metastatic and androgen independent, although mutated p53 may also be expressed in primary tumours (Grignon et al. 1997, Meyers et al. 1998, Ecke et al. 2007).

1.8.1.2 PTEN

Phosphatase and Tensin (PTEN) homolog located on chromosome ten was originally identified as a TSG in 1997 and is frequently mutated and inactivated in breast, brain and prostate cancer (Li et al. 1997). PTEN is an inhibitor of the PI3K signalling pathway that when stimulated goes on to activate effector molecules that induce cell growth, proliferation, survival and motility (Leslie and Downes 2004) Most mutations result in truncation or frameshift resulting in inactivation of the phosphatase subunit (Leslie and Downes 2004) in addition to point mutations (Han et al. 2000).

1.8.1.3 BRAC1 and BRAC2

Breast cancer susceptibility gene 1 (BRAC1) and BRAC2 are tumour suppressor genes that are commonly associated with early onset, hereditary breast cancer (Hall et al. 1990) and sporadic breast cancer (Futreal et al. 1992, Futreal et al. 1994). In response

to DNA damage, BRAC1 is activated via phosphorylation by proliferating cell nuclear antigen (PCNA), antaxia telangiectasia mutated (ATM) kinase, ATM related kinase (ATR) or CHK2 (Thomas et al. 1997, Cortez et al. 1999, Helt et al. 2005, Chaturvedi et al. 1999). Activated BRAC1 then interacts with proteins involved in DNA repair, and also plays a role in transcriptional regulation of cell cycle control genes as reviewed by Yoshida et al (2004) (Yoshida and Miki 2004).

1.9 Overall aims and hypothesis

The overall aim of this thesis was to identify a CSC-targeting agent that induced cell cycle arrest and apoptosis in breast and prostate cancer cell lines cultured in 2D and 3D cell culture.

1.9.1 Hypothesis 1:

- 3D cell culture selects for a cancer stem cell-like phenotype in breast and prostate cancer cells vs 2D cell culture.

Cell lines cultured as monolayers for cell based assays and drug toxicity studies are not reflective of a tissue, or tumour of origin (Knight & Przyborski, 2015). In addition, 2D cell culture selects for the most dominant sub-population that likely represents the most proliferative cells, and may not represent the slow dividing CSC population (Rowehl et al., 2014). Using 3D cell culture, prostate and breast cancer cell lines can be propagated to enrich for spheroid formation which is a CSC characteristic, and induce expression of a CSC phenotype.

1.9.2 Hypothesis 2:

- Nanog-GFP reporters (NRE-GFP) select for CSC-like phenotype in breast and prostate cancer cells
- 3D cell culture selects for Nanog-positive cells

Reporter cell lines that express GFP under the control of a Nanog response element allows the study of CSC and their characteristics in real time, aiding in CSC proliferation in various cell culture environments, location in 2D and 3D cell culture and identification of other CSC markers that may be co-expressed.

1.9.3 Hypothesis 3:

Novel Withanolide derivative LG-02 and Withanolide E (WE) target breast and prostate cancer growth both in 2D and 3D cell culture.

As only 10% of drugs progress through to clinical development, partly due to 2D cell culture being misleading and unreliable, 3D cell culture is more representative of a

tumour microenvironment and assaying for drug responses would be more reflective of drug responses *in vivo*. Withanolide derivatives have been investigated for many years due to their anti-cancerous properties and have recently been identified as CSC targeting agents; however concentrations used to induce a biological affect may have increased toxicity to the host. Identification of a withanolide derivative that has a high therapeutic index and is able to target the bulk of cancer cells in addition to the CSC which normally facilitate tumour reoccurence and a more aggressive phenotype may lead to predictive data and increased reliability of compounds during clinical progression.

2 Comparison of a cancer stem cell phenotype in two dimensional vs three dimensional cell culture

2.1 Introduction

CSC as discussed in chapter 1 are a small population of cells within a tumour that are self-sustaining, and can maintain the bulk of the tumour by dividing symmetrically or asymmetrically in order to maintain the CSC population and the non-tumorigenic cancer cells, which in most cases form the mass of the tumour (Ho 2005, Clarke et al. 2006).

CSC were first identified in 1994 from patients with acute myeloid leukaemia (AML) as cells expressing cell surface markers $CD34^{+}/CD38^{-}$ were able to proliferate extensively and migrate to the bone marrow when transplanted into severe combined immune deficient (SCID) mice, disseminating a leukemic morphology similar to that of leukaemia patients (Lapidot, et al. 1994). Since this discovery, there has been a huge influx of research into the identification of other CSC markers and phenotypes in all cancer types.

2.1.1 Mimicking a tumour microenvironment using three dimensional cell culture

For many years it has been apparent that cells respond to local signals and cues within their environment which in turn has an effect on function, proliferation and differentiation (Baker and Chen 2012). Traditionally, the growth of mammalian cells *in vitro* has been carried out in 2D in which cells are cultured on a flat substrate as monolayers. 2D cell culture flattens and distorts the cell morphology, induces cytoskeleton remodelling and alters the nuclear shape (Knight and Przyborski 2015) which can alter gene and protein expression (Thomas et al. 2002). Vergani et al (2004) has found that culturing cells on different chemical features of the substratum can induce expression of *c-jun, c-myc, c-fos* and collagen, confirming that mechanical factors external to the cell can modulate gene expression through remodelling of the chromatin structure (Vergani, Grattarola and Nicolini 2004). Cells grown in 2D are

polarised and have an uneven distribution of receptors and adhesion molecules, with the majority of adhesion proteins located at the ventral surface in which they attach to the rigid surface (Bokhari et al. 2007b). Growing cells in 2D provides limited information on phenotype, tissue architecture, cellular interactions and drug response and is not representative of the tissue of origin (Knight and Przyborski 2015).

Currently, much focus into cancer research has been to investigate the role of the tumour environment in facilitating tumour growth, migration and drug resistance using 3D cell cultures. As cancer is a complex disease comprised of tumorigenic and malignant cells, and non-cancerous cell types such as endothelial cells, fibroblasts and immune cells (Hanahan and Weinberg 2011), 3D cell culture models have been developed and applied to examine the role of intra- and inter-cellular signalling networks and crosstalk within the tumour microenvironment (Thomas et al. 2002, Knight and Przyborski 2015). Limitations that occur with 2D cell culture grown as monolayers are overcome using a 3D cell culture model as this system can mimic the cellular heterogeneity, hierarchy and complex tissue architecture and represent structures that are present within a tumour microenvironment (Straussman et al. 2012, Chaturvedi et al. 2013b). 3D cell culture can also give mechanistic information about cellular and molecular modifications that occur within the tumour niche (Thoma et al. 2014). 3D cell culture offers an optimal micro environment for proliferation, differentiation and function that can form tissue like structures *in vitro* (Knight and Przyborski 2015) and is more enriching for a CSC phenotype (Ghajar and Bissell 2010, Hirschhaeuser et al. 2010) such as CD44 role in metastasis, ABC transporters in efflux of cytotoxic agents or ALDH role in detoxification.

Figure 2.1 The tumour microenvironment adapted from Thoma, Zimmermann *et al.* 2014 (Thoma et al. 2014). A) A tumour consists of various cell types coexisting to facilitate further growth. Extracellular matrix (ECM) components are secreted by cells and collagenous fibres are formed embedding and encapsulating the tumour offering protection from anti-cancer agents. At the site of invasion, collagenous fibres are aligned. B) An overlay of A emphasising the chemical gradients, physical barriers, and biological/phenotypical zones and niches that would be found within the tumour microenvironment (Thoma et al. 2014).

2.1.2 Types of 3D cell culture

There are two main types of 3D cell culture systems that are being investigated to grow mono or co-cultures, for the simulation of the tumour microenvironment *in vivo* (Thoma et al. 2014). These can either be scaffold-based 3D matrices that are porous, permeable with mechanical characteristics that reflect that of the ECM or liquid based (scaffold-free) that do not rely on any additional support (Knight and Przyborski 2015).

2.1.2.1 Scaffold free 3D cell culture

Scaffold free, 3D cell culture form spheroids from mainly aggregates of cells but can also be from single cell suspensions in which spheroids may be hypoxic due to the oxygen gradient (Fennema et al. 2013) and may include hanging drop method and spheroid formation using ultra-low attachment coated plates (Larson 2015). The hanging drop method has been used to culture cells in 3D to assess cell-cell and cell-stratum cohesion (Foty 2011) however this method can be quite expensive, time consuming and technical. Culturing cells as spheroids using ultra-low attachment plates and serum free medium is simple to do however the plates used are very expensive and spheroid size may not be reproducible.

2.1.2.2 Scaffold-based 3D cell culture

Scaffold-based 3D cell culture may generate spheroids that are derived from a single cell, are heterogeneous with proliferative cells around the outer layer and quiescent cells near the necrotic hypoxic centre (Fennema et al. 2013). Types of scaffold based 3D cell culture may include polymeric hard scaffolds and biological scaffold (Larson 2015).

Polymeric hard scaffolds have been investigated to assess cytotoxic effects of anticancer agents of cells grown in 2D and 3D, and it was discovered that cells grown in polymeric hard scaffolds are more resistant to apoptosis (Bokhari et al. 2007a).

Although polymeric hard scaffolds enrich a more resistant cell population the scaffolds degrade by hydrolysis, producing carbon dioxide and lowering local pH which may induce necrosis (Liu, Liu and Chen 2012). Biological based scaffolds such as collagen or proteoglycans are safer to use as these are bio-degradable and allow host cell deposition of extracellular matrix components when the scaffold is degraded, however some biological components may have poor mechanical properties and it may be difficult to extract cells from some of these matrices for gene expression analysis (Amp, Apos and Brien 2011).

Hydrogels are a scaffold based 3D cell culture material that are used in many biomedical applications due to these being hydrophilic and having similar mechanical properties to native tissues (DeVolder and Kong 2012). A type of hydrogel named alginate has been used in tissue engineering (David et al. 2004) and transplantation (de Vos et al. 2003) due to it being a natural polymer with lack of immunogenicity and good biocompatibility (Burgarski, et al. 1994). Alginate is a natural, anionic compound that is derived from brown seaweed and is structurally similar to macromolecules present *in vivo* (Sakiyama-Elbert and Hubbell 2001). Aqueous alginate is gelated by the addition of crosslinking agents such as divalent cations Ca^{2+} as these can directly bind to the guluronate blocks of one polymer, forming junctions with adjacent polymer chains in an egg-box model of crosslinking (Grant et al. 1973). Alginate gels are advantageous in 3D cell culture as formation by gelation with divalent cations encapsulates cells and does not have any unwanted effects on the cells or biological properties (Li et al. 2013). Limitations of using ionic cross-linked alginate is that these may dissolve due to the exchange of divalent cations with monovalent cations into the surrounding media therefore may not be suitable for long term investigations (Lee and

Mooney 2011), although supplementing medium with divalent cations can limit this process. Extraction of cells under physiological conditions for gene expression analysis can be carried out using an alginate dissolving buffer made up from chelating agents such as sodium citrate and EDTA (Xu et al. 2014).

Culturing cancer cells in alginate has been shown to induce an increased CSC phenotype, tumorigenicity, metastasis and drug resistance than cells cultured using traditional 2D methods (Xu et al. 2014). Xu et al (2014) found culturing hepatocellular carcinoma cell lines in 3D from 3-20 days and compared against 2D cell culture enriched for expression of Oct3/4, Nanog, CD44, CD133 and ABCG2 mRNA expression, CD44 and CD133 protein expressing cells and several matrix metalloproteinases over time in 3D cell culture (Xu et al. 2014).

2.1.3 Study Aims, Objectives and hypothesis

The study aim was to identify a cell culture model that would induce expression of CSC related genes and enrich for a CSC population.

Hypothesis

3D cell culture selects for a cancer stem cell-like phenotype in breast and prostate cancer cells vs 2D cell culture.

The specific objectives of this study were:

To identify the optimum time for culturing cancer cell lines as spheroids using alginate as a 3D cell culture model.

To determine and compare expression levels of CD133 and CD44 in prostate cancer cell lines and CD181, CD44 and CD24 in breast cancer cell lines when cultured in 2D and 3D.

To determine and compare expression when culturing in 2D and 3D of the $CD133^{+}/CD44^{+}$ prostate cancer stem cell phenotype. The $CD44^{+}/CD24^{-}$ breast cancer stem cell phenotype and CD44+/CD181+ and $CD181^{+}/CD24^{-}$ phenotypes.

2.2 Materials and methods

2.2.1 Cell Culture regents:

2.2.1.1 Complete medium

450ml DMEM or RPMI (Thermo Fisher Scientific, Altrincham)

50ml heat-inactivated Foetal Calf Serum (FCS) (Thermo Fisher Scientific)

5ml 100 U/ml penicillin, 100 µg/ml streptomycin (Thermo Fisher Scientific)

2.2.1.2 0.15M NaCl

8.76g $NaCl_2$ (Thermo Fisher Scientific) was dissolved in 1L dH_2O to give a final concentration of 0.15M and autoclaved for 15 minutes at 121°C, psi for 20min..

2.2.1.3 1.2% Alginate

1.2g Sodium alginate (Sigma Aldrich, Dorset) was dissolved in 100ml of 0.15M NaCl and heated at 60°C for ~3hrs until all Sodium alginate had dissolved and then filter sterilised using 0.2µm syringe filters (Fisher Scientific) .

2.2.1.4 0.2M $CaCl_2$

22.2g $CaCl_2$ was dissolved in 1L dH_2O to give a final concentration of 0.2M and autoclaved for 15 minutes at 121°C, psi for 20min.

2.2.1.5 Alginate dissolving buffer

14.2g of Sodium Citrate (55mM) (Thermo Fisher Scientific) and 8.76g EDTA (30mM) (Sigma Aldrich) was added to 1L dH_2O and autoclaved for 15 minutes at 121°C, psi for 20min.

2.2.1.6 Hoechst 33342 Stock solution

Stock solution of 10mg/ml Hoechst 33342 (Thermo Fisher Scientific) in dH_2O was prepared and aliquot into 10µl working solutions and stored at -20°C.

2.2.2 Cell culture methods

2.2.2.1 Cell lines

Cell Line	Tissue	Metastatic site	Morphology	Disease	Age	Gender	Ethnicity	Supplier
Ntera2	Testis	Lung	Epithelial like-differentiation changes phenotype	Malignant pluripotent embryonal carcinoma	22	Male	Caucasian	ATCC
PC3	Prostate	Bone	Epithelial	Grade IV, adenocarcinoma	62	Male	Caucasian	ATCC
Du145	Prostate	Brain	Epithelial	Carcinoma	69	Male	Caucasian	ATCC
LNCAP	Prostate	left supraclavicular lymph node	Epithelial	Carcinoma	50	Male	Caucasian	ATCC
SUM159	Breast	N/A (Infiltrating ductal carcinoma)	Epithelial	Anaplastic-carcinoma		Female	Caucasian	Asterand (NCI)
MCF7	Breast	pleural effusion	Epithelial	Adenocarcinoma	69	Female	Caucasian	ATCC

Table 2. Cell lines. NTera2 cell line is a testicular germ cell line used as a positive control for CSC markers. PC3, DU145 and LNCAP cell lines were used as a model of prostate cancer. SUM159 and MCF7 cell lines were as a used model of breast cancer.

2.2.2.2 Culturing cells

NTera2, MCF7, PC3, DU145 and LNCAP cell lines were all purchased from ATCC and were cultured in 75cm^2 flask (Thermo Fisher) with DMEM complete medium. SUM159 cell lines were obtained from Dr Tom Sayers, National Institutes of Health (NIH), USA and cultured in complete RPMI medium.

2.2.2.3 Passaging of cells

Cell lines were passaged when these were 80% confluent. Culture medium was discarded and cells were washed in 1× Phosphate Buffered Saline (PBS) (Sigma Aldrich) to remove any residual medium. Cells were then removed by adding 3ml of 0.05% Trypsin-EDTA (Sigma Aldrich) per 75cm^2 flask at 37°C for 5-10min until all cells had detached. Inactivation of Trypsin-EDTA was achieved by adding in equal amounts of complete medium.

2.2.2.4 Counting cells

Cells were counted using the Countess Automated Cell Counter (Thermo Fisher Scientific) by mixing 10µl of cell suspension and 10µl of 0.4% (w/v) Trypan Blue (Sigma Aldrich) and adding to a countess chamber slide (Thermo Fisher Scientific). Dead cells that were stained blue by taking up the Trypan blue were excluded from the cell count.

2.2.2.5 3D cell culture using Alginate bead model

5x10^5 cells/ml of 1.2% Sodium Alginate was gently mixed to prevent air bubbles until cells were in a single cell suspension and evenly distributed. Cell suspension was taken up by a syringe and 19G needle. Cell suspension was released into 0.2M $CaCl_2$ (Fisher Scientific) a drop at a time and then incubated at 37°C for 10min to allow the alginate beads to polymerise. $CaCl_2$ was removed and alginate beads were washed twice in 0.15M NaCl, twice in complete medium and incubated in complete medium at 37°C in a humidified, 5% CO_2.

2.2.2.6 Release of tumour spheres from alginate matrix

Alginate beads are washed in 1× PBS and dissolved by placing 1 bead/0.5ml of alginate dissolving buffer for 10mins at 37°C on an orbital shaker at 100g until the bead is fully dissolved. Cell suspension is then centrifuged at 400g to pellet the cells. Alginate dissolving buffer is then removed and cells are suspended in complete medium.

2.2.2.7 Hoechst 33342 and Propidium Iodide stain for apoptosis/necrosis

Cells were stained with Hoechst 33342 and Propidium Iodide to determine the viability of the cells. Hoechst 33342 was used to assay the number of viable and apoptotic cells and Propidium Iodide was used to identify late stage apoptotic and dead cells. Cells were treated with 10µg/ml of Hoechst 33342 and 1µg/ml Propidium Iodide solution (Sigma Aldrich) and incubated for 20-25min at 37°C in a humidified, 5% CO_2 atmosphere. Cells were imaged using the Olympus IX81 inverted fluorescence microscope to assess cell viability using Cell-F software (Olympus).

2.2.2.8 Hoechst 33342 and Propidium Iodide stain of 3D cell culture

Cells cultured in alginate were stained with 10µg/ml of Hoechst 33342 and 1µg/ml Propidium Iodide in complete medium and incubated for 20-25min at 37°C in a humidified, 5% CO_2 atmosphere. Alginate bead containing spheroids are thinly sliced using a disposable scalpel and flattened on a glass slide and coverslip. In other experiments cells were released from alginate as described in (Figure 2.2.2.5) and stained as above. Cells were imaged using the Olympus IX81 inverted fluorescence microscope to assess cell viability using Cell-F software (Olympus).

2.2.3 Principles of flow cytometry

Flow cytometric analysis is a technique that allows the identification of a cell type based on size, granularity and phenotype by passing an individual cell through a detector beam. Using hydrodynamic focussing a single cell suspension can be

separated and focused to allow the passage of single cells, one at a time through a detector beam. The light beams detect the forward and side scatter, which is the amount of light scattered as the beam passes through the cell. The forward scatter (FSC) gives information on the size of the cell and the side scatter (SSC) gives information about the granularity and complexity of the cell. The information obtained from FSC and SSC allow the positive identification of single cells from cellular debris, cell doublets and clumps of cells which would distort the data. FSC and SSC are used in all aspects of flow cytometry, and is an important tool in identifying white blood cells and in cell cycle analysis.

A common application of flow cytometry is the detection of fluorescently labelled antibodies that have bound to an intracellular or cell surface protein of interest. Cells that emit a fluorescent signal can be detected using fluorescent detector beams that have a range of wavelengths. Which fluorescent antibody to use is all dependent on the instrument and detector beams available. For example GFP is excited by the FL1 detector at a wavelength of 400nm with a lesser peak at 475nm. Alexa Fluor647 has an excitation of 650nm and can be detected on the FL4 detector. The information obtained from the FSC, SSC and fluorescence emissions is used to generate a frequency histogram or a dot plot.

Fluorescent activated cell sorting (FACS) is another technique applied to flow cytometry which allows the separation of cells based on different cell characteristics. For example, cells that are GFP positive can be isolated from the heterogeneous cell population using FACS. In the same manner as flow cytometry, after detection of a specific fluorescence cells are given a positive charge whereas negative cells are given a negative charge. Cells are then passed through an electromagnetic deflection system

and separated based on charge, resulting in two phenotypically different cell populations.

Figure 2.2. **Schematic representation of the FACSCalibur optical layout 4 colour detectors as adapted from Becton Dickinson (Dickinson, 2007)**

2.2.3.1 CSC phenotype stain and flow cytometry analysis

$5x10^5$ cells in 1% FCS:PBS were placed in Flow Cytometry Tubes and centrifuged at 1000rpm, 4°C for 5min. The Supernatant was removed leaving up to 100µl of residual 1% FCS and the cell pellet was flicked repeatedly to break up the cells to obtain a single cell suspension. The SUM159 and MCF7 cell lines were incubated with 5µL of 0.2mg/ml PerCP-conjugated anti-mouse/human CD44 (IM7/ #103035), 5µL of 0.2mg/ml Alexafluor 647-conjugated anti-human CD24 (ML5/ #311109) and 5µLof 0.1mg/ml PE-

conjugated anti-human CD181 (8F1/ #320608) (Biolegend). The same concentrations were used for the isotype controls: PerCP-conjugated Rat IgG2b (RTK4530/ #400630), Alexafluor 647-conjugated mouse IgG2a (MOPC-173/#400234) and PE-conjugated mouse IgG2b (MPC-11/ #400314) (Biolegend) for 1hr at 4°C. The PC3, DU145 and LNCAP cell lines were stained with 5µL of 0.2mg/ml PerCP-conjugated anti-mouse/human CD44 (IM7/ #103035) and PE-conjugated anti-human CD133/1(3152C11/ #141204) and the same concentration of isotype controls: PerCP-conjugated Rat IgG2b and PE-conjugated Mouse IgG1. The cells were stained at 4°C for 1hr. Cells were then washed 2x in 1x PBS with centrifugation at 400g to remove excess antibodies and fixed at 4°C overnight in 1% Paraformaldehde (w/v) in PBS (Sigma Aldrich). 10,000 events were acquired using the FACSCalibur and antigen expression was determined using the CellQuest software.

2.3 Results

2.3.1 Expression of cell surface markers CD44 and CD133 in positive control NTera2 cell lines as determined by flow cytometry.

The human embryonal carcinoma cell line NTera2 was used as a positive control for expression of CD44 and CD133. The isotype controls (Mouse and Rat IgG conjugated to PE and Percp) were used to set the gates to distinguish between background fluorescence and positive expression of CD44 and CD133. NTera2 cell line express CD44 and CD133 in 12% and 33% of the cell population (fig 2.3). Dual positivity for cell surface expression of CD44 and CD133 was 3%.

Figure 2.3. Expression of CD133 and CD44 in NTera2 cell line.

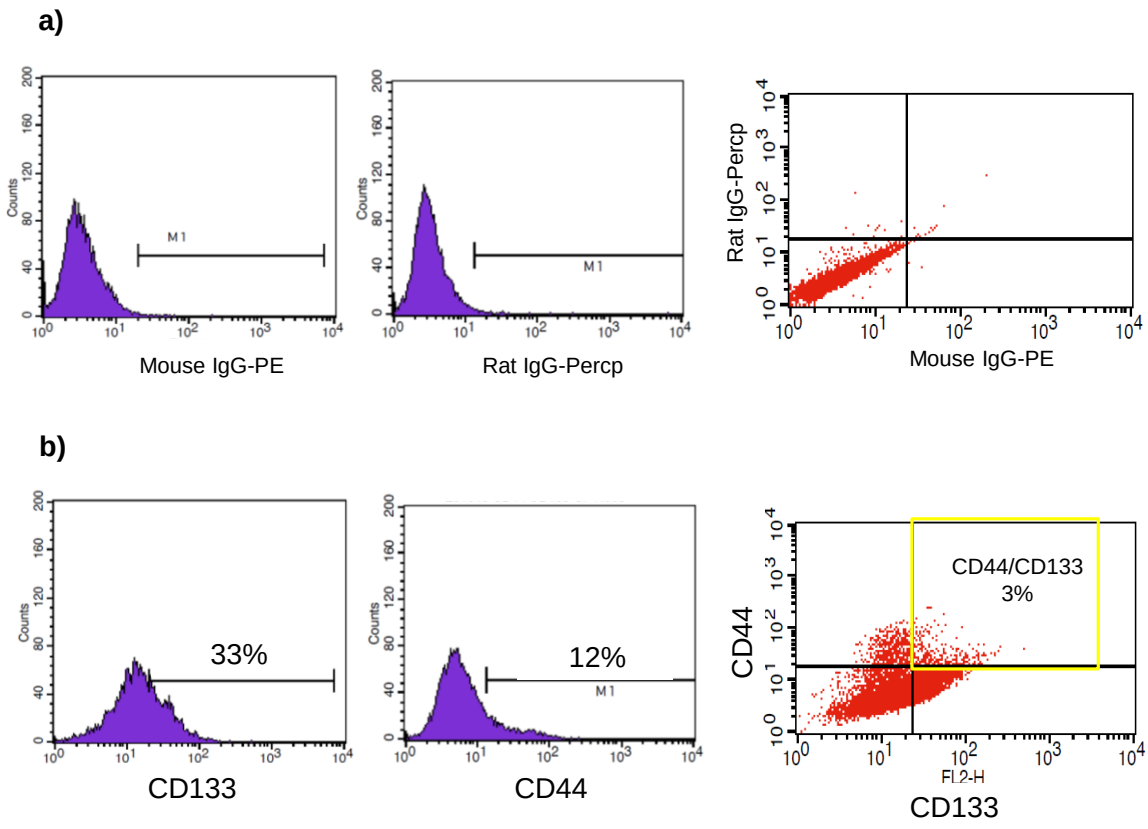

Figure 2.3 Expression of CD133 and CD44 in NTera2 cell line as determined by flow cytometry. a) Respective isotype controls conjugated to PE and Percp were used to incorporate a gate to identify background fluorescence. Everything to the left of the M1 was background fluorescent and taken to be negative. b) Positive expression of CD133 and CD44 was detected in the NTera2 cell line as anything to the right of the M1 line is positive for cell surface markers. Dual positivity for CD44 and CD133 was identified in 3% of the cell population. Histogram plot and dot plot data are representative of 1 independent experiment.

2.3.2 Expression of CD44 and CD133 in prostate cancer cell lines cultured in 2D as determined by flow cytometry.

The PC3 cell line had a 96% population of CD44 expressing cells however CD133 was only expressed in 1% of the population (fig 2.4). DU145 cell line had a basal expression of CD44 in 46% of the cell population and 2% of the population are CD133 positive. The LNCAP cell line had a 1% population of cells that were positive for CD44 and CD133. All data were gathered on the FACSCalibur and analysed using BD CellQuest software.

Figure 2.4. Expression of cell surface markers CD44 and CD133 in prostate cancer cell lines cultured in 2D as determined by flow cytometry.

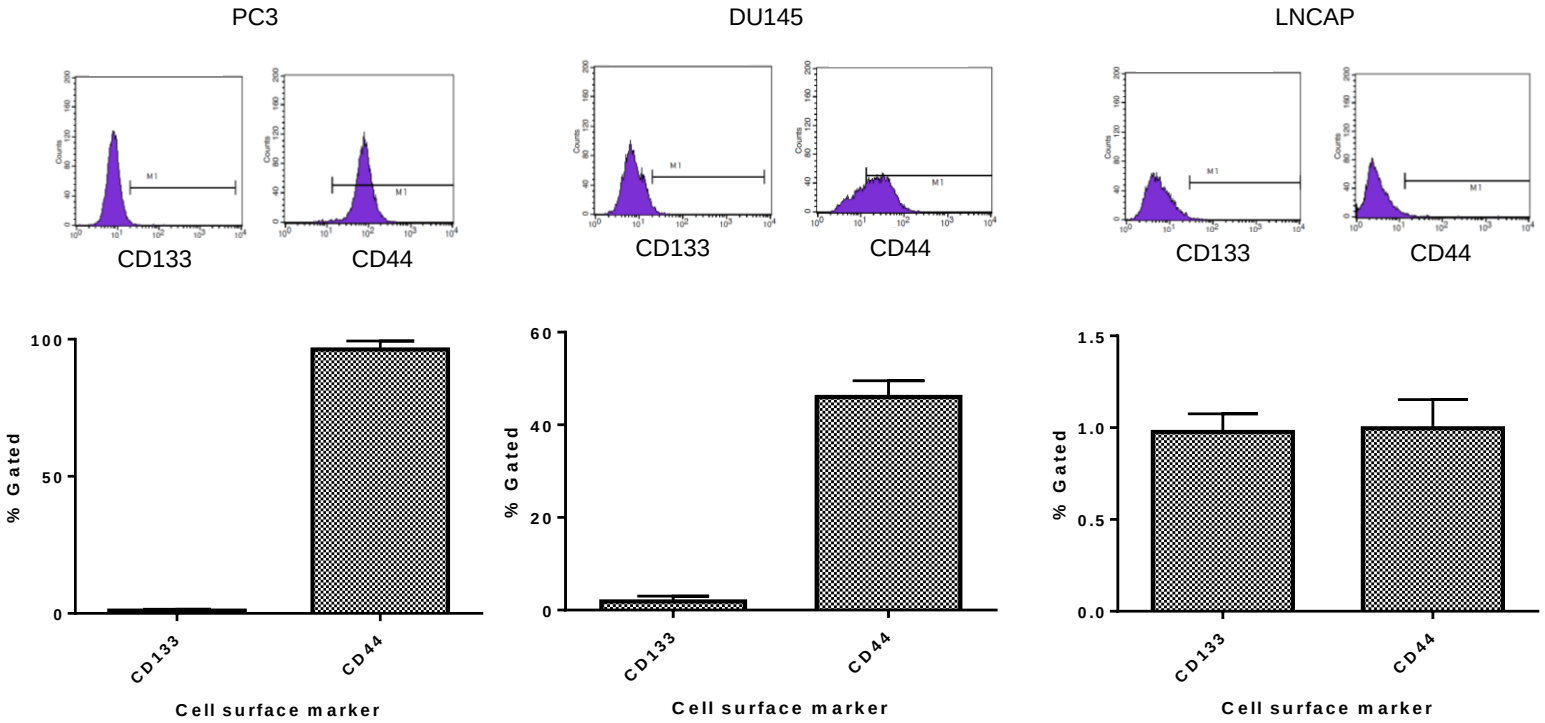

Figure 2.4. Expression of CD133 and CD44 in prostate cancer cell lines grown in 2D. Prostate cancer cell lines were cultured in 2D and stained for basal expression of CD133 and CD44. CD133 expression was very low in all cell lines <2%. PC3 cell lines appeared to express CD44 in almost 100% of the cells whereas CD44 expression in the DU145 and LNCAP cell line was 50% and 1% respectively. All data is represented as mean ± standard error of the mean (SEM) and was carried out in three independent experiments. The histogram plots are representative of three independent experiments.

2.3.3 Dual expression of cell surface markers CD133 and CD44 in prostate cell lines cultured in 2D as determined by flow cytometry.

Prostate cancer cell lines were cultured in 2D to determine basal expression of $CD44^+/CD133^+$ prostate CSC phenotype. The $CD44^+/CD133^+$ phenotype was low as expected in all cell lines grown in 2D as these cells represent the CSC population. The PC3 cell line had a 1% population of cells with the $CD44^+/CD133^+$ phenotype and the DU145 and LNCAP had a 1.7% and 0.6% cell population respectively (fig 2.5). All data were gathered on the FACSCalibur and analysed using BD CellQuest software.

Figure 2.5. Dual expression of cell surface markers CD44 and CD133 in prostate cancer cell lines cultured in 2D as determined by flow cytometry.

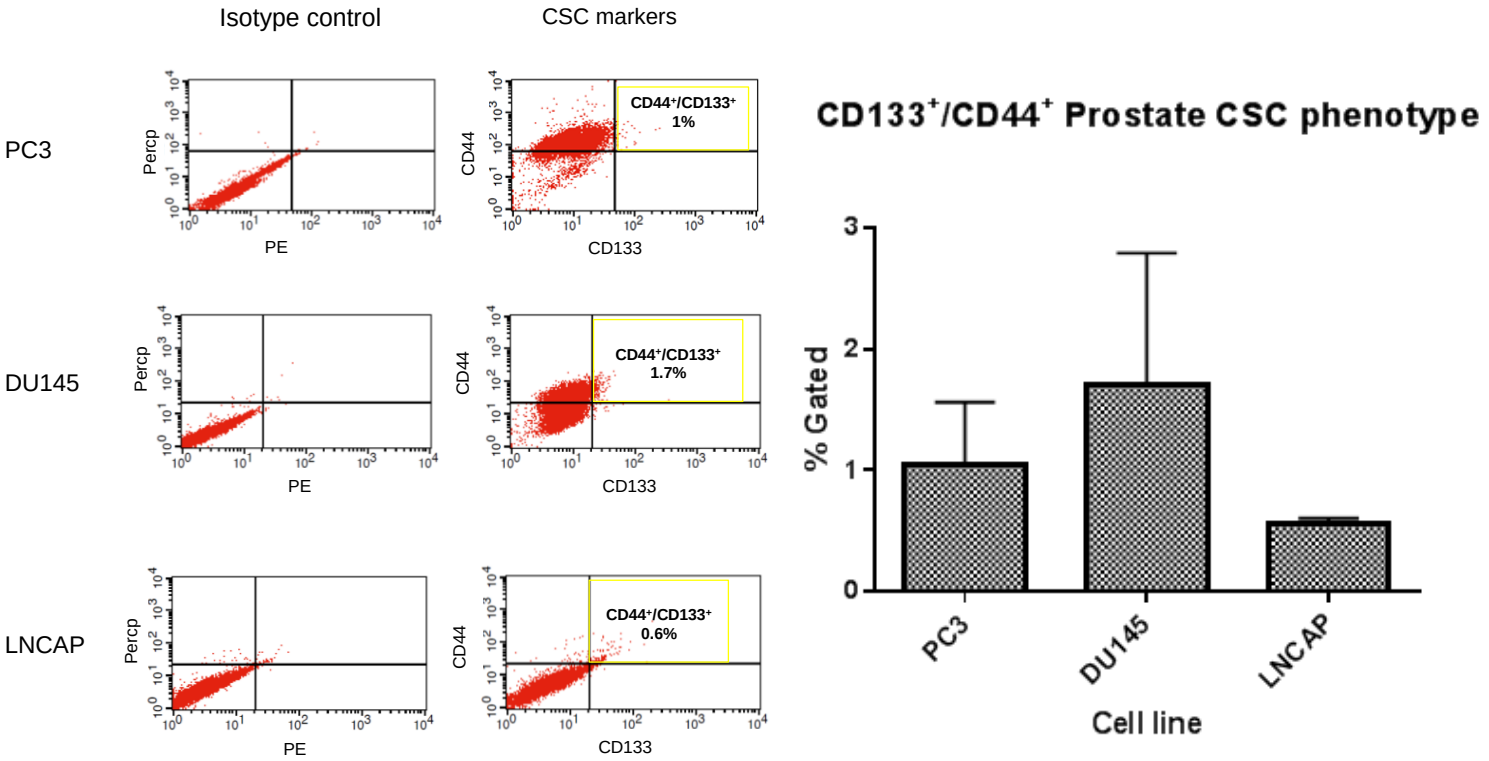

Figure 2.5 Dual expression of CD44 and CD133 in prostate cancer cell lines when cultured in 2D as determined by flow cytometry. Prostate cancer cell lines were seeded in 2D overnight prior to harvesting and antibody stain. Dual expression of CD133 and CD44 was <2% for all cell lines when cultured in 2D. All data is represented as mean ± SEM and was carried out in three independent experiments. The dot plots are representative of 3 independent experiments.

2.3.4 Expression of cell surface markers CD181, CD44 and CD24 in breast cancer cell lines cultured in 2D as determined by flow cytometry.

Breast cancer cell lines were cultured in 2D to determine basal expression of CD181, CD44 and CD24. CD181 was expressed in 7% of MCF7 cells and in 9% of SUM159 cells (fig 2.6). The MCF7 cell line had a population of only 4% of cells with CD44 cell surface marker whereas CD44 was expressed in 100% of SUM159 cells. CD24 is expressed in 70% of the MCF7 cell line and 85% of SUM159 cell line. All data were gathered on the FACSCalibur and analysed using BD CellQuest software.

Figure 2.6. Expression of cell surface markers CD181, CD44 and CD24 in breast cancer cell lines cultured in 2D as determined by flow cytometry.

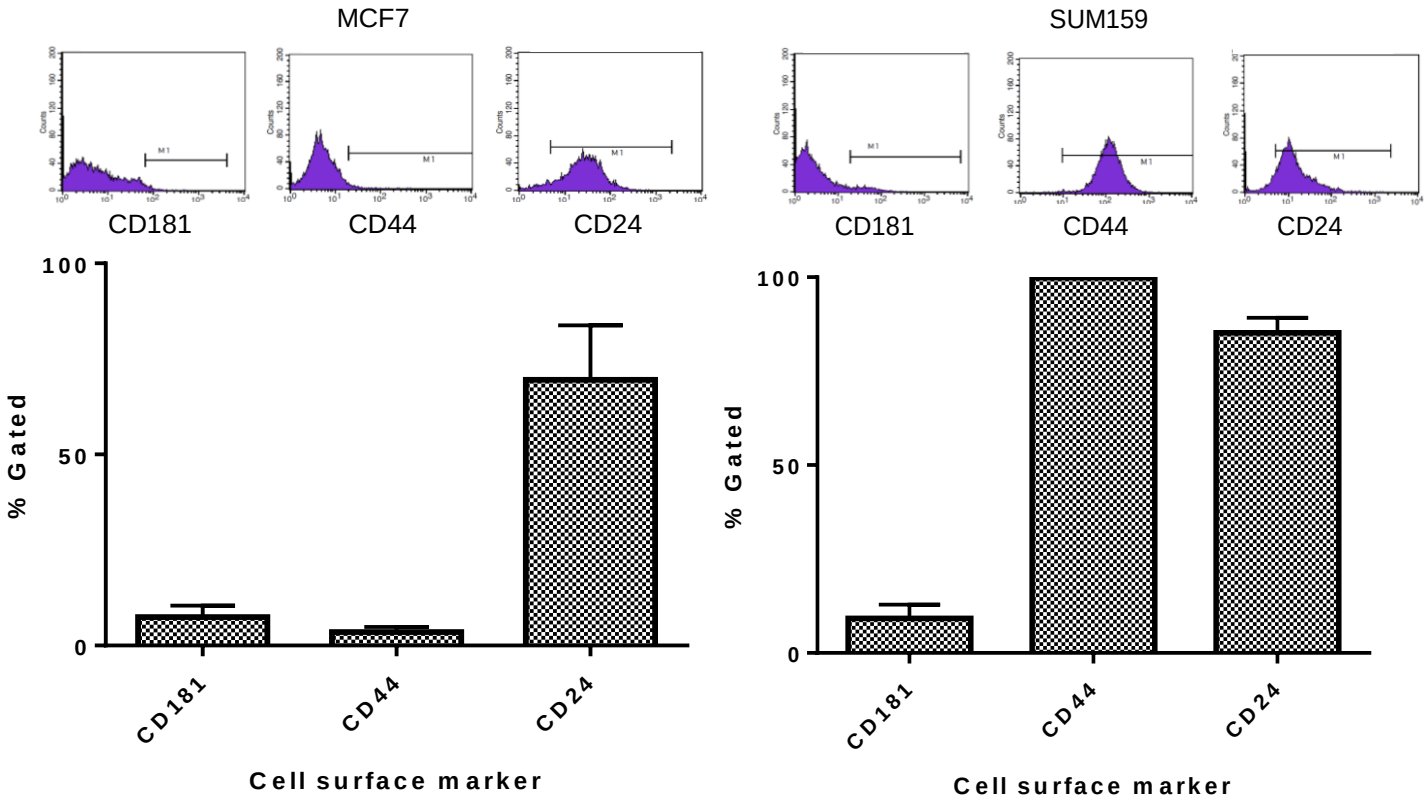

Figure 2.6. Expression of cell surface markers in breast cancer cells lines cultured in 2D. Breast cancer cell lines were seeded in 2D overnight prior to harvesting and antibody stain. MCF7 and SUM159 cell lines had <10% population of cells that were CD181 positivity. CD44 was expressed at low levels in the MCF7 cell line and ubiquitously expressed in SUM159 cell line. CD24 was expressed in 70% of MCF7 cells and in 85% of the SUM159 cell line. All data is represented as mean ± SEM and was carried out in three independent experiments. The histogram plots are representative of three independent experiments.

2.3.5 Expression of breast CSC phenotype in breast cancer cell lines cultured in 2D as determined by flow cytometry.

Expression of basal breast CSC phenotype $CD44^+/CD24^-$ and potential breast CSC phenotypes $CD44^+/CD181^+$ and $CD181^+/CD24^-$ was determined in SUM159 and MCF7 cell line after culturing in 2D.

MCF7 cell line had <1% of cells with the $CD44^+/CD24^-$ breast CSC phenotype. The population of cells with the $CD44^+/CD181^+$ and $CD181^+/CD24^-$ phenotypes was 1% and <1% respectively (figure 2.7).

The SUM159 cell line had a 19% population of cells with the $CD44^+/CD24^-$ breast CSC phenotype. The population of cells with the $CD44^+/CD181^+$ and $CD181^+/CD24^-$ phenotypes was 9% and <1% respectively (figure 2.7).

Figure 2.7. Expression of breast CSC phenotypes^{-} of SUM159 cell line cultured in 2D as determined by flow cytometry.

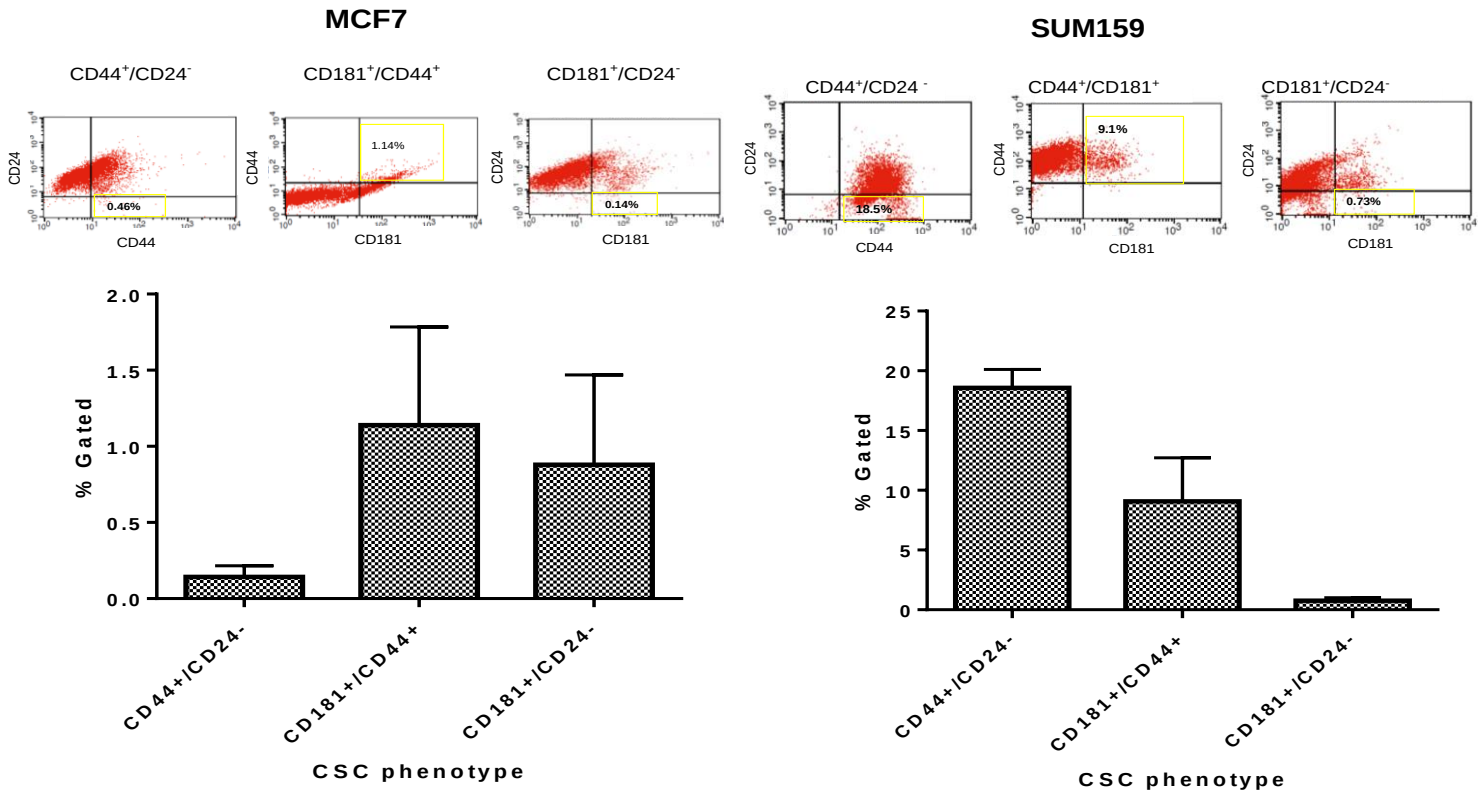

Figure 2.7. Expression of breast CSC phenotype in SUM159 and MCF7 cell lines. Breast cancer cell lines were seeded in 2D overnight prior to harvesting and antibody stain. MCF7 and SUM159 cell lines had a <1% and 19% population of cells with the CD44^{+}/CD24^{-} breast CSC phenotype. The CD44^{+}/CD181^{+} and CD181^{+}/CD24^{-} phenotypes were expressed in ~1% of MCF7 cell line. The SUM159 cell line had a 9% and <1% population of cells with the CD44^{+}/CD181^{+} and CD181^{+}/CD24^{-} phenotypes. All graphical data is represented as mean ± SEM and was carried out in three independent experiments. The dot plots are representative of 3 independent experiments.

2.3.6 Identification of the optimum time for spheroid formation when prostate and breast cancer cell lines are grown in 3D using alginate.

Prostate and breast cancer cell lines were cultured for 0-14 days in alginate acid and stained with Hoechst 33342 and Propidium Iodide to asses for the optimum time point for spheroid formation.

The PC3 cell line readily formed tight clusters of cells from day 7-14. At day 7 these clusters were not tightly packed, however by day 10 these appeared to be uniformed in shape although these were still small in size (<200µm) (fig 2.8). At day 14 these were tightly packed, uniformed, regular shape and larger in size (≥200µm), although not too large that the core of the spheroid would be necrotic. Day 14 was considered to be optimum for assessing the role that the 3D environment would have on cell surface expression and CSC population.

The DU145 cell line did not easily form spheroids, and represented small clusters of cells that had fewer cell-cell interactions than other cell lines investigated due to these being loosely compact (fig 2.8). Further time point in the DU145 cell line (data not shown) demonstrated that these cells failed to grow larger than clusters observed at day 14 and as a result day 14 was chosen for this cell line.

The LNCAP cell line formed medium sized spheroids (~100µm) by day 7 in alginate and by day 14 these spheroids were tightly compact, dense and oblong shape spheroids. Day 14 was chosen as an optimum time point for the LNCAP cell line, and also due to time points used for the other prostate cancer cell lines (fig 2.8).

The SUM159 cells were highly proliferative and formed large clusters of cells by day 7, however these spheroids did not appear to have strong cell-cell interactions due to the

observed loose cell-cell interactions (not tightly compact and spherical). By day 14 the spheroids had obvious necrosis in the core of the spheroid as determined by Propidium Iodide stain, due to uneven O_2 distribution throughout the spheroid. As many of the cells were dead in the centre of the spheroid by day 14, the day 10 time point was taken for the SUM159 cells (fig 2.9).

The MCF7 cell line formed spheroids at day 7, and continued to proliferate by days 10 and 14. At day 14 these appeared tightly compact, dense and spherical in shape. Day 14 was taken as the optimum time point for assessing the effect that a 3D environment has on cell surface expression and CSC phenotype (fig 2.9).

Figure 2.8. Identification of the optimum time for spheroid formation when prostate cell lines are grown in 3D using alginate.

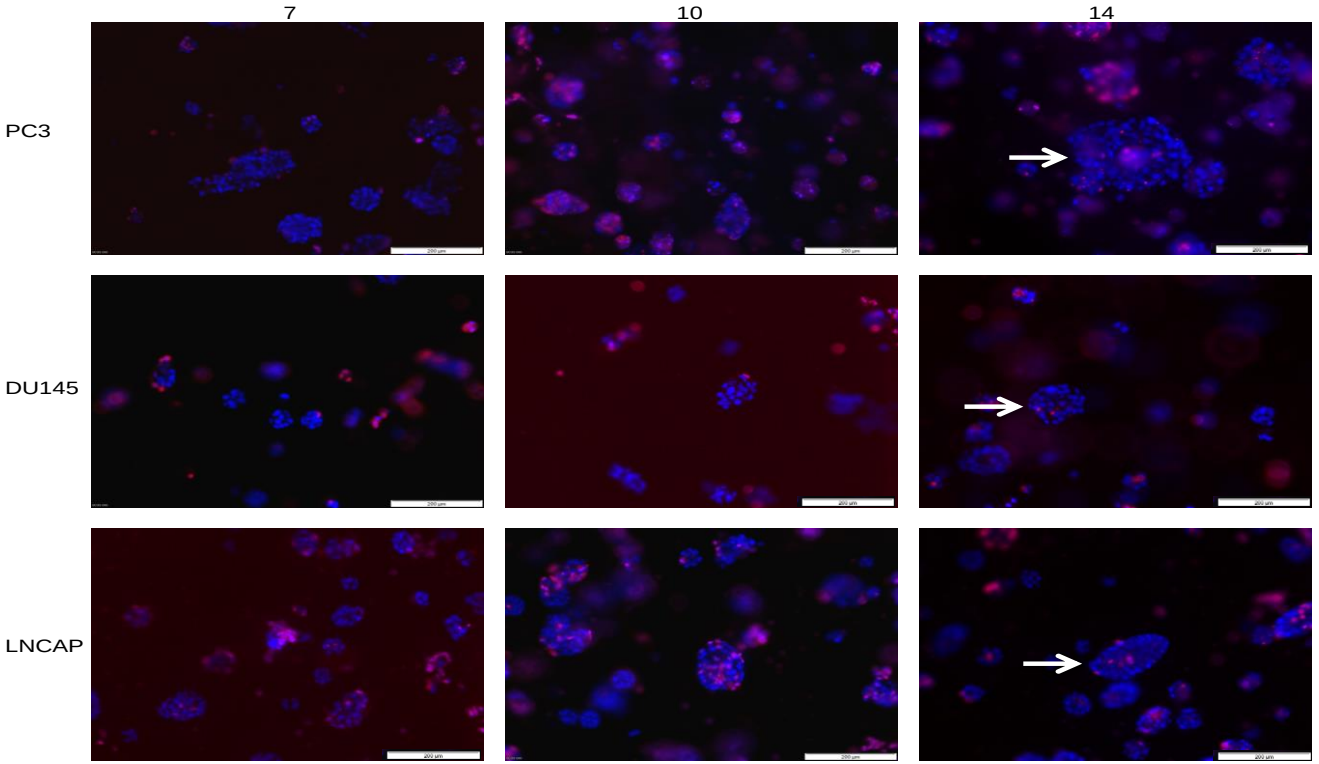

Figure 2.8. Identification of optimum time for spheroid formation when cells are grown in 3D using alginate. Prostate cancer cell lines were cultured for 0-14 days in alginate acid and stained with Hoechst 33342 and Propidium Iodide to asses for the optimum time point for spheroid formation. PC3 cell line readily form spheroids after 7 days as these are tightly compact clusters of cells. By day 14 these spheroids are large, spherical and tightly compact. DU145 failed to form large tightly compact spheroids by day 14. LNCAP cell line formed tightly compact, medium sized, oblong shape spheroids by day 14. All images are representative of 2 independent experiments. Images were captured on the mono-camera using the Olympus IX-81 fluorescent microscope using DAPI and Texas Red filters and scale bar represents 200µm. Arrows point to the optimised size of spheroid.

Figure 2.9. Identification of the optimum time for spheroid formation when breast cancer cell lines are grown in 3D using alginate.

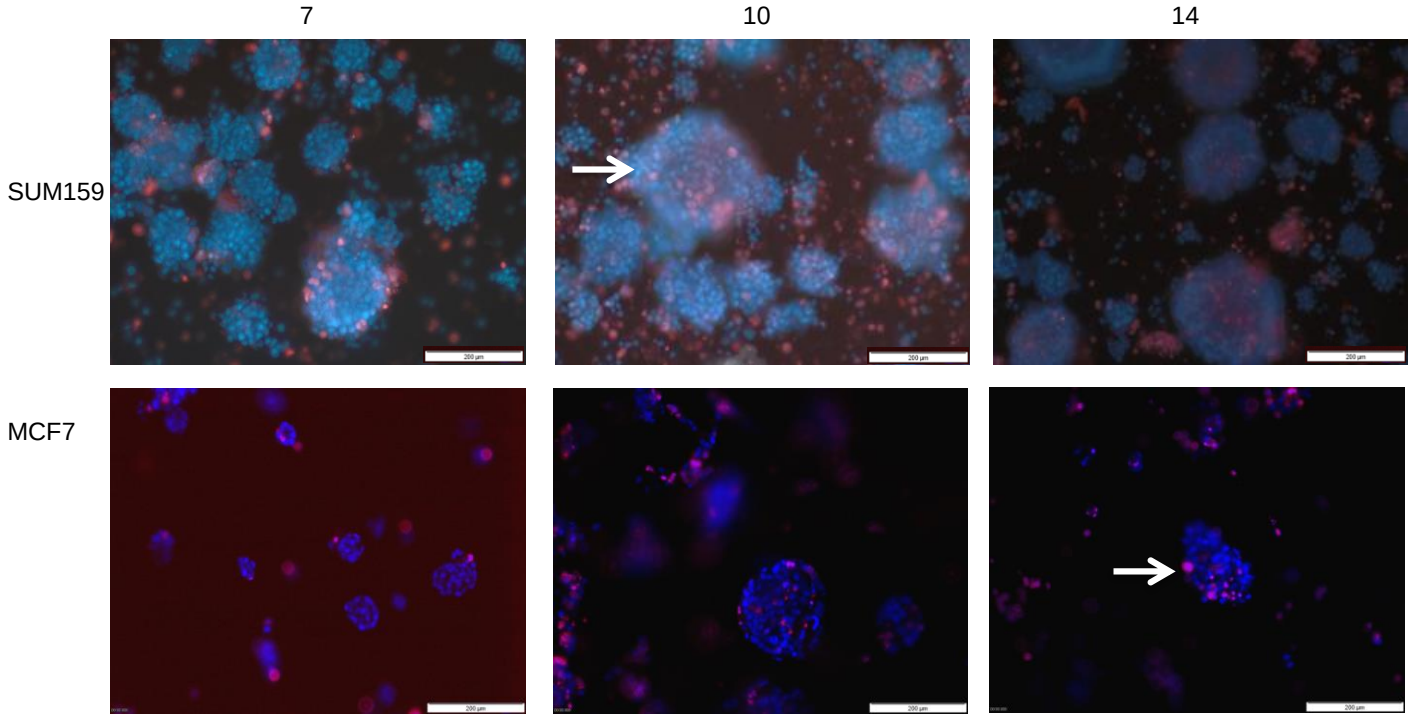

Figure 2.9. Identification of the optimum time for spheroid formation when breast cancer cell lines were cultured in 3D using alginate. Breast cancer cell lines were cultured for 0-14 days in alginate acid and stained with Hoechst 33342 and Propidium Iodide to asses for the optimum time point for spheroid formation. The SUM159 cells were highly proliferative and formed large clusters of cells by day 7 and at day 10 these were tightly compact. At day 14 some necrotic/hypoxic centres were observed. The MCF7 cell line began to form spheroids at day 10 and by day 14 these appeared tightly compact and spherical. All images are representative of 2 independent experiments. SUM159 cell line were imaged using the colour camera using the DAPI and Texas Red filters whereas the MCF7 cell line were captured on a mono-camera using the Olympus IX-81 fluorescent microscope using DAPI and Texas Red filters. Scale bar represents 200µm. Arrows point to the optimised size of spheroid.

2.3.7 Expression of CD133 and CD44 in prostate cancer cell lines cultured in 3D as determined by flow cytometry.

Prostate cell lines were cultured for 14 days in 3D to determine cell surface expression of CD133 and CD44. CD133 was expressed in <2% of PC3, DU145 and LNCAP cell lines cultured in 3D. CD44 was expressed in 15% of PC3 cells and was expressed in 6% and 2% of the DU145 and LNCAP cell populations (fig 2.10). All data was gathered on the FACSCalibur and analysed using BD CellQuest software.

Figure 2.10. Expression of CD133 and CD44 in prostate cancer cell lines cultured in 3D as determined by flow cytometry.

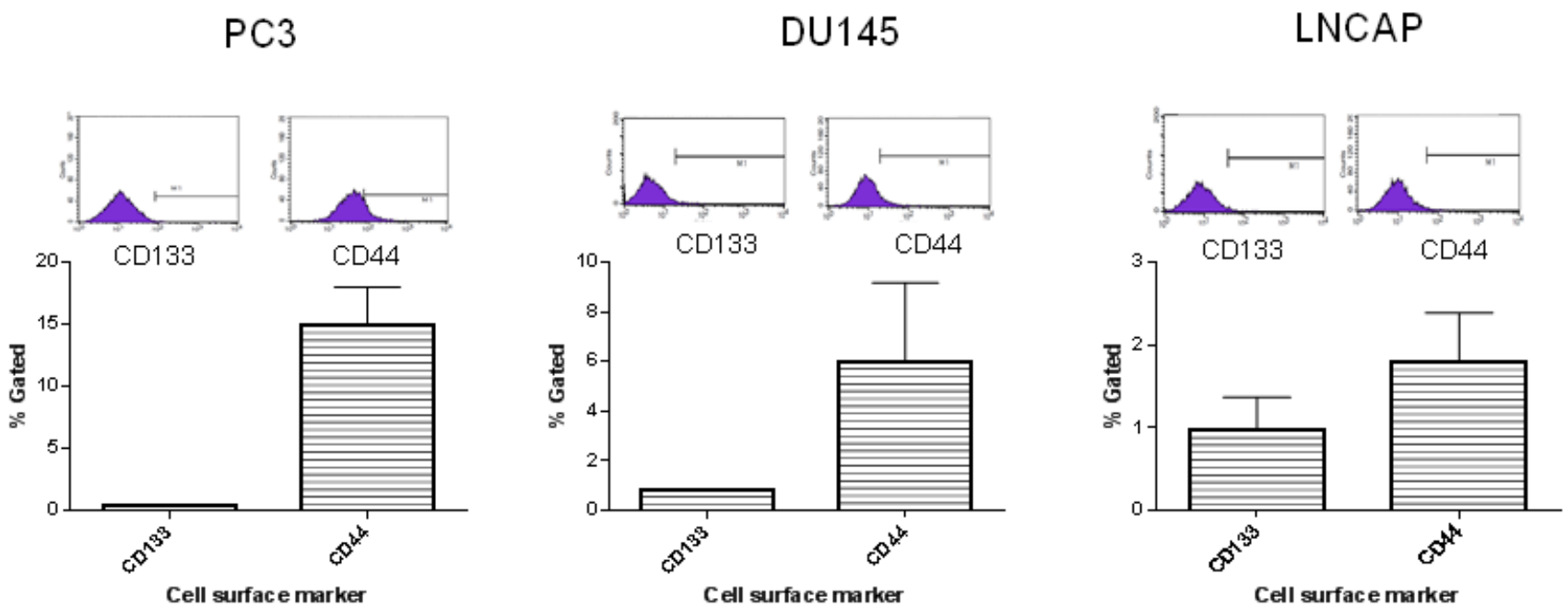

Figure 2.10. Expression of CD133 and CD44 in prostate cancer cell lines cultured in 3D as determined by flow cytometry. Prostate cancer cell lines were cultured for 14 days in 3D and stained to determine if this environment enriched for CD133 and CD44. CD133 expression were very low in all cell lines (<2%). PC3 cell lines appeared to contain approximately 15% of cells that were CD44 positive cells. CD44 expression in the DU145 and LNCAP cell line was 6% and 2% respectively. All graphical data is represented as mean ± SEM and was carried out in three independent experiments. The histogram plots are representative of three independent experiments.

2.3.8 Dual expression of cell surface markers CD133 and CD44 in prostate cancer cell lines cultured in 3D as determined by flow cytometry.

Prostate cancer cell lines were cultured in 3D to determine the effect this environment has on prostate cancer stem cell phenotype $CD133^{+}/CD44^{+}$.

Dual expression of cell surface markers was low in all cell lines. The PC3 cell line had a 0.5% population of $CD133^{+}/CD44^{+}$ cells. The DU145 and LNCAP cell line had similar populations with 0.6% and 0.5% positivity (fig 2.11).

Figure 2.11. Dual expression of cell surface markers CD133 and CD44 in prostate cancer cell lines cultured in 3D as determined by flow cytometry

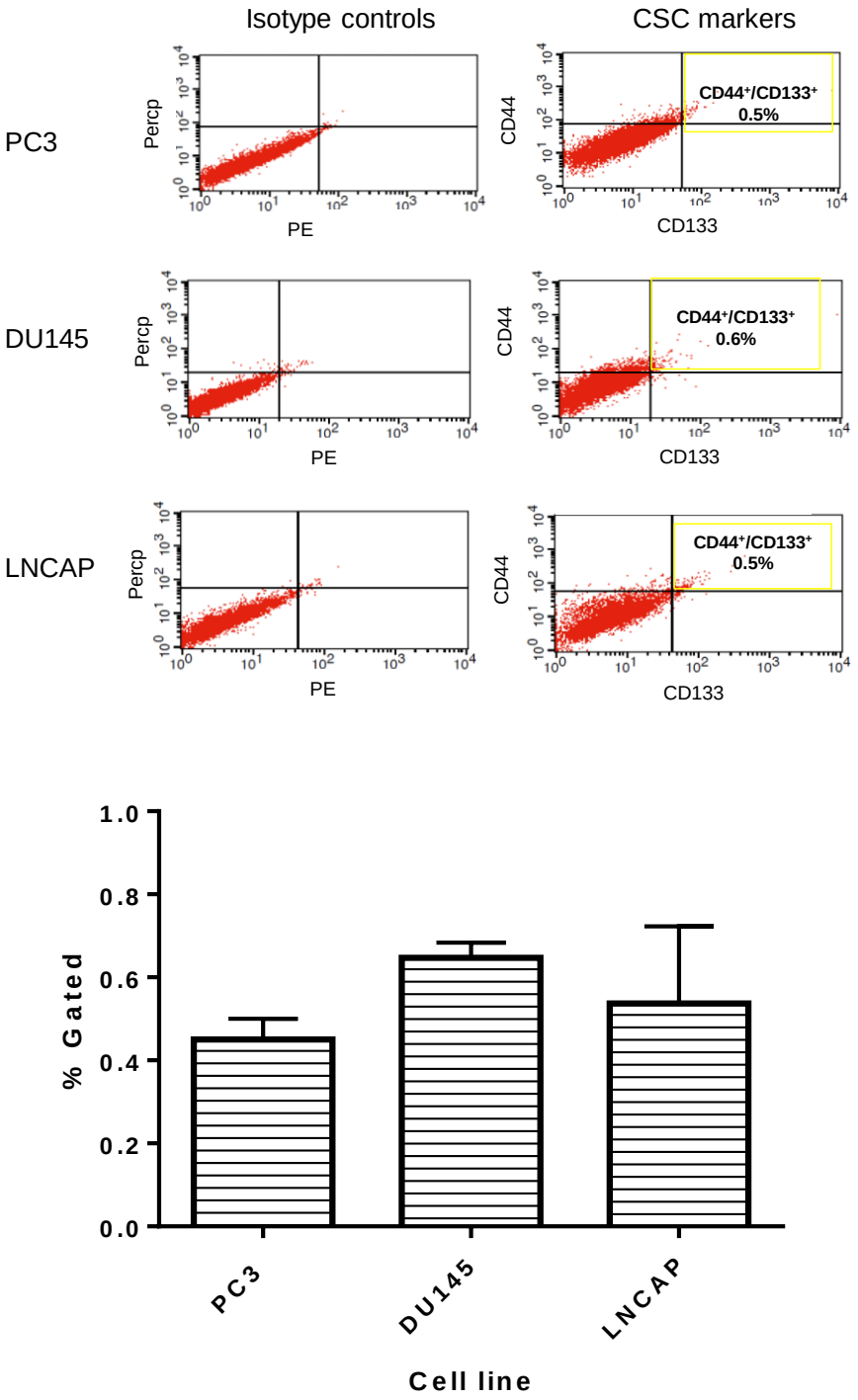

Figure 2.11 Dual expression of cell surface markers CD133 and CD44 in prostate cancer cell lines cultured in 3D. a) Prostate cancer cell lines were cultured in 3D to determine the effect this environment has on prostate cancer stem cell phenotype $CD133^{+}/CD44^{+}$. b) Dual expression of cell surface markers was <1% in all prostate cancer cell lines. All graphical data is represented as mean ± SEM and was carried out in three independent experiments. The dot plots are representative of three independent experiments.

2.3.9 Direct comparison of effects of 2D vs 3D cell culture on cell surface expression of CD133 and CD44 in prostate cancer cell lines.

Cell surface expression of CD133 and CD44 in prostate cancer cell lines cultured in 2D and 3D were directly compared to determine if 3D cell culture does enrich for CSC markers and phenotype as determined by flow cytometry.

CD133 was expressed in ~1% of PC3 cells grown in 2D cell culture, and no significant changes were observed when cells were cultured in 3D. CD44 expression was significantly reduced ($p<0.05$) when culturing in 3D cell culture as a reduction from 96% to 15% was observed (fig 2.12). A reduction of CD44 positive cells was observed when culturing DU145 cells in 3D from 46% to 4%, however this was not significant. There was also a 1% reduction in the CD133 positive DU145 when cultured in 3D although no significance was found. The LNCAP cell line expressed a 1% population of cells that were CD133 and CD44 when cultured in 2D and no significant differences were observed after 14 days of growth in alginate. The prostate CSC phenotype $CD44^{+}/CD133^{+}$ was <2% in all prostate cancer cell lines and was not enriched in PC3, DU145 and LNCAP cell lines as no significant differences between 2D and 3D cell culture was observed.

Figure 2.12. Direct comparison of the expression of CD133 and CD44 cell surface markers and $CD133^{+}/CD44^{+}$ phenotype in prostate cancer cell lines cultured in 2D and 3D cell culture conditions.

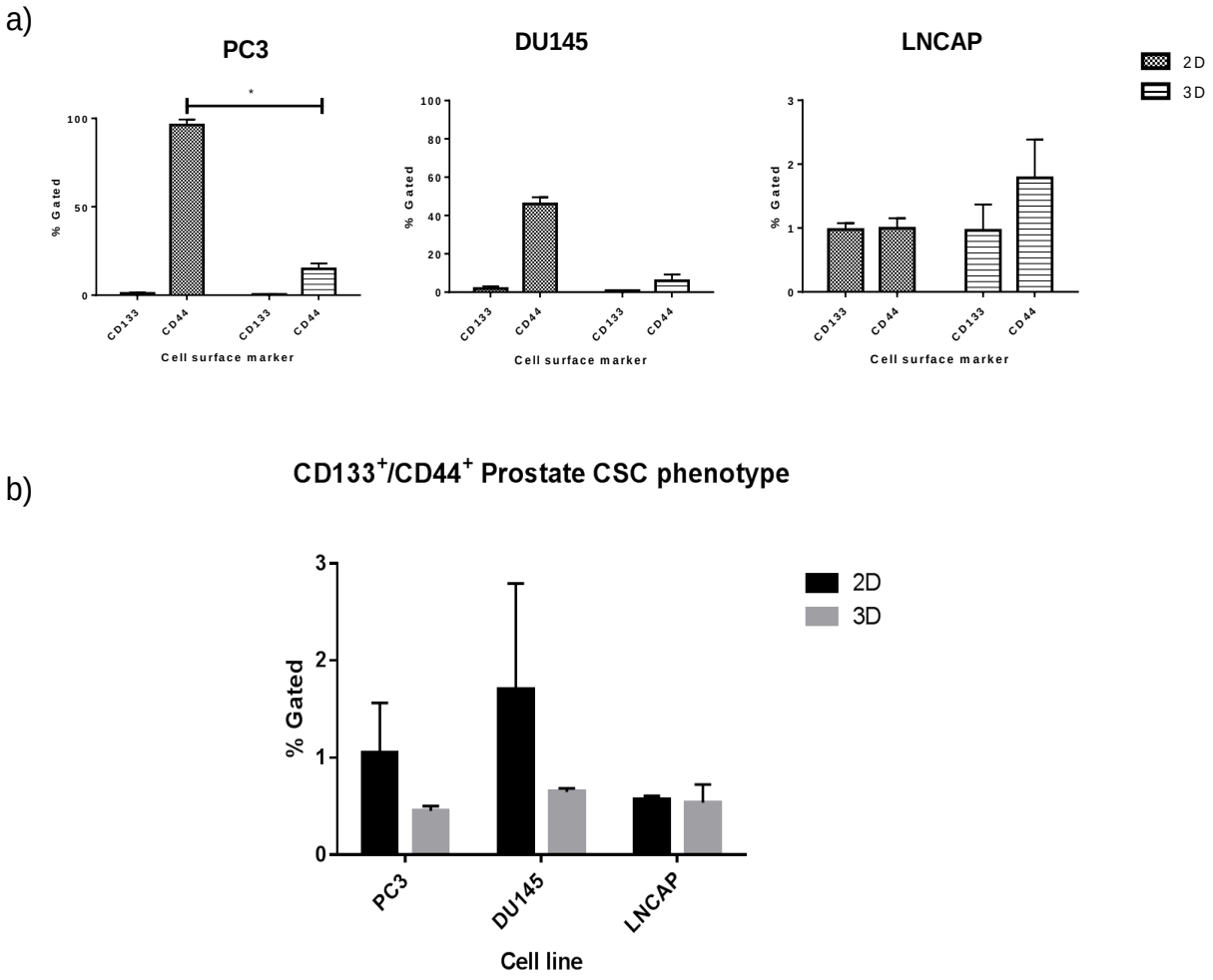

Figure 2.12. Direct comparison of CD133 and CD44 cell surface markers and CD133+/CD44+ phenotype when cells were cultured in 2D and 3D cell culture. All cell lines were seeded in 2D and 3D cell culture prior to harvesting and analysied by flow cytometry. a) A significant reduction in CD44 was observed when PC3 cell lines were cultured in 3D. CD44 was also reduced in DU145 although not significantly. No significant changes in CD44 expression were observed in the LNCAP cell line. No significant changes of CD133 in all cell lines. b) 3D cell culture did not induce the $CD44^{+}/CD133^{+}$ prostate cancer stem cell phenotype. All data is represented as mean ± SEM and was carried out in three independent experiments. Statistical analysis was carried out using nonparametric, Kruskal-Wallis Conover Inman. (<0.05 *).

2.3.10 Expression of CD181, CD44 and CD24 in breast cancer cell lines cultured in 3D as determined by flow cytometry.

Breast cancer cell lines were cultured for 14 days for MCF7 cell line and 10 days for the SUM159 cell line in 3D, to determine cell surface expression of CD44, CD24 and CD181.

CD181, CD44 and CD24 expression was 20%, 18% and 88% respectively when culturing the MCF7 cell line in 3D. The SUM159 cell line has a 44%, 91% and 14% population of CD181, CD44 and CD24 expressing cells (fig 2.13).

Figure 2.13. Expression of CD181, CD44 and CD24 in breast cancer cell lines cultured in 3D as determined by flow cytometry.

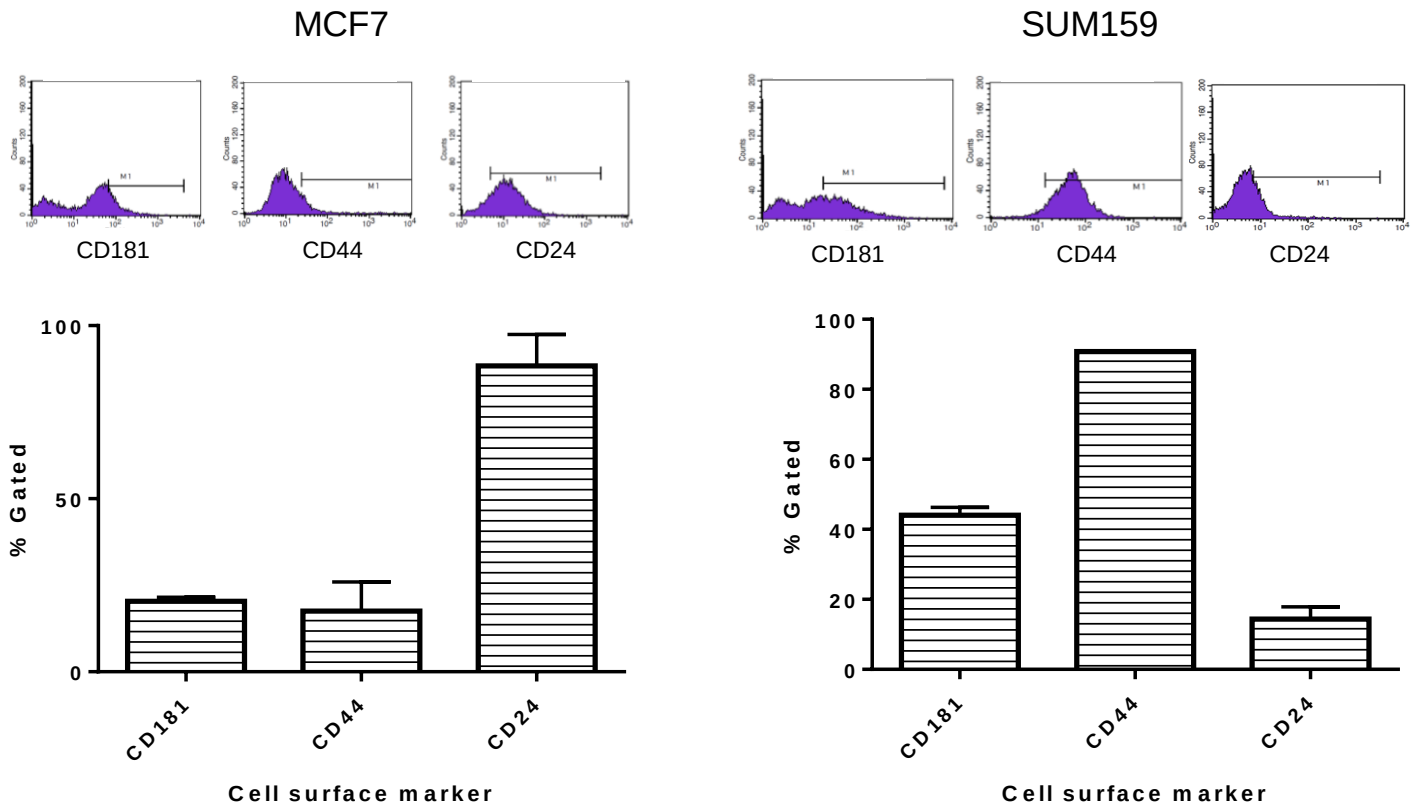

Figure 2.13. Expression of CD181, CD44 and CD24 in breast cancer cell lines cultured in 3D as determined by flow cytometry. MCF7 and SUM159 cell lines were cultured for 14 and 10 days to determine the effects of 3D cell culture on cell surface expression. CD181 was expressed in 20% and 40% of MCF7 and SUM159 cell lines. The MCF7 and SUM159 cell lines had an 18% and 91% population of CD44 expressing cells whereas CD24 was expressed in 88% and 14% of MCF7 and SUM159 cells. Graphical data is represented as mean ± SEM and was carried out in three independent experiments. Histogram plots are representative of 3 independent experiments.

2.3.11 Expression of breast CSC phenotype and 'putative' phenotypes of breast cancer cell lines cultured in 3D cell culture as determined by flow cytometry.

Breast cancer cell lines were cultured in 3D to determine percentage of cells with the $CD44^+/CD24^-$ breast CSC phenotype and $CD181^+/CD44^+$ and $CD181^+/CD24^-$ phenotypes.

The MCF7 cell line has a 1% population of cells with the $CD44^+/CD24^-$ breast CSC phenotype whereas the SUM159 cell line has a 76% cell population (fig 2.14). Expression of phenotypes $CD181^+/CD44^+$ and $CD181^+/CD24^-$ was present in 24% and 20% of MCF7 cells. There was a 42% population with the $CD181^+/CD44^+$ phenotype in the SUM159 cell line and a 36% cell population with the $CD181^+/CD24^-$ phenotype (fig 2.14).

Figure 2.14. Expression of breast CSC phenotype of breast cancer cell lines cultured in 3D.

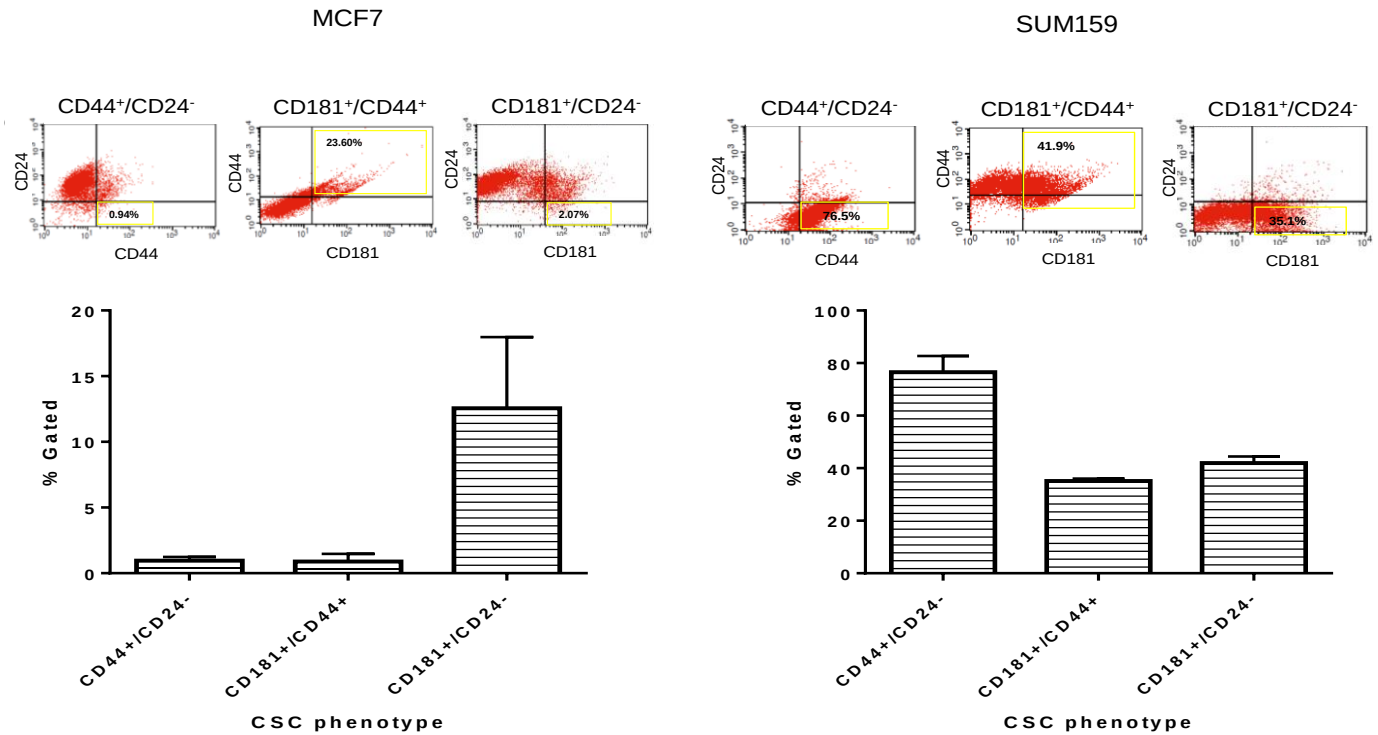

Figure 2.14. Breast CSC phenotype in breast cancer cell lines cultured in 3D. Breast cancer cell lines were cultured in 3D to determine percentage of cells with the $CD44^+/CD24^-$ breast CSC phenotype and $CD181^+/CD44^+$ and $CD181^+/CD24^-$phenotypes. The MCF7 cell line had a 1% cell population with the $CD44^+/CD24^-$ phenotype and 75% of SUM159 cells also had this phenotype. The $CD181^+/CD44^+$ and $CD181^+/CD24^-$ phenotypes were present in 24% and 20% of cells in the MCF7 cell line. The $CD181^+/CD44^+$ and $CD181^+/CD24^-$ phenotypes were present in 42% and 36% of SUM159 cells. Graphical data is represented as mean ± SEM and was carried out in three independent experiments. Histogram plots are representative of 3 independent experiments.

2.3.12 Direct comparison of the effects of 2D and 3D cell culture on cell surface expression of CD181, CD44 and CD24 in breast cancer cell lines and phenotypes.

The MCF7 and SUM159 cell lines were cultured in 2D and 3D, to compare the effect of cell culture environments on cell surface expression of CD44, CD24 and CD181. Also, to investigate if the $CD44^+/CD24^-$ breast cancer stem cell phenotype was enriched in 3D and the $CD44^+/CD181^+$ and $CD181^+/CD24^-$ phenotype as determined by flow cytometry.

3D cell culture enriched for a significant increase in CD181 and CD44 expression in MCF7 cell lines (p *<0.05, **<0.01) however, no significant difference was observed in CD24 expression (fig 2.15). The $CD44^+/CD24^-$ breast CSC phenotype and $CD181^+/CD24^-$ phenotype was significantly induced (p*<0.05) in the MCF7 cell line cultured in 3D. No significant changes in the $CD44^+/CD181^+$ phenotype were found when culturing in 3D.

3D cell culture enriched for a significant increase in CD181 (p<0.005) and a significant reduction in $CD44^+$ (P<0.05) and $CD24^+$ (P<0.005) in the SUM159 cell line. The breast CSC phenotype $CD44^+/CD24^-$ was significantly induced in the SUM159 cell lines (P<0.005). The $CD44^+/CD181^+$ and $CD181^+/CD24^-$ phenotypes were also induced in the SUM159 cell line cultured in 3D (p<0.005). Statistical analysis was carried out using nonparametric, Kruskal-Wallis test with Conover Inman post-hoc test.

Figure 2.15. Direct comparison of the effects of 2D and 3D cell culture on cell surface expression of CD181, CD44 and CD24 in breast cancer cell lines and phenotypes.

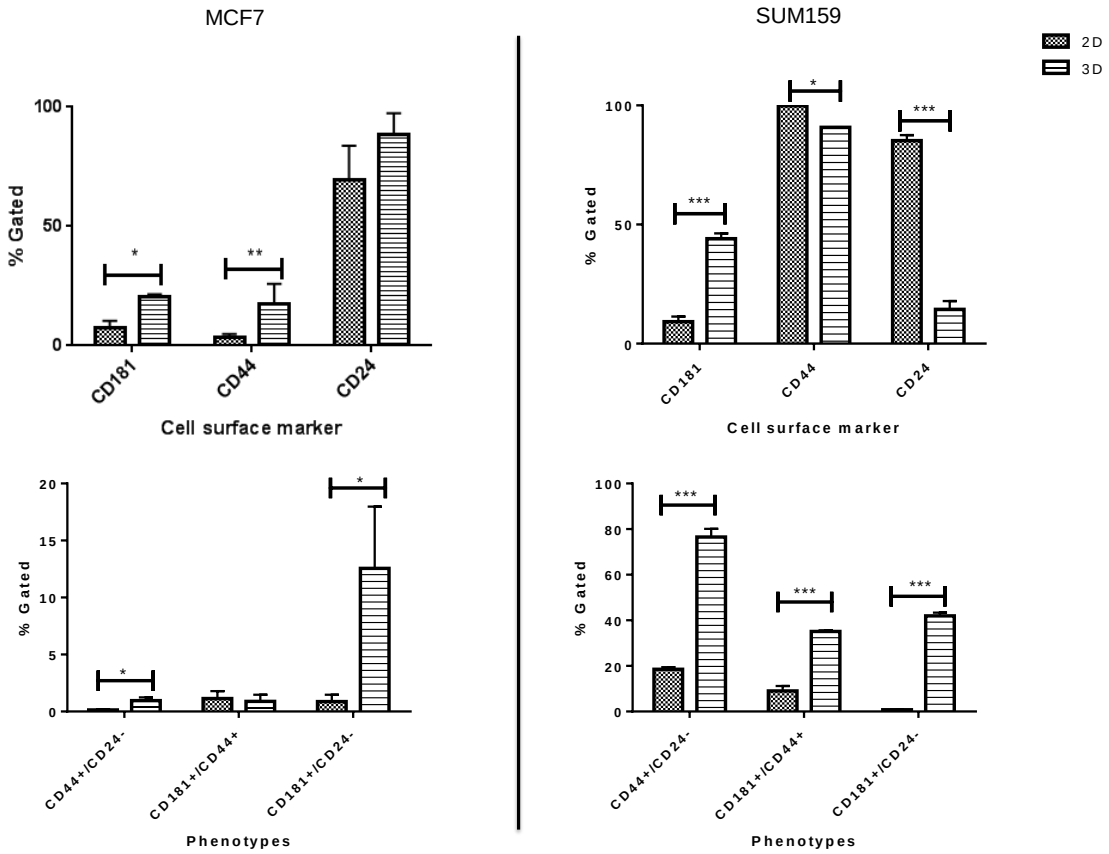

Figure 2.15. Comparison of 2D and 3D cell culture on cell surface expression and phenotype. MCF7 and SUM159 cell lines were cultured in 2D and 3D cell culture to compare the effect of cell culture environments on cell surface expression. The population of cells expressing CD181 and CD44 were significantly induced in MCF7 cell lines cultured in 3D. $CD181^+$ cells were significantly enriched in the SUM159 cell line cultured in 3D whereas a significant reduction in the $CD44^+$ and $CD24^+$ cells was observed. 3D cell culture did enrich for MCF7 and SUM159 cells with the $CD44^{+/}CD24^-$ and $CD181^+/CD24^-$ phenotype and $CD44^+/CD181^+$ population of cells was increased in the SUM159 cell line cultured in 3D. Graphical data is represented as mean ± SEM and was carried out in three independent experiments. Statistical analysis was carried out using nonparametric, Kruskal-Wallis test with Conover-Inman post-hoc test. (<0.05 *, <0.01 ** and < 0.001 ***).

2.4 Discusion

2.4.1 Optimisation of 3D cell culture model using alginate

PC3, DU145, LNCAP and MCF7 cell lines were cultured in alginate as a 3D cell culture model and harvested at day 14 based on their 3D morphology. The SUM159 cell line was selected at day 10 of growth in 3D. The PC3 cell line increased in size from days 7-14 consistent with previous reports (Windus et al. 2012, Fan et al. 2012b). The PC3 cell line had a fairly compact and spherical morphology with no obvious signs of necrosis up to day 14, consistent with previous reports (Fan et al. 2012b, Sheng et al. 2013, Wang et al. 2013a) however, Windus et al, (2012) observed PC3 cell line to be irregular in shape with invasive/stellate radiating tubular processes when cultured in matrigel (Windus et al. 2012). In addition Windus et al, (2012) found that E-cadherin was down-regulated at day 9 and there was an increase in N-cadherin, Vimentin, β1 integrin and chemokine receptor CXCR4 expression indicating a metastatic phenotype (Windus et al. 2012).

The DU145 cell line formed very small clusters that had little cell to cell attachments, and did not appear to form larger spheroids even after 14 days (data not shown) consistent with Chambers et al (2014) (Chambers et al. 2014). Day 14 was chosen due to consistency with the other prostate cancer cell lines and a similar study by Wang et al (2013) in which spheroids were cultured for 14 days in serum free medium (SFM) (Wang et al. 2013a). Wang et al (2013) found that the DU145 cell line formed compact spherical spheroids at day 14 that had an increased population of cells with the $CD44^{+}/CD133^{+}$ phenotype (Wang et al. 2013a). The LNCAP cell line formed spheroids by day 10, consistent with previous reports culturing LNCAP cell line in SFM (Wang et al. 2013b) and by day 14 these were tightly compact and some were oblong shaped consistent with Chambers et al (2014).

The MCF7 cell line formed cluster-like spheroids from day 7, consistent with previous reports in which the MCF7 cell line was cultured in SFM for 7 days (Calvet, Andre and Mir 2014, Manuel Iglesias et al. 2013) and continued to grow by day 10 and 14. Boo et al, (2016) found that culturing MCF7 cells using SFM stimulated adherence of neighbouring cells to form tight juctions, and micropores were present in the interior of the spheroids for nutrient and gas distribution (Boo et al. 2016). The SUM159 cell line was harvested at day 10 as these were largeer than 200µm, compact and spherical. By day 14 the core of the spheroid was probably hypoxic due to the presence of necrotic cells within the core.

2.4.2 Expression of CD44 and CD133 in prostate cancer cell lines

CD44 expression was found to be highly expressed in PC3 and DU145 cell lines and no/low expression in the LNCAP cell line corroborating earlier findings (Wang et al. 2013a) and Verkaik et al, 1999 found CD44 expression is inhibited in the LNCAP cell line due to hypermethylation of the CD44 promoter (Verkaik et al. 1999). Mcfarlane et al (2004) also confirmed CD44 expression in the PC3 cell line but found that DU145 cells were $CD44^{-ve}$ (Draffin et al. 2004). This may be due to the lack of specificity of the antibody for all variants of the CD44 protein. Surprisingly, CD44 expression was significantly reduced when culturing the PC3 cell line in 3D and no significant differences were observed in the DU145 cell line. Primary prostate tumours have been found to have 0.1-0.3% of cells that express CD133, data generated from 40 different samples (Collins et al. 2005) whereas prostate cell lines PC3 and DU145 contain a 1-2% population of CD133 expressing cells. It has been previously found that Androgen receptor positive cells such as LNCAP cells do not express the CD133 cell surface marker (Collins et al. 2005). CD133 expression was not enriched in any of the prostate cell lines when cultured in 3D, contradicting previous reports by Portillo-Lara

et al 2015 in which CD133 was upregulated when cells were cultured as spheroids using a scaffold free system of SFM and ultra-low attachment plates (Portillo-Lara and Alvarez 2015).

2.4.3 Expression of $CD44^+/CD133^+$ prostate cancer phenotype

Expression of the $CD44^+/CD133^+$ phenotype when culturing PC3 cell line in 2D represented a 1% cell population corroborating earlier investigations (Fan et al. 2012b, Rao et al. 2014, Sheng et al. 2013) although Wang et al, (2013) were unable to identify any PC3 cells with this phenotype (Wang et al. 2013a). 3D cell culture did not induce a stem cell phenotype after 14 days growth in alginate. Fan et al, (2012) found that culturing PC3 cells in 3D using SFM and ultra-low attachment plates enriched for a CSC phenotype as an 18 fold increase in cells with the $CD44^+/CD133^+$ phenotype (Fan et al. 2012b). In addition Sheng et al (2013) and Wang et al (2013) also observed an increase in the $CD44^+/CD133^+$ population in the PC3 cell line when culturing in SFM (Sheng et al. 2013, Wang et al. 2013a). Rao et al (2014) found that culturing PC3 cell lines in alginate for 10 days did enrich for the $CD44^+/CD133^+$ phenotype, however these cells demonstrated phenotypic plasticity between 2, 6 and 10 days with the highest proportion of $CD44^+/CD133^+$ at day 2 implying that 3D cell culture for 14 days may be too long as cell surface expression may be diminished (Rao et al. 2014). The $CD44^+/CD133^+$ population represented <2% of the DU145 cell population cultured in 2D, corroborating earlier reports (Wang et al. 2013a) although Oktem et al (2013), previously found that these cells have ~10% cell population with this phenotype when culturing as monolayers (Oktem et al. 2013). Similarly to the PC3 cells cultured in 3D, the $CD44^+/CD133^+$ population was not enriched in the DU145 cell line. A previous study had found that 3D cell culture using SFM did enrich for the $CD44^+/CD133^+$ population in the DU145 cell line. Additionally, culturing only the $CD44^+/CD133^+$ CSC

population as spheroids and in monolayers induced expression of embryonic and mesenchymal lineage gene expression and stem cell related markers such as Sox2 and Oct4 although 3D cell culture was more effective (Oktem et al. 2013). The LNCAP cell line had little/no dual expression of CD44 and CD133 corroborating earlier investigations (Wang et al. 2013a)

2.4.4 Expression of CD44, CD24 and CD181 in breast cancer cell lines

CD44 expression was found to be highly expressed in the SUM159 cells and low expression was found in the MCF7 cell line, consistent with previously published data (Smith and Cai 2012). CD44 expression was significantly induced in the MCF7 cells when cultured in 3D, consistent with Chen et al, (2012) (Chen et al. 2012) and reduced in the SUM159 cell line (100-91%). MCF7 cell line are a luminal cell type and contains a high percentage of cells expressing CD24 when cultured in 2D, consistent with previously published data (Fillmore and Kuperwasser 2007) however the basal cells SUM159 also contain a high population of cells with this phenotype contradicting previous report by Filmore et al 2008 (Fillmore and Kuperwasser 2008). Expression of CD181 in the SUM159 cell line cultured in 2D corrobarates earlier findings by Ginestier et al, 2010 (Ginestier et al. 2010). A significant upregulation of cells expressing CD181 was observed after 3D cell culture, consistent with a previous report in which CD181 receptor was upregulated in a 3D co-culture system (Infanger et al. 2013). CD181 was expressed in the MCF7 cell line grown in 2D confirming previuos data by Pang et al, (2015) (Pang et al. 2015) and was significantly upregulated when cells where cultured in 3D.

2.4.5 Expression of $CD44^+/CD24^-$, $CD44^+/CD181^+$, $CD181^+/CD24^-$ phenotype in breast cancer cell lines

The MCF7 and SUM159 cell lines contain a population of cells with the $CD44^+/CD24^-$ breast CSC phenotype as previously demonstrated by Meyer et al, (2009) (Meyer et al. 2009). Calvet et al (2014) identified that 50% of MCF7 cells cultured in 2D had the $CD44^+/CD24^-$ breast CSC phenotype, and culturing cells in 3D using SFM surprisingly reduced the CSC population, although these cells were cultured for 10 days (Calvet, Andre and Mir 2014). The MCF7 and SUM159 cell lines cultured in 3D enriched for cells with the $CD44^+/CD24^-$ phenotype. Similarly, Chen et al (2012), demonstrated that culturing MCF7 cells in 3D induced a $CD44^+/CD24^-$ phenotype and these cells where more tumourigenic and formed larger tumours in xenograft models (Chen et al. 2012). In addition Boo et al, (2016) found that 3D cell culture of the MCF7 cell line enriched for cells with $CD44^+/CD24^-$ phenotype and these also had an increase in ALDH expression (Boo et al. 2016). As both breast cancer cell lines are enriched for this phenotype in 3D cell culture, future work identifying the CSC population, investigating the role of CSC related genes, drug discovery and responses would be more applicable to cells grown in 3D.

Both MCF7 and SUM159 have a small population of cells with the $CD44^+/CD181^+$ phenotype when grown in 2D and was significantly upregulated in the 3D cell culture model. As CD44 and CD181 expression is associated with a poorer prognosis, their co-expression induction could potentially be a breast CSC marker. Alternatively the $CD181^+/CD24^-$ phenotype was also significantly induced in SUM159 cultured in 3D and although no current literature implies this as a breast CSC marker, further investigation would be needed to elucidate the role it plays.

2.4.6 Concluding remarks

The majority of models used to enrich for the CSC population have used scaffold-free systems in which cells were cultured using SFM in ultra-low attachment plates. The data obtained from these particular studies appeared to enrich for the CSC population of cells with the $CD44^+/\alpha_2\beta_1^{hi}/CD133^+$ or $CD44^+/CD133^+$ prostate cancer stem cell phenotype. Using alginate for culturing PC3, DU145 and LNCAP cells does not appear to enrich for cells with the $CD44^+/CD133^+$ phenotype, even though these cells form characteristic stem cell morphologies *in vitro*. This may be due to the time point chosen for phenotyping these cells grown in alginate as an earlier or possibly later time point may have been applicable for these cell types. Also the alginate concentration may not be representative of the ECM environment and mechanical forces that would be present *in vivo*. However it has been demonstrated for the first time that using alginate as a 3D cell culture tool does enrich for the breast CSC population as a model for breast cancer. The MCF7 and SUM159 cell lines re-express, or upregulate the proportion of cells expressing the $CD44^+/CD24^-$ breast CSC phenotype and CD181 expression alone, or incombination with other markers was also upregulated, indicating a more aggressive, stem like population. To reiterate, 3D cell culture using alginate at the the allocated time points does induce a stem cell phenotype in breast cancer cell lines and subsequent experimental design identifying CSC population and CSC related genes would be based upon this model.

3 Assessment of a Nanog-driven GFP reporter as a marker of CSC

3.1 Introduction

Enriching and inducing a cancer stem cell phenotype *in vitro* can be achieved using various culture conditions such as chemotherapy treatment (Hamilton 2013), hypoxia (Liang et al. 2012) and 3D cell culture (Xu et al. 2014). 3D cell culture can propagate the most primitive of cell types within a heterogeneous population as shown in chapter 3 as an increase in cells with the $CD44^{+}/CD24^{-}$ breast CSC phenotype was found. 3D cell culture using ultra-low attachment plates and cancer stem cell medium has also been used to enrich for the CSC phenotype (Wang et al. 2014a) and enrichment of the CSC population may be partly due to the dispersed O_2 in the centre of the spheroids resulting in a hypoxic environment (Mueller-Klieser, Freyer and Sutherland 1986, Khaitan et al. 2006). Hypoxia has been found to induce a breast CSC phenotype primarily due to the activity of hypoxia inducing factors (HIFs), predominantly hypoxia-inducible factor 1α (HIF-1α) and confers increased invasive and metastatic activity (Conley et al. 2012, Schwab et al. 2012, Chaturvedi et al. 2013a). In normoxia, HIF-1α is hydroxylated, ubiquitinated and degraded by the proteasome, however in hypoxic conditions hydroxylation is inhibited thus allowing activation and dimerization of HIF-1α with constitutively expressed HIF-1ß subunit for the transcriptional activation of target genes (Xiang et al. 2014). In cancer one of the genes that HIF-1α regulates is an embryonic stem cell marker called Nanog (Mathieu et al. 2011).

3.1.1 The embryonic Nanog gene (Nanog) and its retrogene NanogP8

The Nanog gene has been mapped to locus 12p13.31, and in addition, there are 10 nanog pseudogenes, and 1 evolutionary evolved retrogene known as NanogP8 which is located at chromosome 15q14 (Booth and Holland 2004). The Nanog gene is composed of a 5' and 3' UTR, 4 exon sequences and 3 intron sequences that are spliced out during transcription whereas the NanogP8 locus contains only the protein

coding region. Nanog and NanogP8 mRNA share a 99% degree of similarity and only differ by 6 nucleotide substitutions (Booth and Holland 2004), translated to proteins with only 3 amino acid differences (Ambady et al. 2010).

Due to the similarities between these genes, it is likely that they have many similar functions as transgenic mice expressing low levels of NanogP8 protein are normal except for cataract formation. Alternatively high expression of NanogP8 is detrimental, causing developmental abnormalities with many organs (Badeaux et al. 2013) and it is likely that high expression of Nanog would induce similar effects.

3.1.2 Structure and function of Nanog protein

Nanog protein is around 34kDa (Zhang et al. 2005) and its structure is made up of 3 subdomains consisting of the N-terminal which binds to the minor groove of DNA, the homeodomain (residues 96-155) which binds to the major groove of DNA and the C-terminal which contains two transcriptional activator domain ranging from 155-240 and 241-305 (Ambady et al. 2010) and 5 Tryptophan repeats (WXXXX) (ranging from residues 198-243) which facilitates homo and heterodimerization (Wang, Levasseur and Orkin 2008, Mullin et al. 2008). There are six amino acids in the homeodomain (136YKQVKT141) that allow nuclear localization of human Nanog, and within the tryptophan rich region there is a CRM1-indepenent signal for nuclear export which suggest cellular shuttling between compartments within the cell (Chang et al. 2009). Activation of Nanog occurs by dimerization, resulting in the transcriptional activation of downstream targets, although monomeric Nanog can bind to DNA, it is suggested that it has little/no effect on transcription and maintaining pluripotency (Wang, Levasseur and Orkin 2008). Nanog induces the transcription of downstream targets by binding to the consensus sequences: 5’-TAAT(TG)(TG)-3’ or 5’-

(CG)(GA)(CG)C(GC)ATTAN(GC)-3' (Ho et al. 2012). Although Nanog and NanogP8 share a 99% identity the difference in 3 amino acids may affect many aspects of protein function such as activity, dimerization, post translational modifications and transcription.

3.1.3 Role of Nanog role in CSC

Nanog positive cancer cells can divide both asymmetrically and symmetrically to form a heterogeneous cell population (Jeter et al. 2011a, Gong et al. 2012, Wang et al. 2012b, Wang et al. 2014a, Shan et al. 2012). Nanog expression has been detected in most solid and haematological cancers including acute myeloid leukaemia, glioblastoma, breast, prostate and hepatocellular carcinoma (Lipscomb et al. 2007, Hwang, et al. 2013, Lombaerts et al. 2006, Cao et al. 2008, Kong et al. 2010, Xie et al. 2010, Zhou et al. 2011, Shan et al. 2012, Sun et al. 2013a), and in colorectal cancer, human endometrial adenocarcinoma, gastric adenocarcinoma and lung adenocarcinoma, Nanog participates in tumour progression and oncogenesis (Meng et al. 2010, Chiou et al. 2010, Lin, Ding and Li 2012, Zhou et al. 2011). In human endometrial adenocarcinoma Nanog is expressed but not in the benign endometrium (Zhou et al. 2011). In prostate cell lines (Jeter et al. 2011a, Gong et al. 2012) Nanog-expressing cells preferentially form spheroids (Dontu et al. 2003). In prostate cell lines and tumours the CSC population is variable between 0.1%- 2% respectively (Collins et al. 2005, Gong et al. 2012), and Nanog expression is much higher in the CSC population than the bulk of the cells (non-CSC) (Gong et al. 2012). Using siRNA to knockdown Nanog, clonogenic growth and tumourigenicity is significantly reduced in prostate, breast and colon cancer cell lines (Jeter et al. 2009, Han et al. 2012) and in head and neck cancer tissues (Yu et al. 2011). Over-expression of Nanog in MCF7 cells induces resistance to chemotherapy agents by the up-regulation of genes required for cell

survival and detoxification such as Bcl-2, ABCG2, CD133, and ALDH1A1 (Jeter et al. 2011a). NanogP8 has been found to induce cell proliferation (Zhang et al. 2006) and facilitates cell proliferation in gastrointestinal carcinoma (Uchino et al. 2012). In prostate cancer cell lines and gastrointestinal cancer cells, primary tumours and xenograft models, Nanog derived from the NanogP8 locus is most predominantly transcribed (Jeter et al. 2009, Jeter et al. 2011a, Uchino et al. 2012) however in HepG2, MCF-7, colon cancer cell lines, breast, urinary bladder and gastric cancer tissue, Nanog transcripts are derived from both the Nanog and NanogP8 locus (Ishiguro et al. 2012, Zhang et al. 2006). In transgenic mice NanogP8 is biologically functional in development and does not induce spontaneous tumour formation when highly expressed, but had the opposite effect of inhibiting tumourigenesis by depleting stem cell and stem related genes (Badeaux et al. 2013).

3.1.4 Study of Nanog responses using reporter cell lines

Nanog or NanogP8 expression can be investigated *in vitro* by the use of reporter cell lines. Reporter cell lines have been used for many years to investigate the signal transduction pathway, by monitoring the activation of a reporter gene such as luciferase or Green Fluorescent Protein (GFP). In a reporter vector there is a transcription response element (TRE) upstream from the reporter gene, and if a transcription factor such as Nanog binds to the TRE the cells fluoresce or luminesce. Commonly used plasmid based reporter vectors can be delivered into the nucleus of the cell for transient transfection and occasionally stable transfection, but have limitations in regards to transfection efficiency in difficult to transfect cells. Lentiviral expression vectors packaged into pseudoviral particles have a higher transduction efficiency and unlike retroviral systems do not require the cells to be dividing.

Figure 3.1. Nanog Response element Reporter Vector adapted from Systems Biosciences (SBI 2016). The pluripotency response reporters contains 5' and 3' long terminal repeats (LTR) that are located either side of the genes of interest (GOI). The LTR are integrated into the genome of the host cell at LTR or retrotransposon elements, incorporating the Nanog response element (NRE) upstream from reporters. The NRE contains 4 repeated units of ACCCTTCGCCGATTAAGTACTTAAG and is incorporated at the multiple cloning site of the vector that is directly upstream of the minimal cytomegalovirus promoter (mCMV). The mCMV contains binding sites for general transcription factors and RNA polymerase. Downstream from the mCMV is the copepod GFP (copGFP) and Luciferase reporters. Although not shown on the diagram copGFP has been destabilised and tagged for destruction by the proteasome. The T2A peptide is a self-cleaving peptide. The Woodchuck Post-transcriptional Regulatory Element (WPRE) forms a tertiary structure to enhance gene expression.

3.1.5 Proteasome activity as a marker of CSC

Reporter cell lines have been used to identify cells with low 26S proteasome activity as a marker for CSC as cells that are transfected with a plasmid containing the sequence for carboxyl terminus of the murine ornithine decarboxylase (which directs the starting place of degradation) fused to GFP reporter, an increase in Green fluorescent cells identifies cells with low proteasome activity (Pan et al. 2010, Lagadec et al. 2014, Munakata et al. 2016). Cells that have low proteasome activity are more tumorigenic and are resistant to irradiation in head and neck squamous cell carcinoma and patients

with higher proteasome subunit expression lived longer than their counterparts (Lagadec et al. 2014). Lung cancer cell lines cultured in 3D cell culture as spheroids were enriched for cells with decreased 26S proteasome activity reinforcing this CSC phenotype (Pan et al. 2010). In colorectal cancer cell lines, low proteasome activity correlated with increased spheroid formation, increased radio-resistance, chemo-resistance and tumourigenicity (Munakata et al. 2016). Breast cancer cell lines have also been found to have a CSC population that is enriched for cells with low proteasome activity (Vlashi et al. 2013).

3.1.6 Study Aims, Objectives and Hypothesis

The study aim was to assess the role of Nanog and/or NanogP8 using a lentivirus transduced breast cancer cell line, and to identify Nanog/NanogP8 expression in breast and prostate cancer cell lines.

Hypothesis

Nanog-GFP reporters select for CSC-like phenotype in breast and prostate cancer cells and 3D cell culture selects for Nanog-positive cells.

The specific objectives of this study were:

To develop and characterise a lentivirus transduced Nanog-GFP reported cell line in the SUM159 breast cancer.

To determine whether 3D cell culture selects for $CD44^{+ve}$, $CD181^{+ve}$, $CD24^{-ve}$ and Nanog+ve cells cultured in 2D and 3D using a Nanog-GFP reporter assay.

To identify whether Nanog and/or nanogP8 is responsible for Nanog-driven-GFP in these CSC-like cells.

To validate whether observed Nanog-driven GFP in reporter cells reliably correlates with Nanog expression.

To identify Nanog expression in breast and prostate cancer cell lines and determine if the cells express Nanog or NanogP8 protein.

3.2 Methods

3.2.1 Reagents:

3.2.1.1 Cancer stem cell medium

DMEM/F-12 phenol red free (Thermo Fisher Scientific),

1:50 B-27 Supplement (50X), serum free (Thermo Fisher Scientific)

4µg/ml Insulin human recombinant zinc solution (Thermo Fisher Scientific)

0.4% Bovine Serum Albumin (Sigma Aldrich)

20ng/ml Epidermal Growth Factor (EGF) (Peprotech).

100ml of cancer stem cell medium was made up and filter sterilised.

3.2.1.2 Bortezomib

A 100mM stock solution was made by dissolving 38.4mg bortezomib (Selleckchem, Suffolk) in 1ml PBS and stored at -20°C. This was further diluted by serial dilution prior to stimulation of cells.

3.2.1.3 Cell lysis buffer

1ml CelLytic M (Sigma Aldrich) was added to 10µl Protease Inhibitor Cocktail (Sigma Aldrich).

3.2.1.4 10% Sodium dodecyl sulfate polyacrylamide resolving gel

9ml deionised H_2O

3ml 2M Tris (Sigma Aldrich) pH 8.8

3ml Acrylamide/bis-acrylamide, 40% solution (Sigma Aldrich)

10% Ammonium persulphate (Sigma Aldrich)

20µl N,N,N',N'-Tetramethylethylenediamine (Sigma Aldrich)

10% SDS Solution (Thermo Fisher Scientific)

3.2.1.5 Sodium dodecyl sulfate polyacrylamide stacking gel

3.6ml H_2O

0.7ml Tris pH 6.8

50µL 10% SDS solution

0.6 ml Acrylamide/bis-acrylamide, 40% solution

25µl 10% Ammonium persulphate

10µl N,N,N',N'-Tetramethylethylenediamine.

Each layer of the gel was allowed to stand at room temperature until set.

3.2.1.6 1× SDS running buffer

1× SDS running buffer was made up by adding 3g Tris, 14.4g Glycine (Sigma-Aldrich) and 1g SDS (Sigma-Aldrich) to 1L dH_2O.

3.2.1.7 1× Transfer buffer

1× Transfer buffer was made up using 3g Tris (25mM), 12.2g Glycine (190mM) in 900ml dH_2O and incubated at 4°C until chilled. 100ml Methanol was added directly before use.

3.2.1.8 1×Tris buffered Saline (TBS)

2.42g Tris (20mM) and 8.76g $NaCl_2$ (150mM) was added to 1L dH_2O.

3.2.1.9 1×Tris buffered Saline with Tween (TBST)

1L of TBS was added to 0.5ml Tween 20 (Sigma-Aldrich)

3.2.1.10 Blocking solution

5g Blotting-Grade Blocker (Sigma Aldrich) was added to 100ml TBST and inverted until all blotting grade blocker had dissolved.

3.2.1.11 Coomasie Stain

Coomasie stain was made up using 0.1g Brilliant blue r-250 (Sigma-Aldrich), 60ml dH_2O, 30ml Methanol and 10ml glacial acetic acid.

3.2.1.12 Coomasie destain buffer

Coomasie destain buffer was made up with 50ml dH_2O, 40ml Methanol and 10ml Glacial acetic acid.

3.2.1.13 Gel fixing solution

Gel fixing solution was made up using 50ml Ethanol (Sigma Aldrich), 10ml Acetic acid glacial and 40% dH_2O

3.2.1.14 Protein solubulisation buffer

256µl ZOOM 2D Protein solubilizer 1 (Thermo-Fischer Scientific)

2.10µl ZOOM Carrier Ampholytes pH 4-7 (Thermo-Fischer Scientific)

1.14µl 2M DTT (Sigma-Aldrich)

30µl dH_2O

trace of Bromophenol Blue (Sigma-Aldrich).

3.2.1.15 Equilibration buffers

1ml 1× NuPAGE was made up by adding 5ml 4× NuPAGE sample buffer to 15ml dh_2O.

1× sample reducing agent was made up by adding 1ml 10×sample reducing agent to 9ml 1× NuPAGE sample buffer.

3.2.1.16 Alkylating buffer

Alkylating buffer was made up by adding 232mg Iodoacetamide (Sigma-Aldrich) to 10ml 1× NuPAGE Sample buffer.

3.2.1.17 4% Paraformaldehyde

4g Paraformaldehyde (Sigma Aldrich) was added to 100ml 1×PBS (Thermo Fisher Scientific) and dissolved on a magnetic hot plate until all the paraformaldehyde had dissolved.

3.2.1.18 TAE solution

TAE solution was made up using 4.85g Tris (40mM), 1.2g Acetic Acid (20mM) and 0.29g EDTA (1mM) and added to 1L dH_2O.

3.2.1.19 1% agarose gel

1g of agarose was added to 100ml of TAE solution and heated using a microwave until all agarose had dissolved.

When making up the 1% agarose gel, 2µl 5mg/ml Ethidium bromide was added to the gel when the gel solution had cooled enough to handle.

3.2.1.20 Luria Broth (LB) broth

LB broth was made up by adding 25g Luria Broth to 1L dh_2O and autoclaved for 15 minutes at 121°C, psi for 20min. LB broth was allowed to cool before addition of 100µg/ml Ampicillin.

3.2.1.21 LB Agar plates

LB Agar plates was made up by adding 35g LB Broth with agar (Lennox) (Sigma Aldrich) to 1L dh_2O and autoclaved at 121°C, psi for 20min to sterilise and dissolve agar granules. Agar was allowed to cool before addition of 100µg/ml Ampicillin. Agar plates were poured, allowed to set at room temp for 2 hours and stored inverted at 4°C.

3.2.1.22 TE buffer

157mg Tris-HCL (10mM) and 29mg EDTA (1mM) was added to 100ml dH_2O and mixed until dissolved. Solution was adjusted to pH 8. TE buffer was autoclaved at 121°C, psi for 20min for sterilisation.

3.2.2 Cell culture methods:

3.2.2.1 Lentiviral Transduction

Lentivirus transduction was carried out at the NIH, USA in the SUM159 and PC3 cell lines using the pluripotency response reporter that contains the NRE-GFP and a control vector known as the minimal CMV-GFP (Systems Biosystems) but will be referred to as the Control which contains all aspects of the NRE-GFP excluding the NRE. This was carried out to determine if Nanog and/or NanogP8 could bind to the Nanog response element and induce expression of GFP. This was carried out at the NCI, and all subsequent experiments were carried out at SHU.

The SUM159 and PC3 cell lines were seeded at 1×10^4 cells/well in a 48 well plate with complete medium and incubated overnight at 37°C in a humidified, 5% CO_2 atmosphere. Viral particles were thawed on ice and 10ml of complete medium was prepared with 5µg/ml Polybrene (Sigma Aldrich). Viral particles were diluted to 5MOI in 0.1ml complete medium with Polybrene and gently mixed. Culture medium was removed and 0.1ml/well viral stock dilution was added to cells and left overnight at 37°C in a humidified, 5% CO_2 atmosphere. The control well contained everything other than the viral particles. Viral particles were removed and cells were incubated with 0.5ml complete medium and incubated overnight at 37°C in a humidified, 5% CO_2 atmosphere. Cells were passaged to 1:3 to allow transduced cells to proliferate further and incubated for 48hrs. GFP expression was confirmed using fluorescent microscopy. NRE-GFP positive cells were sorted based on GFP expression using FACS.

3.2.2.2 3D cell culture using cancer stem cell medium and Ultra-low attachment plates

SUM159 Parent, Control and NRE-GFP cell lines were seeded at 1×10^5 cells/ well (6 well) or $2x10^3$ (96 well) in an ultralow attachment plate (Sigma Aldrich) and cultured

for 0-7 days in cancer stem cell medium at 37°C in a humidified, 5% CO_2. The medium was carefully changed every 3 days so as to not dislodge the floating spheroids. GFP was assessed using flow cytometry and using fluorescent microscopy.

3.2.2.3 Culturing cells in hypoxia

Cell lines were seeded at $3x10^5$ cells/6 well plate and placed at 37°C in a humidified, 5% CO_2 atmosphere overnight to allow cells to adhere. Plates were then transferred to a Hypoxic Glove Box (Coy Lab, USA) at 37°C with 5% O_2 for between 1-72hrs. At allocated time points medium was collected from wells and cells were washed in 1× PBS and trypsinised using 0.4ml of 0.05% Trypsin-EDTA for 5min. Trysin-EDTA was inactivated using 1ml of complete medium and transferred to the tube containing collected medium. Cells were centrifuged at 1000rpm for 5 mins and supernatant was removed. Cells were fixed for 7min with 1% paraformaldehyde. Paraformaldehyde fixed cells were centrifuged at 37°C and washed twice in 1× PBS. Cells were re-suspended in 1× PBS for flow cytometry analysis using the BD FACSCalibur (Becton Dickinson). For direct comparison the method was carried out for cells incubated at 21% O_2. For cell viability and GFP expression by flow cytometry, medium was removed and cells were washed in 1× PBS and cells used for flow cytometry were fixed for 7min with 4% Paraformaldehyde. For cell viability, cells were stained with 10µM Hoechst 33342 and Propidium Iodide (detailed in figure 2.2.1.6). Cells were imaged using the Olympus IX81 inverted fluorescence microscope using the Cell-F software (Olympus).

3.2.2.4 Treatment of cells with the proteasome inhibitor Bortezomib

Cell lines were seeded at $3x10^5$ cells/6 well plate and $5x10^4$ cells/96 well plate and placed at 37°C in a humidified, 5% CO_2 atmosphere overnight to allow cells to adhere. Cells were then treated with 0-20nM Bortezomib (Selleckchem) for 24h or 72hrs. Cells were harvested and fixed using 4% Paraformaldehyde for flow cytometry analysis.

Alternatively, cells were viewed directly using the Olympus IX81 inverted fluorescence microscope using the Cell-F software (Olympus) prior to harvest and GFP expression was determined.

3.2.3 Western blotting

3.2.3.1 Protein Extraction

Cell lines grown were seeded at $1x10^6$ cells/well (6 well plate) (Thermo Fisher Scientific) with complete medium and incubated overnight at 37°C in a humidified, 5% CO_2 atmosphere. Supernatant was removed and cells were washed in 1× PBS. Cells were lysed with 250µl cell lysis buffer for 15mins at room temperature on an orbital shaker. Cell lysate was removed and centrifuged at 17,000g for 15mins to pellet cellular debris. Protein containing supernatant was removed to a chilled Eppendorf (Thermo Fisher Scientific) and incubated at -20°C for future protein concentration determination.

3.2.3.2 Protein concentration determination using Bicinchoninic Acid Kit

A standard curve for protein concentration was made from a stock solution of 2.5mg/ml of Bovine Serum Albumin (Sigma Aldrich) in cell lysis buffer and serially diluted. Protein concentration was determined for all cell lines using the Bicinchoninic Acid (BCA) Kit following the manufacturer's instructions. Absorbance was read at 560nm using the Perkin Elmer Wallac 1420 Victor2 Microplate Reader.

3.2.3.3 Sodium dodecyl sulfate polyacrylamide gel electrophoresis

20µg of protein was added to 4x Laemmli Sample Buffer (Thermo Fisher) and heated at 95°C for 2mins to denature proteins and placed on ice. Protein and pre-stained protein molecular weight ladder (Thermo Fisher Scientific) was loaded into the wells of a 10% gel and run at 150V for 1hr using the Mini-PROTEAN Tetra Vertical Electrophoresis Cell (BIO-RAD) in 1× SDS running buffer.

3.2.3.4 Protein Transfer and western blot analysis

For protein transfer onto a nitrocellulose membrane a gel was assembled according to the manufactures instructions and transferred onto a nitrocellulose membrane, 0.2 µm using a Mini Trans-Blot Cell (BIO-RAD) at 75V for 1hr in 1× Transfer buffer. The Membrane was briefly washed in TBST before incubating for 1hr at room temperature on an orbital shaker in blocking solution. Blocking solution was removed and membranes incubated in 1:1000 Rabbit Anti-Nanog (D73G4/ #4903S) and 1:5000 Mouse Anti-α-Tubulin (DM1A/ #3763S) (Cell Signaling Technologies, Hertfordshire) in blocking solution at 4°C on an orbital shaker. Primary antibodies were removed and membranes were washed 3x5min in TBST and the membrane was incubated in 1:15,000 IRDye® 800CW-conjugated Donkey anti-Mouse IgG and IRDye® 680RD-conjugated Donkey anti-Rabbit IgG in blocking solution for 1hr at room temperature on an orbital shaker. Secondary antibodies were removed and membranes were washed in 3×10min in TBST. The Membrane was imaged using the Odyssey® CLx Imaging System and data was analysed using the LI-COR Image Studio Software for the Odyssey CLx.

3.2.3.5 Coomasie Blue stain

SDS gels were incubated with coomasie stain overnight on an orbital shaker. Coomasie stained gels were de-stained using coomasie de-staining buffer for up to 1hr on an orbital shaker. Excess stain was removed using dH_2O. Gels were imaged using a digital camera.

3.2.3.6 Silver stain

SDS-PAGE gels were fixed overnight using gel fixing solution prior to silver staining. Silver staining was carried out using the ProteoSilver Plus Silver Stain Kit (Sigma-Aldrich) following the manufacturer's instructions and stop solution was added after

3.30min. Gels were washed for 15min in ultrapure H_2O. Gels were imaged using a digital camera.

3.2.3.7 Optimisation of 2D gel electrophoresis

40µg of protein lysate was solubilized using 256µl ZOOM 2D Protein solubilizer 1, 2.10µl ZOOM Carrier Ampholytes pH 4-7 (Thermo-Fischer Scientific), 1.14µl 2M DTT (Sigma-Aldrich), 30µl dH_2O and a trace of Bromophenol Blue (Sigma-Aldrich). Protein solubilisation solution was added to the ZOOM IPG Runner Cassettes and ZOOM IPG Strip pH 4-7 (Thermo-Fisher Scientific) was then added to the cassette. Cassette was incubated overnight to allow for protein solubilisation. 2D gel electrophoresis was assembled using ZOOM IPG Runner System (Thermo-Fisher Scientific) following the manufacturer's instructions. Isoelectric focusing was as follows:

STEP B Programme	Time in min			
Voltage	1st	2nd	3rd	4th
200	10	20	40	80
450	7	15	30	60
750	7	15	30	60
1200	15	30	60	120

Table 3. Optimising of isoelectric focusing, 1st dimension of 2D gel electrophoresis. Optimisation was carried out to improve focussing of proteins using Step B voltage gated 2D gel electrophoresis. The length of time in which the voltages were applied was doubled until the proteins were focussed.

Zoom strips were then incubated in an equilibration buffer to prepare the sample for SDS-PAGE. 10ml of sample buffer with reducing agent was added to the cassette containing strips, for 15mins on a rotary shaker before it was decanted and then 10ml

of alkylating buffer was added for 15mins room on a rotary shaker. Alkylating buffer was removed and the gels were placed directly on top of a freshly prepared 10% SDS gel as previously detailed in (fig 2.2.1.9) or on to a NuPAGE 4-12% Bis-Tris ZOOM Protein Gels, 1.0 mm, IPG-well (Thermo-Fisher Scientific) for 2nd phase separation. 400µl of 0.5% agarose (Sigma-Aldrich) was added to the top of the gel containing isoelectric focusing strip and SDS-PAGE was carried out as previously described in (fig 3.2.3.3).

3.2.4 Molecular biology

3.2.4.1 RNA extraction

Cell lines were seeded at 1x10^6 in a 6 well plate and incubated overnight at 37°C in a humidified, 5% CO_2 atmosphere. Medium was removed and cells were lysed using 1ml TRI Reagent (Sigma-Aldrich) and incubated at room temperature for 10min. Cellular constituents were collected and 200µl of Chloroform (Sigma-Aldrich) was added. Sample was shaken vigorously and left to stand for 3min until separation occurred. Samples were centrifuged at 12,000g for 10min until separation of proteins, DNA and RNA had occurred. 500µL of the upper aqueous layer containing RNA was taken into a fresh tube. Equal amount of Isopropanol (Fisher Scientific) was added to the RNA and this was stored at -80°C for at least 1hr to allow the RNA to precipitate prior to 15min centrifugation at 12,000g. The RNA pellet was then washed in 70% Ethanol (Sigma-Aldrich) and centrifuged at 8,000g for 5min. The supernatant was carefully precipitated and the RNA pellet was briefly dried on a heated block to remove residual ethanol taking care to not dry out the pellet. RNA pellet was re-suspended in 50µl UltraPure DEPC-Treated Water (Thermo-Fisher Scientific).

3.2.4.2 DNA clean-up

RNA was quantified using the NanoDrop ND-1000 (Thermo Scientific) and analysed using the NanoDrop 1000 3.8.1 software. RQ1 RNase-Free DNase (Promega) was used to digest any contaminating DNA. 1U/µg RQ1 RNase-Free DNase (Promega) was added to 5µl of RNA, 1µl RQ1 RNase-Free DNase 10×Reaction buffer (Promega) and 3µl DEPC treated water and incubated for 30min at 37°C. 1µl RNase-Free DNase stop solution was added and heated at 65°C for 10min to inactivate the enzyme. RNA was incubated at -20°C for subsequent experiments.

3.2.4.3 cDNA synthesis

cDNA synthesis was carried out by adding together 4µl 5x Buffer, 2µl DTT, 0.5µl Random Primers, 0.5µl Super Script II Reverse Transcriptase (Thermo-Fisher Scientific), 9.5µl UltraPure DEPC-Treated Water and 3µl RQ1-treated RNA that had been denatured for 5min at 60°C. The control contained everything other than the Super Script II Reverse Transcriptase (NO RT). Samples were incubated at 37°C for 2hrs to ensure all mRNA had been reverse transcribed.

3.2.4.4 Genomic DNA extraction

Cells were seeded at $1x10^6$ cells/well (6 well plate) and incubated at 37°C in a humidified, 5% CO_2 atmosphere overnight to allow cells to adhere. The following day DNA was extracted using the QIAamp DNA Mini Kit (QIAGEN) following the manufacturer's instructions. The quality of the DNA was determined using the NanoDrop ND-1000 (Thermo Scientific) and analysed using the Nano Drop 1000 3.8.1 software and the A_{260}/A_{280} ratio of the isolated DNA was within 1.6-1.9.

3.2.4.5 PCR and primer concentration optimisation

NTera2 (NTERA2) is a human testicular embryonic carcinoma stem cell line (ATCC) used as a positive control for Nanog expression. NTera2 cDNA was amplified using the

polymerase chain reaction (PCR) to determine if these express Nanog or NanogP8 as detailed below.

Primers were designed to amplify 1240 base pairs from Nanog or NanogP8 cDNA. PCR optimisation was carried out using NTera2 cDNA as these are a positive control for NTera2 expression. PCR was performed on genomic DNA as a positive control for NanogP8.

PCR mastermix was made up using 17.75µl UltraPure DEPC-Treated Water, 2.5µl 1.5mmol MgCl2, 0.5µl Immolase DNA Polymerase (Bioline, London), 2.5µl10x Buffer (Bioline) 1-100pmol 1240 Forward (F) and 1240 (R) primers, 10pmol dNTP (Qiagen) and 1µl cDNA. Touchdown PCR was used for cDNA amplification.

1240F and R primers:

5' Upper 1240F accccagcctttactcttcctacc
5' Lower 1240R tacgatgcagcaaatacgagacct

Touchdown PCR cycling parameters

95°C for 10min

x3 cycles

95°C for 30s

63°C for 30s

72°C for 2min

Then, as above but decreasing anneal temperature by 2°C every 3 cycles, followed by

x30 cycles

95°C for 30s

55°C for 30s

72°C for 2min

3.2.4.6 Agarose Gel Electrophoresis

2µl of 5mg/ml Ethidium Bromide (Sigma-Aldrich) was added to a 1% agarose gel when setting. 10µL PCR products were mixed with 6x DNA Gel Loading Dye (New England Biolab, Hitchin) and run with TAE buffer at 100V for 45mins. Image was captured using UVP BioImaging system and analysed using LabWorks software.

3.2.4.7 Determination of Nanog/NanogP8 expression by RT-PCR-RFPL ananlysis

PCR products that were amplified from NTera2 cDNA and gDNA were subjected to restriction enzyme digest using *A1wNI* as this restriction enzyme recognises a single nucleotide change within the NanogP8 locus or NanogP8 cDNA but not within the Nanog cDNA. This allows for identification of transcription from Nanog or NanogP8 locus.

1µg of PCR product from NTera2 or gDNA was added to 5µL 10× NE Buffer (NEB), 1µl (10U) *AIwN1* (NEB) and topped up to 50µl with DEPC treated water. Sample was gently mixed with a pipette followed by a quick spin down in the microcentrifuge. Sample was incubated at 37°C for 1hr. Samples were then run on a 1% agarose gel for gel electrophoresis.

3.2.5 Plasmid preparation and transformation

Plasmid DNA was synthesised at the National Institute of Health, USA to incorporate the Nanog promoter-GFP, NanogP8 promoter-GFP and the CMV MAX-GFP into a reporter vector to determine if Nanog or NanogP8 was transcribed in cell lines. The CMV MAX-GFP was used as a positive control for transfection.

Figure 3.2 Reporter vectors

Figure 3.2 Reporter vectors. The Nanog promoter-GFP contains 2589bp of the Nanog promoter, upstream from the Nanog start codon sequence. The CMV MAX-GFP contains 819bp of the CMV promoter. Both vectors contain the dsCopGFP and Zeocin resistance. The NanogP8 promoter-GFP has identical features other than the promoter region.

3.2.5.1 Transformation of plasmid DNA

2µg of plasmid DNA: Nanog promoter-GFP, NanogP8 promoter-GFP and CMV MAX-GFP provided by Dr Tom Sayers, NIH USA was gently mixed with 50µl of TOP10 one shot chemically competent E.coli cells (Thermo Fisher Scientific) excluding the negative control that did not contain DNA. Samples were incubated on ice for 30min before heat shock at 42°C for 30s and returned to ice for 5min. 250µl of SOC outgrowth medium (NEB) was added and incubated at 37°C for 1hr. 10µl of transformation cell suspension was added to pre warmed agar plates, streaked and incubated overnight at 37°C. Individual colonies were selected and incubated in 50ml of pre-warmed LB media containing 100µg/ml ampicillin overnight at 37°C, 200rpm. The resulting cultures were subjected to mini-prep (QIAGEN) following manufacturer's instructions. The resulting DNA was stored at -20°C prior to restriction enzyme digest.

3.2.5.2 Restriction enzyme digest of plasmid DNA

Plasmid DNA was digested with *SpeI* restriction enzyme (New England Biolab) following the manufactures instructions. *SpeI* recognises one restriction enzyme site in Nanog promoter-GFP and NanogP8 promoter-GFP and two in the CMV MAX-GFP. Following restriction enzyme digest the plasmid DNA was run on a 1% agarose gel.

3.2.5.3 Midi-Prep

Following successful identification of plasmid: Nanog promoter-GFP, NanogP8 promoter-GFP and CMV MAX-GFP, the colonies that were positive for plasmid DNA were picked and added to 25ml of pre-warmed LB broth and incubated at 37°C for 16hrs and shaken at 300rpm. Bacterial cells were harvested by centrifugation at 6000g for 15min at 4°C prior to Midi-prep using Qiagen midi prep kit. Bacterial cells were re-suspended in BufferP1 containing RNAse and pipetted to remove cell clumps. Bacterial cells were lysed using 4ml of Buffer P2 and vigorously inverted 6 times and incubated

at room temperature for 5min. 4ml of chilled BufferP3 was then added, vigorously inverted 6 times and left on ice for 15mins to precipitate DNA. Lysate was then centrifuged at 20,000g for 30min at 4°C, and the supernatant containing the plasmid DNA was removed and centrifuged again at 20,000g for 15min at 4°C. The tip 100 was then equilibrated using 4ml of Buffer QBT and allowed to empty by gravity flow. The supernatant containing DNA was then added to the tip and allowed to empty by gravity flow and tip was then washed using 2×10ml Buffer QC. In a fresh tube, DNA was eluted from the tip by addition of 5ml of Buffer QF. DNA was then precipitated by the addition of 3.5ml room temperature isopropanol (Fisher) and centrifuged at 15,000g for 30min at 4°C. DNA pellet was then washed with 70% ethanol and centrifuged at 15,000g for 10min at 4°C. Ethanol was carefully removed so as to not dislodge the pellet and left to air dry for 5-10min. DNA was re-dissolved in 150µl buffer TE. DNA was quantified using the NanoDrop ND-1000 (Thermo Scientific) and analysed using the Nano Drop 1000 3.8.1 software. DNA was stored at -20°C for checking its quality using gel electrophoresis and subsequent transfections.

3.2.5.4 Transfection of Nanog reporters using Viromer transfection system

SUM159 and NTera2 cell lines were transfected with a plasmid containing the human Nanog promoter-GFP and NanogP8 promoter-GFP to determine if these cells express any of the Nanog proteins using the Viromer transfection reagents (Lipocalyx, Cambridge).

SUM159 Parent cells were seeded at $3x10^5$ cells/6 well plate overnight to allow cells to adhere. 11ng/ml of vectors containing the Nanog promoter-GFP, NanogP8 promoter-GFP plasmids or CMV Max-GFP was diluted with Buffer Red to 540µl. In a separate tube 57.6µl Buffer red was added to 2.4µl Viromer red and vortexed for 5s. The diluted

plasmid was added to the Viromer and gently mixed, and left for 15min at room temperature to allow complexation of the DNA and Viromers. 300µl of transfection complexes was added to the wells. For the negative control no DNA was added, however TE buffer was used instead. GFP expression was assessed using the Olympus IX81 inverted fluorescence microscope using the Cell-F software (Olympus)

3.2.5.5 Optimising Zeocin concentration

Zeocin concentration was optimised for the selection of stable transfection of Nanog promoter-GFP and NanogP8 promoter-GFP vectors which contain the Zeocin-resistance cassette in to SUM159 and NTera2 cell lines.

Cells were plated at $3x10^5$ cells/6 well plate overnight to allow cells to adhere. The following day Zeocin (Thermo Fisher Scientific) was treated with cells at 0, 25, 50, 100 and 200µg/ml and monitored using light microscopy for up to 72hrs to identify a dose that kills up to 50% of cells, with the remaining cells appearing quiescent and non-proliferative. 100µg/ml was optimum for both SUM159 and NTera2 cell lines as at doses greater than this induced cell death and at less than 100µg/ml, cells were proliferative and continued to proliferate after passage.

3.3 Results

3.3.1.1 Expression of GFP and cell viability in SUM159 cell lines in 2D and 3D cell culture as determined by fluorescent microscopy.

The SUM159 cells were grown in 2D and 3D cell culture to asses for GFP expression and counter stained with Hoechst 33342 and Propidium Iodide and imaged using fluorescent microscopy.

All SUM159 cell lines grown in 2D had a normal, regular nucleus with minimal cell death, as determined by Hoechst 33342/Propidium Iodide staining and fluorescence microscopy (Fig 3.3). The Parent and Control cells exhibited GFP signal below the limit of detection as determined by fluorescent microscopy, whereas GFP expression in the NRE-GFP cell lines was expressed in the nucleus and cytoplasm (Fig 3.3).

SUM159 cell lines grown in 3D were large and compact with some dead/necrotic cells within the core of the spheroids and live viable cells around the outer layer (fig 3.4). No GFP was detected in the Parent cell lines, however some GFP^{+ve} cells were observed in the Control cell line with a similar intensity to NRE-GFP cells. GFP was expressed in the medium-large spheroids in the NRE-GFP cell line whereas the smallest spheroids of <10 cells did not appear to express GFP.

Figure 3.3 The expression of GFP and cell viability in the SUM159 cells in 2D as determined by fluorescent microscopy.

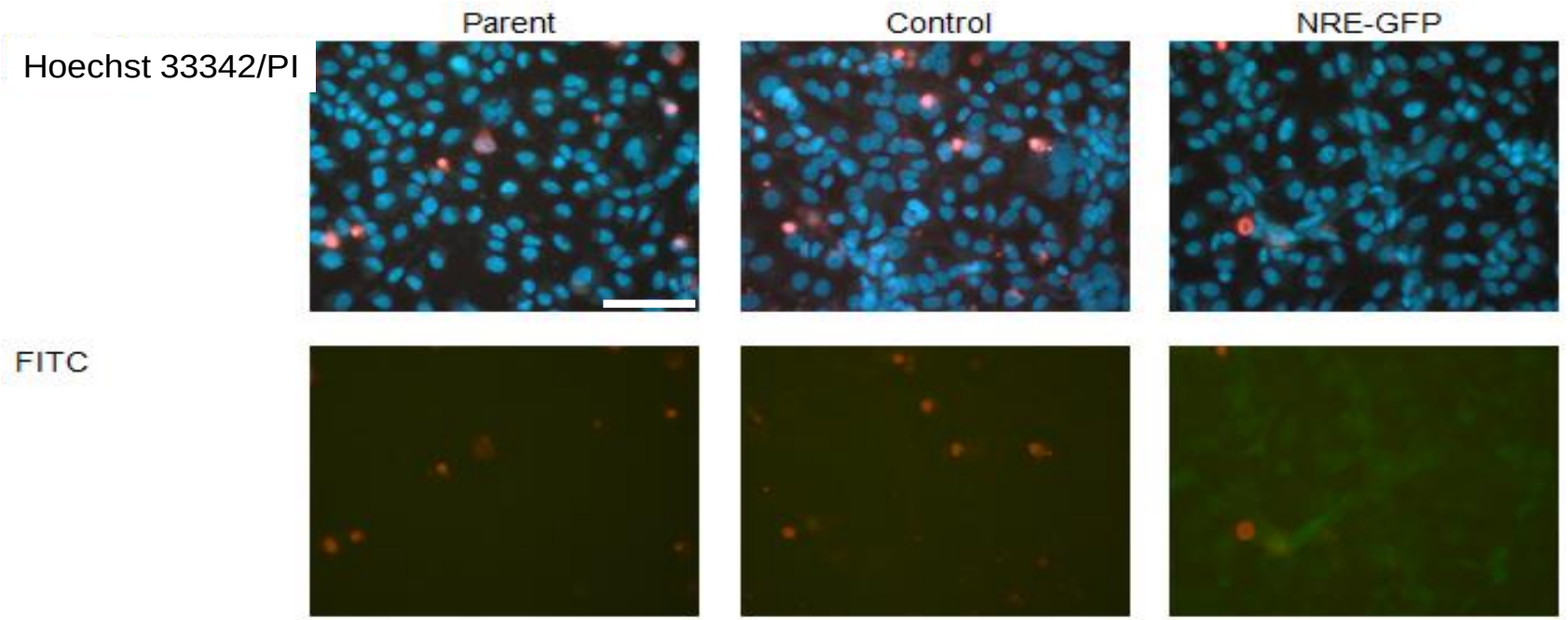

Figure 3.3. The expression of GFP and cell viability of SUM159 cell lines when grown in 2D cell culture as determined by fluorescent microscopy.SUM159 cells were seeded into a 96 well plate overnight and stained with Hoechst 33342 and Propidium Iodide. The Parent, Control and NRE-GFP cells had regular nucleus and low amount of apoptotic and dead cells (<5%) were observed. No GFP was detected in the Parent and Control cells line whereas GFP was abundant in the NRE-GFP cell line. GFP expression was determined using the Olympus IX81 inverted fluorescence microscope using the Cell-F software. Images are representative of two independent experiments. Scale bar represents 200µm.

Figure 3.4 The expression of GFP and cell viability in SUM159 cell lines in 3D as determined by fluorescent microscopy.

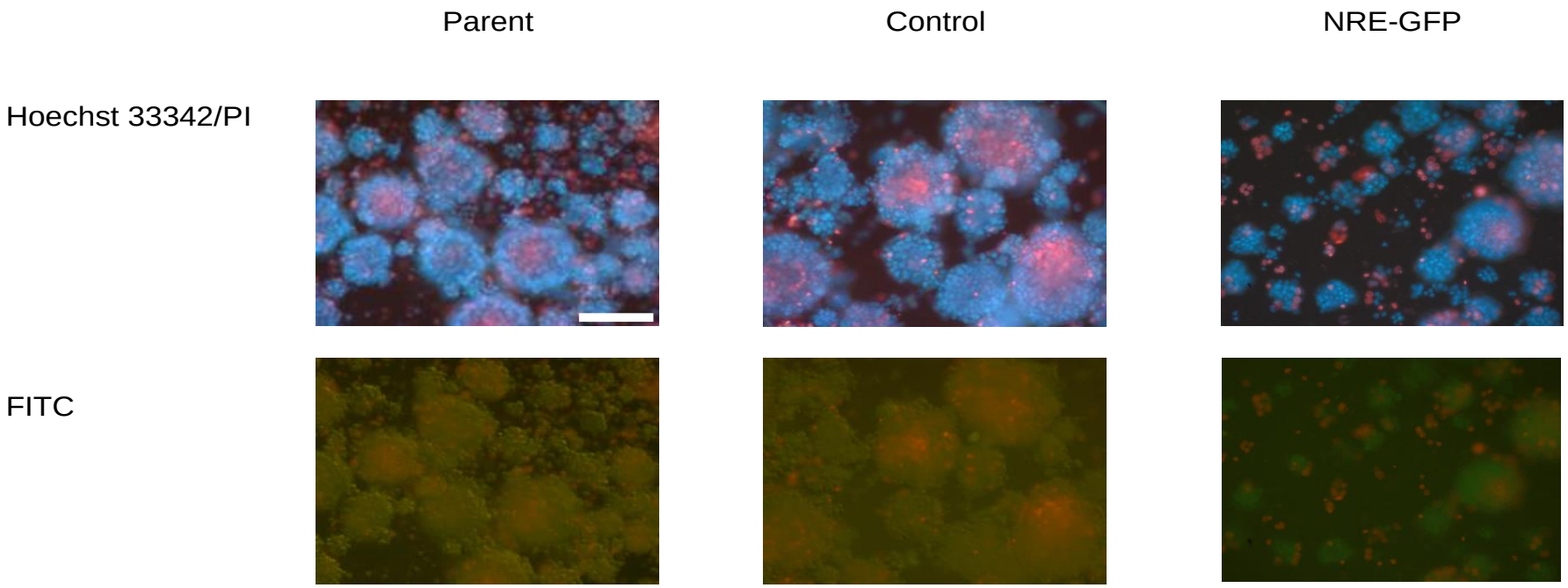

Figure 3.4. The expression of GFP and cell viability in SUM159 cell lines grown in 3D cell culture as determined by fluorescent microscopy. SUM159 cell lines were grown in alginate for 10 days prior to Hoechst 33342 and Propidium Iodide stain. The Parent, Control and NRE-GFP cells grew to large, tightly compact spheroids with some having a necrotic core. The Control cells appeared to proliferate quicker than the Parent and NRE-GFP cell line as these were larger in size. The Parent cells were GFP^{-ve} whereas the Control cell line had some GFP positivity. The NRE-GFP cell line had high GFP expression within spheroids but in some smaller clusters of <10 cells no GFP was observed. GFP expression was determined using the Olympus IX81 inverted fluorescence microscope using the Cell-F software. Images are representative of two independent experiments. Scale bar represents 200µm.

3.3.1.2 The effect of 3D cell culture on CSC surface marker expression as determined by flow cytometry.

SUM159 Parent (untransduced), Control (expressing Min-CMV-driven GFP) and NRE-GFP (expressing Min-CMV-driven GFP with a Nanog response element) cells were grown in 2D and 3D for 10 days to asses for CD44, CD181 and CD24 expression as determined by flow cytometry.

SUM159 Parent, Control and NRE-GFP cells showed no significant differences in expression of CD44, CD24 and CD181 cell surface markers when grown in 2D. SUM159 NRE-GFP has significantly more GFP-positive cell population ($p<0.001$, 34%) when compared to the Parent and Control cells in 2D (fig 3.5).

When culturing cells in 3D a significant decrease in GFP was present in the NRE-GFP cell line ($p<0.001$, 10%) and no significant difference was observed in the Control. Unexpectedly, CD181 expression was significantly increased in the CMVmin-GFP cells ($p<0.001$, 60%) and CD44 and CD24 expression was significantly downregulated ($p<0.001$, 22%, 17%) when compared against the Parent cells. Significant differences in CD181, CD44 and CD24 ($p<0.0001$) was observed in the NRE-GFP when compared against the Control cell lines.

Figure 3.5. The effect of 2D and 3D cell culture on cell surface marker expression in SUM159 cells as determined by flow cytometry.

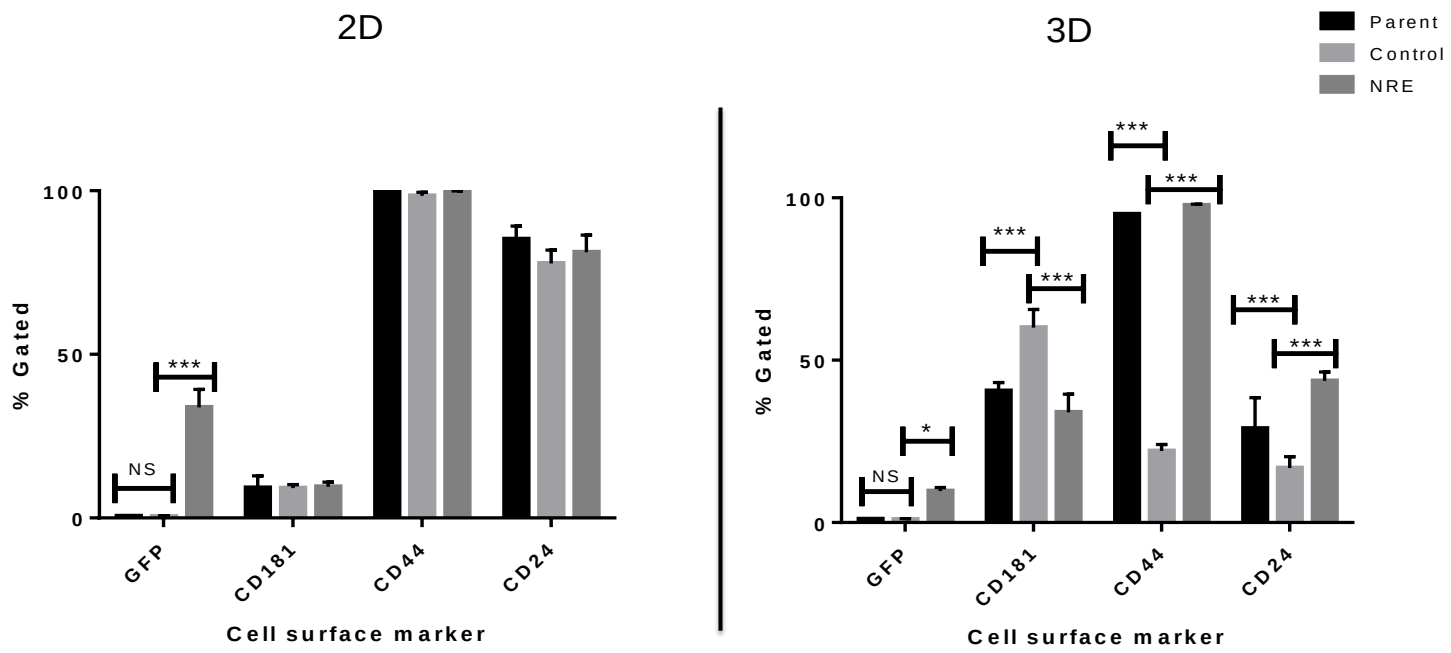

Figure 3.5. The effect of 2D and 3D cell culture on cell surface marker expression in SUM159 cells as determined by flow cytometry. The SUM159 cells were seeded in 2D and 3D cell culture for 10 days prior to harvesting and antibody stain. All SUM159 cells havd the same phenotype when grown in 2D although the NRE-GFP cells has significantly more GFP expression. The Parent and NRE-GFP cells have no significant differences between CD181, CD44, and CD24 when grown in 3D however, the Control (CMVmin-GFP) cells has a significant increase in CD181 expression when compared against the Parent and NRE-GFP cell lines and a significant decrease in CD44 and CD24 expression. All Graphical data is represented as mean ± SEM and was carried out in three independent experiments. Flow cytometry data is representative of 3 independent experiments. Statistical significance was obtained using the nonparametric, Kruskal-Wallis Conover Inman. (<0.05 *, <0.01 ** and < 0.001 ***).

3.3.1.3 The effect of 3D cell culture on cancer stem cell phenotype as determined by flow cytometry.

SUM159 Control and NRE-GFP cells were grown in 2D and 3D for 10 days to determine if there was any co-expression of GFP with any of the cell surface markers and asses for GFP/$CD44^+$, GFP/$CD24^-$, GFP/$CD181^+$, $CD44^+$/$CD181^+$, $CD181^+$/$CD24^-$ potential breast CSC phenotype and $CD44^+$/$CD24^-$ breast CSC phenotype.

GFP positivity was gated from the control (CMVmin-GFP) population as negative therefore no GFP co-expression with other cell markers was determined. A significant decrease in GFP/$CD44^+$ was observed when NRE-GFP was cultured in 3D cell culture and no significant changes were observed in GFP/$CD24^-$, GFP/$CD181^+$. The $CD44^+$/$CD24^-$, $CD44^+$/$CD181^+$ and $CD181^+$/$CD24^-$ CSC phenotype was enriched in 3D cell culture mimicking previously identified data generated from the parental cells (fig 2.3.12). The $CD44^+$/$CD24^-$ breast CSC phenotype was significantly reduced in the Control cells ($p<0.001$) when cultured in 3D and a significant upregulation ($p<0.001$) of the $CD44^+$/$CD181^+$ and $CD181^+$/$CD24^-$ CSC was observed in 3D.

Figure 3.6. The effect of 2D and 3D cell culture on cancer stem cell phenotype in the SUM159 cells as determined by flow cytometry.

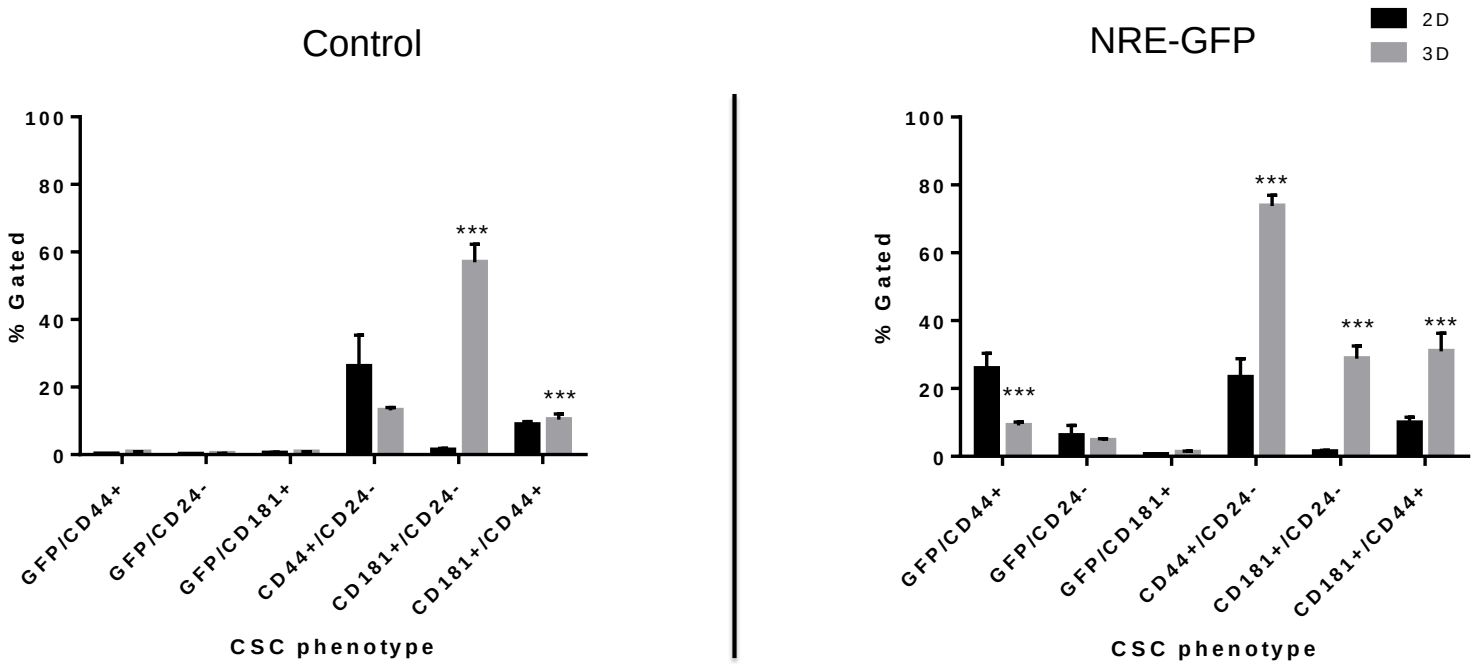

Figure 3.6. The effect of 2D and 3D cell culture on stem cell phenotype in the SUM159 cells as determined by flow cytometry. The SUM159 cells were seeded in 2D and 3D cell culture for 10 days prior to harvesting and antibody stain. No significant increase in the $CD44^{+/}CD24^{-}$ phenotype was observed in the Control cells when culturing in 3D cell culture although the other phenotypes were reflective of the Parent cells. A significant decrease in $GFP/CD44^{+}$ phenotype was found when culturing NRE-GFP cells in 3D cell culture. No significant differences observed in the $GFP/CD24^{-}$ or $GFP/CD181^{+}$ phenotype in 3D cell culture. All other phenotypes mimicked that of the Parent cell line. All Graphical data is represented as mean ± SEM and was carried out in three independent experiments. Statistical significance was obtained using the nonparametric, Kruskal-Wallis test followed by Conover-Inman post-hoc test (<0.05 *, <0.01 ** and < 0.001 ***)

3.3.1.4 Effect of cancer stem cell medium on GFP expression in the SUM159 cell lines as determined by flow cytometry and fluorescent microscopy.

As the SUM159 NRE-GFP cells did not express significantly more GFP expression when grown in alginate 3D cell culture, vs 2D, SUM159 cells were grown in a CSC medium in ultra-low attachment plates for up to 7 days as previous reports have found this to enrich for the Nanog positive CSC population.

There was no GFP signal in the un-transduced Parent cells as expected, and no significant difference in GFP expression in the NRE-GFP cell line cultured in normal and CSC medium at day 1, 4 and 7 however a significant increase in GFP expression was observed at day 4 in the Control (CMV-Min-GFP) cells as determined by flow cytometry ($p<0.05$) (fig 3.7). This was further supported by images captured using fluorescent microscopy (fig 3.9). When assessing GFP expression in all cell lines from days 1-7 there was a significant increase in GFP expression in the Control cell lines from day 1-4 ($p<0.05$) and a significant decrease in GFP expression from day 4-7 ($p<0.05$) when cultured in CSC medium (fig 3.8). No significant changes in GFP could be observed in the Parent and NRE-GFP cells (fig 3.8).

Figure 3.7 Effect of cancer stem cell medium on GFP expression in SUM159 cell lines as determined by flow cytometry.

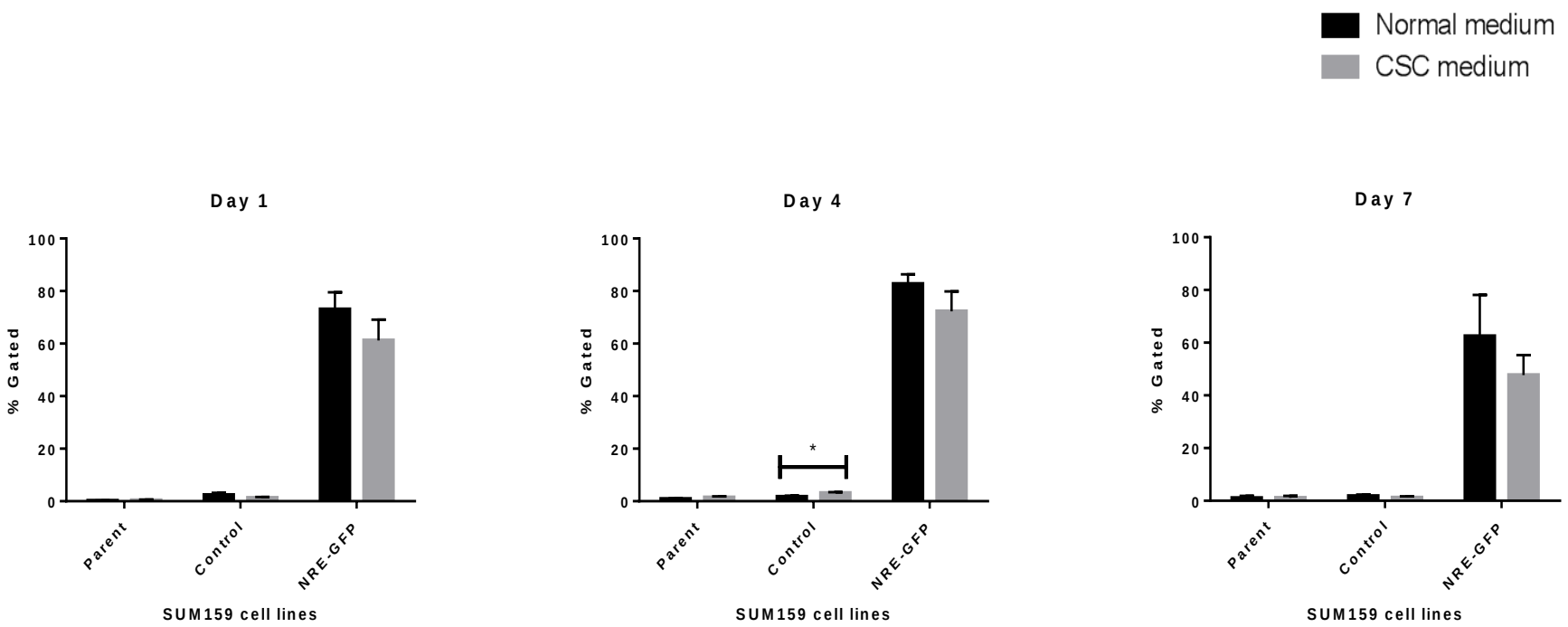

Figure 3.7. The effect of cancer stem cell medium on GFP expression in the SUM159 cells as determined by flow cytometry. SUM159 cells were cultured in a cancer stem cell enriching medium for up to 7 days prior to GFP analysis using the flow cytometer. There were no significant differences in GFP expression in any of the cells at day 1. At Day 4 there was a significant increase in GFP in the Control cells when compared against the Control cell line cultured in complete medium. At day 7 there were no significant differences in all SUM159 cell lines. All Graphical data is represented as mean ± SEM. Flow cytometry data is representative of 3 independent experiments. Statistical significance was obtained using the nonparametric, Kruskal-Wallis test followed by Conover-Inman post-hoc test (<0.05 *).

Figure 3.8 Effect of cancer stem cell medium on GFP expression in SUM159 cells as determined by flow cytometry.

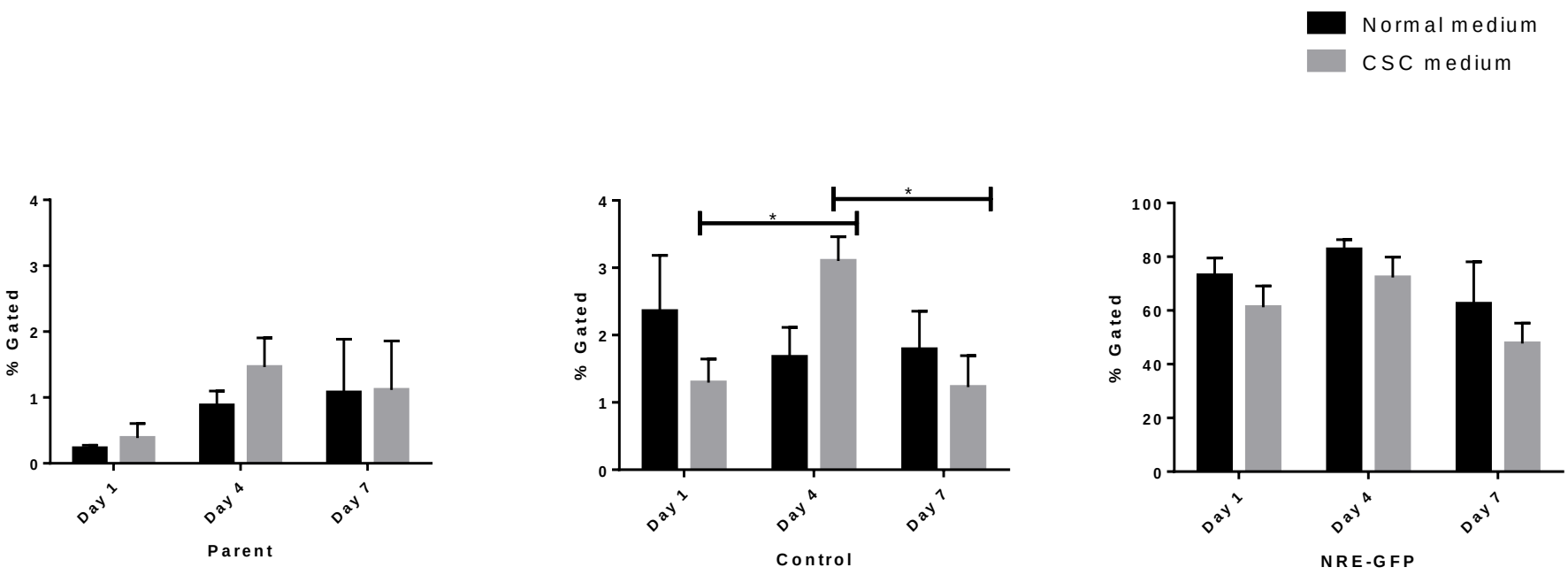

Figure 3.8. The effect of cancer stem cell medium on GFP expression in the SUM159 cell lines as determined by flow cytometry. SUM159 cells were cultured in a cancer stem cell enriching medium for up to 7 days prior to GFP analysis using the flow cytometer. There were no significant differences in GFP expression in the Parent cells overtime when compared against cells cultured in complete medium. There was a significant increase in GFP expression in the Control cells cultured in cancer stem cell medium from Day 1 -4 and a significant decrease in GFP from Day 4-7 ($p<0.05$) No significant differences were observed in the NRE-GFP cells. All Graphical data is represented as mean ± SEM and was carried out in three independent experiments. Statistical significance was obtained using the nonparametric, Kruskal-Wallis test followed by Conover-Inman post-hoc test (<0.05 *).

Figure 3.9 Effect of cancer stem cell medium on GFP expression in the SUM159 cell line as determined by fluorescent microscopy.

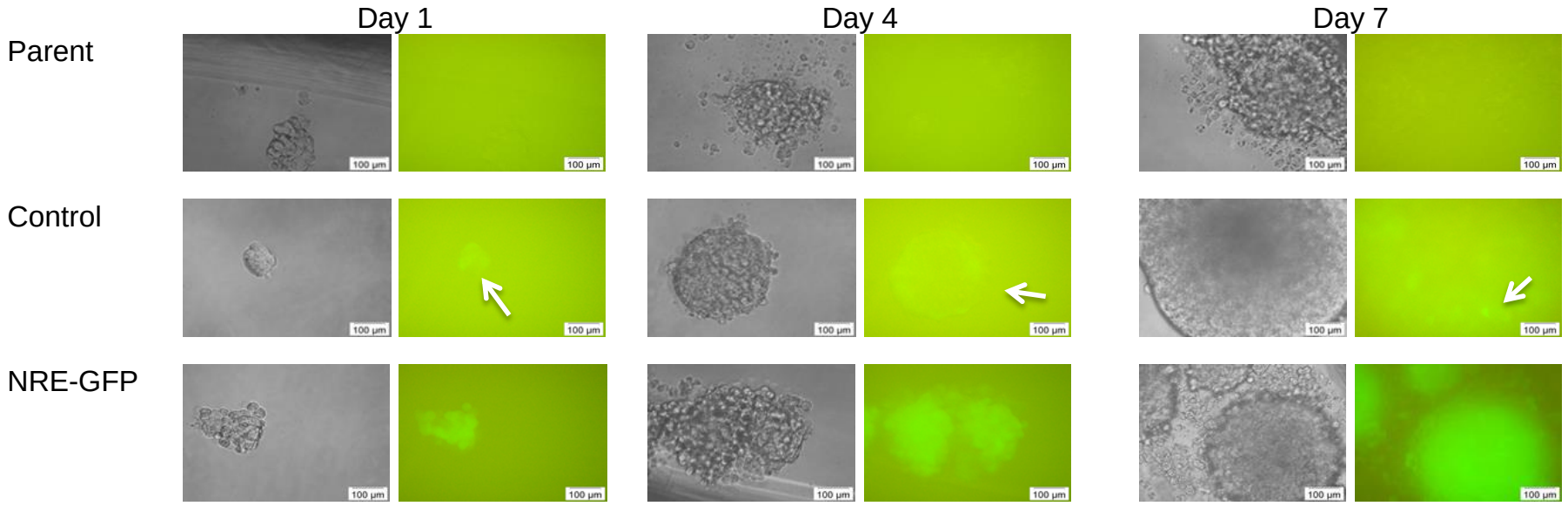

Figure 3.9. The effect of cancer stem cell medium on GFP expression in SUM159 cell lines as determined by fluorescent microscopy. SUM159 cells were cultured in a cancer stem cell enriching medium for up to 7 days prior to GFP analysis using fluorescent microscopy. SUM159 Parent cells had no GFP expression at any of the time points when cultured in cancer stem cell enriching medium. The Control cells appears to have low levels of GFP expression at Day 1, 4 and 7. GFP expression in the NRE-GFP cells appears to be ubiquitously expressed at all-time points and no visual differences can be observed. GFP expression was determined using the Olympus IX81 inverted fluorescence microscope using the Cell-F software. Background auto-flourescence was due to auto-fluorescence of the CSCM. Images are representative of duplicate experiments. Arrows point to GFP^{+ve} cells and spheroids.

3.3.1.5 The effect of 2D vs 3D cell culture on Nanog expression in all SUM159 cell lines as determined by Western blot analysis.

The SUM159 cell line was cultured in 2D and 3D to determine if a 3D cell culture environment would enrich for Nanog expression using Western blot analysis for Nanog protein detection. NTera2 cells used as a positive control for Nanog expression was detected using Western blot analysis, however no Nanog expression was detected when SUM159 cells were cultured in 2D or 3D in all SUM159 cell lines (fig 3.10).

Figure 3.10 The effect of 2D vs 3D cell culture on Nanog expression in all SUM159 cell lines as determined by Western blot analysis.

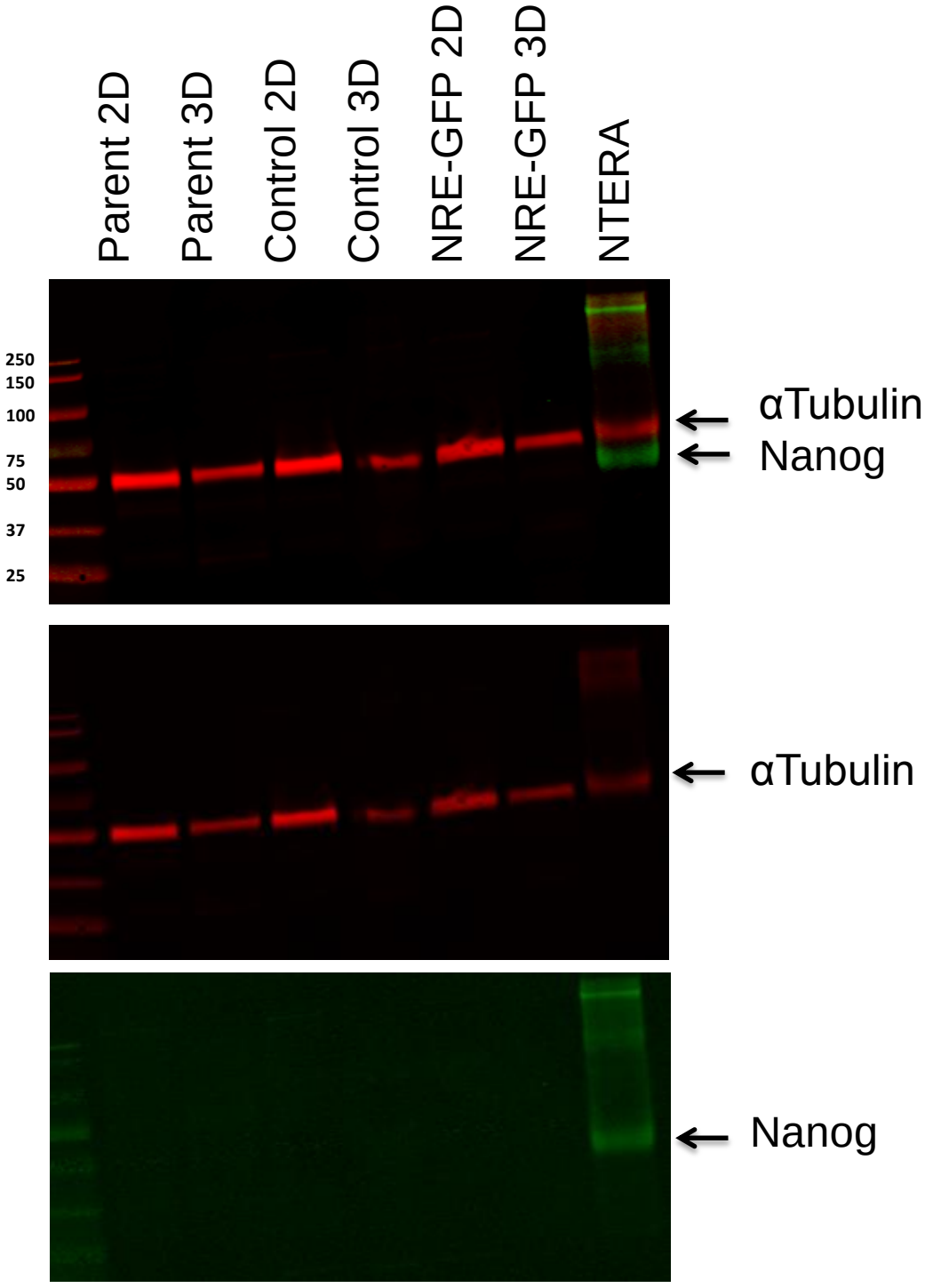

Figure 3.10. The effect of 2D vs 3D cell culture on Nanog expression in the SUM159 cell line as determined by Western Blot analysis. SUM159 cells were lysed from 2D cell culture and after 10 days of 3D cell culture prior to Western blot analysis. SUM159 cells do not appear to express Nanog protein (molecular weight 42 kDa) when cells are grown in 2D or 3D cell culture, however NTera2 cells grown in 2D do express Nanog protein. αTubulin (molecular weight 55 kDa) was used as a loading control. Western blot analysis is representative of 2 independent experiments.

3.3.2 Development of a RT-PCR based assay to differentiate between Nanog or NanogP8 gene expression.

3.3.2.1 Optimisation of PCR

Polymerase chain reaction (PCR) was carried out to determine if the SUM159 cell line express Nanog or NanogP8 mRNA, as Nanog protein (Nanog or NanogP8) was absent or below the limit of detection.

PCR primer pairs designed to amplify 1240bp of Nanog cDNA derived from the NTera2 cell line using touchdown PCR and also the same region of the NanogP8 genomic sequence.

All concentrations of primers appeared to give some product however 10pmol of the forward and reverse primers gave the best signal without any non-specific binding. Concentrations >10pmol resulted in some non-specific binding whereas <10pmol resulted in a low yield of product (fig 3.11).

Figure 3.11 Optimisation of 1240 Forward and Reverse primers

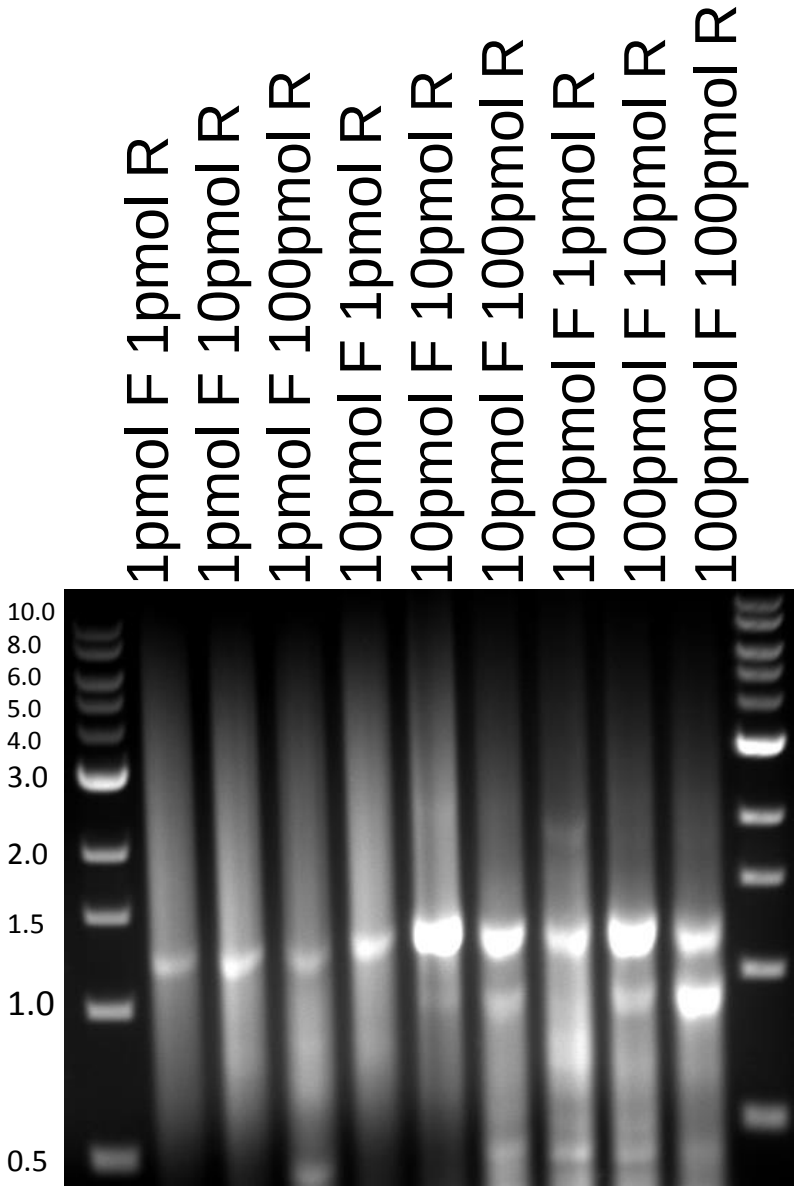

Figure 3.11. Optimisation of 1240 Forward and Reverse primers. Primers were optimised on NTera2 cDNA using touchdown PCR. Primers <10pmol resulted in low yield of product (1240bp) whereas >10pmol resulted in non-specific binding. 10pmol of Forward and Reverse primers were optimum for this reaction. Data is representative of 1 independent experiment.

3.3.2.2 Expression of Nanog or NanogP8 cDNA in the SUM159 cell line as determined by PCR.

SUM159 Parent, Control and NRE-GFP cDNA was subjected to RT-PCR to determine if these cells express Nanog or NanogP8 mRNA. NTera2 cell line was used as a positive control.

All SUM159 cells did not appear to express Nanog or NanogP8 mRNA as no product could be seen in the gel. (Fig 3.12) The NO RT did not have any genomic contamination as no amplification of the NanogP8 genome sequence could be visualised in the gel (Fig 3.12). PCR reaction was successful as Nanog cDNA was amplified using PCR and could be detected after gel electrophoresis (Fig 3.12).

Figure 3.12. Expression of Nanog or NanogP8 cDNA in SUM159 cells as determined by PCR

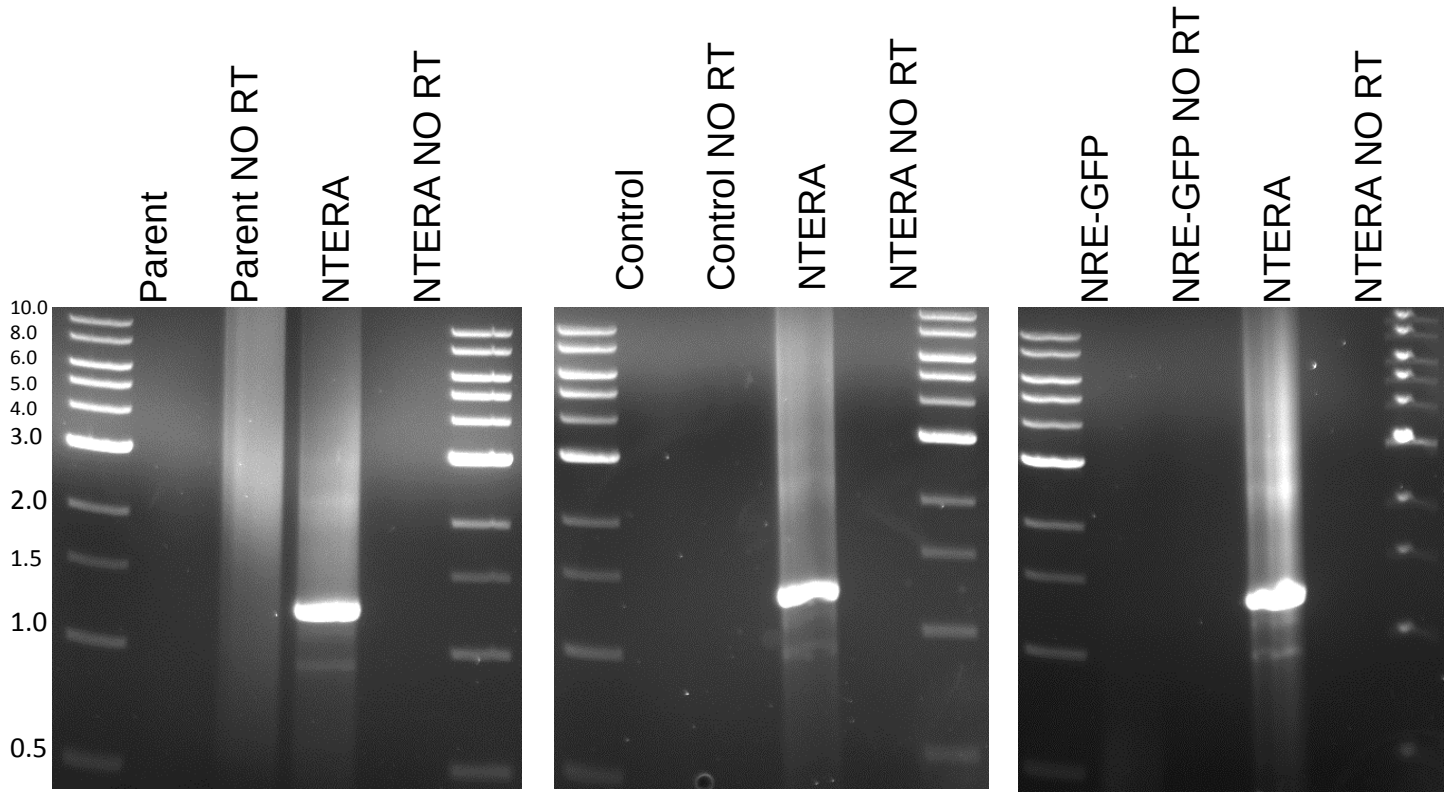

Figure 3.12. Expression of Nanog or NanogP8 cDNA in SUM159 cells as determined by PCR. cDNA from the SUM159 cells was amplified using touchdown PCR to identify if these cell lines express Nanog or NanogP8 mRNA. 1240 Forward and Reverse primers were unable to amplify Nanog cDNA derived from any of the SUM159 cells. PCR was successful in amplifying Nanog cDNA (1240bp) derived from NTera2 cells. Images are representative of two independent experiments. Images were captured using UVP BioImaging system and analysed using LabWorks software.

3.3.2.3 Detection of Nanog or NanogP8 in NTERA2 and gDNA using SNP analysis.

The NTera2 cDNA and gDNA was subjected to restriction enzyme digest using *A1wN1* as this enzyme recognises a point mutation in gDNA (NanogP8) or NanogP8 cDNA that is not present in Nanog cDNA that is expressed in the NTera2 cell line, aiding in the identification of Nanog species.

A1Wn1 did not recognise and cut cDNA derived from the NTera2 cell line confirming that these cells express Nanog from the parental Nanog locus (fig 3.13). *A1Wn1* did recognise and cut at the point mutation within the NanogP8 locus of gDNA further confirming that only Nanog from the parental locus is expressed in NTera2.

Figure 3.13. Detection of Nanog or NanogP8 using SNP analysis.

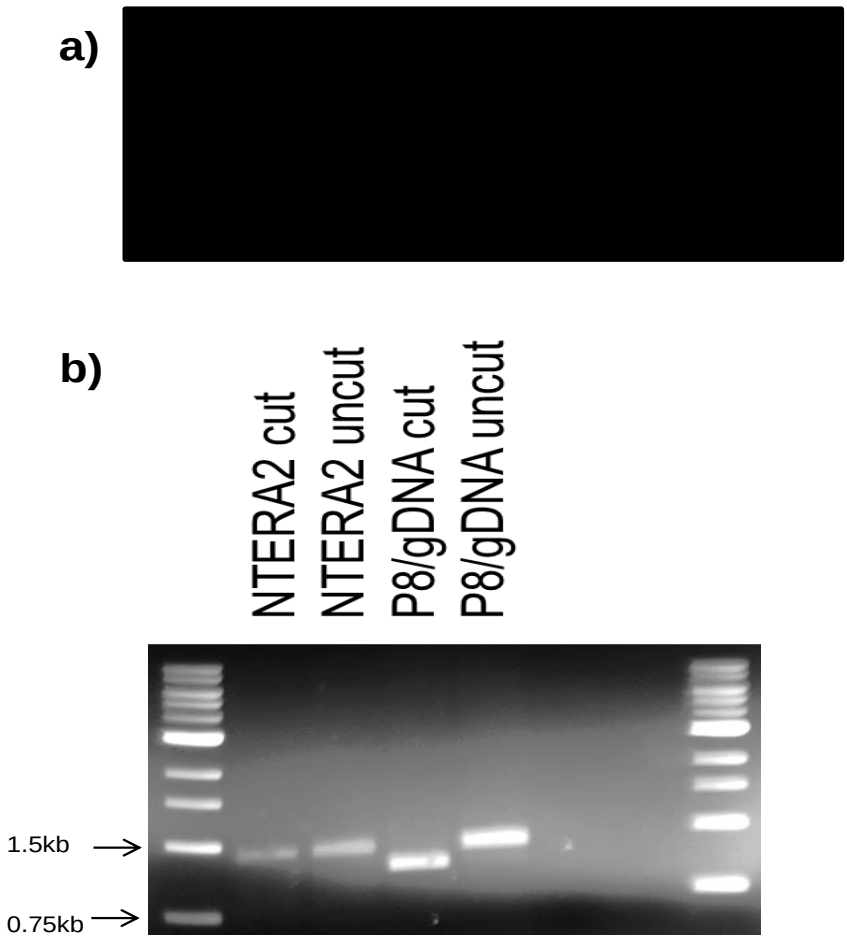

Figure 3.13. Detection of Nanog or NanogP8 using SNP analysis. a) Recognition sequence of *A1wN1*. b) *A1wN1* did not recognise and cut NTera2 cDNA due to these expressing Nanog from the parental locus. *A1wN1* did cut at its recognition sequence of NanogP8 locus from gDNA (1060bp). Images are representative of 1 independent experiment. Image was captured using UVP BioImaging system and analysed using LabWorks software.

3.3.3 Validation of the SUM-159 NRE-GFP reporter model

The SUM159 cell lines did not appear to express Nanog protein in 2D or 3D even though they express GFP, supposedly driven by Nanog protein. Furthermore, a small number of Control cells (CMVmin-GFP) were positive for GFP, and CSC medium experiments (Fig 3.7 and 3.8) showed some GFP positivity in these cells. Therefore to investigate mechanisms that might affect GFP expression independently of Nanog protein, a series of studies was performed to see if GFP could be induced in the NRE-GFP or importantly, CMV-Min-GFP cells.

3.3.3.1 Effect of hypoxia on GFP expression in SUM159 cells as determined by flow cytometry and fluorescent microscopy.

It is known that hypoxia can affect the proteasome-ubiquitin system and given that our reporter relied upon Ub-proteasome to degrade destabilised GFP, hypoxia may result in Nanog-independent effects, such as elevated GFP in the presence of hypoxia.

SUM159 cell lines were assessed for GFP expression after 1-72hr incubation in 21% (normoxia) and 5% (hypoxia) O_2. There were no significant changes in the Parent and Control cell lines in both oxygen concentrations and at any of the time points, however there was a significant increase in GFP expression in the NRE-GFP in normoxia at 48 and 72hrs ($p<0.05$) and at 72hrs in hypoxia ($p<0.05$) (fig 3.14).

Figure 3.14. Effect of normoxia vs hypoxia on GFP expression in SUM159 cell lines as determined by flow cytometry.

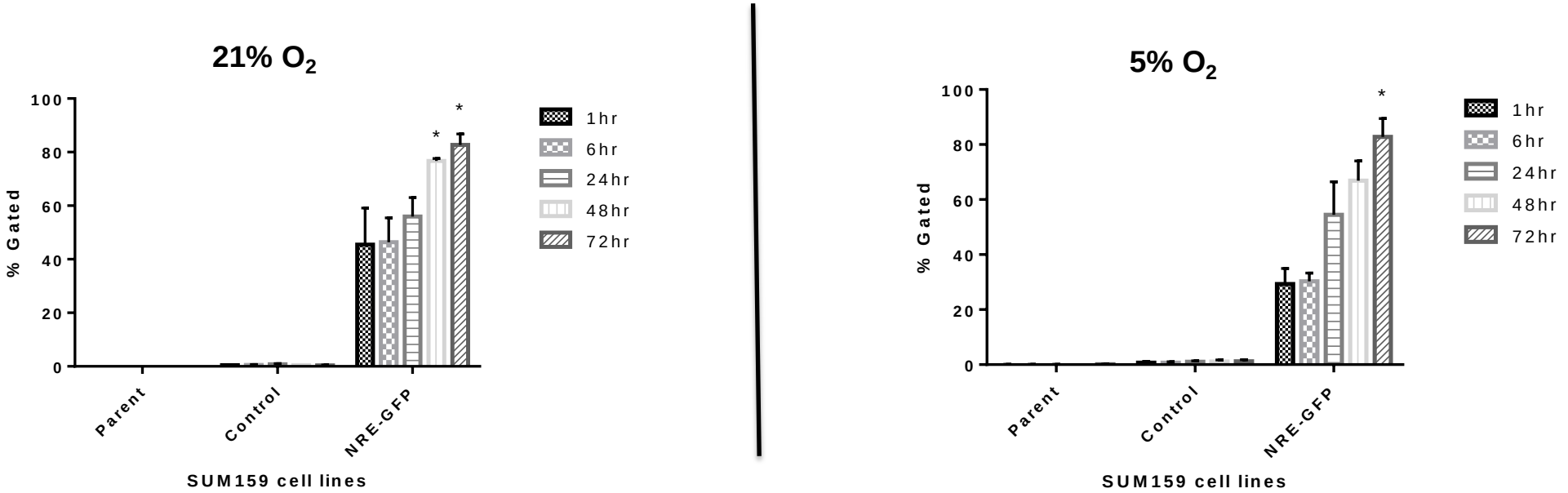

Figure 3.14. The effect of normoxia vs hypoxia of GFP expression in SUM159 cell lines as determined by flow cytometry. The SUM159 cells were incubated in 21% and 5% O_2 for 1-72hrs to assess the effect of Oxygen concentration has on GFP expression. In the normoxic environment there were no significant increase in GFP in the Parent and Control cells, however there was a significant increase in GFP from 48-72hrs ($p<0.05$) in both normoxia and hypoxia in the NRE-GFP cell line. There was no apparent enhanced GFP signal in hypoxia when controlled for effects in normoxia. All graphical data is represented as mean ± SEM and was carried out in three independent experiments. Statistical significance was obtained using the non-parametric, Kruskal-Wallis test followed by Conover-Inman post-hoc test (<0.05).

Figure 3.15. Effect of hypoxia on GFP expression in SUM159 cell line as determined by fluorescent microscopy.

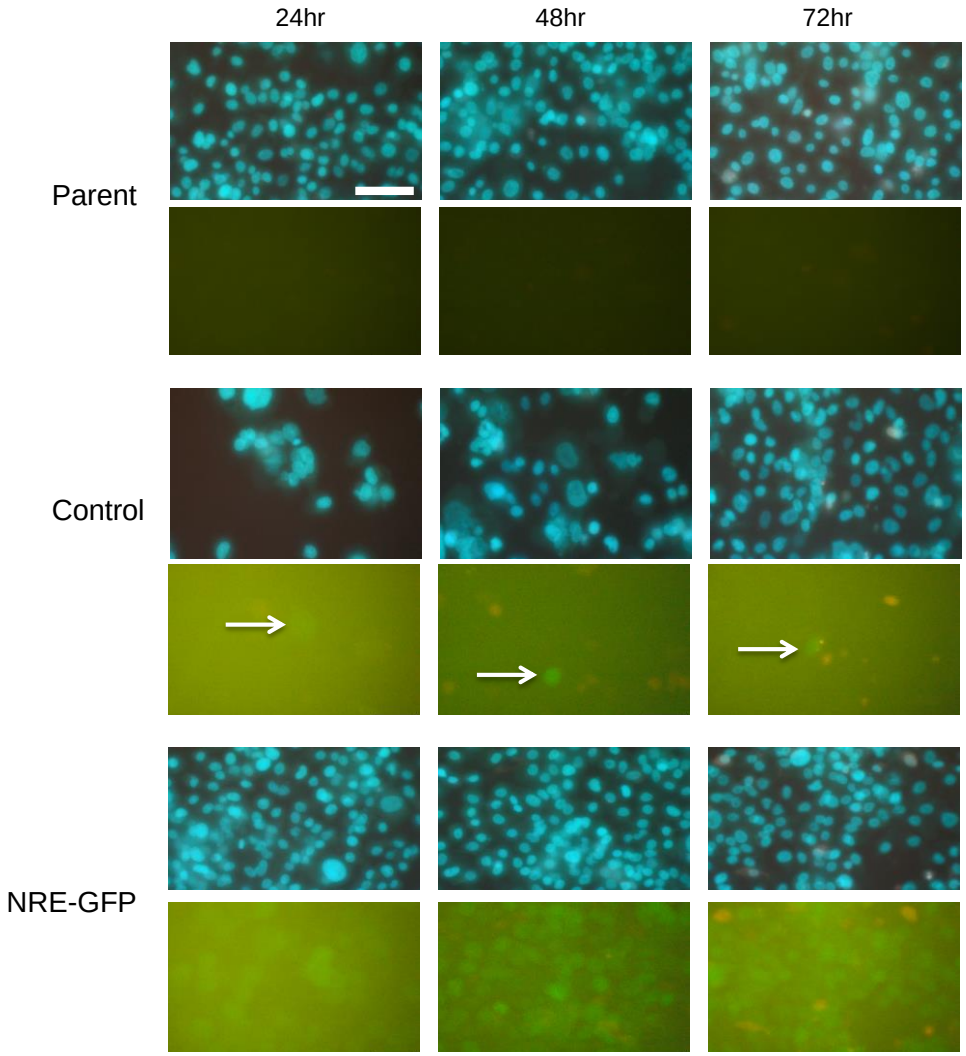

Figure 3.15. Effect of hypoxia on GFP expression in the SUM159 cells as determined by fluorescent microscopy. The SUM159 cells were incubated in 5% O2 for 24, 48 and-72hrs to assess the effect of oxygen concentration has on GFP expression. In the Parent and Control cells no increase in GFP expression was observed at any time points although the Control cell line did have some basal GFP expressing cells. The GFP intensity from 24-48hrs in the NRE-GFP cell line appeared to increase. GFP expression was determined using the Olympus IX81 inverted fluorescence microscope using the Cell-F software. Images are representative of duplicate experiments. Scale bar represents 100µm. Arrows are used to show the GFP positive cells observed in the Control cells.

3.3.3.2 Effect of proteasome inhibition using Bortezomib on GFP expression in SUM159 cell line as determined by flow cytometry and fluorescent microscopy.

As the SUM159 NRE-GFP cells express GFP that does not appear to be under the control of the NRE, a proteasome inhibitor was incubated with the cells to determine if GFP expression may be an artefact of low proteasome activity. If an increase in GFP expression in the Control cells was observed, this may suggest that the GFP derived from the NRE-GFP may have been selected based on low proteasome activity and not Nanog expression. Given that transduced cells were 'selected' for high GFP expression for the CMV-NRE-GFP cell line only, this may reflect an artefact whereby low-proteasome cells, which may represent the CSC phenotype (Pan et al. 2010) were inadvertently selected from the outset. As GFP is destabilised it is tagged for the proteasome for destruction, however if cells contain low proteasome activity an accumulation of GFP may occur. The SUM159 cell line were incubated with 0-20nM of bortezomib for 72hrs to determine the effect of inhibiting the proteasome on GFP expression.

There was a significant increase in GFP signal in the untransduced parent cell line at 10 and 20nM ($p<0.05$, 0.01) which likely represents auto-fluorescence, and a significant increase in GFP was observed at 20nM in the control cell line (fig 3.16). GFP appeared to decrease in the NRE-GFP cells although no significant differences were found. Fluorescent microscopy images confirm this (fig 3.17). Although Parent cells shows increase GFP likely to represent auto fluorescence, the Control cells are distinctly green representing basal GFP under the control of the CMV minimal promoter, potentially representing the CSC population in the NRE-GFP cells.

Figure 3.16. Effect of 72hr proteasome inhibition using Bortezomib on GFP expression in SUM159 cell lines as determined by flow cytometry.

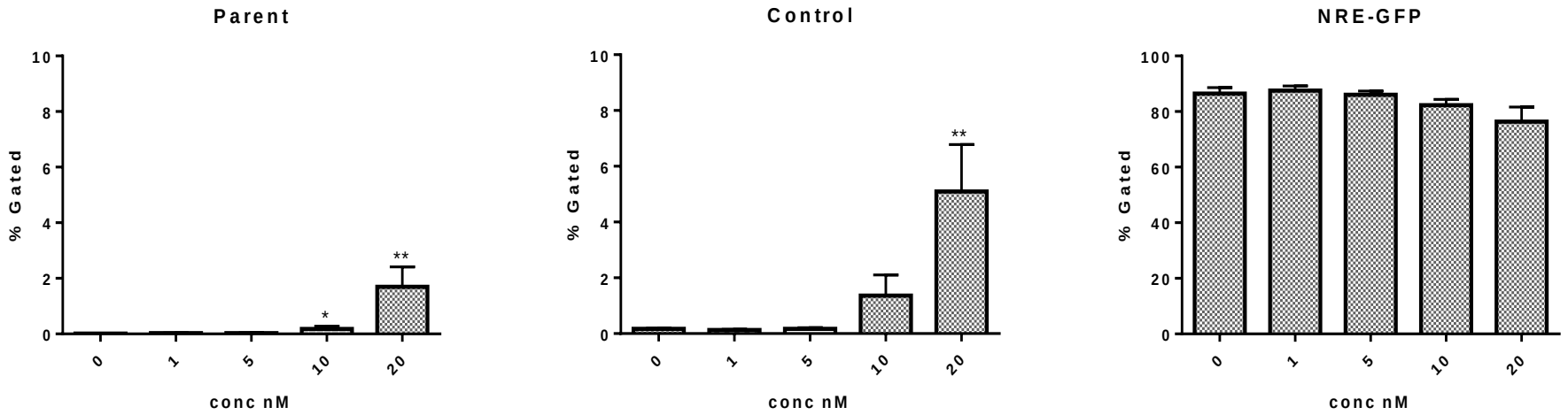

Figure 3.16. The effect of proteasome inhibition using Bortezomib on GFP expression in the SUM159 cells as determined by flow cytometry. SUM159 cells were treated with 0-20nM of Bortezomib for 72hrs prior to GFP analysis. A significant increase in GFP was found in the Parent cells treated at 10 and 20nM of Bortezomib and at 20nM in the Control cells. No significant differences were found in the NRE-GFP cells. All Graphical data is represented as mean ± SEM and was carried out in three independent experiments. Statistical significance was obtained using the nonparametric, Kruskal-Wallis test followed by Conover-Inman post-hoc test (<0.05 *, <0.01 **)

Figure 3.17. The effect of proteasome inhibition using Bortezomib on GFP expression in SUM159 cell lines as determined by fluorescent microscopy.

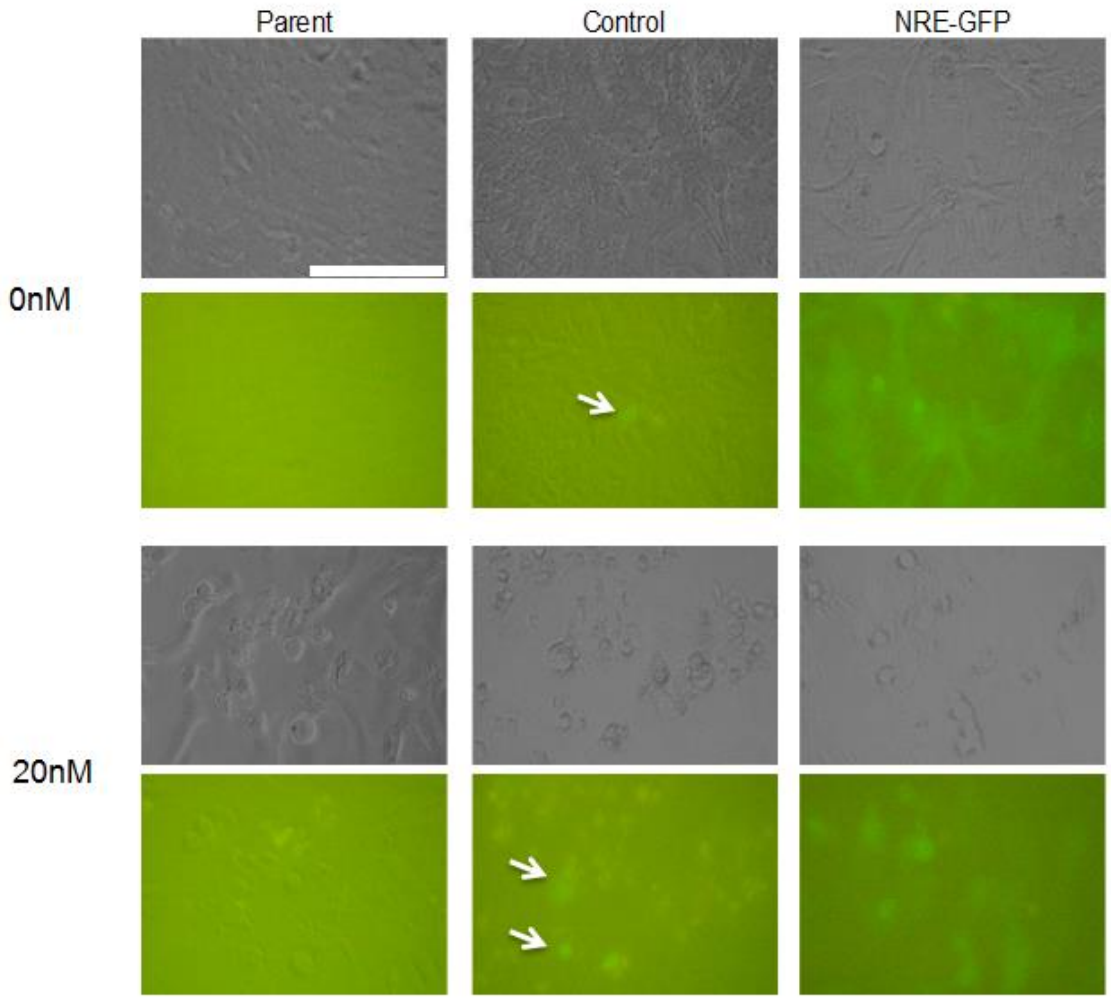

Figure 3.17. The effect of proteasome inhibition using Bortezomib on GFP expression in SUM159 cell lines as determined by fluorescent microscopy. SUM159 Parent cells do not appear to have any increase in GFP expression with 20nM of Bortezomib, however the Control cells does appear to show distinct GFP signal in some cells (arrows). No overt changes in GFP expression were observed in NRE-GFP cell line. GFP expression was determined using the Olympus IX81 inverted fluorescence microscope using the Cell-F software. Images are representative of two experiments. Scale bar represents 100µm.

3.3.3.3 Effect of 24hr proteasome inhibition using Bortezomib on GFP expression as determined by fluorescent microscopy.

A similar experiment was carried out by a Masters student under my supervision to investigate the effects of 20nM bortezomib has on GFP after 24hrs in the Parent and Control cells as 72hrs did induce GFP expression, these cells appeared apoptotic and an increase in auto-fluorescence was observed.

SUM159 Control cells had an accumulation of GFP after 24hr treatment with bortezomib as observed using fluorescent microscopy. GFP was below the level of detection in the untreated sample.

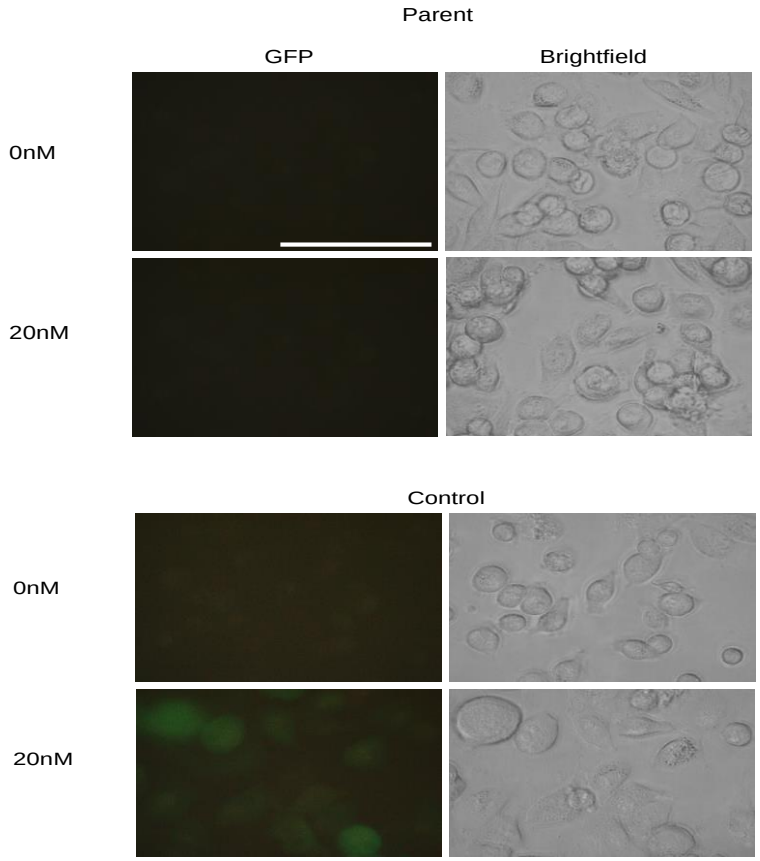

Figure 3.18. Effect of 24hr proteasome inhibition on SUM159 control cells as determined by fluorescent microscopy. There was an increase in GFP in almost all of the Control cells treated with bortezomib. GFP was below the limit of detection in the untreated sample. No GFP expression was observed in the Parent (untransduced) cell line. GFP expression was determined using the Olympus IX81 inverted fluorescence microscope using the Cell-F software. Images are representative of one experiment. Scale bar represents 100µm. Credit: Chris Smith, Masters research project thesis, Sheffield Hallam University,

3.3.3.4 Effect of proteasome inhibition using Bortezomib on GFP expression in NRE-GFP^{lo} cells as determined by fluorescent microscopy.

Epigenetic mechanisms have previously been found to induce the silencing of transfected and transduced sequences. Using a batch of NRE-GFP cells that no longer express basal levels of GFP due to unknown mechanisms, were subjected to bortezomib treatment to determine if these could re-express GFP after proteasome inhibition. If GFP expression can be reverted due to inhibition of the proteasome, this may offer some clarity as to why the control CMV min-GFP induce GFP expression in the absence to Nanog protein and might allow detection of a signal in a similar manner to the effects observed in the Control (CMVmin-GFP) cells where Bortezomib results in a reliable GFP signal.

NRE-GFP was low in the untreated cells as determined by fluorescent microscopy; however after 24hr treatment with bortezomib the NRE-GFP^{lo} cells re-expressed GFP.

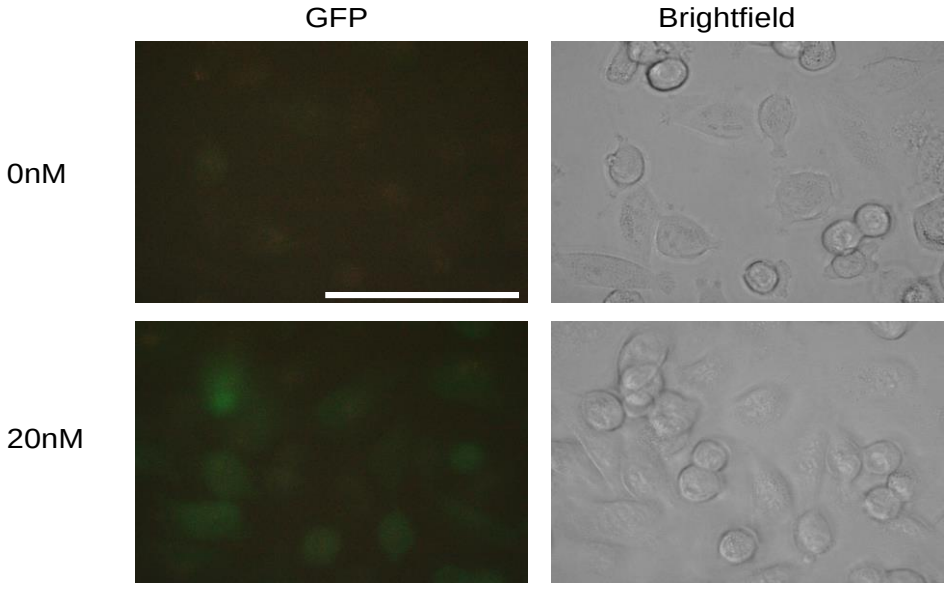

Figure 3.19. Expression of GFP in the NRE-GFP cells after 24hr treatment with bortezomib. There was an increase in GFP in almost all of the NRE-GFP^{lo} cells treated with bortezomib. GFP was below the limit of detection in the untreated sample. GFP expression was determined using the Olympus IX81 inverted fluorescence microscope using the Cell-F software. Images are representative of one experiment. Scale bar represents 100µm. Credit: Chris Smith, Masters research project thesis, Sheffield Hallam University,

3.3.3.5 Expression of Nanog-driven GFP in PC3 cell lines as determined by flow cytometry and fluorescent microscopy.

Due to inconsistencies with the SUM159 lentivirus transduced cells being supposedly NRE-GFP with no apparent Nanog mRNA or protein and GFP expression being induced in the control cell line in CSC medium and proteasome inhibition, the lentivirus transduced PC3 NRE-GFP cell line was investigated as it is reported to express Nanog protein and to validate this reporter model.

PC3; Parent, Control and NRE-GFP were assessed for GFP expression by flow cytometry and fluorescent microscopy. For fluorescent microscopy the cells were counter stained with Hoechst 33342 and Propidium Iodide to assess cell viability.

No significant GFP signal was detected in the PC3 Parent, Control or NRE-GFP cells as determined by flow cytometry and was further confirmed using fluorescent microscopy (fig 3.20).

Figure 3.20. Expression of GFP in PC3 cell line as determined by flow cytometry and fluorescent microscopy.

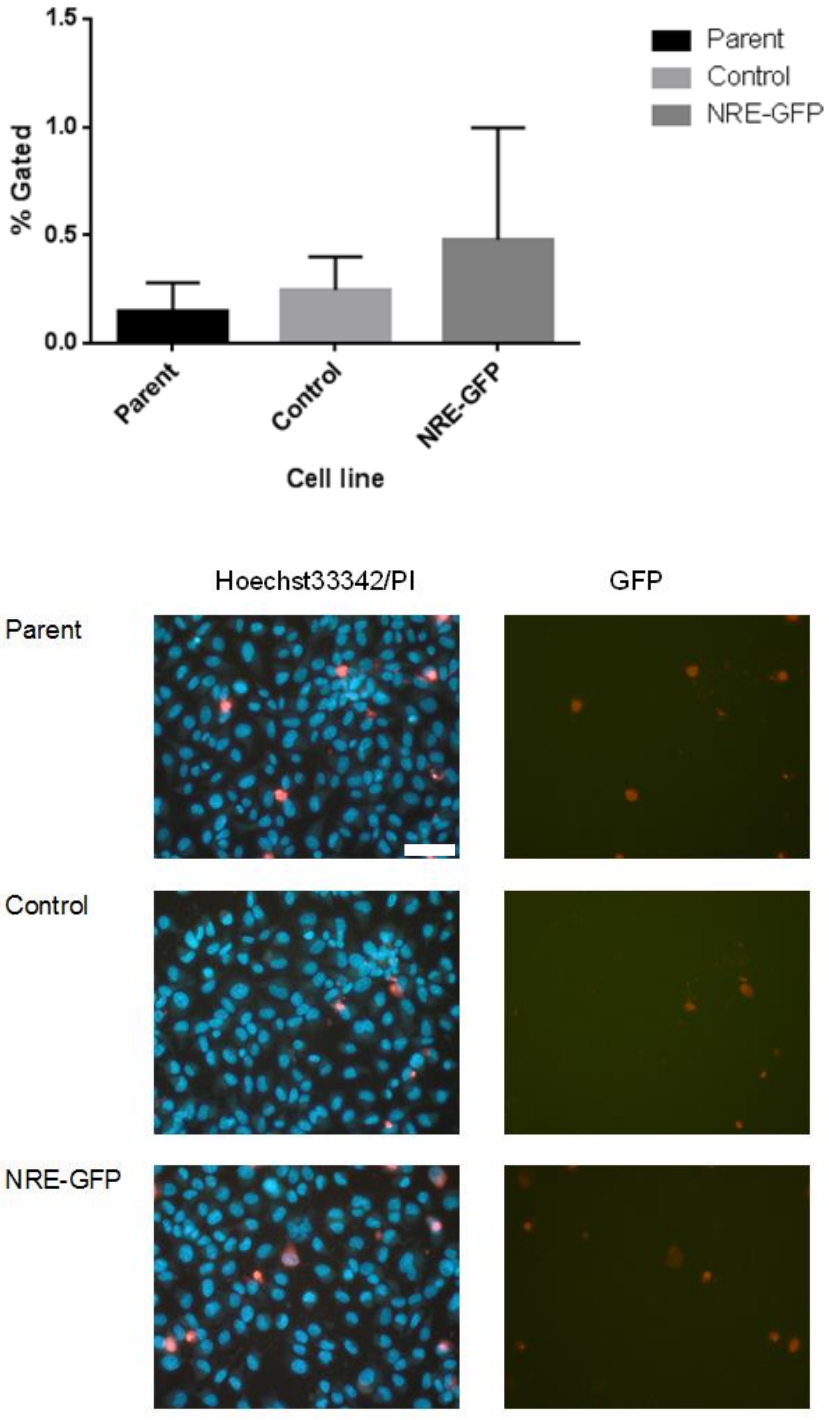

Figure 3.20. Expression of GFP in PC3 cell line as determined by flow cytometry and fluorescent microscopy. No significant GFP expression in Parent, Control and NRE-GFP cells as detected by flow cytometry. Fluorescent microscopy images confirm this. All Graphical data is represented as mean ± SEM and was carried out in three independent experiments. GFP expression was determined using the Olympus IX81 inverted fluorescence microscope using the Cell-F software. Images are representative of duplicate experiments.

3.3.3.6 Expression of GFP in PC3 NRE-GFP in 2D and CSC medium as determined by flow cytometry and fluorescent microscopy

CSC medium significantly increases GFP expression in the SUM159 Control cells. As the PC3 cell line are reported to contain a small proportion of Nanog positive cells (Jeter et al. 2009) these cells were cultured in CSC medium to potentially enrich for the Nanog expressing CSC population. As the PC3 NRE-GFP cells contains a small number of cells that are weakly GFP positive and with the rationale that these cells might express GFP driven by the NRE, the PC3 NRE-GFP was investigated.

Rare GFP positive cells were observed in the PC3 NRE-GFP cells cultured in 2D, however when these were counterstained with Hoechst 33342 this single cell had obvious signs of apoptosis as apoptotic bodies could be seen (Fig 3.21). It is well known that the proteasome reduces in activity during G2 arrest and also apoptosis and as such, destabilised GFP reporters are used for the purpose of identifying such cells (Dantuma et al. 2000).

The PC3 NRE-GFP cells cultured in CSC medium induced GFP expression, however the majority of these cells that had high intensity of GFP showed evidence of apoptosis. When analysing these cells using flow cytometry there was an increase in GFP positivity in cells cultured in CSC medium compared to 2D cell culture; however no increase in Nanog expression was detected. All data was generated in a parallel project by another student (3.21).

Figure 3.21. Expression of GFP in PC3 NRE-GFP in 2D and CSC medium as determined by flow cytometry and fluorescent microscopy

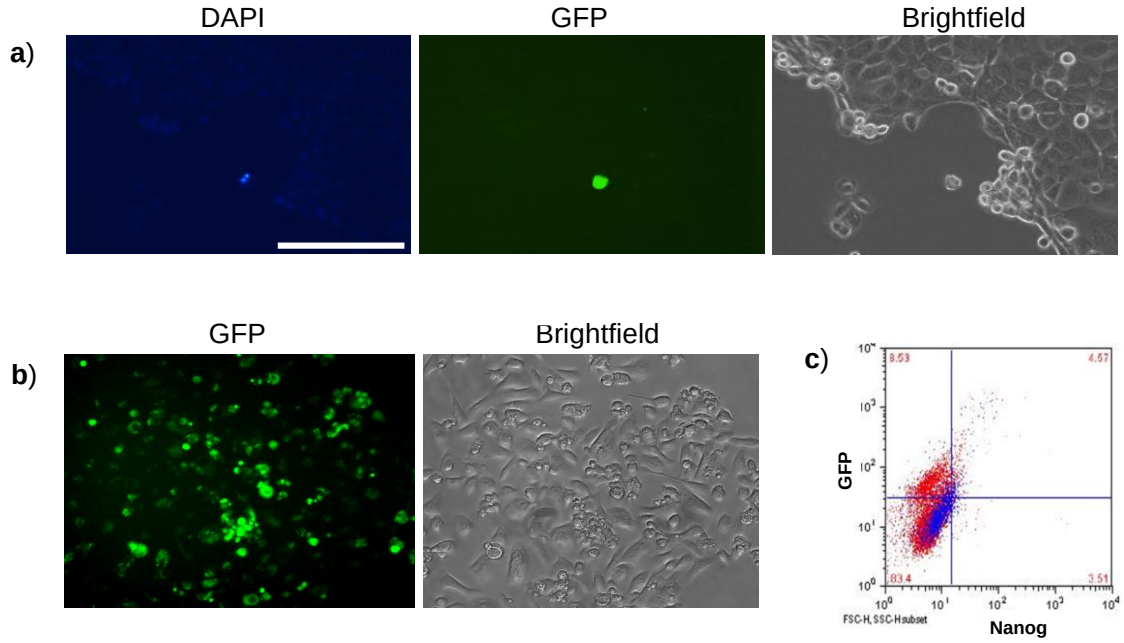

Figure 3.21. Expression of GFP in PC3 NRE-GFP in 2D and CSC medium as determined by flow cytometry and fluorescent microscopy.a) Cells cultured in 2D using complete medium. B) Cells cultured in CSC enriches for apoptotic, GFP positive cells. C) CSC medium (red), Complete medium (blue) CSC medium enriches for GFP positive cells but does not enrich for Nanog expression. Scale bar represents 100µm. Credit: Laura Mulcahy, Undergraduate research project thesis, Sheffield Hallam University

3.3.4 Characterisation of Nanog promoter-GFP or NanogP8 promoter-GFP vector systems

As the GFP in the NRE-GFP did not appear to be expressed in response to the presence of Nanog protein, a different reporter system was investigated. Within this system the promoter of Nanog or NanogP8 was directly placed upstream from GFP instead of the NRE. If transcription factors bind to the promoter region, GFP will be expressed. Therefore the readout of these vectors is a prediction of transcription factor combinations that drive Nanog gene expression, rather than Nanog protein-driven responses as in the lentiviral NRE-CMVmin-GFP vectors. Nanog promoter-GFP and NanogP8 promoter-GFP was engineered in the lab of Dr Tom Sayers, NIH, USA to identify if Nanog or NanogP8 was expressed in cancer cell lines. NTera2 was used as a positive control for parental Nanog expression and SUM159 which probably does not express Nanog protein or is below the limit of detection was used as a negative control. The CMV MAX-GFP obtained from the NIH, USA was used as a positive control for transfection.

3.3.4.1 Restriction enzyme digests of plasmids: Nanog promoter-GFP, NanogP8 promoter-GFP and CMV MAX-GFP

Confirmation of correct identification of plasmids was performed using *SpeI* restriction enzyme to cut plasmid DNA. This was carried out prior to transfection of NTera2 and SUM159 cell lines to confirm identification and expected fragment size of Nanog promoter-GFP, NanogP8 promoter-GFP and CMV MAX-GFP.

Nanog promoter driven-GFP plasmid is 7470bp in length, in its supercoiled form it was observed at 4kb. Linearised with *SpeI* was observed at 7.5kb, consistent with this. NanogP8 promoter-GFP is 7040bp in length and when cut with *SpeI*, it was observed at 7kb. CMV MAX-GFP is a high-level constitutively active promoter driving GFP as a transfection positive control and is 5701bp in length. This plasmid has two restriction

sites and as a result there were two products of expected molecular weight. All plasmids appeared, to be correct in size and had the correct number of restriction sites, therefore these plasmids are likely to be as described. (fig 3.22).

Figure 3.22. Restriction enzyme digests of Nanog or NanogP8 promoter-GFP and CMV MAX-GFP plasmids as determined by gel electrophoresis.

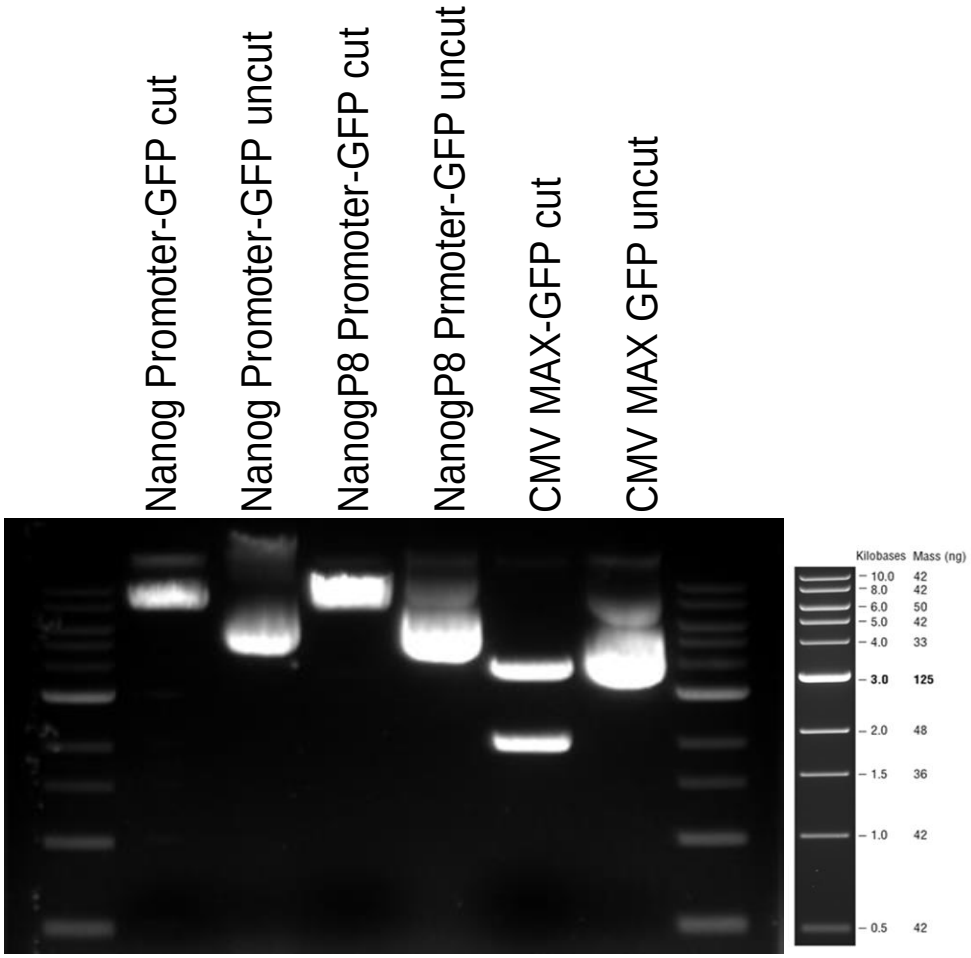

Figure 3.22. Restriction enzyme digests of plasmid after Midi-prep as determined by gel electrophoresis. Plasmids containing the promoters of Nanog or NanogP8-GFP and CMV MAX-GFP were digested using *SpeI* to determine if the correct colony containing plasmid had been selected. The uncut plasmids all appear in their coiled form and as a result these migrate quicker through the gel. The *SpeI* restriction enzyme recognises 1 site in Nanog and NanogP8 promoter-GFP and as a result the plasmids were linearised and migrated through the gel at the expected molecular weight. The *SpeI* restriction enzyme recognises 2 restriction sites within the CMV MAX-GFP plasmid resulting in 2 fragments of DNA at the expected molecular weight. Images are representative of 1 experiment. Images were captured using UVP BioImaging system and analysed using LabWorks software.

3.3.4.2 Expression of GFP after transfection with plasmids containing the promoters of Nanog or NanogP8 as determined by fluorescent microscopy.

NTera2 cell lines were used as a positive control cell line for Nanog promoter activity and the CMV MAX-GFP was used as a positive control for transfection. The SUM159 cell line is unlikely to express Nanog or NanogP8 mRNA and protein or its expression is below the levels of detection. Transfection of the SUM159 cell line with the Nanog or NanogP8 promoter-GFP was used as a negative control for Nanog promoter activity.

SUM159 cell line 'may' express Nanog mRNA derived from the Nanog locus as two independent experiments GFP was detected as seen in (fig 3.23 and 3.24). However the low frequency of such cells suggests they are more likely to represent artefacts. The NTera2 cell line which ubiquitously expresses Nanog protein failed to show any convincing GFP expression after transfection with the Nanog promoter-GFP as only a single cell expressed GFP and was observed in 2 independent experiments. No expression of GFP from the NanogP8 promoter-GFP reporter was detected in SUM159 or NTera2 cells after transfection with the NanogP8 promoter-GFP reporter vector confirming that these cells do not express NanogP8 mRNA. Transfection efficiency as determined by the CMV MAX-GFP reporter was high in the SUM159 cell line, however the NTera2 cell line was much harder to transfect resulting in a lower transfection efficiency.

Figure 3.23. Expression of GFP after transfection with plasmids containing the promoters of Nanog or NanogP8 as determined by fluorescent microscopy (a).

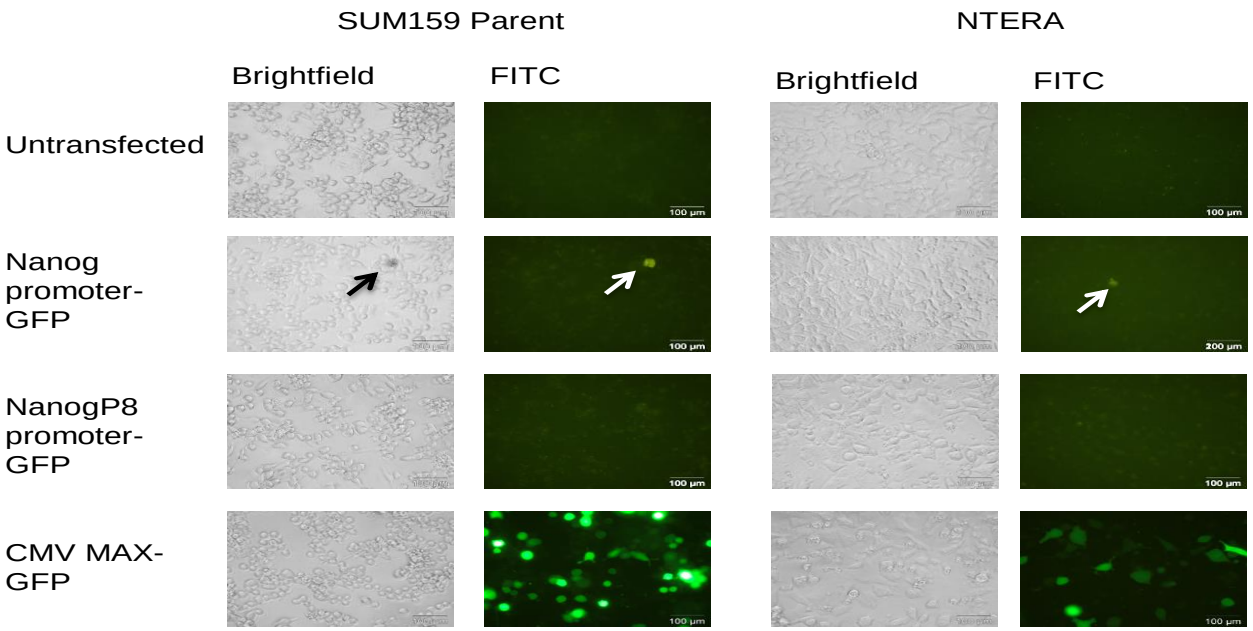

Figure 3.23. Expression of GFP after transfection with plasmids containing the promoters for Nanog or NanogP8 as determined by fluorescent microscopy. SUM159 and NTera2 transfected with the Nanog promoter-GFP appear to have a single cell that is GFP positive, or an artefact of auto-fluorescence. No GFP expression was observed after transfection with the NanogP8 promoter-GFP. The CMV MAX-GFP plasmid used as a positive control for transfection efficiency was successfully transfected into the SUM159 and NTera2 cell lines. GFP expression was determined using the Olympus IX81 inverted fluorescence microscope using the Cell-F software. Images are representative of two independent experiments

Figure 3.24 Expression of GFP after transfection with GFP-reporter plasmid containing the promoters of Nanog as determined by fluorescent microscopy (b).

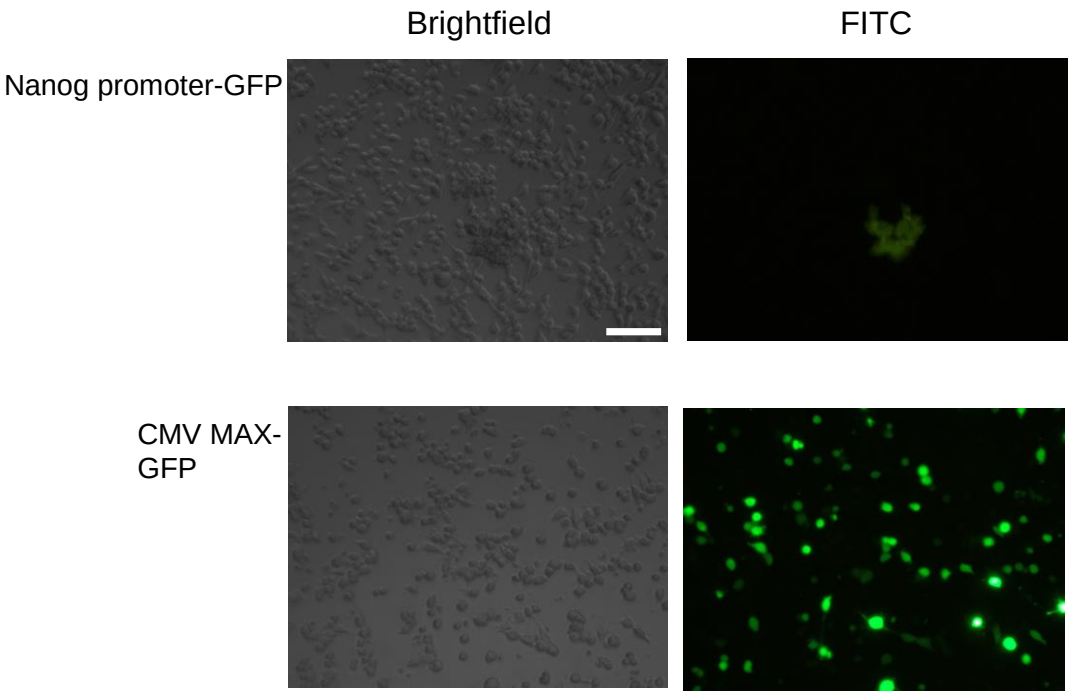

Figure 3.24. The expression of GFP in SUM159 cell line after transfection with plasmids containing the promoters of Nanog or NanogP8 as determined by fluorescent microscopy. SUM159 cell line appeared to express Nanog protein as a cluster of cells are GFP positive after transfection with Nanog promoter-GFP. The plasmid containing CMV MAX-GFP was used as a positive control for transfection efficiency. GFP expression was determined using the Olympus IX81 inverted fluorescence microscope using the Cell-F software. Images are representative of two independent experiments.

3.3.5 Expression of Nanog in breast and prostate cancer cell lines as determined by Western blot analysis.

Reporter cell lines generated to express GFP under the control of the NRE do not appear to express Nanog protein, and the vectors designed to induce GFP under the control of Nanog or NanogP8 promoters did not produce reliable GFP signal in either the positive control cells or SUM159. Western blot analysis was carried out using breast and prostate cancer cell lines cultured in 2D to determine if any of these express Nanog proteins. Actin was used as a loading control (fig 3.25).

Nanog protein expression of ~42kDa was detected in both the NTera2 and DU145 cell line and a smaller isoform of Nanog <42kDa (potentially the core peptide) was detected in the LNCAP cell line. Nanog expression in PC3 and SUM159 cells was at or near the limit of detection and MCF7 cells did not appear to express Nanog protein.

Figure 3.25 Expression of Nanog in breast and prostate cancer cell lines as determined by western blot analysis.

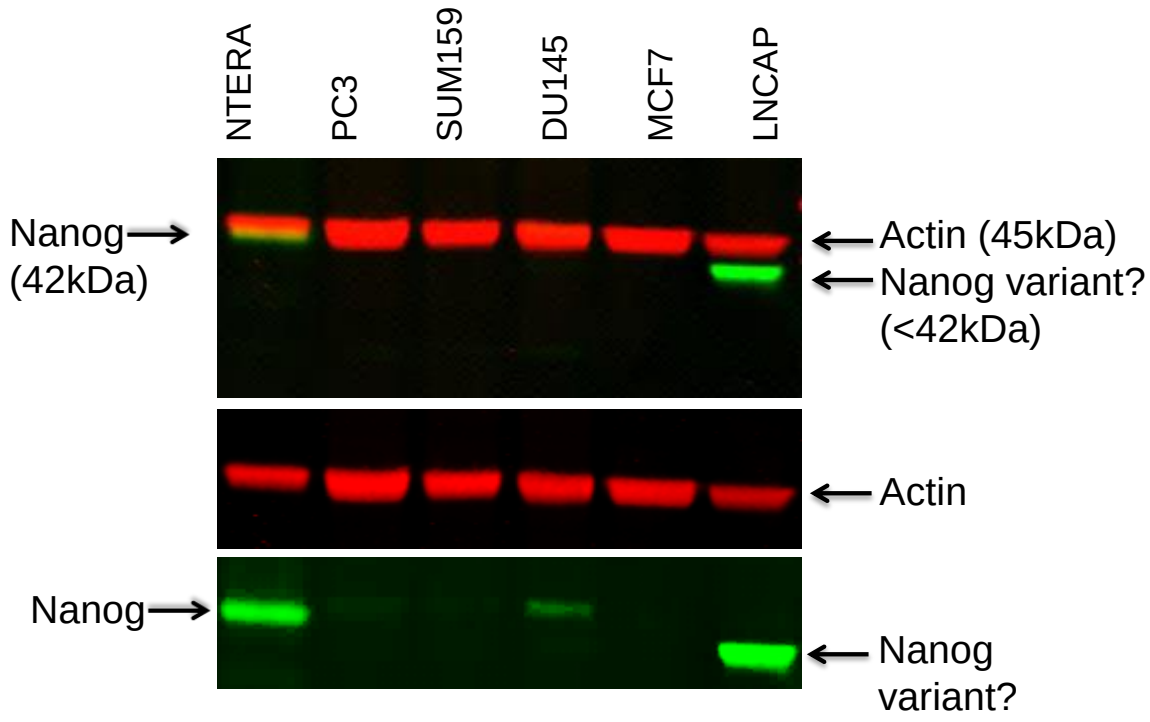

Figure 3.25. Expression of Nanog protein in breast and prostate cancer cell lines as determined by Western blot analysis. Cells grown in 2D cell culture were lysed and probed for the expression of Nanog protein, and Actin was used as a loading control. NTera2 cells express the predicted 42kDa Nanog protein derived from the Nanog gene. DU145 cell line express the same molecular weight species of Nanog but at much lower levels. The LNCAP cell line expresses a variant species of Nanog protein. Western blot analysis is representative of 2 independent experiments. Membrane was imaged using the Odyssey® CLx Imaging System and data was analysed using the LI-COR Image Studio Software for the Odyssey CLx.

3.3.5.1 Optimisation of 2D gel electrophoresis for the identification of Nanog species detected by western blotting.

Nanog expression was detected in NTera2, DU145 and LNCAP cell lines using western blot analysis, although a smaller fragment <42kDa which may represent the core peptide (unmodified) or a Nanog retrogene (fig 3.25). Two dimensional gel electrophoresis (2DGE) was optimised using protein from the NTera2 cell line.

Initial optimisation experiments showed that the isoelectric focusing of NTera2 lysate was not fully optimised as confirmed by the Coomasie Blue staining (fig 3.26) and Western blot analysis. The Actin protein signal was slightly elongated at the correct molecular weight and the Nanog protein signal was smeared across the membrane due to being under focused (fig 3.26).

Subsequent attempts at isoelectric focusing (fig 3.27) revealed that this method was not optimised due to it being under-focused, although Coomasie blue staining was faint it was also apparent from the Western blot analysis as the Actin protein was again slightly elongated at the correct molecular weight but the Nanog protein was split into 2 regions at <pH 5 and 7 (fig 3.27).

As the Coomasie Blue stain was quite faint due to the low amount of protein loading onto the isoelectric focusing strip, the SDS polyacrylamide gels were subjected to silver stain to determine if the isoelectric focusing had been optimised. Figure 3.28 shows examples of a) under-focused and b) correct isoelectric focussing (fig 3.28). These conditions were used for subsequent experiments including 2D Western blotting for Nanog protein.

2D SDS PAGE followed by Western blot analysis using optimised conditions revealed as two individual spots of Nanog in the NTera2 lysate protein sample. Actin was detected ~pH 5.5 and Nanog protein at ~pH 6.6.

2D gel electrophoresis and Western blot analysis failed to detect the aberrant-sized Nanog protein species that had been observed in the LNCAP or DU145 cell lines by Western blotting. Actin was detected at the reported correct pI.

Figure 3.26. Optimisation of 2D gel electrophoresis for the identification of Nanog protein

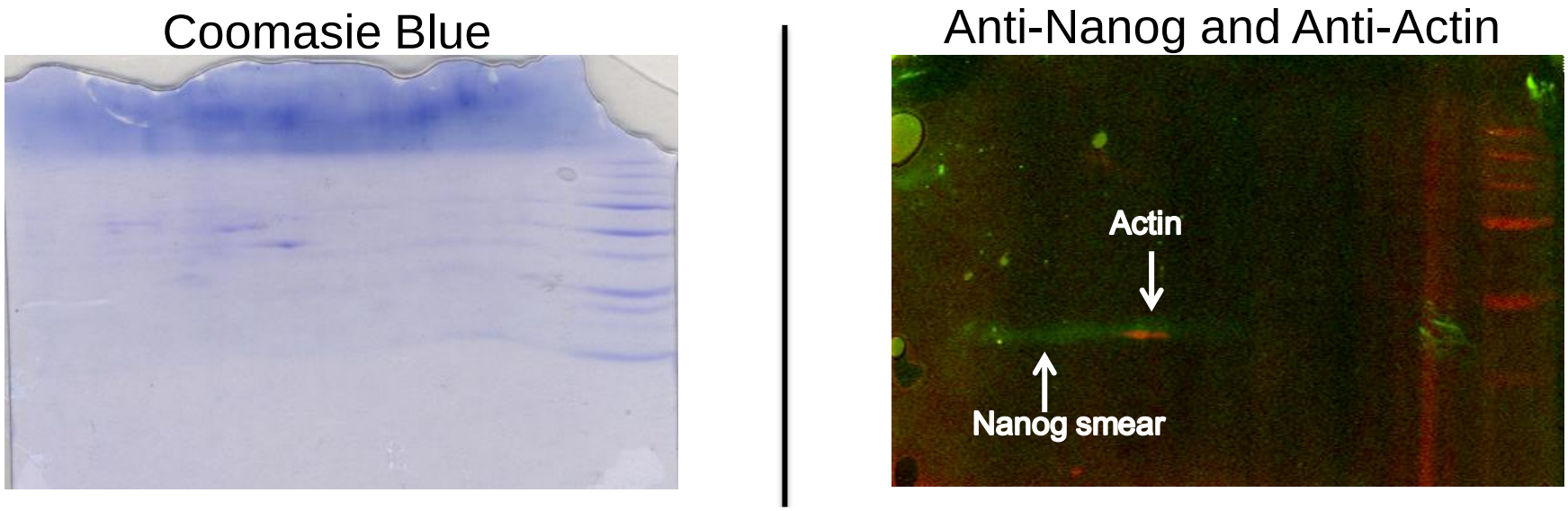

Figure3.26. Optimisation of 2D gel electrophoresis for the identification of Nanog protein. NTera2 protein was subjected to isoelectric focusing to identify Nanog and Actin species. The Coomasie stained gel appears to be quite faint in colour and the proteins appear to be under focused as seen by the smearing. The Western blot analysis of the membrane confirms that the isoelectric focusing is un-resolved due to the smearing of both Actin and Nanog proteins. Membrane was imaged using the Odyssey® CLx Imaging System and data was analysed using the LI-COR Image Studio Software for the Odyssey CLx

Figure 3.27.Optimisation of 2D gel electrophoresis for the identification of Nanog protein.

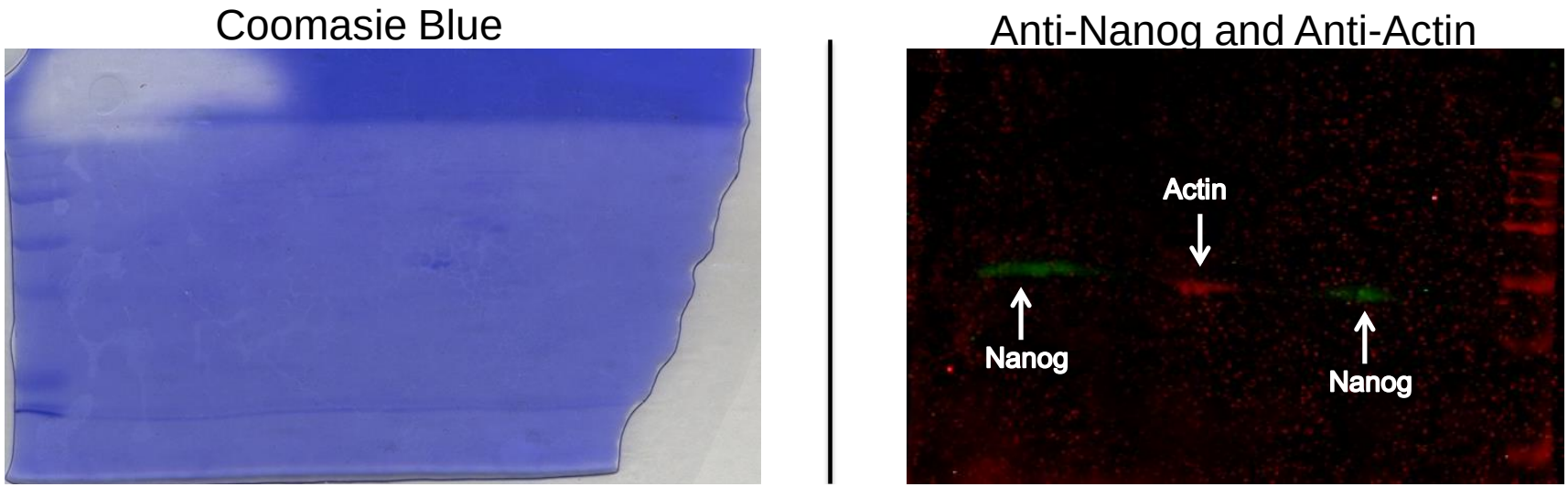

Figure 3.27. Optimisation of 2D gel electrophoresis for the identification of Nanog protein. NTera2 protein was subjected to isoelectric focusing to identify Nanog and Actin species. The Coomasie stained gel appears to be quite faint in colour and the proteins appear to be under focused. The Western blot analysis of the membrane confirm that the isoelectric focusing is un-resolved due to the smearing of both Actin and Nanog proteins located at pH 4 and 6. Membrane was imaged using the Odyssey® CLx Imaging System and data was analysed using the LI-COR Image Studio Software for the Odyssey CLx

Figure 3.28. Optimisation of 2D gel electrophoresis for the identification of Nanog protein.

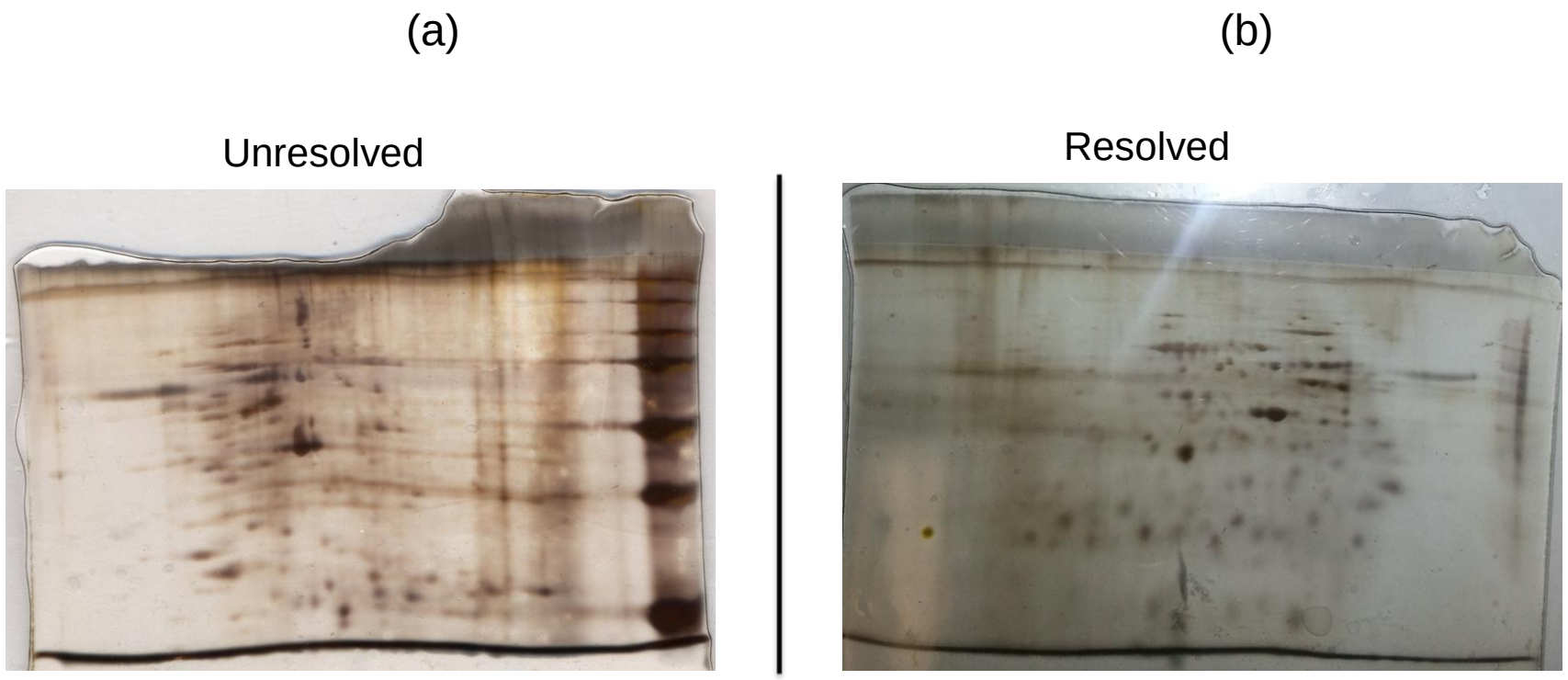

Figure 3.28. Optimisation of 2D gel electrophoresis for the identification of Nanog protein. NTera2 protein was subjected to isoelectric focusing to identify Nanog and Actin species. The silver stained gel in (a) showed an example of isoelectric focussing being slightly under focused due to smearing of protein bands at lower pH values and the higher molecular weight proteins are not fully resolved. b) shows correctly resolved isoelectric focussing with single spots of focused proteins. Membrane was imaged using the Odyssey® CLx Imaging System and data was analysed using the LI-COR Image Studio Software for the Odyssey CLx .

Figure 3.29 Optimisation of 2D gel electrophoresis for the identification of Nanog protein.

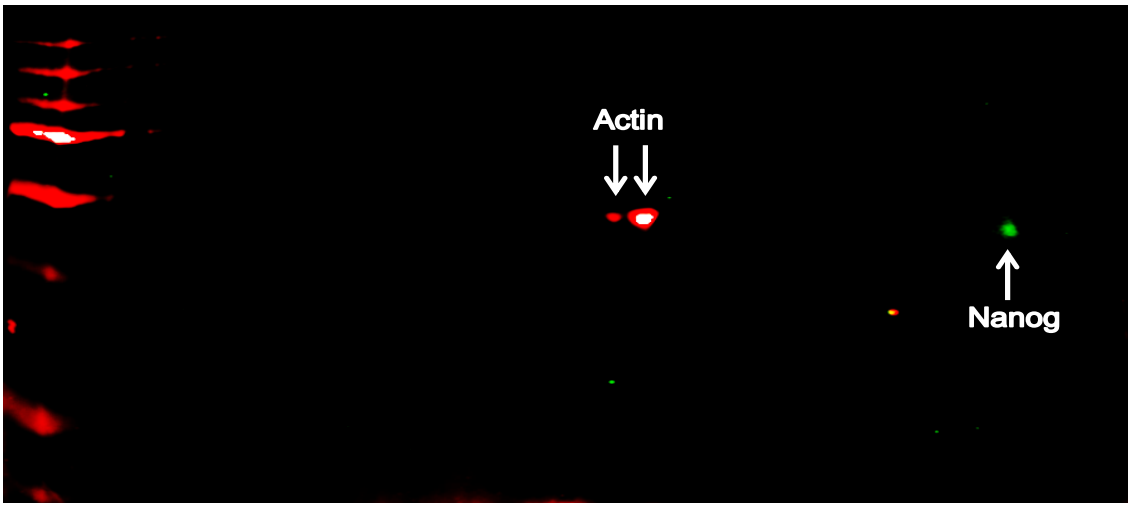

Figure 3.29. Optimisation of 2D gel electrophoresis for the identification of Nanog protein. NTera2 protein was subjected to isoelectric focusing to identify Nanog and Actin species. Actin was fully resolved with an isoelectric point at ~5.5, showing a charged trail, potentially a posttranslational modified Actin species. The predicted pI of Actin is 5.29. Nanog protein appears to be fully resolved with a pI of ~6.6 which is consistent with reported pI for this protein.

Figure 3.30. Identification of Nanog species in DU145 and LNCAP cell lines.

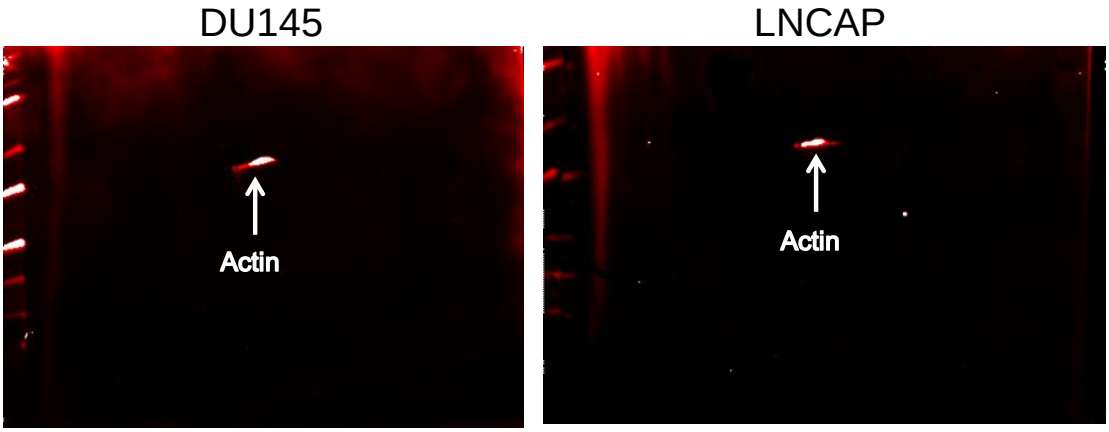

Figure 3.30. Identification of Nanog species in DU145 and LNCAP cell lines. DU145 and LNCAP protein was subjected to isoelectric focusing to identify Nanog and Actin species. Actin was resolved with an isoelectric point at ~5.5, although no charged trail was detected. Nanog protein was not detected in the DU145 or LNCAP cell line. Membrane was imaged using the Odyssey® CLx Imaging System and data was analysed using the LI-COR Image Studio Software for the Odyssey CLx

3.4 Discussion

3.4.1 Characterisation of the Lentivirally-transduced NRE-GFP and CMV-Min-GFP reporter cell lines

Lentivirus transduced cell line were used to determine if there was any correlation and co-localisation between NRE-GFP^{+ve} and CD44, CD24 and CD181 in the breast cancer cell lines as determined by flow cytometry.

All the SUM159 cells cultured in 2D mimicked that of the Parent cells for cell surface expression of CD44, CD24 and CD181. In addition, there were no significant differences in CD44^{+}/CD181^{+}, CD181^{+}/CD24^{-} phenotype and CD44^{+}/CD24^{-} breast CSC in 2D cell culture. The NRE-GFP cell line also mimicked that of the parental cell line when cultured in 3D, however the Control cell line did not correlate with the parental cells. As these are reporter cell lines, and the Control cells should have an identical phenotype to the Parent in both 2D and 3D cell culture, it was surprising to find that the Control cell line was phenotypically different in 3D. In particular CD181 expressing cells were significantly higher in the control cell line and CD24 was significantly downregulated, thus relating to a more aggressive phenotype. In addition CD44 was significantly downregulated, and it has been found that CD44 negative cells correlate with lymph node metastasis and negative for both CD44 and CD24 confirms a high histological grade (Giatromanolaki et al. 2011). The Control cell line cultured in 3D appeared to proliferate much quicker, resulting in much larger spheroids. Xu et al, (2014) also found that culturing cells in alginate resulted in a change of cancer stem related genes in proportion to the size of the spheroids (Xu et al. 2014). Due to the size of the Control cells and strong interactions with neighbouring cells, disassociation of the spheroids into a single cell suspension may have been difficult due to the tight

junctions facilitating robust cell-cell interactions resulting in improper staining of antibodies although every effort was made to avoid this.

As expected there was significantly more GFP in the NRE-GFP reporter cell line than that of the untransduced Parent and Control cell lines however there was no difference between the GFP/$CD44^{+}$, GFP/$CD24^{-}$ and GFP/$CD181^{+}$ phenotype when cultured in 3D, therefore the NRE-GFP did not select for a CSC phenotype in 3D cell culture.

3.4.2 Detection of Nanog in SUM159 cell lines

The SUM159 cell line did not express Nanog mRNA and protein or was below the limit of detection when cultured in 2D and 3D. In addition to this, although there is no apparent expression of Nanog protein there is a significant amount of GFP expression in 2D which surprisingly decreases under 3D cell culture. Previously, it has been found that Nanog expression is upregulated in cancer cell lines cultured in 3D cell culture (Xue et al. 2015, Fujiwara et al. 2013, Xu et al. 2014). SUM159 NRE-GFP cells cultured as 3D spheroids in CSC medium resulted in no induction of NRE-GFP at any time points and likely to be no increase in Nanog expression, however there was a significant increase in GFP in the Control cells in 3D growth. If these Control cells are able to accumulate GFP without Nanog, then presumably this is also possible for the NRE-GFP cells, so experiments were performed to elucidate the mechanism of the false positive of the NRE-GFP and the induced CMVmin-GFP Control cells.

3.4.3 Hypoxia

Since hypoxia is known to induce Nanog expression and can also reduce proteasome activity, hypoxia-induced effects on NRE-GFP cells were assessed. A hypoxic environment did not induce GFP expression, when cultured for up to 72hrs in the NRE-

GFP cell line as there were no differences between normoxia and hypoxia but there was an increase in GFP expression in both 5% (hypoxia) and 21% (normoxia) but this was at the longer time points, possibly due to the cells being more confluent. There was no significant increase in GFP in Control cells, however GFP intensity appeared higher in the rare GFP positive cells after 48 and 72hrs at 5% O_2 as determined by fluorescent microscopy. Hypoxia has been previously found to induce Nanog expression in cell lines, tumour models and ESC (Hasmim et al. 2013, Zhang et al. 2016, Petruzzelli et al. 2014).

3.4.4 Potential role of the proteasome-Lo phenotype on NRE-GFP and Control cells.

Since proteasome-Lo is a CSC marker (Pan et al. 2010) and similar assays to these reporters are used to report proteasome-Lo CSC (Lagadec et al. 2014) we tested whether inhibiting the proteasome, as a mimic of low proteasome activity could affect the NRE-GFP and Control cells. To do this, cells were cultured with the proteasome inhibitor Bortezomib. When the SUM159 cells were subjected to proteasome inhibition, to mimic that of low proteasome activity identified as a potential cancer stem cell marker (Vlashi et al. 2013) there was no overt increase in GFP expression in the NRE-GFP cell line, however these already highly expressed GFP. However in a different batch of NRE-GFP cells that had little GFP expression due to GFP being reduced after every passage (<passage 30) GFP was re-expressed when treated with 20nM of bortezomib. There was also a significant increase in GFP signal in the Control cells, and an increased signal vs untreated cell in the parental cells. Untransduced Parental cells were auto-fluorescent shown by fluorescence microscopy and the signal was more yellow-green than genuine GFP signal, therefore any apparent GFP signal is likely due to these cells containing dead or dying, as it has been found that apoptotic cells auto-fluoresce (Hennings et al. 2009, Levitt et al. 2006). This is supported by the

absence of green cells by fluorescence microscopy in the parental cells, but presence of induced GFP green signal in the Control cells after 72hrs bortezomib treatment. At 24hrs after bortezomib treatment GFP was expressed in almost all of the Control cells, and there was no obvious signs of auto-fluorescence in the Parent cells. Responses were weaker at 72 hours, but GFP subsequently shown to be potently induced at 24 hours in response to 20nM bortezomib. The Control cell line acts by producing low basal levels of GFP which was rapidly degraded, and is ideal for reporter assays so that GFP does not accumulate and hence GFP correlates with recent promoter activity. This basal expression of GFP was increased after proteasome inhibition could be in-part the result of some auto-fluorescence as detected by flow cytometry but also GFP accumulation mimicking what is observed in breast cancer stem cells with low proteasome activity (Vlashi et al. 2013) and microscopy images confirmed the presence of green cells.

Sorting cells based on GFP expression with the notion that the GFP positive cells are Nanog driven identifies major flaws with reporter cell lines. The NRE-GFP cells were sorted at the NIH, USA using FACS to separate the GFP^{+ve} (Nanog driven) from the GFP negative cell populations, however no sorting was carried out on the Control cells as under normal conditions, no overt GFP signal was visible. This is a crucial flaw in this design as selecting based on GFP may be selecting for cells with low proteasome activity or apoptotic cells. Jeter et al (2011) carried out a similar experiment with NanogP8 promoter-GFP in PC3, DU145 and LNCAP cell lines however he did not use a control (Minimal promoter-driven GFP), and separated the cells based on GFP expression prior to expansion and *in vivo* studies. Jeter et al (2011) did show co-expression of GFP and Nanog in the LNCAP cell line but failed to show any for DU145

and PC3 cell lines. Therefore caution should be taken in interpreting such experiments as 'selecting' for proteasome-Lo cells may select for CSC-like cells independently of Nanog expression, however the resulting GFP^{+ve} cells may, independently of Nanog, represent a more CSC-like phenotype than Control cells.

3.4.5 Transfection of SUM159 cell line with Nanog or NanogP8 promoter-GFP.

Transfection of the NTera2 cell line with the Nanog promoter-GFP and NanogP8 promoter-GFP vectors using the Viromer transfection reagent resulted in a low-medium transfection efficiency with the CMV MAX-GFP reporter. Using the Nanog promoter-GFP reporter, very few cells were observed that looked positive for GFP expression therefore Nanog promoter activity. As the NTera2 cell line ubiquitously expressed Nanog protein, even though transfection efficiency is low a substantial amount of these cells should have been positive. This raises doubts as to whether this vector is responding in a manner of which it was designed. The SUM159 cell line was easier to transfect as transfection efficiency using the CMV MAX-GFP reporter vector was high. Some GFP expression was observed after transfection using the Nanog promoter-GFP, suggesting that these may express Nanog protein derived from the Nanog locus as a few cells showed some signal however the signal was not convincingly green.

No GFP was detected after transfection using the promoter of NanogP8-GFP in either cell line. NTera2 cells only express Nanog protein from the Nanog locus, therefor no GFP should have been observed whereas the SUM159 cell line did not appear to express any form of Nanog protein, or it is below the levels of detection.

3.4.6 Expression of Nanog in prostate and breast cancer cell lines

The NTera2 cell line used as the positive control expressed Nanog at the mRNA and protein level, corroborating earlier work (Jeter et al. 2011a, Liu et al. 2014a, Huang et al. 2014). Nanog protein expression was not detected in the PC3 cell line although Gong et al, 2012 found that Nanog expression was extremely low in the bulk population of cells (Gong et al. 2012). The DU145 cell line did however have more expression of the ~42kDa Nanog protein which has been previously identified using Western blot analysis (Kawamura et al. 2015) and immunohistochemistry (Jeter et al. 2009). The LNCAP cell line did not express the ~42kDa Nanog in accordance with Yuan et al, 2007 (Gu et al. 2007) but did express the smaller potentially unprocessed form. This species has also been identified by Jeter et al, 2009 although this group also identified the ~42kDa species in LNCAP cell line (Jeter et al. 2009). The MCF7 cell line appeared not to express Nanog protein or it was below the limit of detection as Jeter et al, 2011 identified the Nanog protein ~42kDa at very low levels (Jeter et al. 2011a). 2D gel electrophoresis and Western blot analysis identified Nanog protein at the predicted pI in the NTera2 cell line, however previously identified Nanog species derived from the DU145 and LNCAP cell lines were undetected using this technique. This may be due to alternative posttranslational modifications of the core peptide altering its pI or these maybe other Nanog species.

3.4.7 Concluding remarks

Using a lentivirus transduced reporter cell line that expresses destabilised GFP in response to NRE is not a suitable model to identify the cancer stem cell population due to the reliability of reporter systems that rely on destabilised GFP. The results clearly show that in the absence of Nanog, the reporter is active and in the Control cells (CMV-min-GFP), the reporter can be switched on by altering the proteasome, CSC

medium and by hypoxia. Furthermore, the insert on the NRE-GFP which is activated by an unknown mechanism, may be periodically silenced in some cell populations. Therefore evidence strongly suggests that this reporter is not a reliable model of Nanog expression.

4 Targeting cancer cells with withanolide derivatives

4.1 Introduction

Recent advances in understanding and identifying the diverse biological factors that contribute to cancer development and progression have led to the development of specific cancer targeting and gene specific agents. Some of these biological factors may be amplified or mutated growth receptors, chromosome amplifications and mutated signaling proteins (Arkenau, Carden and de Bono 2008). Selectively targeting these processes can eradicate the cancerous cells whilst discriminating against normal cells. Many different compounds and biological molecules have been identified for their anti-proliferative and death inducing properties in various cancers.

4.1.1 Targeting breast cancer

Current therapeutic treatments in breast cancer patients are chemotherapy, in addition to hormonal therapy and growth factor signaling inhibition (Blowers and Foy 2009). Patient prognosis and treatment options are determined by the estrogen (ER), progesterone (PR), and human epidermal growth factor receptor 2 (Her-2) receptor status (Arkenau, Carden and de Bono 2008). In 70% of breast cancers these are positive for ER or PR (Arkenau, Carden and de Bono 2008), however overexpression of HER2 in breast cancer indicates a more aggressive and invasive phenotype than Her-2 low breast cancers and are more susceptible to recurrence (Slamon et al. 1987, Slamon et al. 1989). Drugs such as anastrazole, letrozole and exemestane are used in estrogen-responsive cancer cells as these inhibit estrogen synthesis by blocking aromatase, or drugs such as tamoxifen that modulates the estrogen receptor (Early Breast Cancer Trialist, Collaborative Group 1998). As HER2 is overexpressed in up to 30% of breast cancers due to gene amplification, a monoclonal antibody known as trastuzumab (Herceptin) is used to improve survival rates (Slamon et al. 2001). Other targets in breast cancer are vascular endothelial growth factor (VEGF) signaling (Miller et al.

2005) and tyrosine kinase inhibitors of the epidermal growth factor receptor (EGFR) and Her-2 receptor (Geyer et al. 2006).

4.1.2 Targeting Prostate cancer

Prostate cancer was first recognised as being hormonally driven over 65 years ago (Huggins and Hodges 2002) and up until the 1980s the main form of treatment for metastatic prostate carcinoma was surgical castration (Pezaro, Mukherji and De Bono 2012). After this time it was found that using a leutenising hormone releasing hormone (LHRH) analogue could achieve the same survival benefit as surgical removal of the prostate (Huhtaniemi et al. 1991). Advances in hormonal therapy has seen the use of estrogen agonists, LHRH agonists, LHRH antagonists, Anti-androgens (steroidal and nonsteroidal), and ketoconazole to induce castration (Hammerer and Madersbacher 2012).

Drugs such as Diethylstilboestrol were a first line targeted agents used as estrogen agonist as these works to reduce serum testosterone by a negative feedback on the hypothalmic-pituatary axis to suppress LHRH (Hammerer and Madersbacher 2012). Diethylstilboestrol was an effective therapeutic agent at inducing castration but serious concerns were made due to its thrombogenic side effect and increased cardiovascular mortality (Hammerer and Madersbacher 2012) although recent understanding of the estrogen receptor (ER) and its role in normal prostate epithelium and cancer progression has allowed the reevaluation of the role of ERα and more importantly the loss of ERβ in prostate cancer (Oh 2002). Since the 1980s many LHRH agonists were synthesized as these reduce testosterone levels to that achieved by orchiectomy or estrogen agonists (The Leuprodile Study Group 1984). LHRH agonists work by down regulating LHRH receptors therefore suppressing Leutenizing hormone

(LH) and Follicle stimulating hormone (FSH) and decrease testosterone synthesis resulting in testosterone castration levels between 2-4 weeks (Schally 1999, Limonta, Montagnani Marelli and Moretti 2001). Unfortunately in the first few days after treatment an increase in testosterone (flare) is observed causing unwanted side effects such as increased bone pain and acute bladder outlet obstruction in patients with advanced prostate cancer (Labrie et al. 1984). A counteractive measure such as simultaneous administration with anti-androgens for the first 2 weeks inhibits circulating androgen signaling via its receptor (Labrie et al. 1984). LHRH antagonists are also used in androgen deprivation therapy as these induce a rapid decrease in LH, FSH and testosterone as these bind to the LHRH receptor competitively and do not cause a testosterone flare (Mcleod 2003, Trachtenberg et al. 2002). Unfortunately many of the LHRH antagonists that are available are deemed unsuitable in clinical settings as these have been associated with serious and in some instances life threatening histamine mediated side effects (Aus et al. 2005). Anti-androgens used as a monotherapy or in combination with LHRH agonists used in androgen depletion therapy can be classified based on their chemical structure, either steroidal such as cyproterone acetate or non-steroidal such as flutamide and nilutamide (Hammerer and Madersbacher 2012). A study of niluatmide has found that it affects progression-free survival in almost 40% of patients with metastatic prostate cancer (Decensi et al. 1991) and in the treatment of hormone resistant prostate cancer (Desai, Stadler and Vogelzang 2001, Kassouf, Tanguay and Aprikian 2003).

Figure 4.1 Androgen signaling and inhibitor pathway

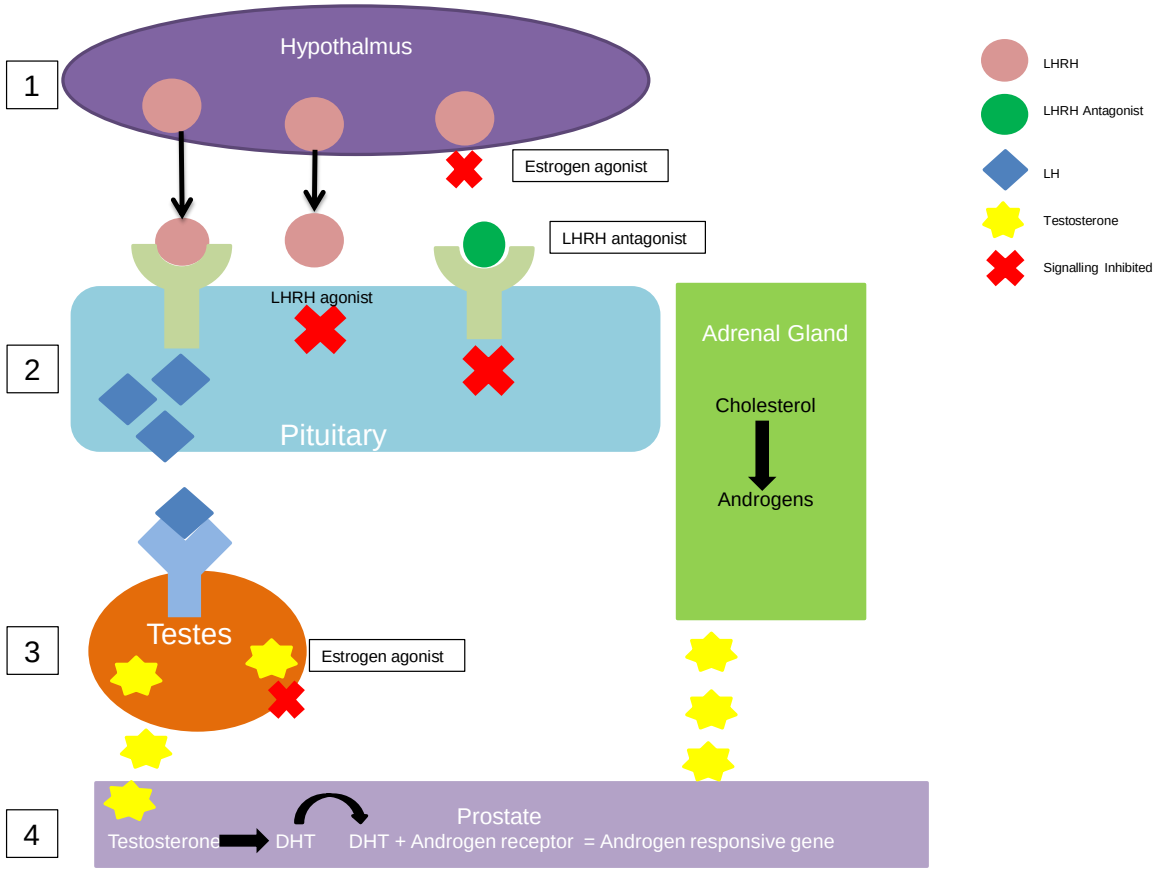

Figure 4.1 Androgen signaling and inhibitor pathway. 1) The hypothalamus releases LHRH which when bound to its receptor induces the production and release of (2) LH from the pituitary. 3) LH when bound to its receptor at the testes induces the release of testosterone which defuses through the membrane of the prostate gland. 4) Testosterone can bind to the androgen receptor or be converted to DHT and then interact with the androgen receptor for nuclear translocation and the upregulation of androgen responsive genes. Another mechanism utilised in cancer is the production and conversion of cholesterol within the adrenal gland to androgens for further androgen signaling. Estrogen agonist can work on the release of LHRH at the hypothalamus and also inhibit the release of testosterone from the testes. LHRH antagonist can down regulate the expression of LHRH receptor whereas LHRH antagonist can competitively bind to the LHRH receptor and inhibit LHRH signaling.

Although hormonal manipulation has a significant effect on castrate levels of testosterone and clinical and biochemical features, most men go on to develop castrate resistance prostate cancer (CRPC) also known as advanced prostate cancer after a period of time (Pezaro, Mukherji and De Bono 2012). The consensus for many years was that CRPC is androgen independent (Hellerstedt and Pienta 2002), however

recent findings have suggested that many patients that have CRPC express androgen dependent genes indicating that they still respond to androgens (Schweizer and Antonarakis 2012). A mechanism for facilitating the advancement of prostate cancer is loss of specificity of the androgen receptor for testosterone and also DHT which has a five fold greater affinity for the receptor than testosterone, and the receptor may become sensitive to progesterone, estrogen and antiandrogens (Taplin et al. 1995). An emerging drug known as Abiraterone has demonstrated positive results in phase III clinical trials for the treatment of CRPC as this selectively and irreversibly inhibits CYP17, an enzyme responsible for the conversion of pregnenolone to androgens (Pezaro, Mukherji and De Bono 2012).

Figure 4.2 Blockage of androgen synthesis with Abiraterone

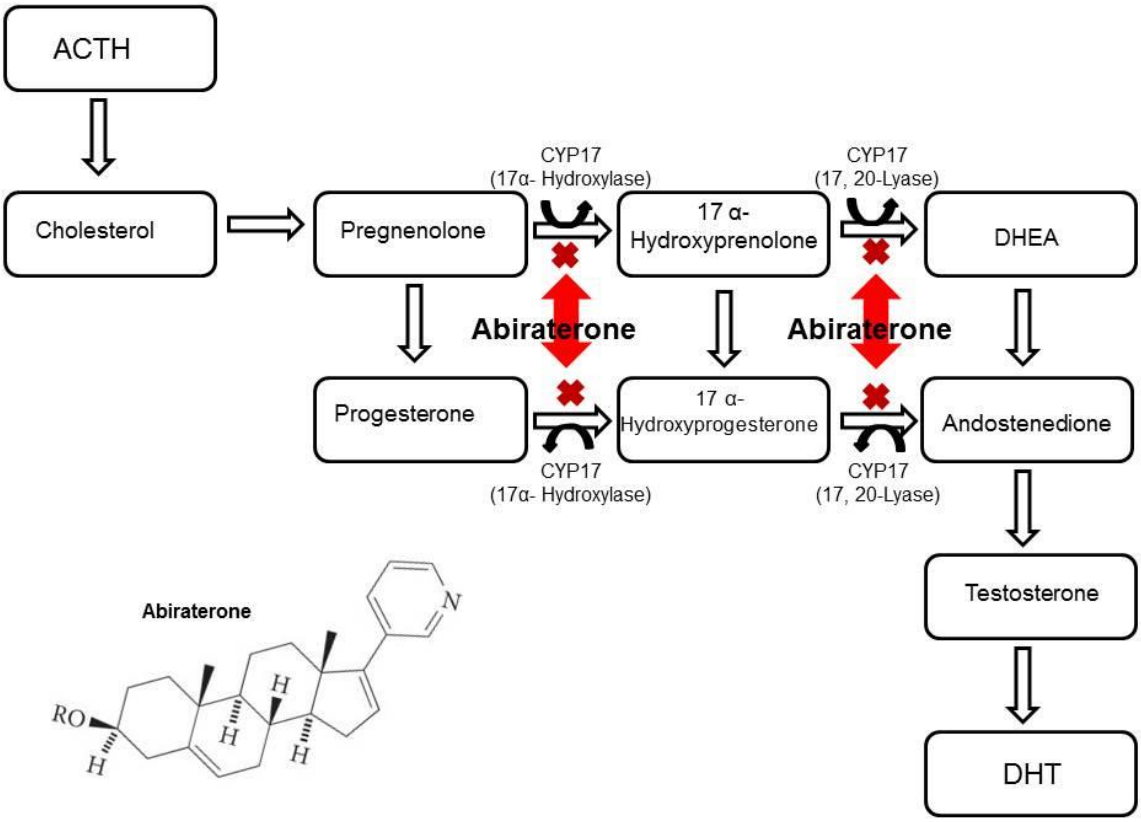

Figure 4.2 Blockage of androgen synthesis with Abiraterone. ACTH is a steroidal molecule that can be converted into cholesterol and various other steroids by cytochrome P450 superfamily members. Pregnenolene is the substrate for CYP17, an enzyme with hydroxylase and lyase properties. Abiraterone is a synthetically derived steroidal compound that when bound to CYP17 inhibits pregnenolene from binding and testosterone and DHT production.

4.1.3 Limitation of currently used therapeutics in cancer

In some cases of advanced CRPC, these have acquired the ability through mutation, brought about by selective pressure and clonal selection to overcome the castrate levels of androgens by upregulation of the androgen receptor to respond to very low levels of androgens (Rehman and Rosenberg 2012), upregulation of intra-tumoral steroidogenesis to facilitate tumour growth (Montgomery et al. 2008) and upregulation of the androgen receptor nuclear coactivators for androgen, target gene transcription in low levels of androgens (Gregory et al. 2001). In addition, alternative splicing of the Androgen receptor induces a constitutively active protein, independent

of hormone levels (Sprenger and Plymate 2014). A translocation of androgen-activated TMPRSS2 with oncogenes ERG or ETV1 has also been identified in many prostate cancers (Tomlins et al. 2005). In advanced breast cancer and CRPC these become more difficult to treat with surgery, radiotherapy and chemotherapy and if metastatic, these are incurable. One potential target in later stage disease would be to target the cancer stem cell population as these contribute to tumour relapse and therapeutic resistance.

Discovery of a novel therapeutic agent with a high therapeutic index, that can discriminate between normal and benign tissues, malignant or metastatic carcinomas would greatly improve treatment options, quality of life and mortality for patients with cancer.

4.1.4 Withanolides

Withanolides are naturally occurring compounds that are derived from the *Solanaceae Sp.* family of plants and have been traditionally used in Chinese and Ayurveda medicine (Singh, et al. 2010). They are steroidal compounds built on an ergostane skeleton of C28 in which oxidization of C-22 and C-26 forms a δ-lactone ring on the nine-carbon side chain (Glotter 1991) and are chemically called 22-hydroxyergostane-26-oic acid 26,22-lactone (Mandal, Dutta et al. 2008). To date there are over 350 withanolides that have been isolated and identified (Chen, He et al. 2011), and all of these are structurally diverse allowing the study of structure-activity, function and biological properties (Wang, Tsai et al. 2012). Withanolides and their derivatives are very interesting compounds as these have a diverse array of biological activities both *in vitro* and *in vivo* such as antimicrobial, insect anti-feedant, anti-inflammatory, immunomodulating, anti-stress, radiosensitizing and anti-tumor (Budhiraja, Krishan and Sudhir 2000).

Figure 4.3. Schematic of withanolide derivatives derived from the *Solanaceae Sp*.

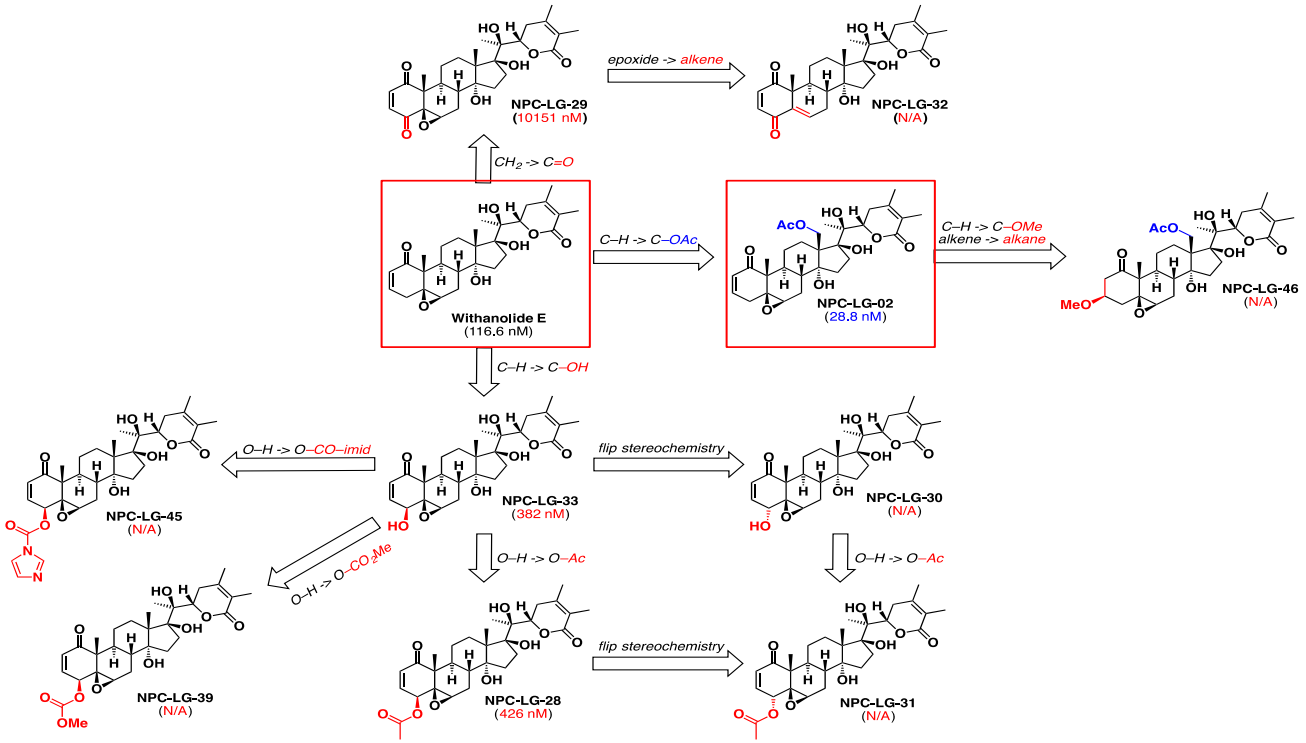

Figure 4.3. Schematic of withanolide derivatives derived from the *Solanaceae Sp*. family or chemically modified. The most widely investigated withanolide derivative known as Withaferin A structure is comprised of the ergostane skeleton of C28 in which oxidization of C-22 and C-26 forms a δ-lactone ring on the nine-carbon side chain. The other derivatives have identical core structures with some additional groups such as hydroxy, methoxy and acetyl to different carbon positions. Withanolide derivatives, Withanolide E (WE) and LG-02 used throughout this chapter are highlighted with a red box. All compounds were provided by Dr Thomas Sawyers at the National Institute of Health (NIH).

Withanolides and some of the derivatives are potent inhibitors of proliferation and induce apoptosis in many types of cancers (Kakar et al. 2014, Roy et al. 2013, Szic et al. 2014). They share a high degree of similarity within the core structure however they are each unique, based on subtle changes in their core structure, and their side chains and have different biological targets and mechanisms of action. Some anti-cancer properties identified are growth inhibition (Kakar et al. 2014) and cell cycle arrest (Szic et al. 2014, Das et al. 2014), apoptosis (Wang et al. 2012a, Hahm, Lee and Singh 2014) , anti-inflammatory, decrease in invasion (Szic et al. 2014) and metastasis and can also target CSC (Kakar et al. 2014).

4.1.5 Cell cycle control in normal and cancer cells

The cell cycle is a normal process of cell growth and division carried out by dividing cells (Curtis 1983). There are two consecutive processes of cell division which are characterized by DNA duplication and segregation of replicated chromosomes into two genetically identical cells (Vermeulen, Van Bockstaele and Berneman 2003). These two processes are mitosis which includes prophase, metaphase, anaphase and telophase and interphase which includes G_1, S and G_2 phases (Norbury and Nurse 1992, Lajtha, Oliver and Ellis 1954). During cell division the cell spends the majority of the time in interphase as this process typically takes up to 23 hours, 12 of these hours are spent in S phase with the remaining time spent in G_1 and G_2 phase and only 1 hour in mitosis (Alberts, Wilson and Hunt 2015). G_1 phase and G_2 phase are gap stages in which cells are allowed time to grow and are also crucial, in order to monitor the internal and external environment (typically growth factor signaling) to ensure conditions are favorable for DNA duplication during S phase and mitosis (Nurse 1990, Moreno and Nurse 1994). G_1 phase is a crucial stage in the cell cycle as cells decide whether they will commit to DNA synthesis in favorable conditions, spend a longer time in G_1 or go

into a specialized resting stage known as G_0 in which cells can remain in an un-proliferative state for days to years or in some non-proliferative cells permanently (Vermeulen, Van Bockstaele and Berneman 2003). If the signals for growth are apparent the cell will pass through an irreversible commitment point at the end of the G_1 phase known as the restriction point and enter S phase (Pardee 1974). Other cell cycle check points and regulatory transition areas are located at the G_2/M transition and at the metaphase to anaphase transition in which cells can withdraw from the cell cycle if problems are detected within the cell or extracellular environment (Gelfant 1977, Rieder et al. 1995).

4.1.6 Cell cycle control system

In order for cell cycle progression a biochemical switch occurs with a number of proteins acting in a binary fashion as the cells goes from interphase to mitosis and cytokinesis (Moreno and Nurse 1994, Pardee 1974, Lajtha, Oliver and Ellis 1954). The central components of this are cyclin dependent kinases (Cdks) binding tightly with their partners known as cyclins (Harper and Adams 2001, Arellano and Moreno 1997). Unlike CdKs that are stably expressed in the cell, cyclin levels are altered throughout each stage of the cell cycle in order to initiate the next phase (Yang, Hitomi and Stacey 2006). Increased levels of cyclin protein interacts with Cdk forming a cyclin-CdK complex at specific stages, followed by a rapid degradation of cyclin protein which further allows cells to progress through the different stages of the cell cycle (Arellano and Moreno 1997). In order for the cyclin-Cdk to be fully activated a Cdk-activating kinase phosphorylates the complex at the active site, causing a conformational change ensuing for cyclin-Cdk phosphorylation of target proteins (Bockstaele et al. 2006, Pavletich 1999). Although cyclical changes of cyclin levels are the predominant way of controlling Cdk activity other mechanisms are in place during the cell cycle (Bockstaele

et al. 2006) such as phosphorylation at the roof of the cyclin-Cdk complex inhibits activity. In addition, binding of Cdk inhibitor proteins such as p27, p21 and p16 to the complex distorts the structure of the complex and active site rendering it inactive (Blain 2008, Hall, Bates and Peters 1995). In vertebrates there are four classes of cyclins, namely Cyclin D, E, A and B with three isoforms of cyclin D and 4 types of Cdks that are expressed in different stages of the cell cycle (Morgan 1997). If DNA is damaged, un-replicated or the chromosome is unattached to the spindle the cell will remain in the gap phases or at the Metaphase to Anaphase transition until intracellular defects have been rectified (Cohen-Fix and Koshland 1997, Tinker-Kulberg and Morgan 1999, Musacchio and Salmon 2007). Alternatively the cells will be primed to undergo apoptosis (Bartek and Lukas 2001).

Figure 4.4. Phases of the cell cycle

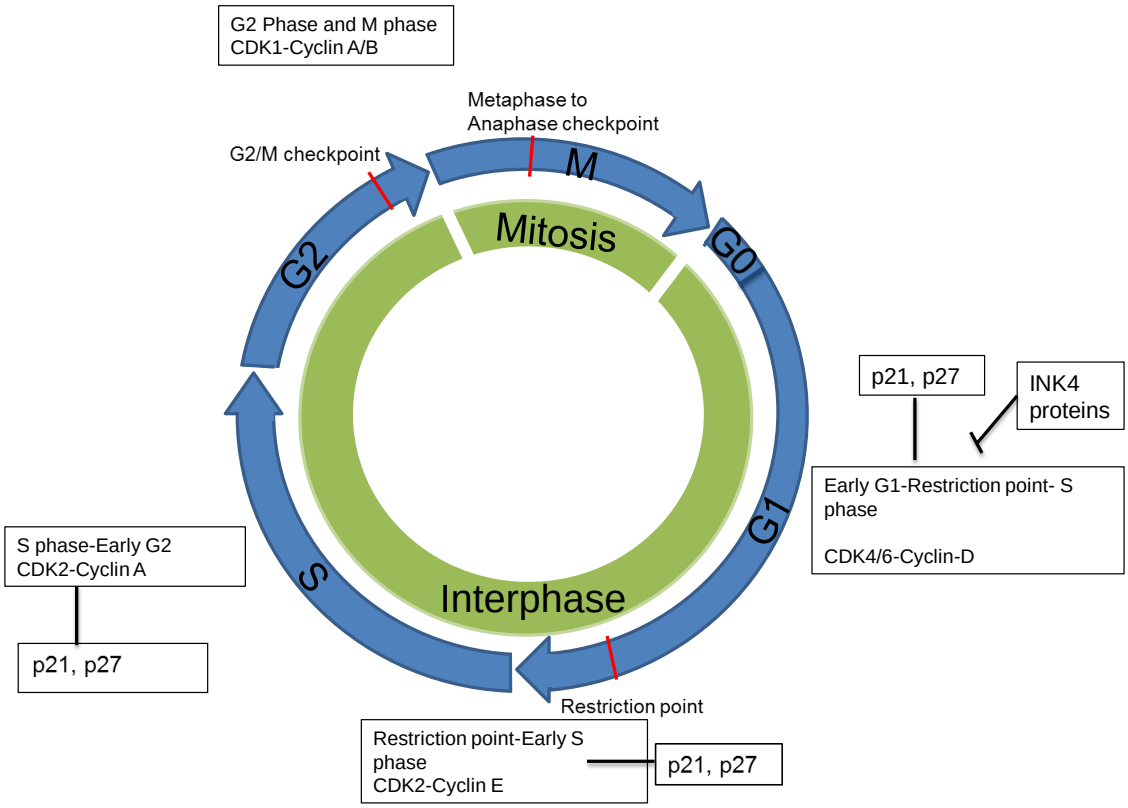

Figure 4.4 Phases of the cell cycle as adapted from (Alberts, Wilson and Hunt 2015). The cell cycle consists of 2 phases called interphase and mitosis. Interphase consists of 3 gap phases named G0, G1 and G2 phase in which the cell is deciding whether or not to undergo a round of cell proliferation or remain in a gap/resting state temporarily, permanently or undergo apoptosis. S phase is where DNA duplication is taking place. Mitosis can be further divided into prophase, metaphase, anaphase and telophase. Various proteins are responsible for regulating the cell cycle such as cyclin and cyclin dependent kinases that drive the cell cycle or inhibitors such as p21, p27 and INK4.

Stage of cell cycle	Cyclin	Cdk	Function	Stage in the cell cycle levels decrease
G1	D	4, 6	Induces G1/S cyclins	S
G1/S	E	2	Drive progression through G1/S	S
S	A	2, 1	Stimulates DNA replication	Mitosis
M	B	1	Stimulates entry into mitosis	Mid-mitosis

Table 4. Cyclin and Cyclin dependent kinases location throughout the cell cycle.

As previously mentioned, the cyclin-CdK complexes are responsible for driving the cell cycle by phosphorylation of target proteins (Pavletich 1999, Bockstaele et al. 2006). During G1 and S phase CDK4-cyclin D1, CDK2-cyclin E, and CDK2-cyclin A complexes, differentially inactivates the tumour suppressor protein retinoblastoma (RB) (Zarkowska and Mittnacht 1997). pRB is a nuclear phosphoprotein that in its hypophosphorylated state interacts with a transcription factor, known as E2F (Lundberg and Weinberg 1998) resulting in no transactivation of G1 phase target genes, however when pRB is hyperphosphorylated E2F can no longer interact with this growth inhibitory complex, facilitating the progression into S-phase of the cell cycle (Lees et al. 1993).

4.1.7 Apoptosis

Type 1 programmed cell death (PCD), commonly referred to as apoptosis is a normal process required for cellular destruction (Kerr, Wyllie and Currie 1972) This process is imperative during embryogenesis (Lorda-Diez et al. 2015), remodeling of the tissue architecture in order to maintain tissue homeostasis (Harada et al. 2004) , proper development and functioning of the immune system (Elmore 2007) ageing and in many diseased states (Zhang and Herman 2002). Neurodegenerative diseases, ischemic damage, autoimmune disorders and in many types of cancer, too much or too little apoptosis has occurred resulting in a diseased phenotype (Elmore 2007). In normal conditions when a cell undergoes apoptosis, a cascade of biochemical events occurs in order to dispose of unwanted cells and this process is facilitated by extrinsic and/or intrinsic signaling.

4.1.8 Morphology of apoptosis

In the early stages of apoptosis the morphology of the cell is altered as cell shrinkage takes place, cells are smaller in size with the cytoplasm being denser and organelles tightly packaged (Kerr, Wyllie and Currie 1972). Pykonosis also occurs at this stage and is the most characteristic feature of apoptosis (Elmore 2007). Extensive blebbing of the cell membrane precedes pykonosis followed by karyorrhexis and the formation of apoptotic bodies. Organelles and DNA are packaged into intact plasma membranes (apoptotic bodies) (Elmore 2007) to prevent intracellular components being released into the extracellular matrix thus preventing an immune response and secondary necrosis for the engulfment and removal by macrophages (Fadok et al. 2001, Kurosaka et al. 2003).

Figure 4.5. Morphology of Apoptosis.

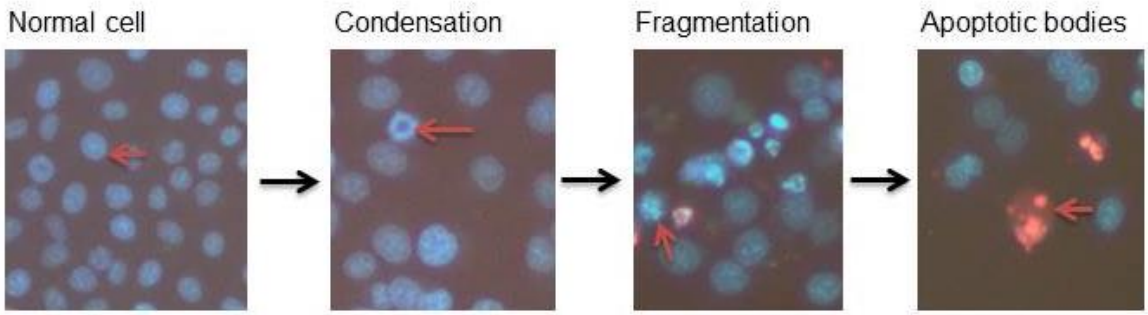

Figure 4.5 Morphology of Apoptosis. In a normal cell the nucleus appears regular in shape with a dispersed appearance of Hoechst 33342 stain (blue). After apoptotic signaling classical nuclear morphological changes are apparent. DNA condenses, and blebs, before DNA fragmentation occurs into apoptotic bodies. Finally cell becomes permeablised and dies as shown by Propidium Iodide entry (red)

4.1.9 Extrinsic signaling

Extrinsic signaling is the process in which cells respond to an extracellular stimuli binding to a member of the tumor necrosis factor (TNF) receptor gene family (Locksley, Killeen and Lenardo 2001). Members of this family have a high degree of similarity as these share a cysteine-rich extracellular domain and a cytoplasmic death domain consisting of 80 amino acids (Ashkenazi and Dixit 1998). The ligands and their subsequent receptors that are responsible for death receptor mediated apoptosis are FasL/FasR, TNF-α/TNFR1, TWEAK/DR3, TRAIL/DR4 and TRAIL/DR5 (Chicheportiche et al. 1997, Ashkenazi and Dixit 1998, Rubio-Moscardo et al. 2005). Intracellularly, the death domain roles are crucial in transmitting the death signal from the surface of the cell to the intracellular signaling pathway (Elmore 2007).

When ligands binds to receptors, this causes them to cluster and recruits adaptor proteins to the death domain such as FADD (FasL/FasR) or TRADD then the recruitment of FADD and RIP in TNF-α signaling (Hsu, Xiong and Goeddel 1995, Wajant 2002).This then becomes a death inducing signaling complex (DISC) that is able to recruit in pro-

caspase 8 and cause its auto-catalytic activation (Kischkel et al. 1995). The catalytic activation of caspase-8 at the DISC can then directly cleave and activate executioner caspases resulting in a caspase cascade (Wen et al. 2012).

4.1.10 Intrinsic signaling

Intrinsic signaling does not require an external stimuli binding to a receptor but a diverse array of intracellular signaling molecules that act directly on targets and are mitochondrial mediated events. Events that occur could act positively on inducing apoptosis such as radiation, hypoxia and toxins or absence of growth factors, cytokines and hormones (Shimizu et al. 1996, Dewey, Ling and Meyn 1995, Tesh 2010, Araki et al. 1990, Lorenzo and Saatcioglu 2008). Detection of intracellular stimuli within the cell causes the inner mitochondrial membrane permeability transition pore to open and the loss of membrane potential (Saelens et al. 2004). Cytochrome C, Smac/DIABLO serine protease HtrA2/Omi are pro-apoptotic proteins that are released from the intermembrane space into the cytosol to activate the caspase dependent mitochondrial pathway (Du et al. 2000, Garrido et al. 2006). Caspase-9 accumulation and activation is caused due to the binding of Cytochrome C and Apoptotic peptidase factor 1 (Apaf-1) thus causing Apaf1 oligomerisation and procaspase-9 at to form the apoptosome (Chinnaiyan 1999, Hill et al. 2004). Inhibitor of apoptosis proteins are repressed by the release of Smac/DIABLO and HtrA2/Omi from the mitochondria to further promote apoptosis (van Loo et al. 2002, Schimmer 2004).

4.1.11 Role of caspases in apoptotic signaling

Caspases are found in every cell and in total there have been 14 caspases identified, with two thirds of these being involved in apoptosis (Wen, Lin et al. 2012). These have been categorized into initiator caspase-2, -8, -9 and -10 executioner caspase-3, -6, and -7 and inflammatory caspases-1, -4 and -5. Initiator caspases are present as inactive

zymogens that upon dimerization exhibit proteolytic activity by cleavage of proteins at aspartic acid residues, however executioner caspases are present as inactive dimers and are only activated by initiator caspase mediated cleavage to form a functional mature protein (Rai, Tripathi et al. 2005). As previously stated, initiator caspases-8 and -10 are responsible for induction of apoptosis via the extrinsic signaling pathway and can directly activate executioner caspases, or the intrinsic signaling pathway for the activation of caspase-9 prior to caspase-3, 6 and -7 caspase activation (Chang and Yang 2000). Executioner caspases differ from initiator caspases in that they work directly on the destruction of the cell by the simultaneous cleavage of peptide substrates responsible for maintaining cellular integrity (Slee, Adrain and Martin 2001, Walsh et al. 2008).

4.1.12 Cell survival/anti-apoptotic signaling

In some instances survival factors can suppress apoptosis and drive cell cycle progression by interfering with intracellular regulatory factors. Insulin-like growth factor-1 and neurotrophins are survival factors that bind to extracellular receptors and stimulate the activation of many kinases such as phosphatidylinositol 3-kinase, which in turn lead to the activation of a serine/threonine kinase known as Akt. When Akt is phosphorylated it becomes activated, and can go on to phosphorylate and inhibit other protein functions such as those of pro-apoptotic proteins BAD (Datta et al. 1997) and Caspase-9 (Cardone et al. 1998). Inactivation of BAD, renders BAD unable to oppose anti-apoptotic protein BCL2 therefore apoptosis does not occur when pAkt is present. Phospho-Akt can also inactivate other proteins that are involved in regulating the cell cycle such as GSK-3beta (Zhao et al. 2012). Activated GSK-3beta can phosphorylate and inactivate Cyclin D, therefore inhibiting cell cycle progression, however if pAkt inactivates GSK-3beta Cyclin D will remain in its active state to drive

cell proliferation (van Weeren et al. 1998). In addition, phospho-Akt can also alter p27 function as phosphorylation of p27 induces cytoplasmic accumulation and prevents nuclear translocation and cell cycle arrest (Liang et al. 2002).

4.1.13 Autophagy

Autophagy also known as "cell eating" is an essential process to maintain cellular homeostasis in which intracellular components of the cell such as the mitochondria, aggregated proteins and other cellular constituents are brought to and degraded by the lysosome, recycled and may be reused to make macromolecules or for metabolism (Glick, Barth and Macleod 2010). Autophagy requires a number of steps: The autophagasome membrane is formed and this then recruits and encloses damaged organelles or proteins into the membrane, the membrane then fuses to encapsulate intracellular components. The autophagosome then fuses with an endosome-lysosome and the lysosome degrades the internal material (Mizushima 2007). A key marker that is ubiquitously expressed in mammalian cells and used to identify cells undergoing autophagy is that of microtubule-associated protein light chain 3 (LC3) as this associates with the membrane of autophagasomes (Kabeya et al. 2000). The conversion of LC3-I to LC3-II by a process known as lipidation is imperative for elongation of an autophagasome, and due to the correlation between the number of autophasomes and the amount of LC3-II, or LC3-I/LC3-II ratio, it is used as a marker for autophagic activity (Kabeya et al. 2000).

Generally speaking autophagy has been identified as a pro-survival response in order to recycle intracellular constituents in response to processes such as nutrient depravation, irradiation, and hypoxia, (Li, Chen and Gibson 2013b, Wu et al. 2014, Lai, Chang and Sun 2016) but can lead to cell death (Guillermo Mariño et al. 2014).

4.1.14 Study Aims, Objectives and hypothesis

The study aim was to assess the anti-tumour effects of withanolide derivatives on cell cycle arrest and apoptosis in breast and prostate cancer cell lines with a particular emphasis on androgen receptor-dependent signaling in prostate cancer.

Hypothesis

Novel Withanolide derivative LG-02 and Withanolide E target breast and prostate cancer growth both in 2D and 3D cell culture

Specific aims and objectives were:

To compare the anti-proliferative activity of novel Withanolide derivatives vs. Withaferin A in breast and prostate cancer cell lines in 2D growth vs. 3D alginate bead assay.

To determine if LG-02 and WE are effective at growth inhibition in hormone dependent/independent breast and prostate cancer cell lines.

To determine if LG-02 and WE are effective at inducing apoptosis and or autophagy in hormone dependent/independent breast and prostate cancer cell lines.

To determine if withanolides have any anti-androgenic properties.

To identify changes in protein expression in response to withanolide derivatives in breast and prostate cancer cell lines.

4.2 Materials and Methods

4.2.1 Cell culture

4.2.1.1 Withanolide derivatives

The withanolide derivatives (synthesised at National Cancer Institute, USA) were supplied at 10mM in Dimethyl sulfoxide (DMSO) (Sigma Aldrich). Aliquots were made up with 5µl 10mM withanolide derivative and 5µl DMSO (1mM) and incubated at -20°C for subsequent use. For working solution 10µl of 1mM withanolide derivative was added 9.990 ml medium for a 1000nM solution and was serially diluted for all concentrations (500, 250, 125, 62.5, 31.3, 15.6, 7.8nM). The control contained 0nM of withanolide derivative and 0.1% DMSO (1ul DMSO in 999ml complete medium).

4.2.1.2 MTS Assay

Cells were plated into a 96 well plate at $5x10^4$ cells/ well 24hrs prior to withanolide treatment. Cell culture medium was removed and cells were treated with 0-1000nm withanolide derivatives for 72hrs. In empty cells, medium only was added. Cell viability was carried out using CellTiter 96 AQueous Non-Radioactive Cell Proliferation Assay (MTS) (Promega, Southampton) following manufactures instructions and the MTS reagent was incubated with the LNCAP cells for 90min. The absorbance from the medium only wells was subtracted from the absorbance from control wells and treated wells to remove background. Absorbance was read at 490nM on the Wallac Victor^2 (Perkin Elmer).

4.2.1.3 Crystal Violet Assay

Crystal violet solution 0.5% was prepared using 0.5g Crystal violet (Sigma Aldrich) and dissolved in 25ml Methanol (Fisher Scientific, Loughborough) and 75ml dH_2O.

Cells were plated into a 96 well plate at $5x10^4$ cells/ well 24hrs prior to withanolide treatment. Cell culture medium was removed and cells were treated with 0-1000nm

withanolide derivatives for 72hrs. Cell culture medium was removed and cells were washed twice in 1× PBS, carefully to not dislodge cells. Cells were incubated with 100% Methanol for 5min at room temperature. Methanol was discarded and plates left to air dry. Cells were incubated with 0.5% Crystal Violet Solution for 20mins at room temperature. Crystal Violet Solution was aspirated and washed three times with deionised water. 10% Glacial Acetic Acid (Sigma Aldrich) was added for 20mins to solubilize crystals. Absorbance read at 560nM on the Wallac Victor^2.

4.2.1.4 Assessment of apoptosis using Nucview 488 Caspase-3 activity assay

Cells were seeded at 3 x10^5 cells/well (6 well plate) and left to adhere overnight. Cells were treated with 0-1000nM withanolide derivatives as previously described (fig 4.2.1.1) and incubated at 37°C in a humidified, 5% CO_2 atmosphere for 48hrs. The Nucview 488 Caspase-3 Assay kit for live cells (Biotium, Cambridge) was performed following the manufacturer's instructions. The Capase-3 inhibitor Ac-DEVD-CHO was also used following the manufacturer's instructions but failed to inhibit Caspase-3 activity. Caspase-3 activity was detected on the BD FACSCalibur (Becton Dickinson). Analysis was carried out using the FlowJo software (Becton Dickinson). Cells were imaged using the Olympus IX81 inverted fluorescence microscope to assess cell viability using Cell-F software

4.2.1.5 Cell cycle analysis by Flow Cytometry

Cells were seeded at 3 x10^5 cells/well (6 well plate) and left to adhere overnight. Cells were treated with 0-1000nM withanolide derivatives as previously described (fig 4.2.1.1) and incubated at 37°C in a humidified, 5% CO_2 atmosphere for 24hrs. After 24hrs cell culture medium was removed and placed into a flow cytometry tube (Becton-Dickinson). Cells were washed with 1ml of 1×PBS and then placed in a flow tube. 300µl of 0.05% Trypsin-EDTA was added to each well and incubated at 37° C until

all cells had detached. Cells were then placed into corresponding flow tube and centrifuged at 400g at 4°C for 5min to pellet the cells. Supernatant was removed and cells were washed in ice cold 1× PBS. Cells were centrifuged and washed again with Ice cold PBS and PBS was discarded. Ice cold 80% Ethanol (Sigma Aldrich) was added to cells a drop at a time whilst mixing cells to prevent clumping. These were then left for 48hrs at -20°C. Cells were centrifuged at 400g and ethanol was discarded. Cells were incubated with 50µg/ml Propidium Iodide and 0.1U/ml RNase (Sigma Aldrich) overnight at 4°C. Cell cycle analysis was determined using the FACSCalibur and data analysis was carried out using FlowJo software.

4.2.1.6 Western Blot

20µg of protein lysate was loaded on to a Mini-PROTEAN TGX Precast Gels (BIO RAD) and run at 200V for 22min. Following SDS PAGE gels were transferred to a Trans-Blot Turbo Transfer System (BIO RAD) following the manufacturer's instructions for 10min. Membrane was then incubated in 100% MeOH for <1min, allowed to air dry and then briefly incubated again in MeOH. Membrane was then rinsed in dH_2O and equilibrated in TBS for 1 min. Membranes were incubated with primary antibodies detailed below, diluted in 5% w/v BSA in TBS and 0.1% Tween-20 overnight at 4°C on an orbital shaker.

Antibody	Clone	dilution	Supplier
GAPDH Rabbit mAb-	D16H11	1:10000	Cell signaling Technologies (CST)
Androgen Receptor Rabbit mAb	EPR1535(2)	1:1000	Abcam
PSA/KLK3 Rabbit mAb	D6B1	1:1000	CST
p21 Rabbit mAb	12D1	1:1000	CST
p14 ARF mouse mAb	4C6/4	1:1000	CST
p27 Kip1 Rabbit mAb	D69C12	1:1000	CST
p53 mouse mAb	1C12	1:1000	CST
Cyclin B1 Rabbit mAb	4138	1:1000	CST
Cyclin D1 Rabbit mAb-	92G2	1:1000	CST
Phospho-Akt Rabbit mAb	d9E	1:2000	CST
Cdk2 Rabbit mAb	78B2	1:1000	CST
Cdk4 Rabbit mAb	D9G3E	1:1000	CST
LC3B Rabbit mAb	D11	1:1000	CST
Caspase-3 Rabbit mAb	9662	1:1000	CST

Table 5. The antibodies that were used in protein detection after withanolide treatment.

The following day membranes were washed 3×5 min in TBST and incubated in HRP-conjugated secondary Abs for 1 hour at room temperature. The membranes were washed in 3 ×10 min in TBST on an orbital shaker. Membranes were then incubated with 6 ml of West Dura Extended Duration Substrate (Thermo Fisher) for 5-7min, excess substrate and removed and membranes were placed in a clear plastic wrap and were exposed to X-ray film for 30s-2hrs dependent upon protein concentration and detection. X-ray film was developed using an automated developing system.

Following development membrane was stripped using Restore Western Blot Stripping Buffer (Thermo Fisher) for 15mins at room temperature on an orbital shaker, washed in TBST and re-probed overnight with primary antibody.

4.3 Results

4.3.1.1 The effect of withanolide derivatives on the LNCAP cell line as determined by the MTS assay.

To assess the growth inhibitory effects of Withanolide derivatives an MTS assay was performed after 72hr treatment with a series of withanolide derivatives (Provided from Tom Sayers, NCI) to determine the most potent inhibitor of cell proliferation. LG-02 was the most potent withanolide derivative at inducing growth inhibition in the LNCAP cell line with an IC_{50} value of 28.88nM. IC_{50} values for LG-28, LG-29, LG-33, WE and WFA was 426.1, >1000, 382.6, 116.6 and >1000nM respectively (fig 4.6).

Figure 4.6. The effect of withanolide derivatives on LNCAP cell line as determined by the MTS assay.

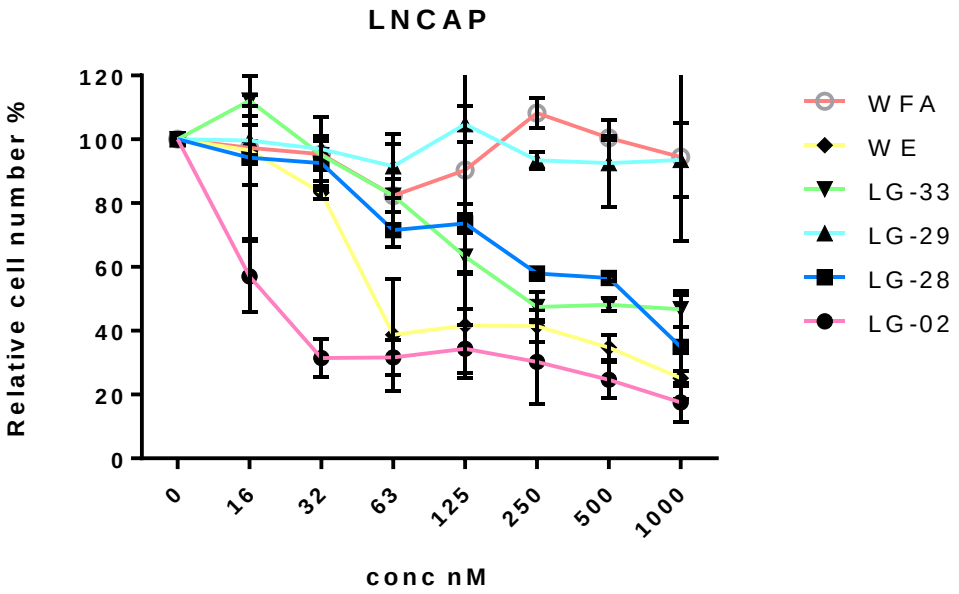

Figure 4.6. The effect of withanolide derivatives on LNCAP cell line as determined by the MTS assay. The LNCAP cell line was subjected to withanolide derivative treatment for 72hr for investigating the most potent growth inhibitor and the relative cell number was determined using the MTS assay. Data was generated in triplicate and displayed as two independent experiments.

4.3.1.2 Effects of LG-02 and WE on proliferation in breast and prostate cancer

A crystal violet assay was performed after 72hrs of LG-02 and WE treatment to determine which of the withanolide derivative was the most potent inhibitor of breast and prostate cancer growth. LG02 and WE has a significant effect on growth inhibition in all cell lines as determined by the nonparametric Kruskal-Wallis, Conover Inman test (<0.05=*, <0.01=** and < 0.001=***) (fig 4.7). A significant reduction in proliferation of SUM159 cells occurred at all doses above 16nM with LG-02 treatment with increasing growth inhibition in a dose dependent manner; however growth was only significantly inhibited at 1000nM with WE treatment. IC_{50} was undetermined with both compounds in the SUM159 cell line. A significant reduction in MCF7 cell proliferation was observed from 16nM ($p<0.005$) with LG-02 treatment with increasing dose responsive inhibition and at all doses above 31nM WE. IC_{50} values for LG-02 and WE treatments were 73.57nM and 358.3nM respectively. LG-02 has a significant effect on growth inhibition in PC3 cell lines at all does above 16nM ($p=<0.05$). WE displayed a significant effect on growth of PC3 cell line at all doses above 31nM ($p<0.005$). IC_{50} was determined for LG-02 treatment at 146.3nM and 365.3nM for WE in PC3 cells. A significant inhibition in growth of DU145 cells was observed at all doses above 61nM for LG-02 treatment ($p<0.05$) and 250nM WE ($p=<0.001$) and IC_{50} values are 208.9nM and 537.3nM respectively. A significant reduction in growth of LNCAP cells was observed at all doses above 16nM ($p=<0.05$) for LG-02 and 125nM WE ($p=<0.001$). IC_{50} was 62.12nM and 154.8nM. To note, there is relatively good concordance between the MTS (Fig 4.6) and crystal violet assay (FIG 4.7) for the LNCAP cell line treated with LG-02 and WE

Figure 4.7. The effect of LG-02 and WE on relative cell number as determined by the crystal violet assay.

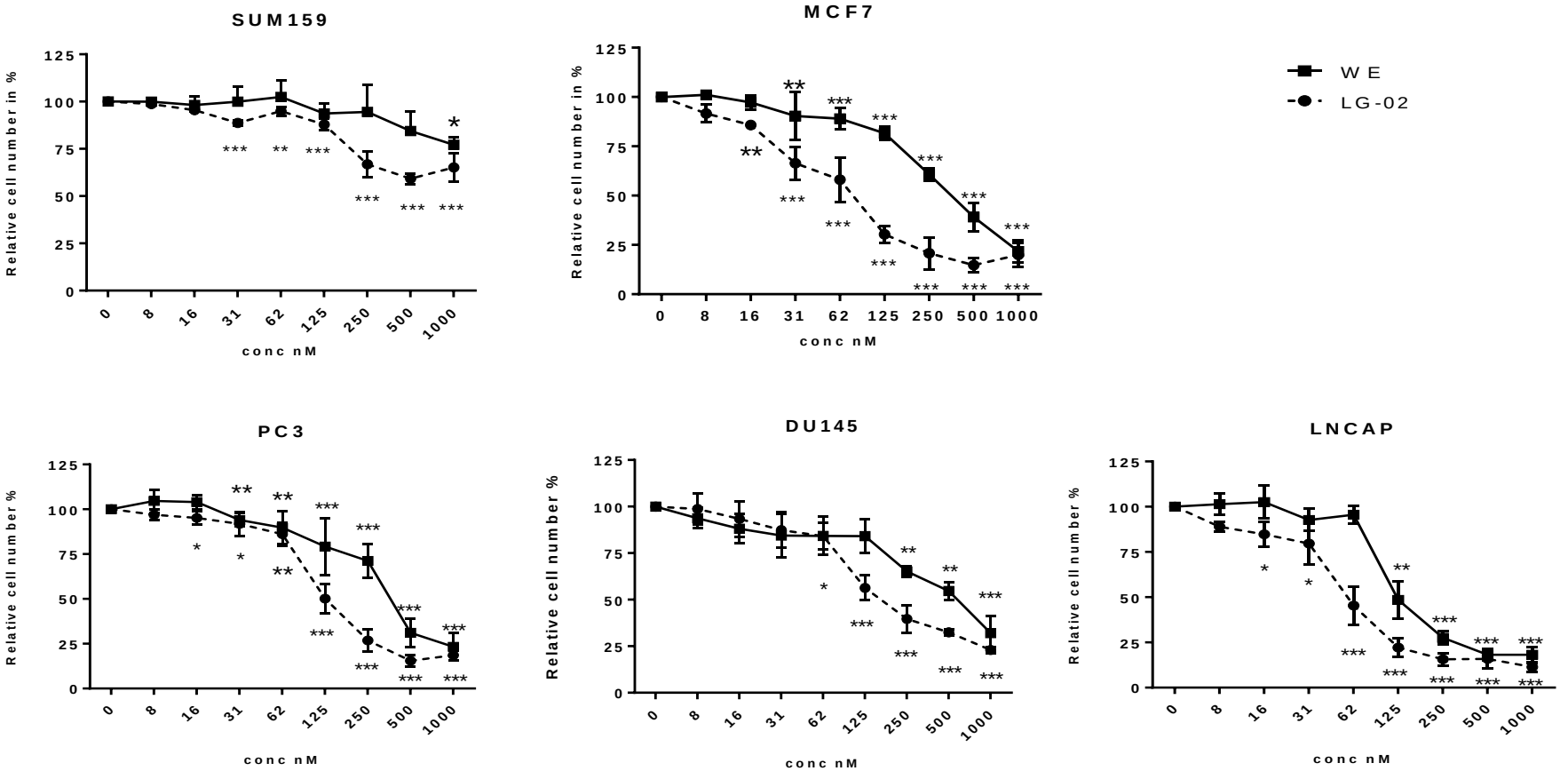

Figure 4.7. Comparison of the phase of cell cycle (control) vs the phase of cell cycle (treated). Breast and prostate cancer cell lines were subjected to 72hr incubation of 0-1000nM of LG-02 and WE to determine the most potent inhibitor of proliferation and identify the most sensitive cell lines. LG-02 is clearly more potent than WE at growth inhibition and LNCAP are the most sensitive cell line as determined from the IC_{50} values. Statistical significance was obtained using the nonparametric, Kruskal-Wallis Conover Inman. (<0.05 *, <0.01 ** and < 0.001 ***). All data is represented as mean ± SEM and was carried out in triplicate.

Cell Line	LG-02 IC_{50}	WE IC_{50}
SUM159	UNDETERMINED	UNDETERMINED
MCF7	73.57nM	358.3nM
PC3	146.3nM	365.3nM
DU145	208.9nM	537.3nM
LNCAP	62.12nM	154.8nM

Table 6. The IC_{50} for breast and prostate cancer cell lines after 72hr incubation with withanolide derivatives. The IC_{50} was determined after three independent experiments using the Graph Pad Prism software**.**

4.3.1.3 LG-02 and WE effect on the cell cycle.

The SUM159, MCF7, PC3, DU145 and LNCAP cell lines were investigated to determine if LG-02 and WE induced cell cycle arrest at G1 or G2/M-phase of the cell cycle after 24hrs treatment.

LG-02 induced a significant G1-phase accumulation and reduced the number of cells in G2/M-phase following treatment with LG-02 at 1000nM (p value <0.001, and p value <0.05) in the SUM159 cell line, however no significant differences were found after WE treatment (fig 4.8).

LG-02 induced a significant number of cells in S-phase (p value <0.01) in MCF7 cell line, however no differences were observed at G1 or G2/M-phase (Figure 4.9). No significant difference in cell cycle accumulations was observed in the MCF7 cell line after WE treatment (Fig 4.9).

A significant accumulation of PC3 cells in G1-phase of the cell cycle and a reduction in cells at G2/M-phase at 250nM of LG-02 treatment, and a reduction of cells in S-phase

was also found at 1000nM (p value <0.05 *, <0.01 **, <0.001 ***) (Figure 4.8). A similar effect was determined after WE treatment in PC3 cells (Figure 4.10).

A reduction in DU145 cells in S-phase was determined at 250nM LG-02 and a significant increase in cells at G2/M-phase at 1000nM ($p < 0.05$) (Fig 4.11). WE induced S-phase depletion of DU145 cells at 1000nM ($P < 0.05$) but no significant difference was found in G1 or G2/M-phase (Fig 4.11).

Cell cycle arrest was most pronounced in the LNCAP cell line as a good correlation between dose response and growth inhibition was observed confirming that the LNCAP cell line was more sensitive to LG-02 and WE in accordance with the IC_{50} value (Fig 4.12). In particular a G1-phase accumulation was found from 63nM LG-02 and a significant reduction in the number of cells in S and G2/M-phase at 250nM ($p < 0.05$, 0.01) (Fig 4.12). WE induced G1 phase accumulation and reduced the number of cells in G2/M-phase at 63nM ($p < 0.05$).

Figure 4.8 The effect of LG-02 and WE on the SUM159 cell line as determined by cell cycle analysis.

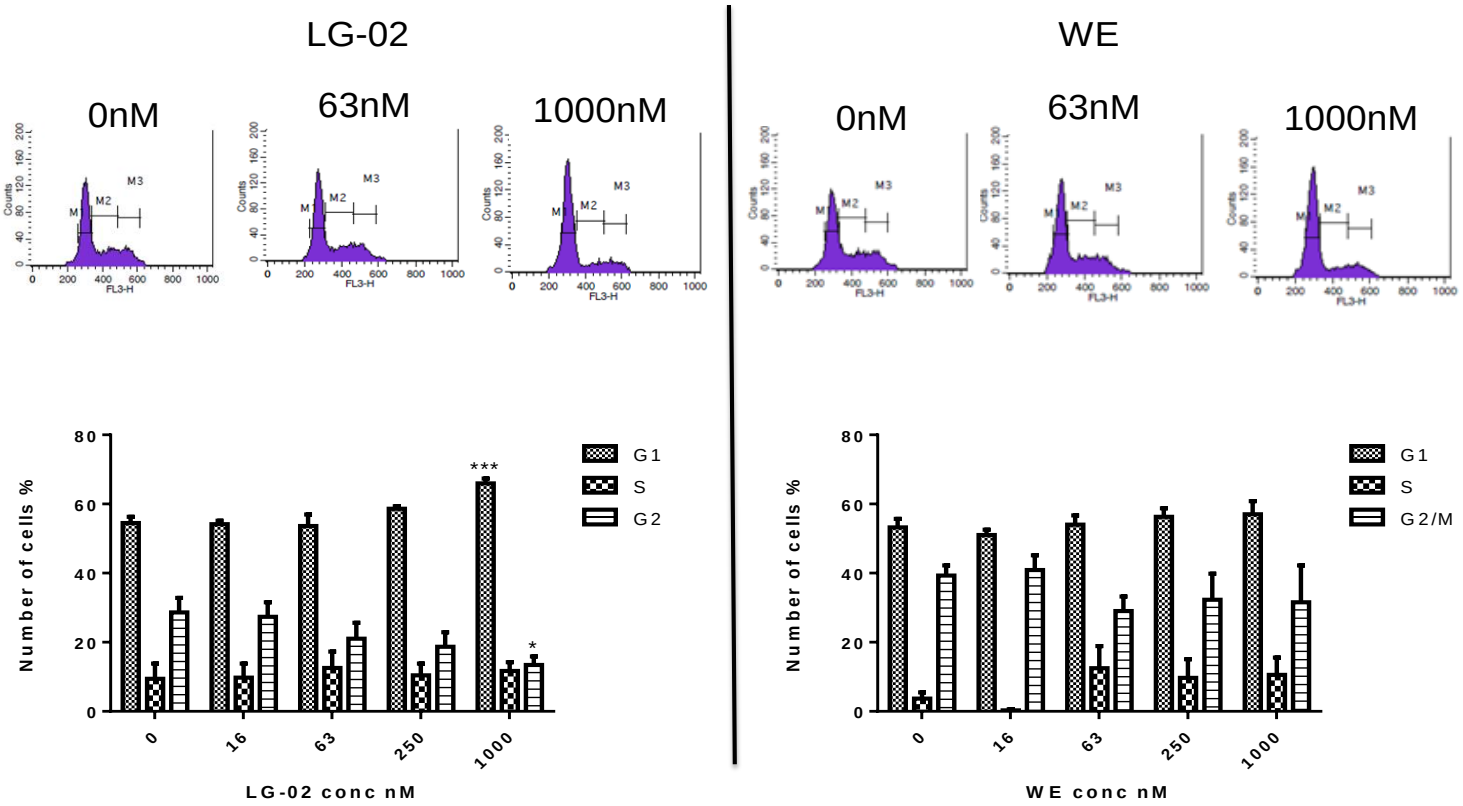

Figure 4.8. The effect of LG-02 and WE on the SUM159 cell line as determined by cell cycle analysis. The SUM159 cell line was treated with LG-02 and WE for 24hr prior to harvesting the cells and supernatant for cell cycle analysis. LG-02 induced a significant amount of G1 accumulation at 1000nM, however WE appeared to have no significant effect at any concentration. All data is represented as mean ± SEM and was carried out in triplicate. Statistical significance was obtained using the nonparametric, Kruskal-Wallis Conover Inman. (<0.05 *, <0.01 ** and < 0.001 ***).

Figure 4.9 The effect of LG-02 and WE on the MCF7 cell line as determined by cell cycle analysis.

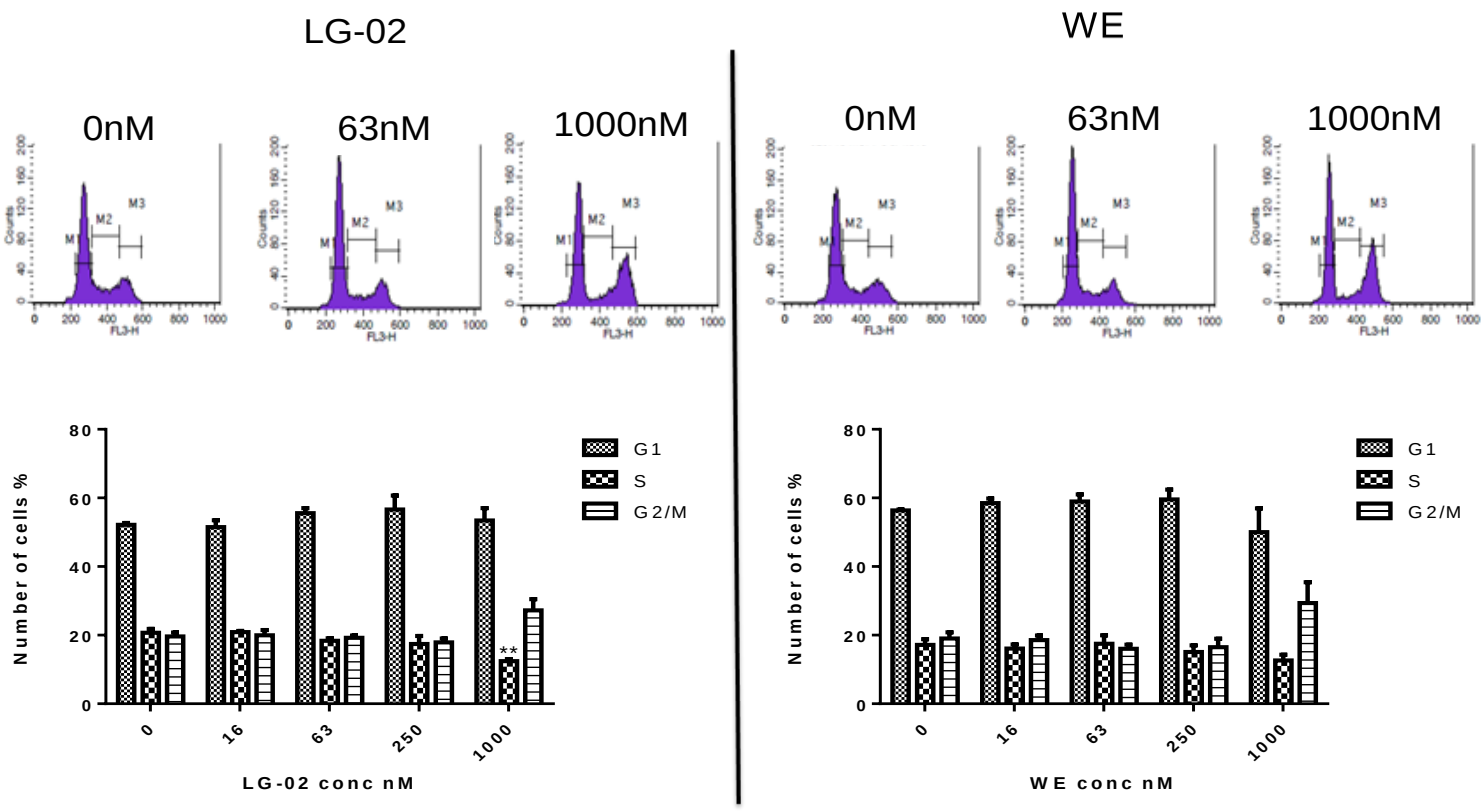

Figure 4.9. The effect of LG-02 and WE on the MCF7 cell line as determined by cell cycle analysis. The MCF7 cell line was treated with LG-02 and WE for 24hr prior to harvesting the cells and supernatant for cell cycle analysis. LG-02 induced a significant S phase reduction at 1000nM, however WE appeared to have no significant effect at any concentration. All data is represented as mean ± SEM and was carried out in triplicate. All data is represented as mean ± standard error and was carried out in triplicate. Statistical significance was obtained using the nonparametric, Kruskal-Wallis Conover Inman. (<0.05 *, <0.01 ** and < 0.001 ***).

Figure 4.10 The effect of LG-02 and WE on the PC3 cell line as determined by cell cycle analysis.

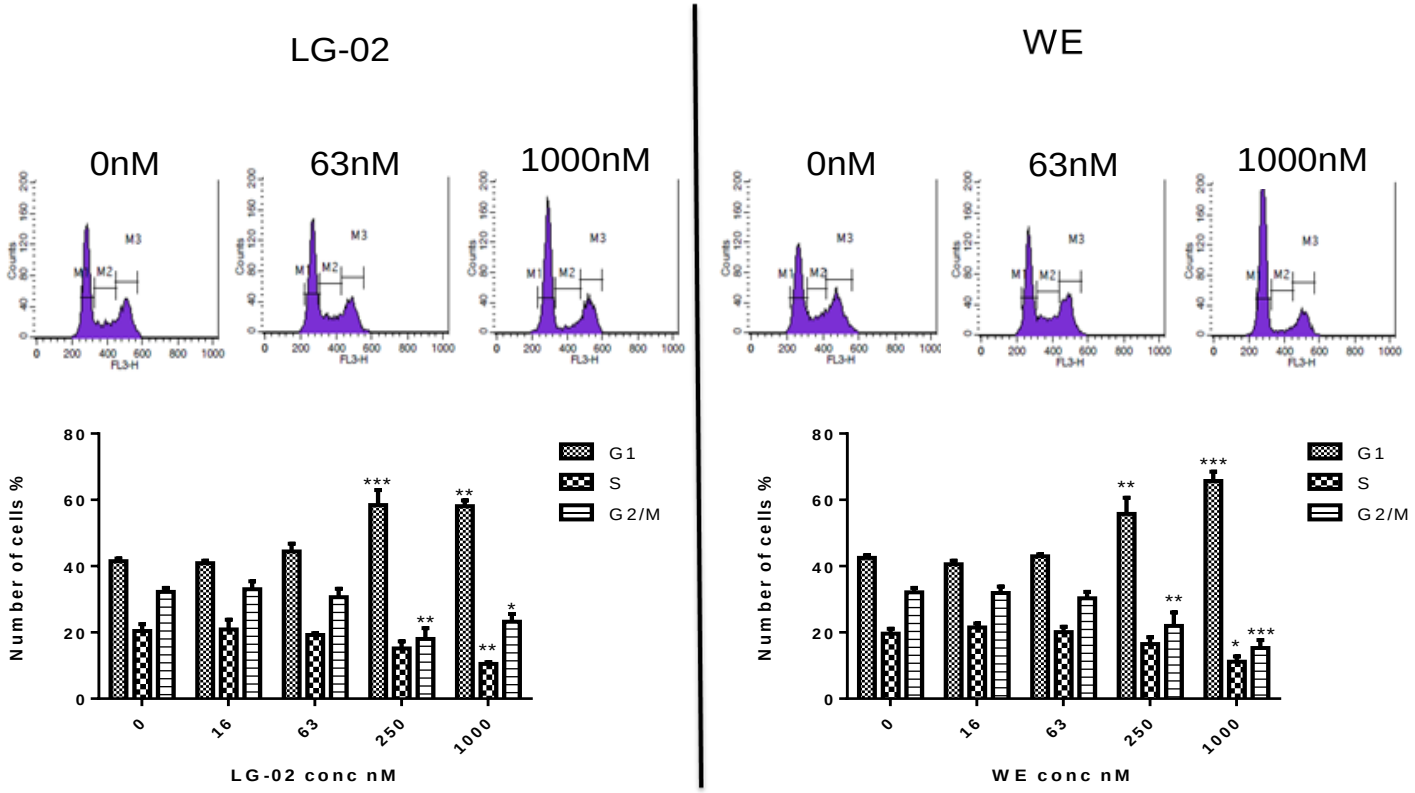

Figure 4.10 The effect of LG-02 and WE on the PC3 cell line as determined by cell cycle analysis. The PC3 cell line was treated with LG-02 and WE for 24hr prior to harvesting the cells and supernatant for cell cycle analysis. LG-02 induced a significant amount of G1 accumulation at 250nM with a concomitant G2 phase reduction, with a similar effect after WE treatment. All data is represented as mean ± standard error and was carried out in triplicate. All data is represented as mean ± SEM and was carried out in triplicate. Statistical significance was obtained using the non-parametric, Kruskal-Wallis Conover Inman. (<0.05 *, <0.01 ** and < 0.001 ***).

Figure 4.11 The effect of LG-02 and WE on DU145 cell line as determined by cell cycle analysis.

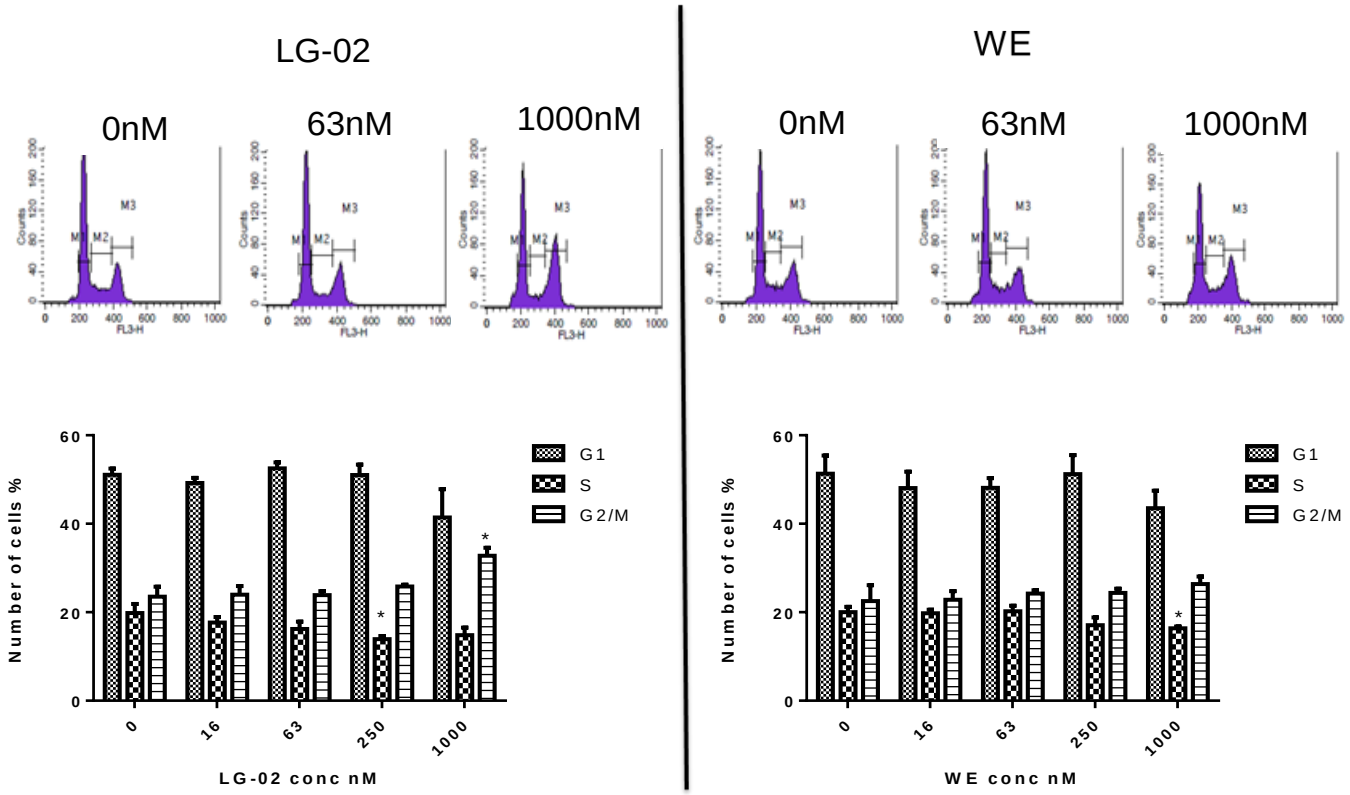

Figure 4.11 The effect of LG-02 and WE on the DU145 cell line as determined by cell cycle analysis. The DU145 cell line was treated with LG-02 and WE for 24hr prior to harvesting the cells and supernatant for cell cycle analysis. LG-02 induced a significant reduction in number of cell in S phase at 250nM and a significant G2/M accumulation at 1000nM (P value <0.05) whereas WE only induced an S phase reduction at 1000nM (P value <0.05). All data is represented as mean ± SEM and was carried out in triplicate. Statistical significance was obtained using the nonparametric, Kruskal-Wallis Conover Inman. (<0.05 *, <0.01 ** and < 0.001 ***).

Figure 4.12 The effect of LG-02 and WE on the LNCAP cell line as determined by cell cycle analysis

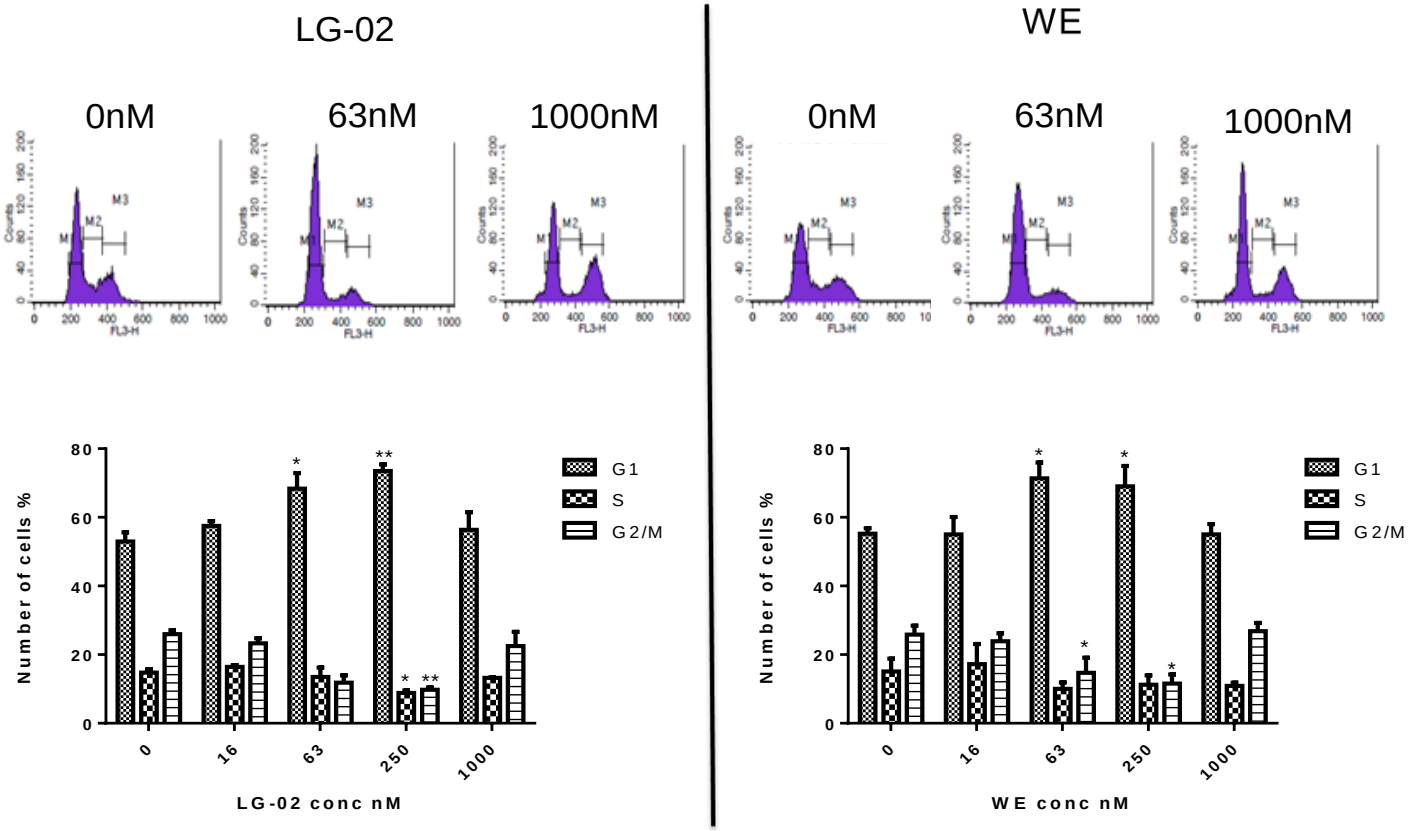

Figure 4.12. The effect of LG-02 and WE on the LNCAP cell line as determined by cell cycle analysis. LG-02 induced a significant amount of G1 accumulation at 63nM followed by a significant decrease in cells in S and G2/M phases of the cell cycle at 250Nm.A significant G1 accumulation with a concomitant G2/M reduction was observed at 63nM WE treatment. All data is represented as mean ± SEM and was carried out in triplicate. Statistical significance was obtained using the nonparametric, Kruskal-Wallis Conover Inman. (<0.05 *, <0.01** and < 0.001***).

4.3.1.4 Effect of LG-02 and WE effect on apoptosis.

Cell viability was assessed after 24hrs treatment with LG-02 and WE using Hoechst 33342 and Propidium Iodide stain on all cell lines except from the SUM159 cell line as these cells did not respond to either agent. LG-02 and WE induced <15% apoptosis in the MCF7 cells at 1000nM (Fig 4.13). LG-02 appears more potent at inducing apoptosis in the PC3 cells than WE treated cells as a significant amount of apoptosis was observed at 500nM ($p < 0.05$), however a similar effect was not observed at 1000nM (Fig 14). WE had no effect on inducing apoptosis in the PC3 cell line at any concentration (Fig 14). LG-02 was more potent at inducing apoptosis in the DU145 cells as a significant response was observed at 125nM ($p < 0.05$), similar effects was not observed after WE treatment until 250nM (Fig 15). Both withanolides had a similar dose response in the LNCAP as a significant value was obtained from 250nM ($p < 0.01$). All cell lines displayed an apoptotic dose response although most significant responses were at higher doses. The LNCAP cell line however displayed growth inhibition at lower doses (Fig 4.16), even in the absence of apoptosis.

Figure 4.13 The effect of LG-02 and WE in the MCF7 cell line as determined by Hoechst 33342 stain and Propidium Iodide.

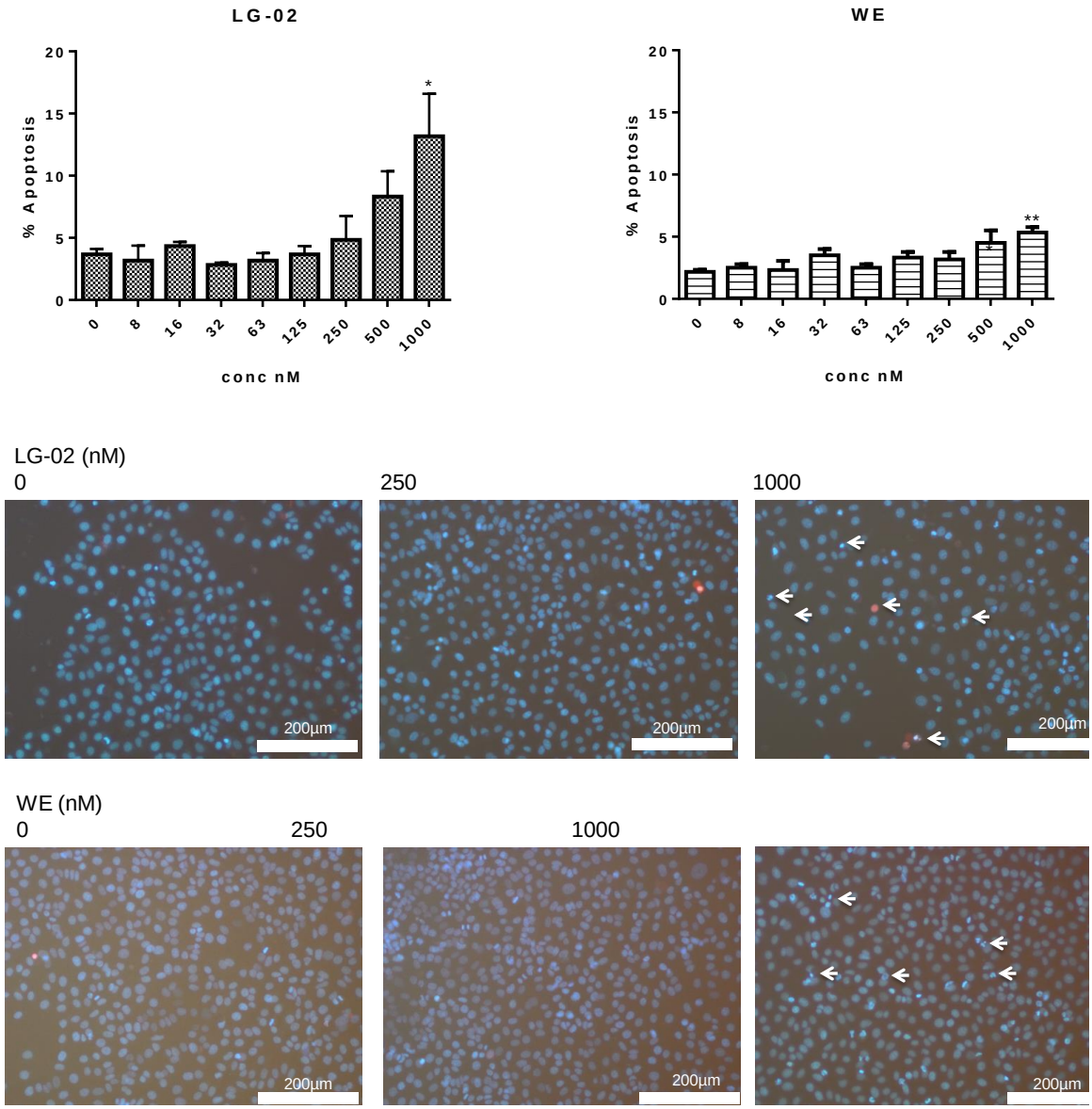

Figure 4.13 The apoptotic effect of 24hr treatment with LG-02 and WE on the MCF7 cell line as determined by Hoechst 33342 stain and Propidium Iodide. MCF7 cell lines were treated with 0-1000nM LG-02 and WE for 24hours to asses for apoptotic effects of these compounds. Both LG-02 and WE have a significant effect on apoptosis at 1000nM. All data is represented as mean ± SEM and was carried out in triplicate. Statistical significance was obtained using the nonparametric, Kruskal-Wallis Conover Inman. (<0.05 *, <0.01 ** and < 0.001 ***). Arrows indicate apoptotic or dead cells.

Figure 4.14 The effect of LG-02 and WE on the PC3 cell line as determined by Hoechst 33342 stain and Propidium Iodide

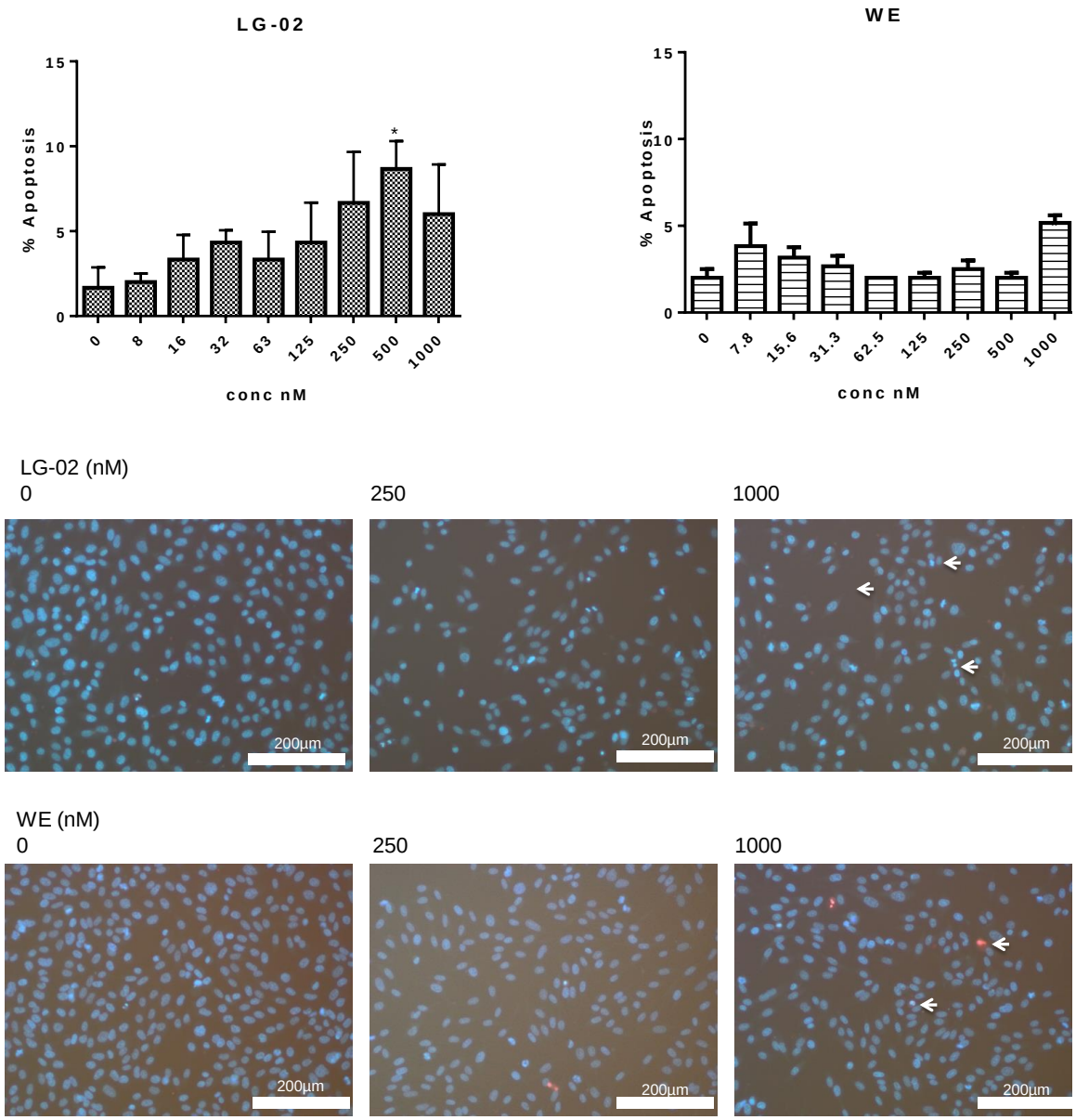

Figure 4.14 The apoptotic effect of 24hr treatment with LG-02 and WE on the PC3 cell line as determined by Hoechst stain and Propidium Iodide. The PC3 cell lines were treated with 0-1000nM LG-02 and WE for 24HRS to asses for apoptotic effects of these compounds. LG-02 induced a significant amount of apoptosis at 500nM although no significant differences were observed at 1000nM whereas no apoptotic effects were observed with WE treatment. All data is represented as mean ± SEM and was carried out in triplicate. Statistical significance was obtained using the nonparametric, Kruskal-Wallis Conover Inman. (<0.05 *, <0.01 ** and < 0.001 ***). Arrows indicate apoptotic or dead cells.

Figure 4.15 The effect of LG-02 and WE on the DU145 cell line as determined by Hoechst 33342 stain and Propidium Iodide

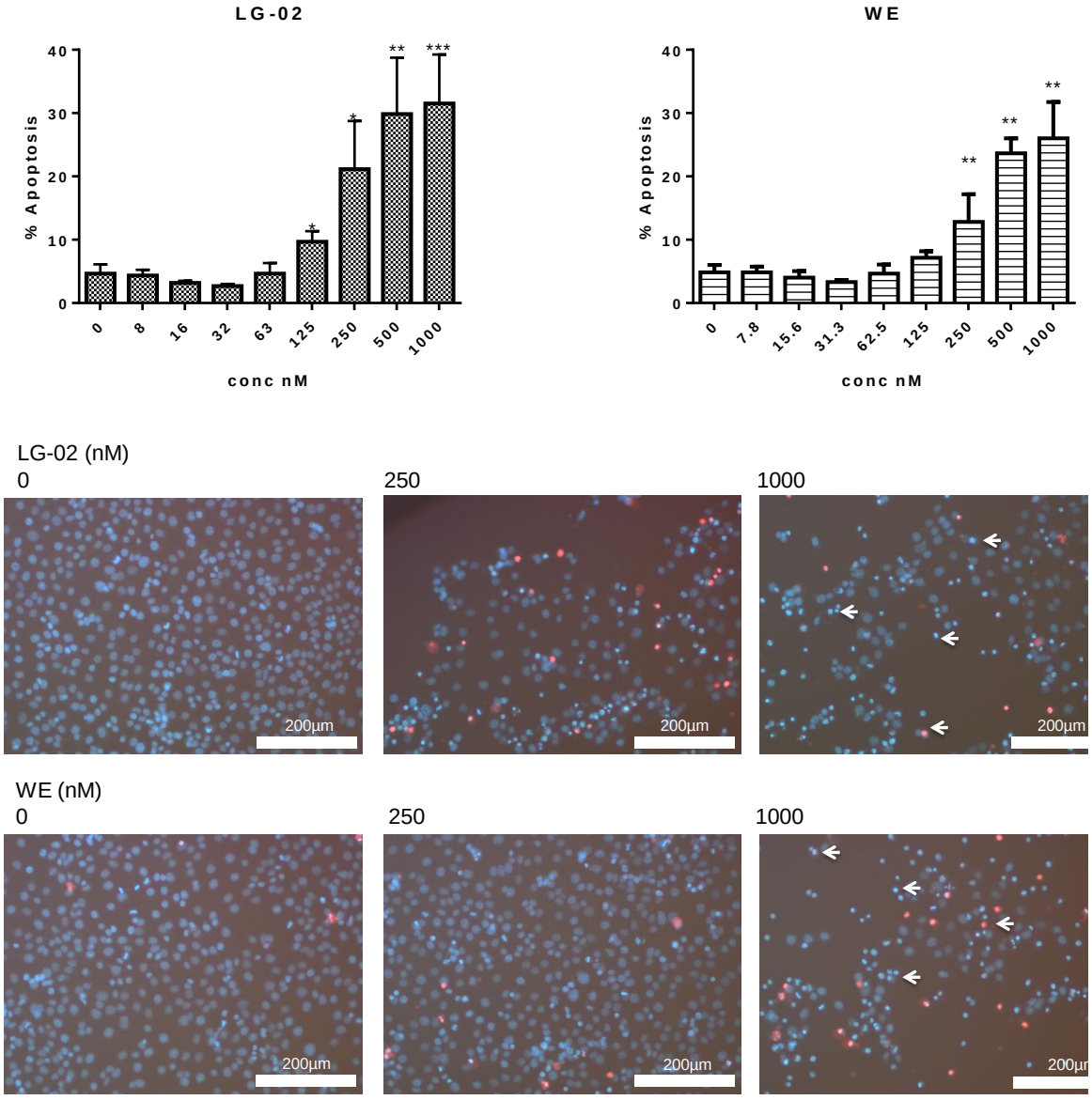

Figure 4.15 The apoptotic effect of 24hr treatment with LG-02 and WE on the DU145 cell line as determined by Hoechst 33342 stain and Propidium Iodide. LG-02 had a significant effect on apoptosis from 125nM with a continued dose response, however a significant effect was not observed with WE incubation until 250nM. All data is represented as mean ± SEM and was carried out in triplicate. Statistical significance was obtained using the nonparametric, Kruskal-Wallis Conover Inman. (<0.05 *, <0.01 ** and < 0.001 ***). Arrows indicate apoptotic or dead cells.

Figure 4.16 The effect of LG-02 and WE on the LNCAP cell line as determined by Hoechst 33342 stain and Propidium Iodide.

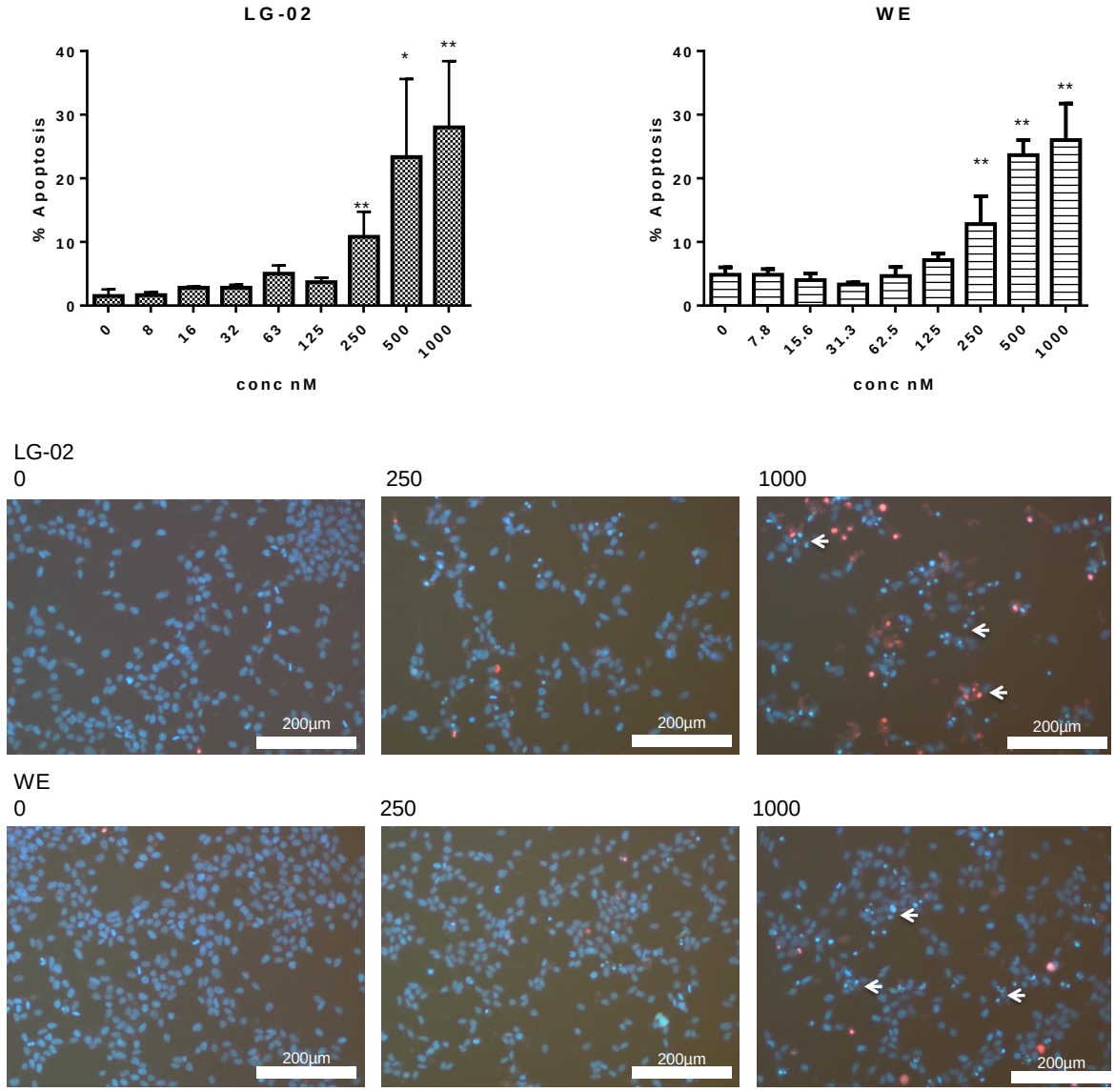

Figure 4.16 The apoptotic effect of 24hr treatment with LG-02 and WE on the LNCAP cell line as determined by Hoechst 33342 stain and Propidium Iodide. LG-02 and WE had a significant effect on apoptosis from 250nM with a continued dose response although LG-02 had more late stage apoptosis but similar death overall. All data is represented as mean ± SEM and was carried out in triplicate. Statistical significance was obtained using the nonparametric, Kruskal-Wallis Conover Inman. (<0.05 *, <0.01 ** and < 0.001 ***). Arrows indicate apoptotic or dead cells.

4.3.1.5 Assessment of Caspase-3 activation by LG-02 and WE

The Caspase-3 assay was used as a confirmatory test for apoptosis after 24hours incubation with LG-02 and WE and detected using the FACSCalibur. No significant levels of caspase-3 activity were detected with both withanolides in the MCF7 and PC3 cell lines as consistent with Figures 4.13, 4.14, 4.17 and 4.18. MCF7 cells did not express Caspase-3 therefore no Caspase-3 activation although these cells are able to undergo apoptosis through other executioner caspase activity. Caspase-3 assay confirmed data generated from the Hoechst 33342 and Propidium Iodide stain in PC3 cell line (Fig4.18). Caspase-3 was active in the DU145 cell line at 250 and 1000nM of LG-02 WE which correlates with previous Hoechst 33342 and Propidium Iodide stain (see Figure 4.19). The LNCAP cell line demonstrated a slight increase in Caspase-3 activity at 1000nM with LG-02 and WE (fig 4.20).

Figure 4.17 The effect of LG-02 and WE treatment on the MCF7 cell line as determined by the Caspase-3 assay.

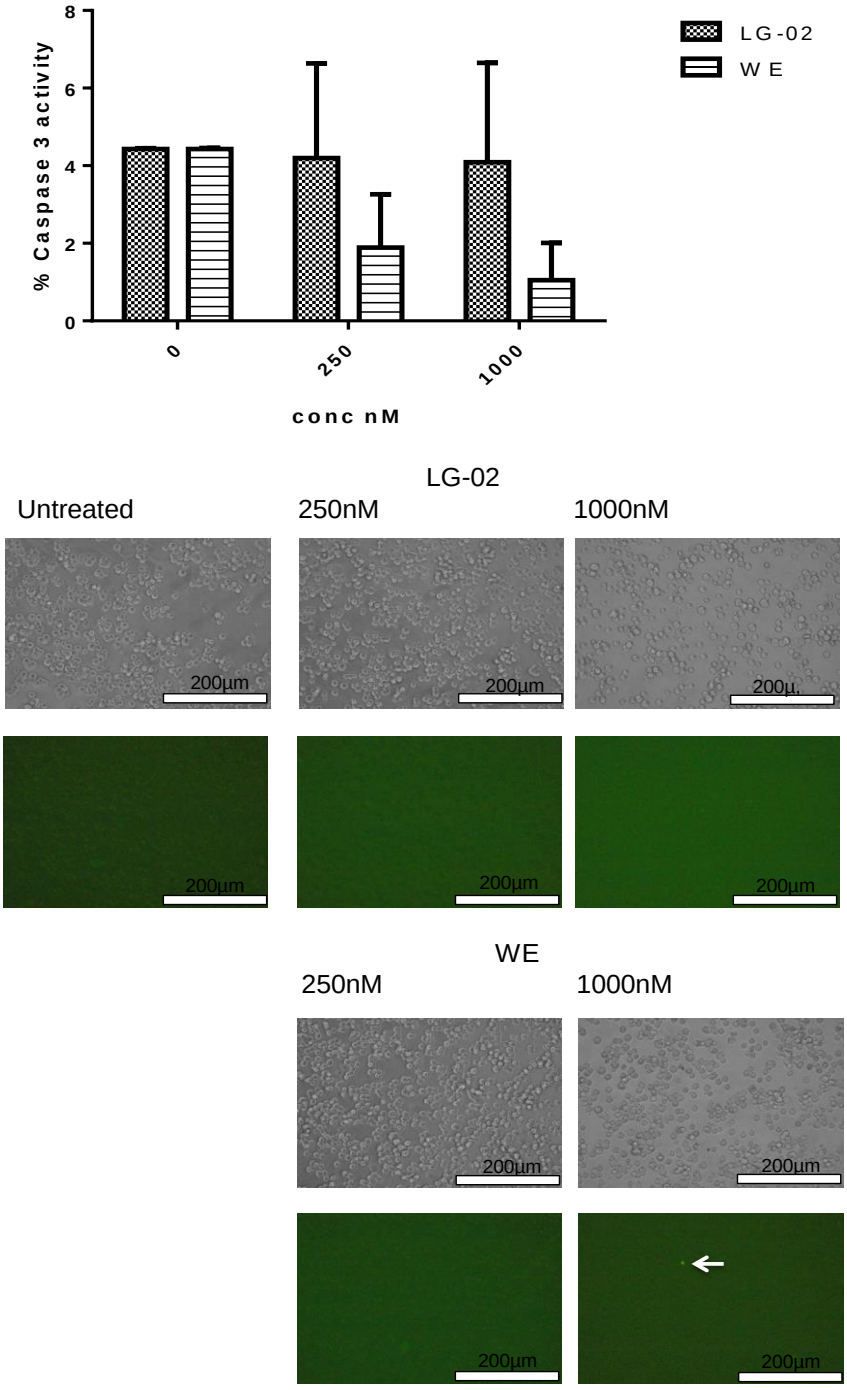

Figure 4.17 The effect of 24hr incubation with LG-02 and WE treatment in the MCF7 cell line as determined by the Caspase-3 assay. The MCF7 cell line was treated with 0-1000nM LG-02 and WE to asses for apoptotic effects of these compounds. Caspase-3 activities could not be determined as MCF7 cell line does not express a functional copy this gene. Data is representative of two independent experiments. Arrow indicate cell with caspase-3 activity.

Figure 4.18 The effect of 24hr incubation with LG-02 and WE on the PC3 cell line as determined by the Caspase-3 assay.

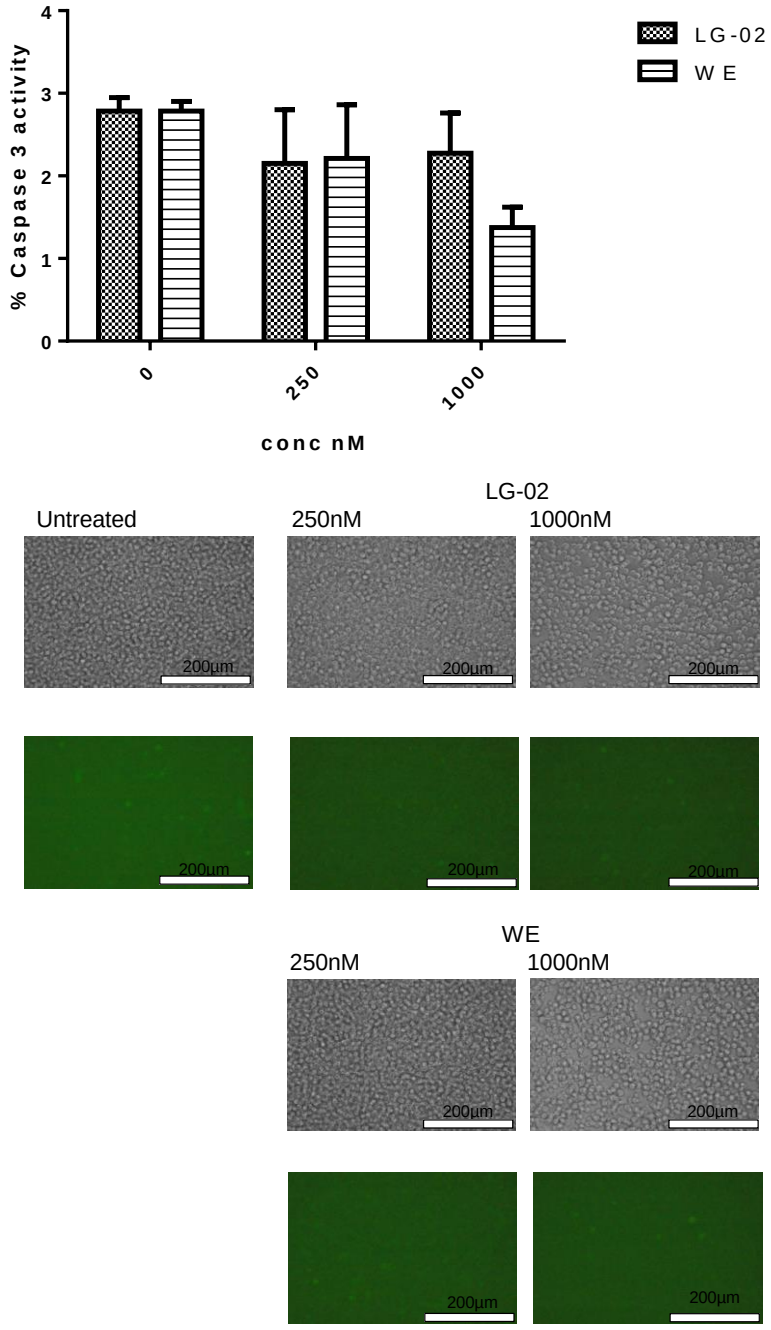

Figure 4.18. The effect of 24hr incubation with LG-02 and WE treatment on the PC3 cell line as determined by the caspase-3 assay. The PC3 cell lines were treated with 0-1000nM LG-02 and WE to asses for apoptotic effects of these compounds. No caspase-3 activity was determined with either of the withanolide derivatives. Data is representative of two independent experiments.

Figure 4.19 The effect of after 24hr incubation with LG-02 and WE treatment on the DU145 cell line as determined by the Caspase-3 assay.

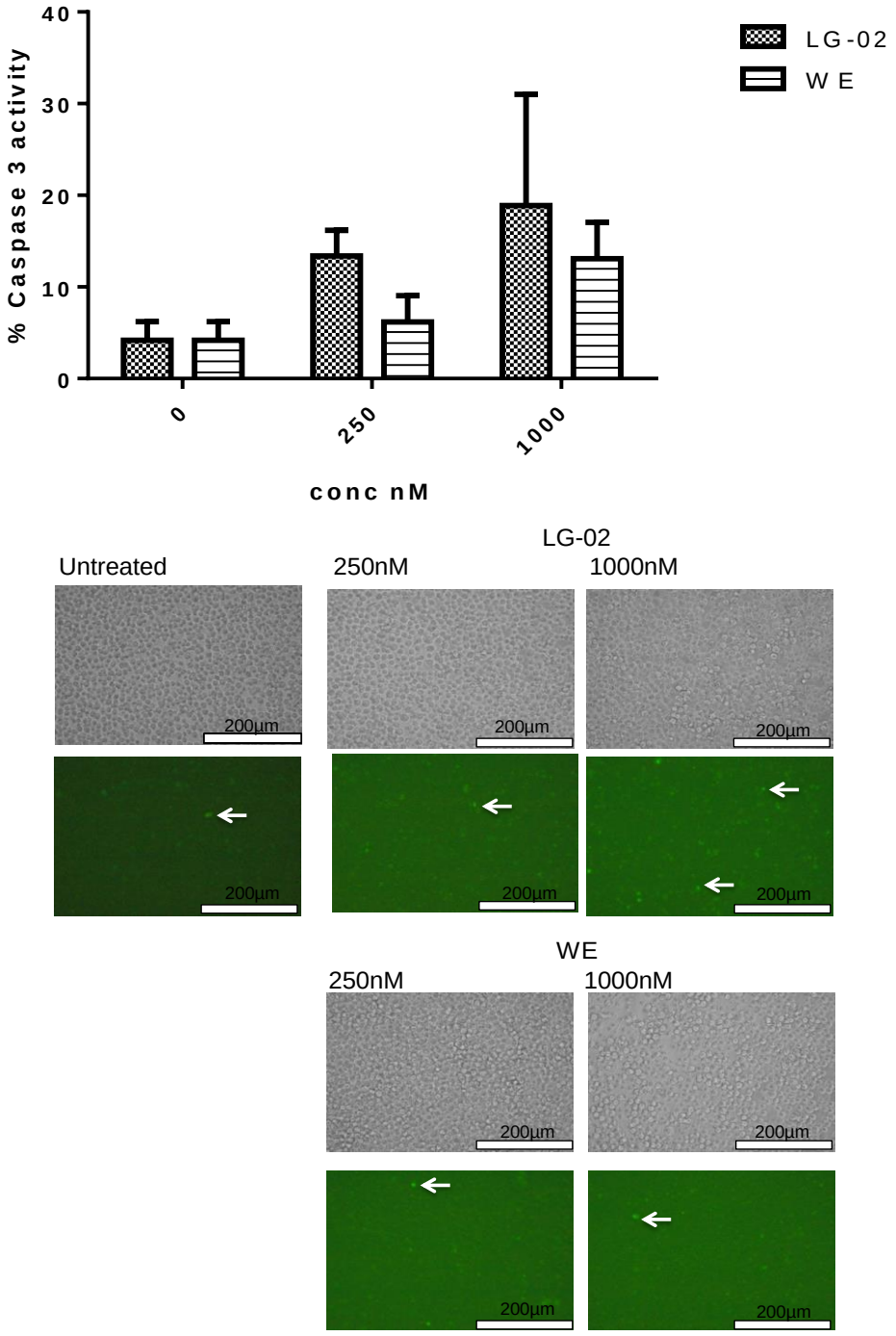

Figure 4.19. The effect of 24hr incubation with LG-02 and WE treatment on the DU145 cell line as determined by the caspase-3 assay. The DU145 cell lines were treated with 0-1000nM LG-02 and WE to asses for apoptotic effects of these compounds. Caspase-3 activity was observed at both concentrations of withanolides and appears to be dose responsive at increasing concentrations. Data is representative of two independent experiments. Arrows indicate cells with caspase-3 activity.

Figure 4.20. The effect of after 24hr incubation with LG-02 and WE treatment on the LNCAP cell line as determined by the Caspase-3 assay.

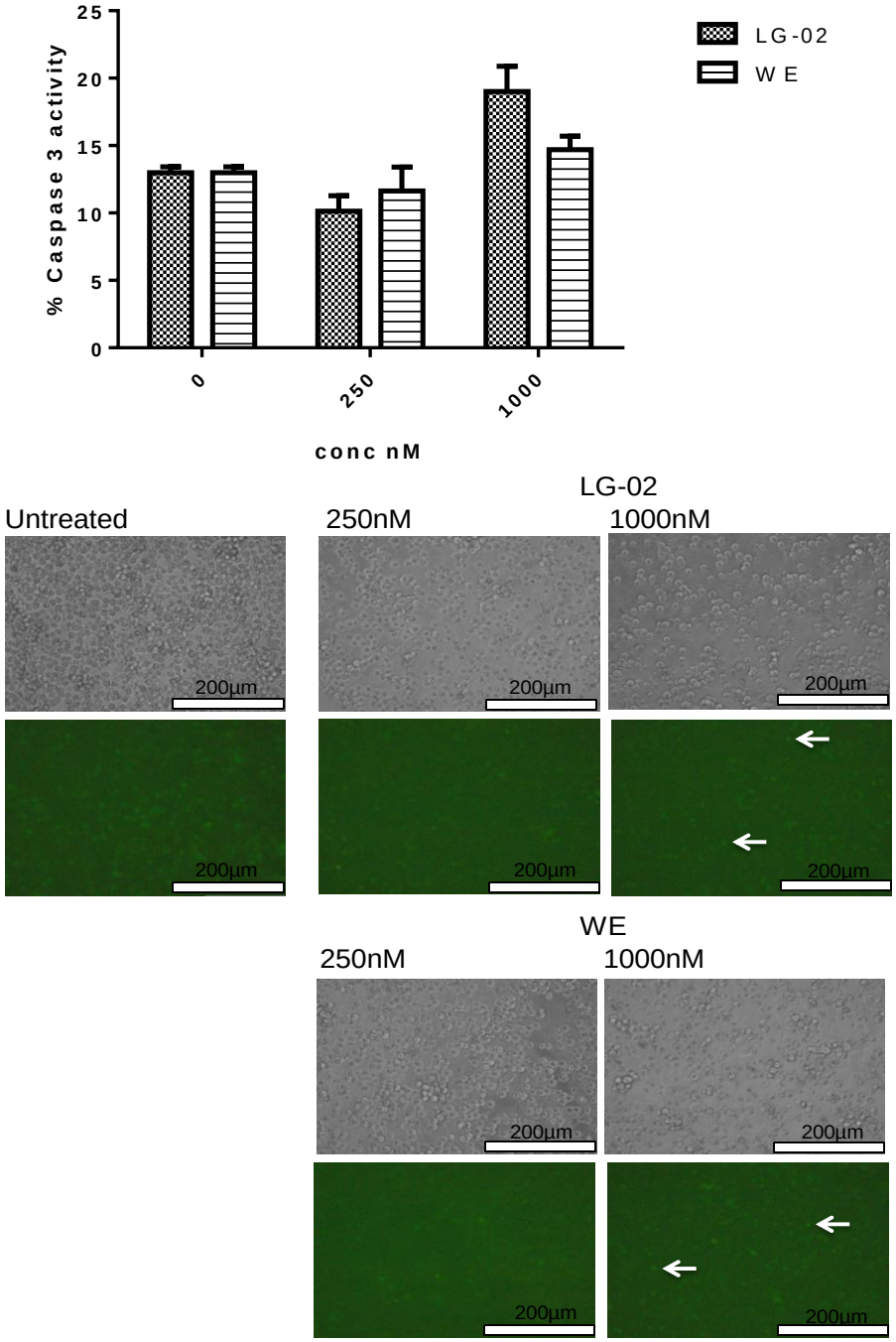

Figure 4.20. The effect of 24hr incubation with LG-02 and WE treatment in LNCAP cell line as determined by the caspase-3 assay. The LNCAP cell lines were treated with 0-1000nM LG-02 and WE to asses for apoptotic effects of these compounds. Caspase-3 activity appears to be induced at 1000nM of LG-02 and WE however background levels of caspase-3 were high in control cells. Data is representative of two independent experiments. Arrows indicate cells with caspase-3 activity.

4.3.2 Effects of withanolides on protein expression

4.3.2.1 Induction of Apoptosis and or Autophagy in prostate cell lines

Prostate cancer cell lines were investigated for apoptosis and or autophagy activation as these were more sensitive to withanolide induced growth inhibition and apoptosis than the breast cancer cell lines. Cell lines were incubated with withanolides for 72 hours prior to cell lysis and western blot analysis. Caspase-3 appeared to be upregulated in the withanolide treated DU145 cell line and was unchanged in the PC3 and LNCAP cell lines, however no cleaved Caspase-3 was evident confirming that of Figures 4.18, 4.19 and 4.20 and further reinforcing that LG-02 and WE mechanism of action are growth inhibition particularly at lower doses. The autophagy marker LC3B was upregulated in all cell lines after LG-02 and WE treatment and an increase in the conversion of LC3B-I to LC3B-II was observed consistent with autophagasome formation and autophagy (Fig 4.21).

Figure 4.21. The effect of LG-02 and WE on Caspase-3 expression and activity and LC3B as determined by Western Blot analysis.

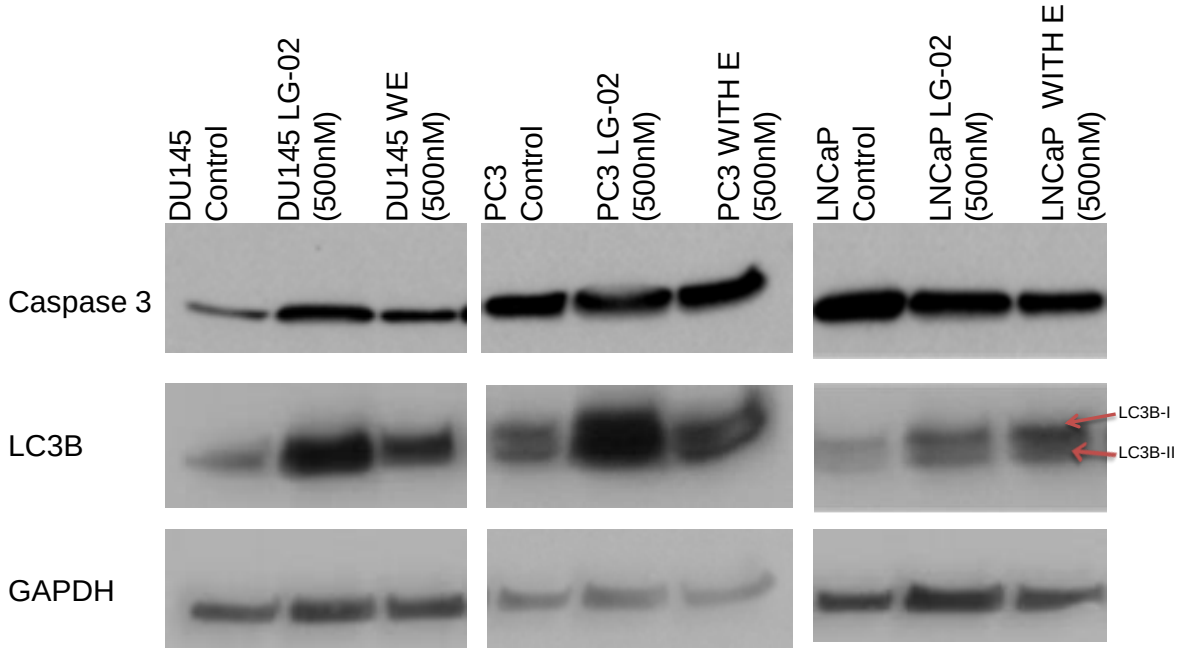

Figure 4.21. The effect of LG-02 and WE on caspase-3 expression and activity and LC3B as determined by Western Blot analysis. Prostate cancer cell lines were subjected to withanolide derivative treatment for 72 hours and a Western blot analysis was performed to asses for cell survival or apoptotic marker. Caspase-3 was upregulated in the DU145 cell line with both LG-02 and WE however no differences was observed in the PC3 and LNCAP cell lines. Although total Caspase-3 (35kDa) was detectable by Western blotting no cleaved Caspase-3 (17kDa) was observed. LC3B was upregulated by both withanolide derivatives in all cell lines. GAPDH was used as a loading control. Data is representative of two independent experiments.

4.3.2.2 The effect of LG-02 and WE in prostate cancer cell lines as determined by Western Blotting.

Proteins responsible for cell cycle regulation were investigated in response to LG-02 and WE at 500nM after 72hrs in DU145, PC3 and LNCAP cell lines.

Cyclin D bound to CDK4/6 is responsible for driving the cell through G1-phase of the cell cycle and was upregulated in the DU145 cell line with both withanolide treatments (Fig 4.22) consistent with Figure 4.11 of the cell cycle analysis of G2/M-phase accumulation. Cyclin D levels were reduced in the PC3 LG-02 treated cells and abolished in the LG-02 treated LNCAP cells (fig 4.22) consistent with PC3 cell being arrested in the G1 phase of the cell cycle (Fig 4.10), however WE had no effect in the PC3 cells and little in the LNCAP cells (fig 4.22).

Cyclin B expression, when bound to its reciprocal Cdk drives the cells through G2/M-phase of the cell cycle, into mitosis and was consistently low in all DU145 samples (fig 4.22). Cyclin B levels were abolished after LG-02 treatment in both PC3 and LNCAP cell lines and reduced after WE treatment (Fig 4.22) consistent with Figure 4.10 and 4.11.

CDK2 that is constitutively expressed in cells and when bound with Cyclin E drives the cells through G1/S-phase of the cell cycle was upregulated in DU145 cells after LG-02 and WE treatment (Fig 4.22) and also corroborates Figure 4.11 in that these cells pass G1-phase of the cell cycle and are stuck in G2/M-phase. CDK2 expression was low in the untreated PC3 cells and inhibited after both withanolide treatments (Fig 4.22). No effect was observed in the LNCAP cells (Fig 4.22).

CDK4 expression when bound to Cyclin E in G1-phase facilitates cell cycle progression and was potentially upregulated after LG-02 treatment (Fig 4.22) although no changes were observed in the PC3 or LNCAP cell lines (Fig 4.22).

$p14^{ARF}$ a tumour suppressor protein that indirectly activates p53, was upregulated after LG-02 and WE treatment in the DU145 cell line (fig 4.22) blocking the cell in G1 or G2 phase of the cell cycle. No expression of $p14^{ARF}$ was found in the PC3 and LNCAP cell lines (Fig 4.22) however PC3 cells are $p14^{ARF}$ negative (Creighton et al. 2010).

p21 is responsible for cell cycle arrest during G1 and G2/M-phase of the cell cycle and was induced after LG-02 and WE treatment in all cell lines (Fig 4.22).

p27 that acts similarly to p21 at inhibiting cyclin-Cdks activity was unchanged in the DU145 and PC3 cell lines and upregulated with both withanolides in the LNCAP cell line (Fig 4.22).

The tumour suppressor protein p53 was present and unchanged in the p53 positive cell line DU145, and absent in the p53 null cell line PC3 after LG-02 and WE treatment. Interestingly, no difference in p53 expression was observed in the LNCAP cells after LG-02 treatment but was induced after WE treatment (Fig 4.22). GAPDH was used as a loading control.

Figure 4.22.The effect of LG-02 and WE in prostate cancer cell lines as determined by Western Blotting

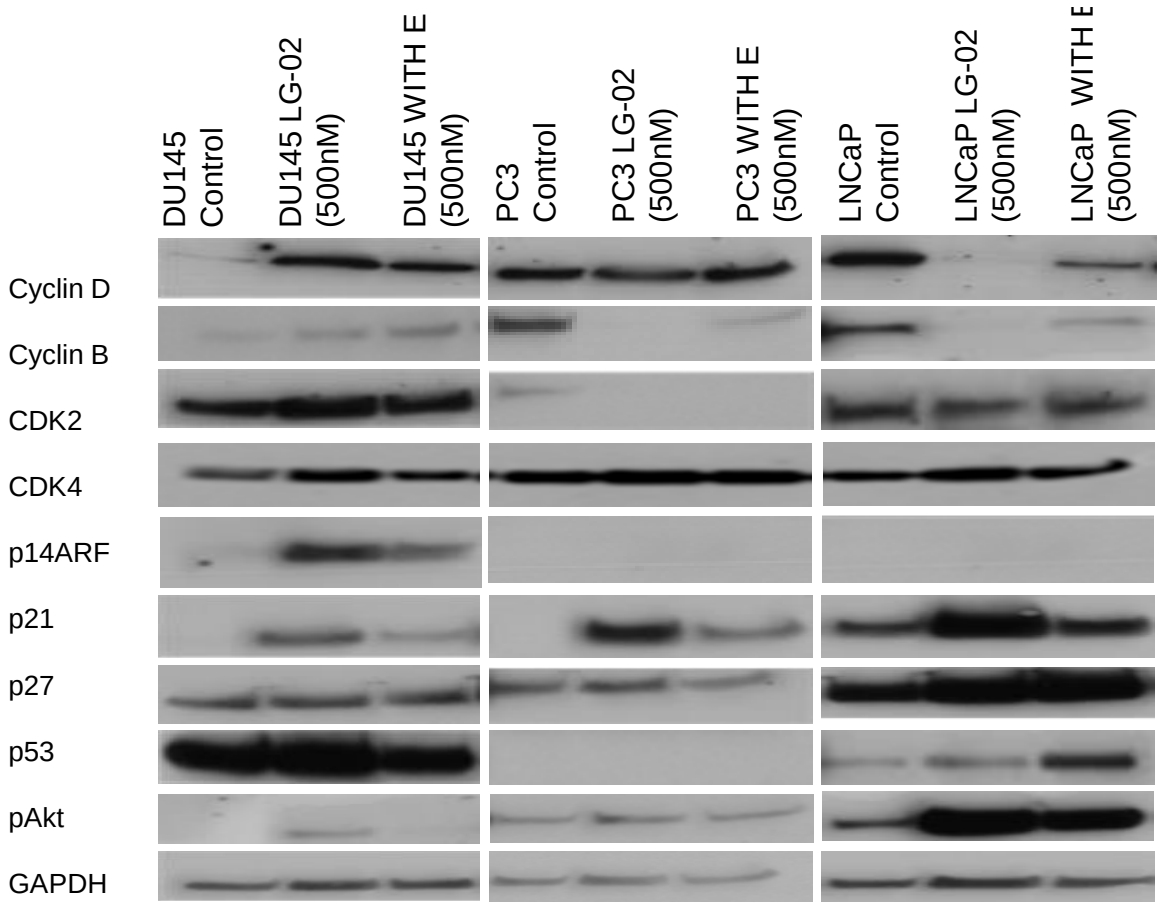

Figure 4.22 The effect of LG-02 and WE in prostate cancer cell lines as determined by Western Blotting. Cell cycle regulatory proteins were probed after 72 hour treatment with LG-02 and WE to determine if any of these genes were upregulated or down-regulated in response to the compounds. Cyclin D was upregulated in the DU145 cells after treatment with LG-02 and WE, unchanged in the PC3 treated cells and down regulated in LNCAP cells. No change was observed in CDK2 and CDK4 expression after incubation with LG-02 and WE in the DU145 and LNCAP cells and CDK2 expression was down regulated in the PC3 cells. p14ARF was upregulated in the treated DU145 cells but was not expressed in the PC3 and LNCAP cell line. p21 was upregulated in all cell lines after treatment with LG-02 and WE. p27 was upregulated in the treated LNCAP cell line and unchanged in the DU145 and PC3 cell lines. No change in p53 expression was observed in the DU145 and p53 null PC3 cells after treatment. pAkt was upregulated in the LNCAP cells after LG-02 and WE treatment and in the LG-02 treated DU145 cells. GAPDH was used as a loading control.

4.3.2.3 The effect of incubation of LG-02 and WE in prostate cancer cell lines for 24 hours as determined by Western Blotting.

Fig 4.22 shows the effects of WE and LG-02 at 72 hours. To asses changes at earlier time points, cells were challenged with WE or LG-02 for 24 hours prior to Western blotting.

p21, p27 and Cyclin D expression was investigated in the PC3 and LNCAP cell lines only as data generated from figure 4.22 demonstrated that 500nM of LG-02 and WE was sufficient at inducing G1 phase accumulation in as little as 24hr incubation with LG-02 and WE.

p21 expression was upregulated in the PC3 and LNCAP cell lines after 24hrs treatment with WE. LG-02 and WE did not appear to have any significant effect on p27 expression in the PC3 cell line, however both compounds did induce p27 expression in the LNCAP cell line. Cyclin D was unaffected in the PC3 cell line with both compounds and was inhibited in the LNCAP cell line (fig 4.23).

Figure 4.23. The effect of 24 hour incubation LG-02 and WE in prostate cancer cell lines as determined by Western Blotting.

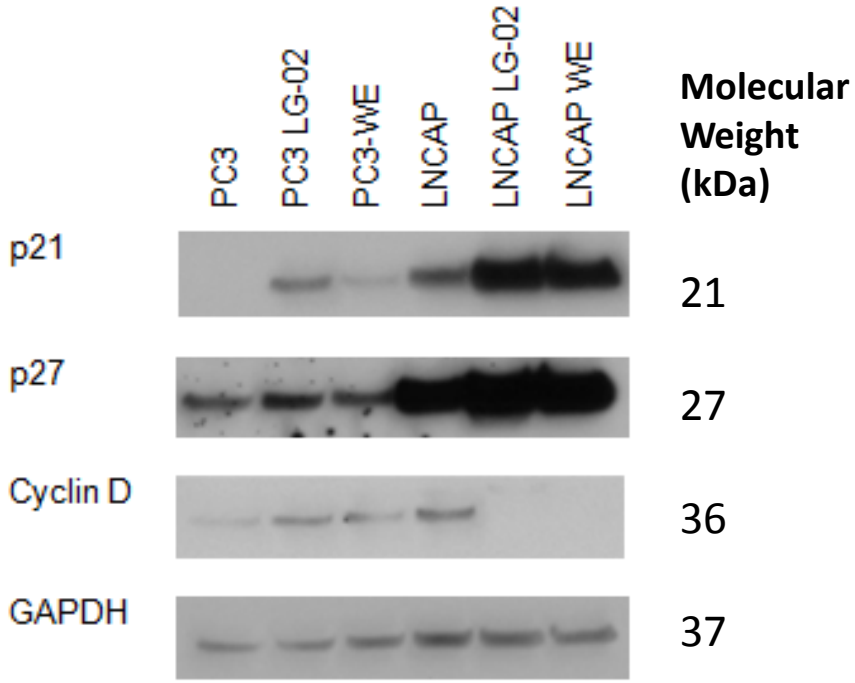

Figure 4.23 The effect of 24 hour incubation LG-02 and WE in prostate cancer cell lines as determined by Western Blotting. Cell cycle regulatory proteins were probed after 24 hours treatment with LG-02 and WE to determine whether these genes were upregulated or downregulated in response to the compounds. Data is representative of 1 independent experiment.

4.3.2.4 Effects of 24 hour treatment of withanolides on androgen responsive genes

Androgen independent PC3 cells and Androgen responsive LNCAP cells were investigated to determine if LG-02 and WE have an effect on the androgen pathway particularly the LNCAP cells as these cells have the lowest IC_{50} value and appeared to be the most sensitive cells to the withanolides. The PC3 cell line is androgen independent and as a result does not express the androgen receptor or PSA, therefore these cells were negative for these proteins. PSA and Androgen receptor was reduced after 24 hours of LG-02 and WE treatment in the LNCAP cells and PSA expression was almost abolished by 72 hours (Figure 4.24). GAPDH was used as a loading control.

Figure 4.24. The effect of LG-02 and WE on PC3 and LNCAP cell lines as determined by Western Blotting

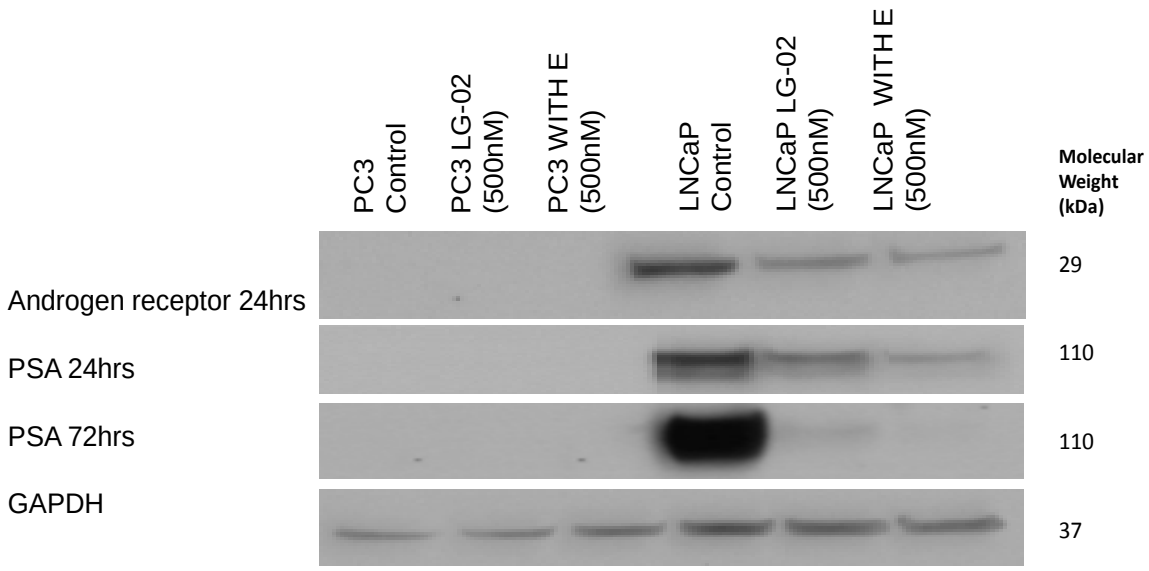

Figure 4.24. The effect of LG-02 and WE on PC3 and LNCAP cell lines as determined by Western blotting. Androgen responsive proteins were investigated to determine the effect of the withanolide derivatives on protein expression in the PC3 and LNCAP cell lines. Androgen receptor-negative/PSA-negative PC3 cells did not express the androgen receptor or PSA. Data is representative of two independent experiments.

4.3.3 The effect of LG-02 and WE on 3D growth and spheroid formation of breast and prostate cancer cells as determined by Hoechst 33342 and Propidium Iodide stain.

Due to LG-02 and WE having a similar effect of inducing cell cycle arrest and induction of apoptosis in prostate and breast cancer cell lines, these were seeded into alginate to assess if growth of spheroids would be inhibited after 7 days of treatment with LG-02 only.

LG-02 had an effect on spheroid formation in the SUM159 cell lines at 1000nM, as a reduction in the number and size of the spheroids was observed. Similar results were observed in MCF7 cells although this was observed from 250nM, and at 1000nM only a small population of cells were able to form spheroids (Fig 4.25). The number and size of the spheroids from the PC3 cells was reduced from 63nM of LG-02 and WE and no spheroids were observed from 250nM of LG-02 (Fig 4.25). Spheroid formation was reduced in the DU145 cell line at 250nM LG-02 and was completely inhibited at 1000nM of both withanolide (Fig 4.25). LNCAP spheroid formation was reduced from 63nM of LG-02 and ~1% of cells treated with 1000nM LG-02 were able to form a spheroid, although these were much smaller in size than the untreated cells.

Figure 4.25. The effect of 7 day incubation on LG-02 on spheroid formation in breast and prostate cancer cell lines

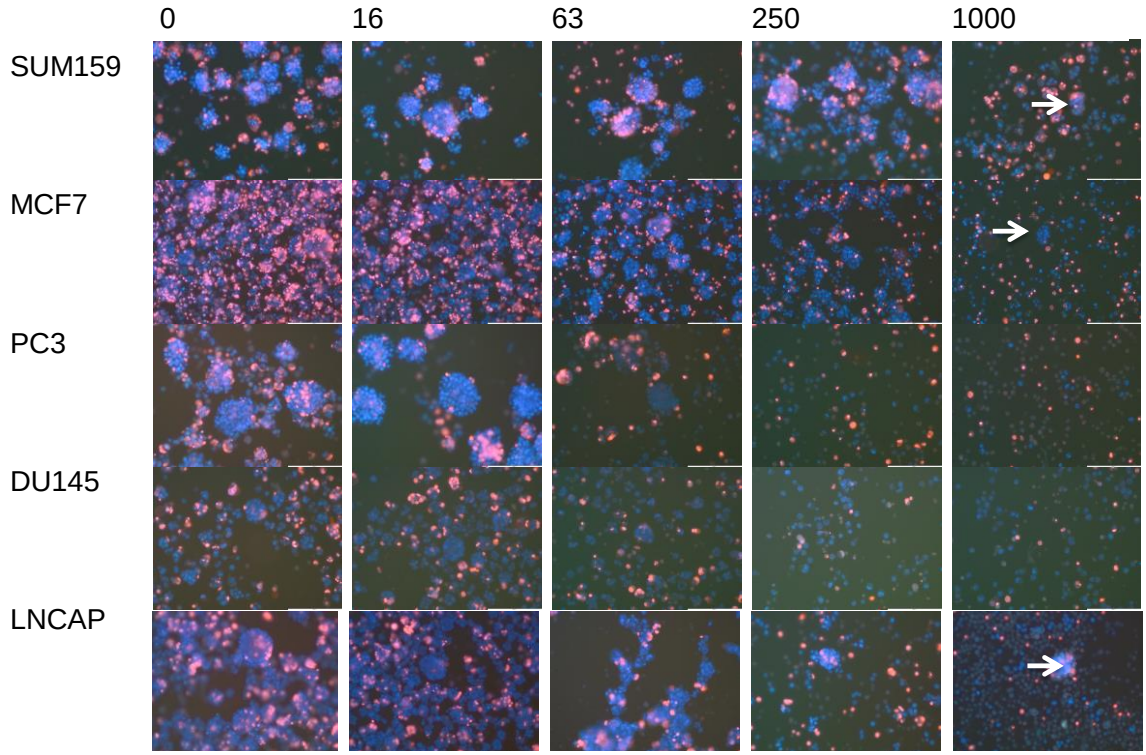

Figure 4.25. The effect of 7 day incubation of LG-02 on spheroid formation in breast and prostate cancer cell lines. LG-02 was more potent at inhibiting spheroid formation in the prostate cancer cell lines as a reduction in the size of spheoids was observed >63nM. However the LNCAP cell line was still able to form a single spheroid at 1000nM. LG-02 reduced spheroid formation capacity by 1000nM in the MCF7 cell line and slowed down growth in the SUM159 cell line. Images are represented of 2 independent experiments. Scale bar represents 200µm. Arrows indicate spheroids that were able to proliferate at the highest dose of LG-02.

4.4 Discussion

4.4.1 Structure function relationship of withanolide derivatives

LG-02 was the most potent withanolide derivative at inducing growth inhibition in the LNCAP cell line with an IC_{50} of 30-60nM followed by WE at 120-150nM as determined by the MTS and Crystal Violet assay. WE and other derivatives except from Withaferin A are all 17Beta hydroxywithanolides which changes the spatial position of the lactone ring (alpha in WE, beta in Withaferin A), therefore these have very different molecular shapes. This is likely to play a role in the biological activity observed. The LG-02 compound differs from WE as it has an acetate at position 18 which increases biological activity whereas LG-29 has a ketone at position 4 that diminishes activity. LG-33 also has reduced activity due to the OH at position 4. Therefore minor modifications in the basic WE skeleton backbone can have major effects on biological effects *in vitro.*

4.4.2 Effect of LG-02 and WE in breast cancer cell lines

4.4.2.1 Effect of LG-02 and WE in SUM159 cell line

SUM159 cells were the least sensitive of all the cell lines to the treatment with withanolides and as a result no IC_{50} was determined, however a previous report has found that these cells are sensitive to WFA with an IC_{50} value of around 1000nM (Antony et al. 2014). At 1000nM of LG-02 there was a significant increase of cells in the G1-phase of the cell cycle and a reduction in the number of cells in the G2/M-phase which does indicate G1-phase cell cycle arrest. WE had no effect on the cell cycle as no significant changes were observed. In an earlier experiment by Lee et at (2014) found that at 2000nM WFA induced G2/M-phase cell cycle arrest, confirming that at lower doses LG-02 is more potent at inducing cell cycle arrest. This difference in cell cycle arrest is likely due to LG-02 and WFA having different targets of the cell cycle and it has

been found that WFA induces securin accumulation found during mitosis, preventing DNA separation and cytokinesis (Antony et al. 2014). The SUM159 cells seeded in alginate and spiked with 1000nM of LG-02 or WE for 7 days resulted in a significantly smaller mammospheres (spheroids). This data is consistent with previous reports of WFA targeting the bCSC population by reducing the number and size of spheroids and also reducing the $CD44^{high}/CD24^{low}/ESA^{+}$ fraction although concentrations of WFA were much higher (Kim and Singh 2014). Although the size of the spheroids were much smaller than the control, these spheroids may be generated from a true breast CSC, as previous findings have found that stem cells are slower growing than differentiated cell types (Moore and Lyle 2011).

4.4.2.2 Effect of LG-02 and WE in MCF7 cell line

The MCF7 cell line is extremely sensitive to LG-02 as a significant reduction in growth was observed with an IC_{50} of 73.57nM, however these cells were not as sensitive to WE. Currently the most potent withanolide at growth inhibition and inducing apoptosis in this cell line is WFA with an IC_{50} of 576> 1000nM, indicating that LG-02 would be a better therapeutic agent than WFA in treating ER breast cancer(Wang et al. 2012a, Zhang et al. 2011). Spheroid formation was inhibited in a dose dependent manner with LG-02 and WE treatment and Kim et al 2014 also found a similar effect with WFA in the size and number of spheroids with similar concentrations. Previous reports have found that WFA at nanomolar concentrations was sufficient at reducing the invasiveness of MCF7 cells, a characteristic of CSC brought about by interacting and disassembling vimentin (Thaiparambil et al. 2011). The mechanism of action of WFA is that the C3 on the A ring interacts with Cys328 on the vimentin α-helix inducing vimentin aggregation, de-polymerisation at the leading edge and Ser56 vimentin phosphorylation (Thaiparambil et al. 2011). As LG-02 and WE share a high degree of similarity, and also

contain C3 on the A ring, it could be suggested that these also interact with vimentin, reduce invasiveness, and could impart be responsible for spheroid inhibition, although this is unlikely as WE does not induce dramatic cell morphology changes as observed after WFA incubation (Henrich et al. 2015). To note, spheroid formation was not fully abolished as a single cell was able to self-renew and form an individual spheroid, much smaller than that of the control but with the potential to proliferate further. Data generated from the cell cycle analysis was inconclusive after LG-02 treatment as only a significant reduction in cells in S-phase was observed and as a result G1 or G2/M cell cycle arrest could not be confirmed, although it did appear to be G2/M arrest no significant changes could be found. Previously, it has also been found that the MCF7 cell line has a defective G1 and mitotic spindle checkpoint (Morse et al. 2005). WE appeared to have no effect on the cell cycle from 0-1000nM concentrations. Previously, Lee et al. 2014 had found that 2000nM of WFA induced the MCF7 cell lines to undergo G2/M cell cycle arrest (Antony et al. 2014) although Zhang et al 2011 found that 500nM was sufficient to induce cell cycle arrest. At 1000nM of either withanolides, MCF7 cells underwent apoptosis as confirmed by the Hoechst 33342 and Propidium Iodide stain. Treating cells with 1000nM of WFA for 24hrs resulted in a similar amount of apoptosis (Zhang et al. 2011). The caspase-3 assay as expected indicated no caspase-3 activation as MCF7 cell lines did not express this gene due to a 47 base pair deletion located within exon 3 of the CASP-3 gene (Jänicke et al. 1998) but have been found to undergo apoptosis after incubating with 5000nM WFA via caspase-7 activation although this concentration is 5-times greater than that used for LG-02 and WE (Wang et al. 2012a).

4.4.3 Effect of LG-02 and WE in Androgen-independent prostate cancer cell lines: PC3 and DU145

The PC3 cells had an IC_{50} of <500nM after 72hr treatment with both withanolides, however currently investigated withanolide derivatives have an IC_{50} of greater than 500nM (Aalinkeel et al. 2010, Nishikawa et al. 2015) indicating that LG-02 and WE are more potent than the previously investigated withanolide derivatives. LG-02 and WE appeared to have a different effect in the PC3 and DU145 cell lines as these were found to undergo G1 and G2/M cell cycle arrest respectively, indicating that these withanolides have cell specific targets, however previous data has found that WFA induces G2/M cell cycle arrest in both cell lines (Roy et al. 2013, Reyes-Reyes et al. 2013). G1 cell cycle arrest was further confirmed in the PC3 cells due to the up-regulation of p21, that may potentially bind to and inhibit cyclinD/Cyclin dependent kinase activity (Gartel and Tyner 2002). G1 cell cycle arrest was further facilitated by the down regulation of Cdk2 in PC3 cells as this enzyme is crucial in facilitating the progression of G1 to S-phase of the cell cycle. Cyclin B is crucial in the M-phase of the cell cycle and was also down regulated in the PC3 cells after withanolide treatments and corroborates earlier findings after WFA treatment (Roy et al. 2013). Cyclin D, CDK2 and CDK4 expression are upregulated after LG-02 and WE treatment in the DU145 cells. The increase in Cyclin D expression facilitates the progression of cells through the restriction point and into S-phase. In addition to this there is also an up-regulation of $p14^{ARF}$ and p21 after withanolide treatment, further confirming that increased expression leads to G2/M cell cycle arrest. Cyclin B levels remain unchanged after treatment although Roy et al (2013) found that WFA downregulated Cyclin B although concentrations used were greater that 1000nM (Roy et al. 2013). Both withanolides have a significant effect on spheroid formation in the PC3 and DU145 cell lines as by

1000nM, no spheroid formation was observed. A recent paper by Xu et al. (2015) has shown that using a PC3 xenograft model in mice; LG-02 treatment is successful at reducing the size of a tumour (Xu et al. 2015). The PC3 cells appeared to undergo little/no apoptosis after withanolide treatment, as confirmed by their nuclear morphology, the Caspase-3 assay and also Caspase-3 expression whereas the DU145 cells showed a higher amount (>20%) of apoptosis, Caspase-3 activation using the Caspase-3 assay and an increase in Caspase-3 protein expression consistent with previous data of withanolide derivatives (Reyes-Reyes et al. 2013), however the primary effect of the withanolides is growth inhibition but may also induce caspase-independent apoptosis at higher concentrations. A withanolide derivative known as Physangulidine A can compromise the colony forming capacity in the PC3 and DU145 cells in a dose dependent manner from 2500nM and abolishes all self-renewal capabilities at 5000nM (Reyes-Reyes et al. 2013) however LG-02 and WE are 5 times more potent than other derivatives at spheroid formation inhibition. PC3 cells are negative for the androgen receptor and PSA and are consistent with previous findings (Tai et al. 2011). Phosphorylated Akt (pAkt) remains unchanged in the PC3 control and withanolide treated cell lines. pAkt is undetectable in the DU145 control, and WE treated samples after 72 hours however an upregulation of this kinase is observed after 72 hours LG-02 treatment.

4.4.4 Effects of LG-02 and WE in the Androgen-dependent cell line LNCAP

The LNCAP cells are extremely sensitive to growth inhibitory and apoptotic effects of withanolides, particularly LG-02. This supports previous reports of LNCAP growth inhibition induced by LG-02 (Xu et al. 2015) and other withanolide derivatives (Minguzzi et al. 2002, Nishikawa et al. 2015). The LNCAP cell line was the most sensitive cell line to withanolide derivatives induced growth inhibition however

Okuzaki et al, 2015 has found that androgen independent cell lines PC3 and DU145 were more sensitive to 2000nM WFA, demonstrating that LG-02 and WE may have a different/additional target protein to WFA in the LNCAP cells, particularly at lower concentrations. The withanolides had a significant dose dependent effect on spheroid formation as the majority of cells remained as individual cells, likely to be cytostatic, although a cluster of cells derived from a single cell was able to overcome the cytotoxic effects of the withanolides even at the highest concentrations. Using a LNCAP xenograft model in mice, LG-02 was successful at reducing the size of a tumour (Xu et al. 2015). G1-phase accumulation was observed from 63nM of both withanolides characterised by an increase in G1 events and a concomitant reduction of events in S and G2/M phase however by 1000nM no significant differences was observed, likely caused by the cell cycle being arrested at both G1 and G2/M phase. When treated with 500nM of withanolides there was a clear decrease in cyclin D and B expression and an increase in p21 and p27 expression signifying potential simultaneous G1 and G2/M cell cycle arrest. Another report by Yang et al (2006) found that WFA induces p27 accumulation (Yang, Shi and Dou 2007). A significant proportion of cells were apoptotic when treated from 250nM of both withanolides, as determined by their nuclear morphology which contrasts with their resistance to WFA induced apoptosis (Nishikawa et al. 2015). A substantial reduction in PSA and androgen receptor expression was seen after 24 hours of 500nM withanolides treatment and by 72 hours almost all expression of PSA was diminished indicating that androgen responsive genes are targeted and downregulated. A similar study by Xu et al (2015) determined that PSA mRNA was downregulated after incubation with LG-02 using a high-throughput gene expression screen (Xu et al. 2015). Down regulation of the androgen receptor in LNCAP cells after addition of 5-10µM of WFA (much higher than that used in this

study) was first identified by Yang et al (2007) in which they had found that WFA inhibits chymotrypsin like activity in the 26S proteasome (Yang, Shi and Dou 2007). As proteasome activity is crucial in androgen receptor transactivation (Lin et al. 2002) inhibiting proteasome activity may in part, explain the effects of LG-02 and WE on the androgen receptor expression although this is unlikely as Henrich et al (2015) found that WFA is a weak proteasome inhibitor and WE has negligible effects on proteasome activity (Henrich, Brooks et al. 2015). PSA expression is transcriptionally activated by the androgen receptor therefore a reduction in this receptor would reduce expression of PSA (Jia et al. 2003). In addition, PSA has also been found to regulate androgen receptor signaling as it controls androgen receptor mRNA and protein levels (Saxena et al. 2012). A significant upregulation of pAkt is observed after response to LG-02 and WE treatment, likely due to the PI3K/Akt and AR pathway regulating each other by reciprocal negative feedback, in which inhibition of any of the pathway leads to activation of the other (Carver et al. 2011). A previous report has found that androgen deprivation therapy leads to an increase in PI3K and Akt activity, promoting survival, androgen independency and castrate resistance prostate cancer (Murillo et al. 2001).

4.5 Concluding remarks

LG-02 and WE are the most effective withanolide derivatives at inducing cell cycle arrest as compared to previously investigated withanolides, in particular WFA is a highly reactive molecule and is generally used at high concentrations. Prostate cancer cell lines were much more sensitive to withanolides than the breast cancer cell lines. Mechanisms of action of both compounds were predominantly growth inhibition and some apoptosis at high concentrations. These compounds also inhibited the 3D formation of spheroids in the androgen dependent cell lines but only slowed growth in the breast cancer cell line, and a single LNCAP cell was able to overcome cytotoxic

effects of these compounds generating a spheroid similar in size to that of the untreated sample. This was likely, to be due to an increase in Akt activity, promoting cell survival after androgen ablation. The Actual mechanisms of action of LG-02 and WE on androgen signaling still unknown but it is more potent in the androgen dependent LNCAP cell line at inducing cell cycle arrest. LG-02 could potentially be used as a therapeutic in cases of castrate resistant prostate cancer as these are sensitive to the growth inhibitory effects and do not rely on PI3K/Akt for survival. In androgen dependent carcinomas LG-02 and WE would have an initial effect on androgen signaling but is likely to lead to castrate-resistance prostate cancer and should only be used in combination with other compounds that can target the PI3K/Akt pathway.

5 General Discussion

5.1 Introduction

Most drug discovery processes rely on cell based assay as these are simple, fast and cost effective and avoid large scale, cost intensive animal testing. Cell based assays measure cellular responses to external stimuli such as drugs or compounds. The majority of cell based assays use traditional 2D cell culture in which cells are grown as a monolayer on a flat, rigid substrate. 2D cell culture does not take into account that *in vivo*, cells are usually surrounded by other cells and ECM components. As a result 2D cell culture may give misleading, unreliable and non-predictive data (Birgersdotter, Sandberg and Ernberg 2005, Bhadriraju and Chen 2002). In drug discovery, the standard process in screening is 2D cell culture, animal models leading onto clinical trials however only 10% of compounds progress through clinical development, partly due to the data collected from 2D cell culture is altered due to the cells unnatural microenvironment (Edmondson et al. 2014). Recently, much of the focus into cell based assays is the development of 3D cell culture models as these represent more accurately the actual microenvironment where cells reside in tissues and also enriches for the CSC population that may be absent when cells are cultured in 2D.

The first part of this study was to investigate the prostate and breast cancer stem cell phenotypes $CD44^+/CD133^+$ (Collins et al. 2005) and $CD44^+/CD24^-$ (Bhat-Nakshatri et al. 2010, Ghebeh et al. 2013) in 2D, in addition to 'proposed' breast CSC phenotypes $CD44^+/CD181^+$ and $CD181^+/CD24^-$. It was determined that the prostate cell lines had a low percentage of cells with the $CD44^+/CD133^+$ phenotype. This was not concerning as it is expected that the bulk of cancer cells are differentiated and that CSC accounts for ~1% of the population in tumours or cell lines (Collins et al. 2005, Gong et al. 2012). In addition, long-term culture of cancer cell lines in monolayers facilitates selection of the

most dominant cell sub-populations, which may not be representative of the slow growing CSC (Rowehl et al. 2014). The breast cancer cell line MCF7 had a population of <1% of cells with the $CD44^+/CD24^-$ phenotype, whereas triple negative, highly aggressive SUM159 cells had a basal expression of 18%. $CD181^+/CD44^+$ and $CD181^+/CD24^-$ phenotype was also investigated in the MCF7 cell line cultured in 2D resulting in a 1% and <1% 'proposed' CSC population. Again, the SUM159 had a much higher population of cells with the $CD181^+/CD44^+$ and $CD181^+/CD24^-$ phenotypes. Prostate and breast cancer cell lines cultured in 3D using alginate did support spheroid formation however the DU145 cell line were unable to grow 3D spheroids larger than 200μm, although these cells remained viable. 3D cell culture was then investigated to determine if alginate could enrich for the prostate cancer stem cell phenotype after 14 days culture in 3D. At this given time point there was no significant increase in cells with the prostate CSC phenotype when compared against cells cultured in 2D, suggesting that at the optimised time point and concentration, alginate does not enrich for a prostate CSC population. In addition, CD44 expression decreased in the PC3 and DU145 cell line cultured in 3D. Investigations into the $CD44^+/CD24^-$ breast CSC phenotype of cells cultured in 3D found that there was a 6-fold increase in MCF7 and 4-fold increases in the SUM159 cell line. The $CD181^+/CD24^-$ population was also significantly increased in both cell lines whereas the $CD181^+/CD44^+$ cell population was only induced in the SUM159 cell line phenotype.

Previous studies have found that alginate-based 3D cell culture can enrich for the CSC population as an up-regulation of CSC markers have been found in a murine breast cancer model (Qiao et al. 2016), hepatocellular carcinoma and head and neck squamous carcinoma cell lines cultured in 3D (Xu et al. 2014). This study was the first

of its type using alginate as a 3D cell culture tool used to mimic the tumour microenvironment *in vitro* for enrichment of the CSC population in human breast cancer cell lines.

Although the prostate CSC population was not enriched in 3D, identification of an enriched CSC population in breast cancer cell lines set the precedence for further study and clarification of the breast CSC population, further supported by previous literature confirming this.

5.1.1 Does Nanog expression correlate with CSC phenotypes?

Nanog is a transcription factor that regulates self-renewal in embryonic and adult tissue specific stem cells (Loh et al. 2006, Boyer et al. 2005) and has also been identified in many cancer types (Lipscomb et al. 2007, Hwang, et al. 2013, Lombaerts et al. 2006, Cao et al. 2008, Kong et al. 2010, Xie et al. 2010, Zhou et al. 2011, Shan et al. 2012, Sun et al. 2013a). Several studies have found that Nanog maintains pluripotency in CSC and also offers resistance to chemotherapy agents (Jeter et al. 2011a), involved in metastasis and invasion and facilitates tumour reoccurrence (Wang, Chiou and Wu 2013). An investigation was carried out using the SUM159 reporter cell line that had a NRE-GFP reporter incorporated into its genome via lentiviral transduction, and was used to determine if NRE-GFP is co-expressed with CD44, CD24- and CD181. Preliminary studies revealed that there was no significant difference between the NRE-GFP and GFP^{-ve} cell population with any of the CSC markers. The SUM159 NRE-GFP cells when cultured in 2D had a basal expression of GFP in 34% of the cell population which was significantly downregulated in 3D cell culture. Much of the literature investigating Nanog expression has found that Nanog is induced in 3D cell culture (Xu et al. 2014) and in hypoxia (Mathieu et al. 2011) that was

present in the core of the spheroids. As the other CSC markers in this study were induced in 3D it was surprising to find NRE-GFP was not. GFP expression was also investigated in the SUM159 cell line cultured in 3D using CSC medium and it was found to not induce NRE-GFP expression, however GFP was significantly induced in the Control cells (CMVmin-GFP) in the absence of a NRE. Interestingly in a parallel project, PC3 NRE-GFP cells that were cultured in CSC medium enriched for GFP expression but not Nanog. Nanog protein expression was investigated using Western blot analysis of SUM159 cells cultured in 2D and 3D. Surprisingly Nanog was not expressed at a protein level, or was below the limit of detection. This resulted in more questions than answers as to what was driving GFP in these cells. PCR was also carried out to determine if Nanog or NanogP8 mRNA was expressed and it was determined that Nanog does not appear to be expressed at the mRNA level. For both Nanog protein and mRNA the NTera2 cell line was used as a positive control confirming that the assays worked. With questions still unanswered, subsequent experiments were carried out to identify the source of the GFP signal in the NRE-GFP.

5.1.2 Factors affecting GFP in the NRE-GFP and CMVmin-GFP reporter cell lines

As the NRE-GFP expressed GFP in the absence of Nanog, investigations into GFP inducers was carried out. It was found that hypoxia did not induce GFP expression in the SUM159 cell line as no significant differences were observed when compared against normoxia, however GFP intensity in the CMVmin-GFP cells resembled that of NRE-GFP after 24hr incubation in hypoxia. As GFP was induced in the Control (CMVmin-GFP) cell line cultured in CSC medium in the absence of the NRE, it was thought that GFP expressed in the NRE-GFP cell line may have been selected based on low proteasome activity and not Nanog positivity, since destabilised GFP from the construct is degraded by the proteasome keeping basal levels below the limit of

detection. Investigations using the proteasome inhibitor bortezomib were carried out to mimic low proteasome activity as previous investigations have identified proteasome^{Lo} as a marker of CSC (Vlashi et al. 2013). No significant differences were observed in the NRE-GFP cell line after 72 hour treatment with bortezomib, however a significant increase in GFP was observed in the Control (CMVmin-GFP) cell line and a more profound effect after 24 hours. Interestingly a batch of NRE-GFP cells that progressively decreased their expression of GFP were identified. Loss of a stem cell reporter (NRE-GFP) could be due to a) differentiation of cells (Lin et al. 2005) or b) long term culture in 2D may reduce the CSC population (Rowehl et al. 2014) or c) gene silencing due to histone modifications or CpG methylation near the transduced reporter vector (Mutskov and Felsenfeld 2004). Irrespective of the mechanism of silencing, these cells re-expressed GFP after bortezomib treatment, suggesting that the construct was active to a similar level to the CMVmin-GFP control. This data is supportive of the notion of reporter cell lines selected on the basis of dsGFP may not be selecting for gene of interest but could be due to low proteasome activity (Pan et al. 2010, Lagadec et al. 2014, Munakata et al. 2016) or early stage apoptosis (Dantuma et al. 2000). As the NRE-GFP reporter cells were not selected for based on Nanog expression these may or may not represent the CSC population and targeting this population with novel CSC-targeting agents such as withanolide derivative would be unsuccessful based on their phenotype. Using a different reporter vector, the NTera2 cell line used as a positive control for Nanog expression and the SUM159 cell line as a negative control were transfected with vectors containing the Nanog promoter-GFP or Nanog-P8 promoter-GFP, in which GFP expression would be in response to Nanog gene regulation and not Nanog protein-GFP. This was carried out to optimise the transfection protocol, following onto creating other reporter cell lines in order to

target and eradicate the CSC population and assay in real time. After transfection, the NTera2 and SUM159 cells failed to generate any convincingly GFP positive cells, likely due to the poorly designed vectors. Investigations into Nanog or NanogP8 expression was then carried out to identify if Nanog is actually expressed in breast and prostate cancer cell lines.

5.1.3 Nanog expression in breast and prostate cancer cell lines

Nanog appeared to be expressed in the DU145 cells at 42kDa, and a smaller Nanog species was detected in the LNCAP cell line. In order to elucidate if these Nanog species are derived from the Nanog or NanogP8 locus, 2D gel electrophoresis and Western blot were optimised on the NTera2 cell line. The DU145 and LNCAP cell lines have previously been found to express NanogP8 (Jeter et al. 2011b, Jeter et al. 2009), although Kawamura et al (2015) found that DU145 cells express Nanog and NanogP8 (Kawamura et al. 2015). Unfortunately, no Nanog species could be detected after isoelectric focusing in the DU145 or LNCAP cell lines, likely to be due to a) NanogP8 protein pI does not fall between the pH 4-7, b) Nanog or NanogP8 proteins have differing post-translational modifications not observed in the NTera2 cell line or c) Truncated Nanog or NanogP8 proteins altering the pI. Identifying transcription factors that regulate NanogP8 expression would offer great knowledge into the mechanism that facilitates its expression. To date, there is no literature available that has identified transcription factors responsible for NanogP8 expression and little convincing evidence of naturally occurring nanogP8 protein.

As the Nanog positive cell population were not easily identifiable, withanolide derivatives that were assumed to target the CSC population could not be used with the

NRE-GFP cell lines and preliminary data would be gathered using 2D cell culture and progress onto 3D cell culture in un-transduced breast and prostate cancer cell lines.

5.1.4 Targeting CSC with withanolide derivatives

Withanolide derivatives are a natural steroidal compound found in *Withania somnifera,* also known as Winter Cherry that possesses anticancer properties. Withaferin A has been investigated extensively for its anti-cancer properties (Kakar et al. 2014, Roy et al. 2013, Szic et al. 2014) and as a CSC targeting agent (Kakar et al. 2014). The aim of the final part of the study was to investigate novel withanolides that were more potent than Withaferin A and induce growth inhibition and cell death in breast and prostate cancer cell lines and eradicate the CSC population that induce tumour re-occurrence. In this study it was found that LG-02 and WE were more potent growth inhibitors than Withaferin A, in the LNCAP cell line and at higher concentrations induced some apoptosis. The SUM159 cell line was the most resistant to growth inhibition and an IC_{50} could not be established. The prostate cancer cell lines were more sensitive to LG-02 and WE than the breast cancer cell lines, in particular the LNCAP cell line and it is thought that these may target the androgen signalling as a previous study using high throughput screening found that LG-02 inhibited PSA mRNA transcription (Xu et al. 2015). LG-02 and WE had similar biological targets *in vitro* although LG-02 was the most potent likely due to the acetate at position 18 increasing activity. Both compounds induced cell cycle arrest in the prostate cell lines and induced the expression of proteins involved in cell cycle arrest in accordance with previous reports of proteins targeted using withanolide derivatives, although these were used at higher concentrations (Roy et al. 2013, Reyes-Reyes et al. 2013). LG-02 was able to inhibit spheroid formation in the PC3 and DU145 cell lines from 250nM and slowed the growth in the MCF7 and SUM159 cell line however a single spheroid

was able to form in the LNCAP cell line, even at the highest concentration. This may be due to pAkt induction in the LNCAP cell line as observed in this study and as a secondary proliferative pathway when Androgen response pathways is inhibited (Murillo et al. 2001), facilitating growth and potentially leading to castrate resistance in this cell line. It is likely that LG-02 may target the CSC population in the PC3 and DU145 cell lines as 3D growth was inhibited and individual cells were dead or quiescent although long term incubation with LG-02 and WE may lead to propagation and resistance in remaining cells.

5.1.5 Conclusion

In this study it has been shown for the first time that 3D cell culture using alginate can enrich for the breast CSC population however this model in not universally applicable to all cancer types. 3D cell culture does not enrich for Nanog expression in the SUM159 cell line, due to Nanog expression being below the limit of detection. It has also been demonstrated for the first time that LG-02 and WE were able to target the heterogeneous cell population and potential CSC population in the PC3 and DU145 cell lines. LG-02 and WE appear to selectively target the androgen response pathway, and proteins involved in cell cycle arrest. In addition, this study for the first time shows a decrease in PSA and Androgen receptor in the LNCAP cell line confirming and extending Xu et al (2015) that identified mRNA reduction of PSA using high-throughput gene expression screen.

5.2 Future Directions

5.2.1 Does the CD44+/CD181+ phenotype represent a CSC population?

Identification of an increased population of cells with the $CD44^{+}/CD181^{+}$ phenotype using 3D cell culture has identified a population of cells that are potentially more stem like and may represent a more universally accepted breast CSC population. A Hoechst efflux assay, ALDH1A activity and invasion assay could be carried out to determine if this population was representative of the breast CSC population when compared against cells with the $CD44^{+}/CD24^{-}$ phenotype.

5.2.2 Does LG-02 and WE treatment lead to drug resistance or castrate resistance cell populations?

It has been demonstrated that a small population of LNCAP cells cultured in 3D are resistant to LG-02 effects but what has not been established is whether these cells acquired resistance to the Withanolides or are these cells representative, or originating from a CSC population. Also, are these androgen-resistant subpopulations emerging from androgen-sensitive populations and if so, what are the mechanisms of LG-02/WE.

Future directions would be to culture the LNCAP cell line on a larger scale for subsequent phenotyping for CSC markers. Another experimental design would be to culture in charcoal stripped FBS to determine if these cells proliferate in the absence of androgens. In addition, pAkt was upregulated in response to LG-02 and WE, probably due to the androgen signalling mechanism being impaired offering resistance to this compound. Inhibition of the pAkt pathway as a secondary treatment may aid in eradicating this population of cells.

Future work would require re-treatment of isolated cultures of resistant spheroids with withanolides and comparing to untreated to determine if the resistant phenotype stable or not. Further investigations would be to determine if the cells that repopulate

3D spheroids representative of CSCs and get to the point of a 99.9% kill and study the surviving cells that are present in the LNCAP cell line, at 1000nM LG-02. The bulk in the spheroid may be differentiated but also resistant, so the spheroid 'originates from a CSC' but isn't comprised of them.

Further investigation would be carried out to determine if withanolide resistance is associated with Androgen-resistance. Since resistance was only seen in AR-dependant cell line, and clearly AR signalling is down-regulated in Withanolide treatment, as would be observed in charcoal-stripping (no androgens) or Bicalutimide treatment, then it could be presumed that the resistant cells that emerge are androgen-resistant. This is known to occur with the LNCAP and anti-androgens. Given that abiraterone is a steroidal structure with some similarities to withanolide derivatives and inhibits androgen biosynthesis due to interactions with CYP17 enzyme, LG-02 and WE may have a similar mechanism of action. Alternatively, the resistant population could be treated with siRNA for the androgen receptor and growth could be monitored to determine if this population no longer required androgen signalling via the androgen receptor for proliferation.

If cells are androgen-dependent, it is important to know where the AR-targeted effects are. Androgen dependent cells could be treated with LG-02 or WE and investigate for blockade of androgen biosynthesis pathways using HPLC. HPLC allows the detection of steroids from a sample and could be used to determine if steroid biosynthesis was impaired after incubation with withanolide derivatives. If a particular steroid was no longer synthesised this would offer further information as to LG-02 and WE mechanisms of action as these may target the CYP enzymes (see fig 4.2) that are involved in steroid biosynthesis.

6 References

AALINKEEL, Ravikumar, et al. (2010). Genomic Analysis Highlights the Role of the JAK-STAT Signaling in the Anti- proliferative Effects of Dietary Flavonoid—' Ashwagandha' in Prostate Cancer Cells. *Evidence-based complementary and alternative medicine,* **7** (2), 177-187.

AIGNER, S., et al. (1998). CD24 mediates rolling of breast carcinoma cells on P-selectin. *FASEB journal : Official publication of the federation of american societies for experimental biology,* **12** (12), 1241-1251.

AIGNER, S., et al. (1997). CD24, a mucin-type glycoprotein, is a ligand for P-selectin on human tumor cells. *Blood,* **89** (9), 3385-3395.

AKASHI, T., SHIRASAWA, T. and HIROKAWA, K. (1994). Gene expression of CD24 core polypeptide molecule in normal rat tissues and human tumor cell lines. *Virchows archiv : An international journal of pathology,* **425** (4), 399-406.

ALBERTS, Bruce, WILSON, John H. and HUNT, Tim (2015). *Molecular biology of the cell.* Sixth edition / Bruce Alberts [with six others] ; with problems by John Wilson, Tim Hunt.. ed., Garland Science.

AL-HAJJ, M., et al. (2003). Prospective identification of tumorigenic breast cancer cells. *Proceedings of the national academy of sciences of the united states of america,* **100** (7), 3983-3988.

AMBADY, S., et al. (2010). Expression of NANOG and NANOGP8 in a variety of undifferentiated and differentiated human cells. *The international journal of developmental biology,* **54** (11-12), 1743-1754.

Amp, Apos and BRIEN, Fergal J. (2011). Biomaterials & scaffolds for tissue engineering. *Materials today,* **14** (3), 88-95.

ANAND, P., et al. (2008). Cancer is a preventable disease that requires major lifestyle changes. *Pharmaceutical research,* **25** (9), 2097-2116.

ANTONY, Marie L., et al. (2014). Growth arrest by the antitumor steroidal lactone withaferin a in human breast cancer cells is associated with down- regulation and covalent binding at cysteine 303 of β-tubulin. *Journal of biological chemistry,* **289** (3), 1852-1865.

ANTONY, M. L., et al. (2010). Changes in expression, and/or mutations in TGF-beta receptors (TGF-beta RI and TGF-beta RII) and Smad 4 in human ovarian tumors. *Journal of cancer research and clinical oncology,* **136** (3), 351-361.

ARAKI, S., et al. (1990). Apoptosis of vascular endothelial cells by fibroblast growth factor deprivation. *Biochemical and biophysical research communications,* **168** (3), 1194-1200.

ARELLANO, M. and MORENO, S. (1997). Regulation of CDK/cyclin complexes during the cell cycle. *The international journal of biochemistry & cell biology,* **29** (4), 559-573.

ARKENAU, Hendrik-Tobias, CARDEN, Craig P. and DE BONO, Johann S. (2008). Targeted agents in cancer therapy. *Medicine,* **36** (1), 33-37.

ASHKENAZI, A. and DIXIT, V. M. (1998). Death receptors: signaling and modulation. *Science (new york, N.Y.),* **281** (5381), 1305-1308.

AUS, G., et al. (2005). EAU Guidelines on Prostate Cancer. *European urology,* **48** (4), 546-551.

BABA, T., et al. (2009). Epigenetic regulation of CD133 and tumorigenicity of CD133+ ovarian cancer cells. *Oncogene,* **28** (2), 209-218.

BADEAUX, M. A., et al. (2013). In vivo functional studies of tumor-specific retrogene NanogP8 in transgenic animals. *Cell cycle (georgetown, tex.),* **12** (15).

BAGGIOLINI, Marco and CLARK-LEWIS, Ian (1992). Interleukin-8, a chemotactic and inflammatory cytokine. *FEBS letters,* **307** (1), 97-101.

BAIXERAS, E., et al. (2001). The proliferative and antiapoptotic actions of growth hormone and insulin-like growth factor-1 are mediated through distinct signaling pathways in the Pro-B Ba/F3 cell line. *Endocrinology,* **142** (7), 2968-2977.

BAKER, B. M. and CHEN, C. S. (2012). Deconstructing the third dimension: how 3D culture microenvironments alter cellular cues. *Journal of cell science,* **125** (Pt 13), 3015-3024.

BARRANDON, Y. and GREEN, H. (1987). Three clonal types of keratinocyte with different capacities for multiplication. *Proceedings of the national academy of sciences of the united states of america,* **84** (8), 2302-2306.

BARTEK, J. and LUKAS, J. (2001). Mammalian G1- and S-phase checkpoints in response to DNA damage. *Current opinion in cell biology,* **13** (6), 738-747.

BAUM, B., SETTLEMAN, J. and QUINLAN, M. P. (2008). Transitions between epithelial and mesenchymal states in development and disease. *Seminars in cell & developmental biology,* **19** (3), 294-308.

BEAVER, C. M., AHMED, A. and MASTERS, J. R. (2014). Clonogenicity: holoclones and meroclones contain stem cells. *PloS one,* **9** (2), e89834.

BECKHARDT, R. N., et al. (1995). HER-2/neu oncogene characterization in head and neck squamous cell carcinoma. *Archives of otolaryngology--head & neck surgery,* **121** (11), 1265-1270.

BHADRIRAJU, K. and CHEN, C. S. (2002). Engineering cellular microenvironments to improve cell-based drug testing. *Drug discovery today,* **7** (11), 612-620.

BHAT-NAKSHATRI, P., et al. (2010). SLUG/SNAI2 and tumor necrosis factor generate breast cells with CD44+/CD24- phenotype. *BMC cancer,* **10** , 411-2407-10-411.

BIRGERSDOTTER, A., SANDBERG, R. and ERNBERG, I. (2005). Gene expression perturbation in vitro--a growing case for three-dimensional (3D) culture systems. *Seminars in cancer biology,* **15** (5), 405-412.

BISSELL, M. J., RIZKI, A. and MIAN, I. S. (2003). Tissue architecture: the ultimate regulator of breast epithelial function. *Current opinion in cell biology,* **15** (6), 753-762.

BLAIN, Stacy W. (2008). Switching cyclin D- Cdk4 kinase activity on and off. *Cell cycle (georgetown, tex.),* **7** (7), 892.

BLANPAIN, C. and FUCHS, E. (2014). Stem cell plasticity. Plasticity of epithelial stem cells in tissue regeneration. *Science (new york, N.Y.),* **344** (6189), 1242281.

BLOWERS, Elaine and FOY, Sharon (2009). Breast cancer overview: Current treatments. *Practice nursing,* **20** (6), 282-286.

BOCKSTAELE, L., et al. (2006). Regulated Activating Thr172 Phosphorylation of Cyclin-Dependent Kinase 4(CDK4): Its Relationship with Cyclins and CDK â€œInhibitorsâ€. *Molecular and cellular biology,* **26** (13), 5070-5085.

BOESCH, M., et al. (2016). High prevalence of side population in human cancer cell lines. *Oncoscience,* **3** (3-4), 85-87.

BOFFETTA, Paolo and HASHIBE, Mia (2006). *Alcohol and cancer.* Amsterdam ;, The Lancet oncology, **7** (2), 149-156.

BOKHARI, M., et al. (2007a). Culture of HepG2 liver cells on three dimensional polystyrene scaffolds enhances cell structure and function during toxicological challenge. *Journal of anatomy,* **211** (4), 567-576.

BOKHARI, Maria, et al. (2007b). Culture of HepG2 liver cells on three dimensional polystyrene scaffolds enhances cell structure and function during toxicological challenge. *Journal of anatomy,* **211** (4), 567-576.

BOO, L., et al. (2016). MiRNA Transcriptome Profiling of Spheroid-Enriched Cells with Cancer Stem Cell Properties in Human Breast MCF-7 Cell Line. *International journal of biological sciences,* **12** (4), 427-445.

BOOTH, H. Anne F. and HOLLAND, Peter W. H. (2004). Eleven daughters of NANOG. *Genomics,* **84** (2), 229-238.

BOSTWICK, David G. (2000). *Prostatic intraepithelial neoplasia.* Philadelphia, Pa.] :, Current urology reports, **1** (1), 65-70.

BOSTWICK, David G. and QIAN, Junqi (2004). *High-grade prostatic intraepithelial neoplasia.* New York, NY :, Modern pathology., **17** (3), 360-379.

BOYER, L. A., et al. (2005). Core transcriptional regulatory circuitry in human embryonic stem cells. *Cell,* **122** (6), 947-956.

BRADY, G., et al. (2007). Upregulation of IGF-2 and IGF-1 receptor expression in oral cancer cell lines. *International journal of oncology,* **31** (4), 875-881.

BRANDOLINI, L., et al. (2015). Targeting CXCR1 on breast cancer stem cells: signaling pathways and clinical application modelling. *Oncotarget,* **6** (41), 43375-43394.

BRONNER, C. E., et al. (1994). Mutation in the DNA mismatch repair gene homologue hMLH1 is associated with hereditary non-polyposis colon cancer. *Nature,* **368** (6468), 258-261.

BRUGAROLAS, J., et al. (1995). Radiation-induced cell cycle arrest compromised by p21 deficiency. *Nature,* **377** (6549), 552-557.

BUDHIRAJA, R., KRISHAN, P. and SUDHIR, S. (2000). Biological Activity of Withanolides. **59** , 904-911.

BUDILLON, A., et al. (1991). UP-REGULATION OF EPIDERMAL GROWTH- FACTOR RECEPTOR INDUCED BY ALPHA-INTERFERON IN HUMAN EPIDERMOID CANCER-CELLS. *Cancer research; cancer res.,* **51** (4), 1294-1299.

BURGARSKI, B', et al. (1994). *Electrostatic droplet generation: Mechanism of polymer droplet formation.* New York] :, AIChE journal, **40** (6), 1026-1031.

BURGER, Patricia E., et al. (2009). High aldehyde dehydrogenase activity: a novel functional marker of murine prostate stem/progenitor cells. *Stem cells (dayton, ohio),* **27** (9), 2220-2228.

BURKHART, Deborah L. and SAGE, Julien (2008). Cellular mechanisms of tumour suppression by the retinoblastoma gene. *Nature reviews cancer,* **8** (9), 671.

BUTLER, L. M., et al. (1998). Down-regulation of Fas gene expression in colon cancer is not a result of allelic loss or gene rearrangement. *British journal of cancer,* **77** (9), 1454-1459.

BYAR, D. P. (1973). Proceedings: The Veterans Administration Cooperative Urological Research Group's studies of cancer of the prostate. *Cancer,* **32** (5), 1126-1130.

CABRERA, M. C., HOLLINGSWORTH, R. E. and HURT, E. M. (2015). Cancer stem cell plasticity and tumor hierarchy. *World journal of stem cells,* **7** (1), 27-36.

CALVET, C. Y., ANDRE, F. M. and MIR, L. M. (2014). The culture of cancer cell lines as tumorspheres does not systematically result in cancer stem cell enrichment. *PloS one,* **9** (2), e89644.

CAMPAGNOLI, C., et al. (2001). Identification of mesenchymal stem/progenitor cells in human first-trimester fetal blood, liver, and bone marrow. *Blood,* **98** (8), 2396-2402.

CAMPREGHER, C., LUCIANI, M. G. and GASCHE, C. (2008). Activated neutrophils induce an hMSH2-dependent G2/M checkpoint arrest and replication errors at a (CA)13-repeat in colon epithelial cells. *Gut,* **57** (6), 780-787.

Cancer Research UK, (2015). Last accessed August 2015 at http://www.cancerresearchuk.org/.

CAO, Jian, et al. (2008). Membrane type 1 matrix metalloproteinase induces epithelial-to-mesenchymal transition in prostate cancer. *The journal of biological chemistry,* **283** (10), 6232-6240.

CARDONE, M., et al. (1998). Regulation of cell death protease caspase- 9 by Akt-mediated protein phosphorylation. *Molecular biology of the cell; mol.biol.cell,* **9** , 246A-246A.

CARVER, Brett s, et al. (2011). Reciprocal Feedback Regulation of PI3K and Androgen Receptor Signaling in PTEN- Deficient Prostate Cancer. *Cancer cell,* **19** (5), 575-586.

CHAFFER, Christine L. and WEINBERG, Robert A. (2011). A perspective on cancer cell metastasis. *Science (new york, N.Y.),* **331** (6024), 1559-1564.

CHAMBERS, K. F., et al. (2014). 3D Cultures of prostate cancer cells cultured in a novel high-throughput culture platform are more resistant to chemotherapeutics compared to cells cultured in monolayer. *PloS one,* **9** (11), e111029.

CHANG, David F., et al. (2009). Molecular characterization of the human NANOG protein. *Stem cells (dayton, ohio),* **27** (4), 812-821.

CHANG, H. Y. and YANG, X. (2000). Proteases for Cell Suicide: Functions and Regulation of Caspases. *Microbiology and molecular biology reviews,* **64** (4), 821-846.

CHATURVEDI, P., et al. (1999). Mammalian Chk2 is a downstream effector of the ATM-dependent DNA damage checkpoint pathway. *Oncogene,* **18** (28), 4047-4054.

CHATURVEDI, P., et al. (2013a). Hypoxia-inducible factor-dependent breast cancer-mesenchymal stem cell bidirectional signaling promotes metastasis. *The journal of clinical investigation,* **123** (1), 189-205.

CHATURVEDI, Pallavi, et al. (2013b). Hypoxia- inducible factor-- dependent breast cancer-- mesenchymal stem cell bidirectional signaling promotes metastasis.(Research article). *Journal of clinical investigation,* **123** (1), 189.

CHEN, L., et al. (2012). The enhancement of cancer stem cell properties of MCF-7 cells in 3D collagen scaffolds for modeling of cancer and anti-cancer drugs. *Biomaterials,* **33** (5), 1437-1444.

CHEN, N. and DEBNATH, J. (2010). Autophagy and tumorigenesis. *FEBS letters,* **584** (7), 1427-1435.

CHEN, Tianji, DU, Juan and LU, Guangxiu (2012). Cell growth arrest and apoptosis induced by Oct4 or Nanog knockdown in mouse embryonic stem cells: a possible role of Trp53. *Molecular biology reports,* **39** (2), 1855-1861.

CHENG, N., et al. (2008). Transforming growth factor-beta signaling-deficient fibroblasts enhance hepatocyte growth factor signaling in mammary carcinoma cells to promote scattering and invasion. *Molecular cancer research : MCR,* **6** (10), 1521-1533.

CHENG, Y., et al. (2012). MK-2206, a novel allosteric inhibitor of Akt, synergizes with gefitinib against malignant glioma via modulating both autophagy and apoptosis. *Molecular cancer therapeutics,* **11** (1), 154-164.

CHIBA, K., et al. (2015). Cancer-associated TERT promoter mutations abrogate telomerase silencing. *eLife,* **4** , 10.7554/eLife.07918.

CHIBA, Tetsuhiro, et al. (2006). Side population purified from hepatocellular carcinoma cells harbors cancer stem cell-like properties. *Hepatology (baltimore, md.),* **44** (1), 240-251.

CHICHEPORTICHE, Y., et al. (1997). TWEAK, a new secreted ligand in the tumor necrosis factor family that weakly induces apoptosis. *The journal of biological chemistry,* **272** (51), 32401-32410.

CHINNAIYAN, A. M. (1999). The apoptosome: heart and soul of the cell death machine. *Neoplasia (new york, N.Y.),* **1** (1), 5-15.

CHIOU, Shih-Hwa, et al. (2010). Coexpression of Oct4 and Nanog enhances malignancy in lung adenocarcinoma by inducing cancer stem cell-like properties and epithelial-mesenchymal transdifferentiation. *Cancer research,* **70** (24), 10433-10444.

CHODAK, Gerald (2006). Prostate cancer: epidemiology, screening, and biomarkers. *Reviews in urology,* **8 Suppl 2** , S3.

CHUA, V. Y., et al. (2016). Activity of ABCG2 Is Regulated by Its Expression and Localization in DHT and Cyclopamine-Treated Breast Cancer Cells. *Journal of cellular biochemistry,* **117** (10), 2249-2259.

CHUTE, John P., et al. (2006). Inhibition of aldehyde dehydrogenase and retinoid signaling induces the expansion of human hematopoietic stem cells. *Proceedings of the national academy of sciences of the united states of america,* **103** (31), 11707-11712.

CLARKE, A. R., et al. (1993). Thymocyte apoptosis induced by p53-dependent and independent pathways. *Nature,* **362** (6423), 849-852.

CLARKE, Michael F., et al. (2006). Cancer stem cells--perspectives on current status and future directions: AACR Workshop on cancer stem cells. *Cancer research,* **66** (19), 9339-9344.

COHEN-FIX, Orna and KOSHLAND, Doug (1997). The anaphase inhibitor of Saccharomyces cerevisiae Pds1p is a target of the DNA damage checkpoint pathway. *Proceedings of the national academy of sciences of the united states of america,* **94** (26), 14361-14366.

COLE, S. P., et al. (1992). Overexpression of a transporter gene in a multidrug-resistant human lung cancer cell line. *Science (new york, N.Y.),* **258** (5088), 1650-1654.

COLLINS, A. T., et al. (2005). Prospective identification of tumorigenic prostate cancer stem cells. *Cancer research,* **65** (23), 10946-10951.

COLLINS, A. T., et al. (2001). Identification and isolation of human prostate epithelial stem cells based on α 2 β 1 -integrin expression. *Journal of cell science,* **114** (21), 3865-3872.

CONLEY, S. J., et al. (2012). Antiangiogenic agents increase breast cancer stem cells via the generation of tumor hypoxia. *Proceedings of the national academy of sciences of the united states of america,* **109** (8), 2784-2789.

COOK, R., et al. (2015). Direct involvement of retinoblastoma family proteins in DNA repair by non-homologous end-joining. *Cell reports,* **10** (12), 2006-2018.

CORTEZ, D., et al. (1999). Requirement of ATM-dependent phosphorylation of brca1 in the DNA damage response to double-strand breaks. *Science (new york, N.Y.),* **286** (5442), 1162-1166.

CORTI, Stefania, et al. (2006). Identification of a primitive brain-derived neural stem cell population based on aldehyde dehydrogenase activity. *Stem cells (dayton, ohio),* **24** (4), 975-985.

CREIGHTON, C. J., et al. (2010). Molecular profiling uncovers a p53-associated role for microRNA-31 in inhibiting the proliferation of serous ovarian carcinomas and other cancers. *Cancer research,* **70** (5), 1906-1915.

CROKER, Alysha K., et al. (2009). High aldehyde dehydrogenase and expression of cancer stem cell markers selects for breast cancer cells with enhanced malignant and metastatic ability. *Journal of cellular and molecular medicine,* **13** (8B), 2236-2252.

CURTIS, Helena (1983). *Biology.* New York, N.Y., Worth Publishers.

DAMDINSUREN, B., et al. (2006). TGF-beta1-induced cell growth arrest and partial differentiation is related to the suppression of Id1 in human hepatoma cells. *Oncology reports,* **15** (2), 401-408.

DANG, Hien, et al. (2011). Snail1 induces epithelial-to-mesenchymal transition and tumor initiating stem cell characteristics. *BMC cancer,* **11** (1), 396-396.

DANTUMA, N. P., et al. (2000). Short-lived green fluorescent proteins for quantifying ubiquitin/proteasome-dependent proteolysis in living cells. *Nature biotechnology,* **18** (5), 538-543.

DAS, T., et al. (2014). Withaferin A modulates the Spindle assembly checkpoint by degradation of Mad2-Cdc20 complex in colorectal cancer cell lines. *Biochemical pharmacology,* **91** (1), 31-39.

DATTA, S. R., et al. (1997). Akt phosphorylation of BAD couples survival signals to the cell-intrinsic death machinery. *Cell,* **91** (2), 231.

DAVID, Bertrand, et al. (2004). In Vitro Assessment of Encapsulated C3A Hepatocytes Functions in a Fluidized Bed Bioreactor. *Biotechnology progress,* **20** (4), 1204-1212.

DAVOLI, T., DENCHI, E. L. and DE LANGE, T. (2010). Persistent telomere damage induces bypass of mitosis and tetraploidy. *Cell,* **141** (1), 81-93.

DE BEÇA, Francisco Ferro, et al. (2013). Cancer stem cells markers CD44, CD24 and ALDH1 in breast cancer special histological types. *Journal of clinical pathology,* **66** (3), 187-191.

DE VOS, Paul, et al. (2003). Long- term biocompatibility, chemistry, and function of microencapsulated pancreatic islets. *Biomaterials,* **24** (2), 305-312.

DEAN, M. and ALLIKMETS, R. (1995). Evolution of ATP-binding cassette transporter genes. *Current opinion in genetics & development,* **5** (6), 779-785.

DECENSI, A. U., et al. (1991). Monotherapy with nilutamide, a pure nonsteroidal antiandrogen, in untreated patients with metastatic carcinoma of the prostate. The Italian Prostatic Cancer Project. *The journal of urology,* **146** (2), 377-381.

DESAI, Apurva, STADLER, Walter M. and VOGELZANG, Nicholas J. (2001). Nilutamide: possible utility as a second- line hormonal agent. *Urology,* **58** (6), 1016-1020.

DEVOLDER, R. and KONG, H. J. (2012). Hydrogels for in vivo-like three-dimensional cellular studies. *Wiley interdisciplinary reviews.systems biology and medicine,* **4** (4), 351-365.

DEWEY, W. C., LING, C. C. and MEYN, R. E. (1995). Radiation-induced apoptosis: relevance to radiotherapy. *International journal of radiation oncology, biology, physics,* **33** (4), 781-796.

DOHERTY, R. E., et al. (2011). Aldehyde dehydrogenase activity selects for the holoclone phenotype in prostate cancer cells. *Biochemical and biophysical research communications,* **414** (4), 801-807.

DONTU, G., et al. (2003). In vitro propagation and transcriptional profiling of human mammary stem/progenitor cells. *Genes & development,* **17** (10), 1253-1270.

DRAFFIN, Jayne E., et al. (2004). CD44 potentiates the adherence of metastatic prostate and breast cancer cells to bone marrow endothelial cells. *Cancer research,* **64** (16), 5702.

DU, C., et al. (2000). Smac, a mitochondrial protein that promotes cytochrome c-dependent caspase activation by eliminating IAP inhibition. *Cell,* **102** (1), 33-42.

DU, L., et al. (2008). CD44 is of functional importance for colorectal cancer stem cells. *Clinical cancer research : An official journal of the american association for cancer research,* **14** (21), 6751-6760.

DUBROVSKA, Anna, et al. (2009). The role of PTEN/ Akt/ PI3K signaling in the maintenance and viability of prostate cancer stem- like cell populations.(MEDICAL SCIENCES)(phosphatase and tensin homolog)(Author abstract)(Report). *Proceedings of the national academy of sciences of the united states,* **106** (1), 268.

Early Breast Cancer Trialist, Collaborative Group (1998). Tamoxifen for early breast cancer: an overview of the randomised trials. *The lancet,* **351** (9114), 1451-1467.

EASTHAM, J. A., et al. (1995). Association of p53 mutations with metastatic prostate cancer. *Clinical cancer research : An official journal of the american association for cancer research,* **1** (10), 1111-1118.

ECKE, T. H., et al. (2007). TP53 mutation in prostate needle biopsies--comparison with patients follow-up. *Anticancer research,* **27** (6B), 4143-4148.

EDMONDSON, R., et al. (2014). Three-dimensional cell culture systems and their applications in drug discovery and cell-based biosensors. *Assay and drug development technologies,* **12** (4), 207-218.

ELMORE, S. (2007). Apoptosis: a review of programmed cell death. *Toxicologic pathology,* **35** (4), 495-516.

Emmanuelle Charafe-Jauffret, et al. (2010). Aldehyde Dehydrogenase 1–Positive Cancer Stem Cells Mediate Metastasis and Poor Clinical Outcome in Inflammatory Breast Cancer. *Clinical cancer research,* **16** (1), 45-55.

EPSTEIN, J. I., et al. (2005). The 2005 International Society of Urological Pathology (ISUP) Consensus Conference on Gleason Grading of Prostatic Carcinoma. *The american journal of surgical pathology,* **29** (9), 1228-1242.

EVAN, G. and LITTLEWOOD, T. (1998). A matter of life and cell death. *Science (new york, N.Y.),* **281** (5381), 1317-1322.

EVAN, G. I. and VOUSDEN, K. H. (2001). Proliferation, cell cycle and apoptosis in cancer. *Nature,* **411** (6835), 342-348.

FADOK, V. A., et al. (2001). Loss of phospholipid asymmetry and surface exposure of phosphatidylserine is required for phagocytosis of apoptotic cells by macrophages and fibroblasts. *The journal of biological chemistry,* **276** (2), 1071-1077.

FAN, L., et al. (2012a). Loss of E-cadherin promotes prostate cancer metastasis via upregulation of metastasis-associated gene 1 expression. *Oncology letters,* **4** (6), 1225-1233.

FAN, Q. M., et al. (2014). Tumor-associated macrophages promote cancer stem cell-like properties via transforming growth factor-beta1-induced epithelial-mesenchymal transition in hepatocellular carcinoma. *Cancer letters,* **352** (2), 160-168.

FAN, Xinlan, et al. (2012b). Effective enrichment of prostate cancer stem cells from spheres in a suspension culture system. *Urologic oncology: Seminars and original investigations,* **30** (3), 314-318.

FANG, D. D., et al. (2010a). Expansion of CD133(+) colon cancer cultures retaining stem cell properties to enable cancer stem cell target discovery. *British journal of cancer,* **102** (8), 1265-1275.

FANG, Xianfeng, et al. (2010b). CD24: from A to Z. *Cellular and molecular immunology,* **7** (2), 100.

FEINBERG, A. P. and VOGELSTEIN, B. (1983). Hypomethylation distinguishes genes of some human cancers from their normal counterparts. *Nature,* **301** (5895), 89-92.

FELTHAUS, O., et al. (2011). Cancer stem cell-like cells from a single cell of oral squamous carcinoma cell lines. *Biochemical and biophysical research communications,* **407** (1), 28-33.

FENNEMA, Eelco, et al. (2013). Spheroid culture as a tool for creating 3D complex tissues. *Trends in biotechnology,* .

FERGUSON, L. R., et al. (2015). Genomic instability in human cancer: Molecular insights and opportunities for therapeutic attack and prevention through diet and nutrition. *Seminars in cancer biology,* **35 Suppl** , S5-24.

FERRALDESCHI, R., et al. (2015). PTEN protein loss and clinical outcome from castration-resistant prostate cancer treated with abiraterone acetate. *European urology,* **67** (4), 795-802.

FILLMORE, C. M. and KUPERWASSER, C. (2008). Human breast cancer cell lines contain stem-like cells that self-renew, give rise to phenotypically diverse progeny and survive chemotherapy. *Breast cancer research : BCR,* **10** (2), R25.

FILLMORE, Christine and KUPERWASSER, Charlotte (2007). Human breast cancer stem cell markers CD44 and CD24: enriching for cells with functional properties in mice or in man? *Breast cancer research : BCR,* **9** (3), 303-303.

FOTY, R. (2011). A simple hanging drop cell culture protocol for generation of 3D spheroids. *Journal of visualized experiments : JoVE,* **(51). pii: 2720. doi** (51), 10.3791/2720.

FRIXEN, U. H., et al. (1991). E-cadherin-mediated cell-cell adhesion prevents invasiveness of human carcinoma cells. *The journal of cell biology,* **113** (1), 173-185.

FROMOWITZ, F. B., et al. (1987). Ras P21 Expression in the Progression of Breast Cancer. *Human pathology,* **18** (12), 1268-1275.

FUJIWARA, D., et al. (2013). The usefulness of three-dimensional cell culture in induction of cancer stem cells from esophageal squamous cell carcinoma cell lines. *Biochemical and biophysical research communications,* **434** (4), 773-778.

FULFORD, L. G., et al. (2006). Specific morphological features predictive for the basal phenotype in grade 3 invasive ductal carcinoma of breast. *Histopathology,* **49** (1), 22-34.

FUTREAL, P. A., et al. (1994). BRCA1 mutations in primary breast and ovarian carcinomas. *Science (new york, N.Y.),* **266** (5182), 120-122.

FUTREAL, P. A., et al. (1992). Detection of frequent allelic loss on proximal chromosome 17q in sporadic breast carcinoma using microsatellite length polymorphisms. *Cancer research,* **52** (9), 2624-2627.

GANGEMI, R. M., et al. (2009). SOX2 silencing in glioblastoma tumor-initiating cells causes stop of proliferation and loss of tumorigenicity. *Stem cells (dayton, ohio),* **27** (1), 40-48.

GARRIDO, C., et al. (2006). Mechanisms of cytochrome c release from mitochondria. *Cell death and differentiation,* **13** (9), 1423.

GARTEL, A. L. and TYNER, A. L. (2002). *The role of the cyclin- dependent kinase inhibitor p21 in apoptosis.* Molecular Cancer Therapeutics; Mol.Cancer Ther., **1** (8), 639-649.

GEHO, David H., et al. (2005). Physiological mechanisms of tumor-cell invasion and migration. *Physiology (bethesda, md.),* **20** (3), 194-200.

GELFANT, S. (1977). A new concept of tissue and tumor cell proliferation. *Cancer research,* **37** (11), 3845-3862.

GERBER, H. P., et al. (1999). VEGF is required for growth and survival in neonatal mice. *Development (cambridge, england),* **126** (6), 1149-1159.

GEYER, Charles E., et al. (2006). Lapatinib plus capecitabine for HER2- positive advanced breast cancer. *The new england journal of medicine,* **355** (26), 2733.

GHAJAR, Cyrus M. and BISSELL, Mina J. (2010). Tumor engineering: the other face of tissue engineering.(Report). *Tissue engineering, part A: Tissue engineering,* **16** (7), 2153.

GHEBEH, H., et al. (2013). Profiling of normal and malignant breast tissue show CD44high/CD24low phenotype as a predominant stem/progenitor marker when used in combination with Ep-CAM/CD49f markers. *BMC cancer,* **13** , 289-2407-13-289.

GIATROMANOLAKI, A., et al. (2011). The CD44+/CD24- phenotype relates to 'triple-negative' state and unfavorable prognosis in breast cancer patients. *Medical oncology (northwood, london, england),* **28** (3), 745-752.

GIDEKEL, S., et al. (2003). Oct-3/4 is a dose-dependent oncogenic fate determinant. *Cancer cell,* **4** (5), 361-370.

GINESTIER, C., et al. (2010). CXCR1 blockade selectively targets human breast cancer stem cells in vitro and in xenografts. *JOURNAL OF CLINICAL INVESTIGATION,* **120** (2), 485-497.

GIROD, S. C., et al. (1998). Proliferative activity and loss of function of tumour suppressor genes as ‘biomarkers’ in diagnosis and prognosis of benign and preneoplastic oral lesions and oral squamous cell carcinoma. *British journal of oral & maxillofacial surgery,* **36** (4), 252-260.

GLEASON, D. F. (1992). Histologic grading of prostate cancer: a perspective. *Human pathology,* **23** (3), 273-279.

GLICK, Danielle, BARTH, Sandra and MACLEOD, Kay F. (2010). *Autophagy: cellular and molecular mechanisms.* Chichester, UK, J.Pathol., **221** (1), 3-12.

GLOTTER, E. (1991). Withanolides and related ergostane-type steroids. *Natural product reports,* **8** (4), 415-440.

GOEL, H. L., et al. (2008). Integrins in prostate cancer progression. *Endocrine-related cancer,* **15** (3), 657-664.

GOEL, H. L. and MERCURIO, A. M. (2013). VEGF targets the tumour cell. *Nature reviews.cancer,* **13** (12), 871-882.

GOGAT, K., et al. (2004). VEGF and KDR gene expression during human embryonic and fetal eye development. *Investigative ophthalmology & visual science,* **45** (1), 7-14.

GOKSEI, G., et al. (2013). Wnt1 gene expression alters heterogeneous population of prostate cancer cells; decreased expression pattern observed in CD133(+)/ CD44(+) prostate cancer stem cells. *Cancer research; cancer res.,* **73** (8).

GONG, Chen, et al. (2012). Implication of expression of Nanog in prostate cancer cells and their stem cells. *Journal of huazhong university of science and technology.medical sciences = hua zhong ke ji da xue xue bao.yi xue ying de wen ban = huazhong keji daxue xuebao.yixue yingdewen ban,* **32** (2), 242-246.

GOTTESMAN, M. M., FOJO, T. and BATES, S. E. (2002). Multidrug resistance in cancer: role of ATP-dependent transporters. *Nature reviews.cancer,* **2** (1), 48-58.

GOULD, V. E., et al. (1990). Coexpression patterns of vimentin and glial filament protein with cytokeratins in the normal, hyperplastic, and neoplastic breast. *The american journal of pathology,* **137** (5), 1143-1155.

GRANSTEIN, R. D. and MATSUI, M. S. (2004). UV radiation-induced immunosuppression and skin cancer. *Cutis,* **74** (5 Suppl), 4-9.

GRANT, Gregor T., et al. (1973). Biological interactions between polysaccharides and divalent cations: The egg- box model. *FEBS letters,* **32** (1), 195-198.

GREGORY, C. W., et al. (2001). A mechanism for androgen receptor- mediated prostate cancer recurrence after androgen deprivation therapy. *Cancer research; cancer res.,* **61** (11), 4315-4319.

GRIGNON, D. J., et al. (1997). p53 status and prognosis of locally advanced prostatic adenocarcinoma: a study based on RTOG 8610. *Journal of the national cancer institute,* **89** (2), 158-165.

GU, G., et al. (2007). Prostate cancer cells with stem cell characteristics reconstitute the original human tumor in vivo. *Cancer research,* **67** (10), 4807-4815.

Guillermo Mariño, et al. (2014). Self- consumption: the interplay of autophagy and apoptosis. *Nature reviews molecular cell biology,* **15** (2), 81.

GUPTA, PB, CHAFFER, CL and WEINBERG, RA (2009). Cancer stem cells: mirage or reality? *Nature medicine,* **15** (9), 1010-1012.

GUREL, B., et al. (2010). NKX3.1 as a marker of prostatic origin in metastatic tumors. *The american journal of surgical pathology,* **34** (8), 1097-1105.

GUSTERSON, B. A., et al. (1982). Distribution of myoepithelial cells and basement membrane proteins in the normal breast and in benign and malignant breast diseases. *Cancer research,* **42** (11), 4763-4770.

GUSTERSON, Barry A. and STEIN, Torsten (2012). Human breast development. *Seminars in cell and developmental biology,* **23** (5), 567-573.

HAEGEL, H., DIERICH, A. and CEREDIG, R. (1994). CD44 in differentiated embryonic stem cells: surface expression and transcripts encoding multiple variants. *Developmental immunology,* **3** (4), 239-246.

HAHM, Eun-Ryeong, LEE, Joomin and SINGH, Shivendra V. (2014). Role of mitogen-activated protein kinases and Mcl-1 in apoptosis induction by withaferin A in human breast cancer cells. *Molecular carcinogenesis,* **53** (11), 907.

HAINAUT, P., et al. (1998). IARC Database of p53 gene mutations in human tumors and cell lines: updated compilation, revised formats and new visualisation tools. *Nucleic acids research,* **26** (1), 205-213.

HALL, J. M., et al. (1990). Linkage of early-onset familial breast cancer to chromosome 17q21. *Science (new york, N.Y.),* **250** (4988), 1684-1689.

HALL, M., BATES, S. and PETERS, G. (1995). Evidence for different modes of action of cyclin-dependent kinase inhibitors: p15 and p16 bind to kinases, p21 and p27 bind to cyclins. *Oncogene,* **11** (8), 1581-1588.

HAMBURGER, A. and SALMON, S. E. (1977). Primary bioassay of human myeloma stem cells. *The journal of clinical investigation,* **60** (4), 846-854.

HAMILTON, Olszewski U. (2013). Chemotherapy- induced Enrichment of Cancer Stem Cells in Lung Cancer. *Journal of bioanalysis & biomedicine,* **s9** .

HAMMERER, Peter and MADERSBACHER, Stephan (2012). Landmarks in hormonal therapy for prostate cancer. *BJU international,* **110** , 23-29.

HAN, Jinghua, et al. (2012). RNA interference-mediated silencing of NANOG reduces cell proliferation and induces G0/G1 cell cycle arrest in breast cancer cells. *Cancer letters,* **321** (1), 80-88.

HAN, S. Y., et al. (2000). Functional evaluation of PTEN missense mutations using in vitro phosphoinositide phosphatase assay. *Cancer research,* **60** (12), 3147-3151.

HANAHAN, D. and FOLKMAN, J. (1996). Patterns and emerging mechanisms of the angiogenic switch during tumorigenesis. *Cell,* **86** (3), 353-364.

HANAHAN, D. and WEINBERG, R. A. (2000). The hallmarks of cancer. *Cell,* **100** (1), 57-70.

HANAHAN, D. and WEINBERG, R. A. (2011). Hallmarks of cancer: the next generation. *Cell,* **144** (5), 646-674.

HANNON, G. J. and BEACH, D. (1994). p15INK4B is a potential effector of TGF-beta-induced cell cycle arrest. *Nature,* **371** (6494), 257-261.

HARADA, A., et al. (1994). Essential involvement of interleukin-8 (IL-8) in acute inflammation. *Journal of leukocyte biology,* **56** (5), 559-564.

HARADA, T., et al. (2004). Apoptosis in human endometrium and endometriosis. *Human reproduction update,* **10** (1), 29-38.

HARPER, J. W. and ADAMS, P. D. (2001). *Cyclin- dependent kinases.* Chem.Rev., **101** (8), 2511-2526.

HASMIM, M., et al. (2013). Cutting edge: Hypoxia-induced Nanog favors the intratumoral infiltration of regulatory T cells and macrophages via direct regulation of TGF-beta1. *Journal of immunology (baltimore, md.: 1950),* **191** (12), 5802-5806.

HAY, E. D. (2005). The mesenchymal cell, its role in the embryo, and the remarkable signaling mechanisms that create it. *Developmental dynamics : An official publication of the american association of anatomists,* **233** (3), 706-720.

HAYFLICK, L. and MOORHEAD, P. S. (1961). The serial cultivation of human diploid cell strains. *Experimental cell research,* **25** , 585-621.

HEAPHY, C. M., et al. (2011). Prevalence of the alternative lengthening of telomeres telomere maintenance mechanism in human cancer subtypes. *The american journal of pathology,* **179** (4), 1608-1615.

HEIMARK, R. L., TWARDZIK, D. R. and SCHWARTZ, S. M. (1986). Inhibition of endothelial regeneration by type-beta transforming growth factor from platelets. *Science (new york, N.Y.),* **233** (4768), 1078-1080.

HELLAWELL, G. O., et al. (2002). Expression of the type 1 insulin-like growth factor receptor is up-regulated in primary prostate cancer and commonly persists in metastatic disease. *Cancer research,* **62** (10), 2942-2950.

HELLERSTEDT, Beth A. and PIENTA, Kenneth J. (2002). The Current State of Hormonal Therapy for Prostate Cancer. *CA: A cancer journal for clinicians,* **52** (3), 154-179.

HELT, C. E., et al. (2005). Ataxia telangiectasia mutated (ATM) and ATM and Rad3-related protein exhibit selective target specificities in response to different forms of DNA damage. *The journal of biological chemistry,* **280** (2), 1186-1192.

HENNINGS, L., et al. (2009). Dead or alive? Autofluorescence distinguishes heat-fixed from viable cells. *International journal of hyperthermia : The official journal of european society for hyperthermic oncology, north american hyperthermia group,* **25** (5), 355-363.

HENRICH, C. J., et al. (2015). Withanolide E sensitizes renal carcinoma cells to TRAIL-induced apoptosis by increasing cFLIP degradation. *Cell death & disease,* **6** , e1666.

HESS, David A., et al. (2004). Functional characterization of highly purified human hematopoietic repopulating cells isolated according to aldehyde dehydrogenase activity. *Blood,* **104** (6), 1648-1655.

HIGGINS, C. F. (1992). ABC transporters: from microorganisms to man. *Annual review of cell biology,* **8** , 67-113.

HILGENDORF, K. I., et al. (2013). The retinoblastoma protein induces apoptosis directly at the mitochondria. *Genes & development,* **27** (9), 1003-1015.

HILL, M. M., et al. (2004). Analysis of the composition, assembly kinetics and activity of native Apaf-1 apoptosomes. *The EMBO journal,* **23** (10), 2134-2145.

HIRAGA, T., ITO, S. and NAKAMURA, H. (2011). Side population in MDA-MB-231 human breast cancer cells exhibits cancer stem cell-like properties without higher bone-metastatic potential. *Oncology reports,* **25** (1), 289-296.

HIRSCHHAEUSER, Franziska, et al. (2010). Multicellular tumor spheroids: An underestimated tool is catching up again. *Journal of biotechnology,* **148** (1), 3-15.

HO, Anthony D. (2005). Kinetics and symmetry of divisions of hematopoietic stem cells. *Experimental hematology,* **33** (1), 1-8.

HO, Baotran, et al. (2012). Nanog increases focal adhesion kinase (FAK) promoter activity and expression and directly binds to FAK protein to be phosphorylated. *The journal of biological chemistry,* **287** (22), 18656-18673.

HOFMANN, M., et al. (1993). A link between ras and metastatic behavior of tumor cells: ras induces CD44 promoter activity and leads to low-level expression of metastasis-specific variants of CD44 in CREF cells. *Cancer research,* **53** (7), 1516-1521.

HONETH, G., et al. (2008). The CD44+/CD24- phenotype is enriched in basal-like breast tumors. *Breast cancer research : BCR,* **10** (3), R53.

HSIEH, J. T., et al. (1995). Tumor suppressive role of an androgen-regulated epithelial cell adhesion molecule (C-CAM) in prostate carcinoma cell revealed by sense and antisense approaches. *Cancer research,* **55** (1), 190-197.

HSU, H., XIONG, J. and GOEDDEL, D. V. (1995). The TNF receptor 1-associated protein TRADD signals cell death and NF-kappa B activation. *Cell,* **81** (4), 495-504.

HUANG, C. E., et al. (2014). Enhanced chemosensitivity by targeting Nanog in head and neck squamous cell carcinomas. *International journal of molecular sciences,* **15** (9), 14935-14948.

HUANG, Emina H., et al. (2009). Aldehyde dehydrogenase 1 is a marker for normal and malignant human colonic stem cells (SC) and tracks SC overpopulation during colon tumorigenesis. *Cancer research,* **69** (8), 3382-3389.

HUGGINS, C. and HODGES, C. V. (2002). Studies on prostatic cancer: I. The effect of castration, of estrogen and of androgen injection on serum phosphatases in metastatic carcinoma of the prostate. 1941. *The journal of urology,* **168** (1), 9-12.

HUHTANIEMI, Ilpo, et al. (1991). Response of Circulating Gonadotropin Levels to GnRH Agonist Treatment in Prostatic Cancer. *Journal of andrology,* **12** (1), 46-53.

HWANG, Michael S., et al. (2013). *miR-221/222 Targets Adiponectin Receptor 1 to Promote the Epithelial-to-Mesenchymal Transition in Breast Cancer.* United States, PloS one, **8** (6), e66502.

HYNES, N. E. and STERN, D. F. (1994). The biology of erbB-2/neu/HER-2 and its role in cancer. *Biochimica et biophysica acta,* **1198** (2-3), 165-184.

IDOWU, M. O., et al. (2012). CD44(+)/CD24(-/low) cancer stem/progenitor cells are more abundant in triple-negative invasive breast carcinoma phenotype and are associated with poor outcome. *Human pathology,* **43** (3), 364-373.

IMAMICHI, Y. and MENKE, A. (2007). Signaling pathways involved in collagen-induced disruption of the E-cadherin complex during epithelial-mesenchymal transition. *Cells, tissues, organs,* **185** (1-3), 180-190.

INFANGER, David W., et al. (2013). Glioblastoma stem cells are regulated by interleukin- 8 signaling in a tumoral perivascular niche. *Cancer research,* **73** (23), 7079.

ISAACS, J. T. and COFFEY, D. S. (1989). Etiology and disease process of benign prostatic hyperplasia. *The prostate.supplement,* **2** , 33-50.

ISHIGURO, Tatsuya, et al. (2012). Differential expression of nanog1 and nanogp8 in colon cancer cells. *Biochemical and biophysical research communications,* **418** (2), 199-204.

ITO, H., et al. (2005). Radiation-induced autophagy is associated with LC3 and its inhibition sensitizes malignant glioma cells. *International journal of oncology,* **26** (5), 1401-1410.

JACKSON, D., et al. (1992). CD24, a signal-transducing molecule expressed on human B cells, is a major surface antigen on small cell lung carcinomas. *Cancer research,* **52** (19), 5264-5270.

JAIN, Abhinav K., et al. (2012). p53 regulates cell cycle and microRNAs to promote differentiation of human embryonic stem cells. *PLoS biology,* **10** (2), e1001268.

JANG, Tae Jung, JEON, Kyu Ha and JUNG, Ki Hoon (2009). Cyclooxygenase-2 expression is related to the epithelial-to-mesenchymal transition in human colon cancers. *Yonsei medical journal,* **50** (6), 818-824.

JÄNICKE,R.U., et al. (1998). Caspase- 3 is required for DNA fragmentation and morphological changes associated with apoptosis. *The journal of biological chemistry,* **273** (16), 9357.

JETER, Collene R., et al. (2009). Functional evidence that the self-renewal gene NANOG regulates human tumor development. *Stem cells (dayton, ohio),* **27** (5), 993-1005.

JETER, Collene R., et al. (2011a). NANOG promotes cancer stem cell characteristics and prostate cancer resistance to androgen deprivation. *Oncogene,* **30** (36), 3833-3845.

JETER, Collene R., et al. (2011b). NANOG promotes cancer stem cell characteristics and prostate cancer resistance to androgen deprivation. *Oncogene,* **30** (36), 3833-3845.

JI, P., et al. (2016). CD44hiCD24lo mammosphere-forming cells from primary breast cancer display resistance to multiple chemotherapeutic drugs. *Oncology reports,* **35** (6), 3293-3302.

JIA, Li, et al. (2003). Androgen receptor activity at the prostate specific antigen locus: steroidal and non- steroidal mechanisms. *Molecular cancer research : MCR,* **1** (5), 385.

JIANG, Bing-Hua and LIU, Ling-Zhi (2008). PI3K/ PTEN signaling in tumorigenesis and angiogenesis. *BBA - proteins and proteomics,* **1784** (1), 150-158.

JIN, B. and ROBERTSON, K. D. (2013). DNA methyltransferases, DNA damage repair, and cancer. *Advances in experimental medicine and biology,* **754** , 3-29.

JIN, C., et al. (2015). Side population cell level in human breast cancer and factors related to disease-free survival. *Asian pacific journal of cancer prevention : APJCP,* **16** (3), 991-996.

Joëlle Roche, et al. (2013). Global Decrease of Histone H3K27 Acetylation in ZEB1-Induced Epithelial to Mesenchymal Transition in Lung Cancer Cells. *Cancers,* **5** (2), 334-356.

KABEYA, Yukiko, et al. (2000). LC3, a mammalian homologue of yeast Apg8p, is localized in autophagosome membranes after processing. *EMBO journal,* **19** (21), 5720-5728.

KAHN, B., COLLAZO, J. and KYPRIANOU, N. (2014). Androgen receptor as a driver of therapeutic resistance in advanced prostate cancer. *International journal of biological sciences,* **10** (6), 588-595.

KAKAR, S. S., et al. (2014). Withaferin a alone and in combination with cisplatin suppresses growth and metastasis of ovarian cancer by targeting putative cancer stem cells. *PloS one,* **9** (9), e107596.

KARTNER, N., et al. (1985). Detection of P-glycoprotein in multidrug-resistant cell lines by monoclonal antibodies. *Nature,* **316** (6031), 820-823.

KASSOUF, W., TANGUAY, S. and APRIKIAN, A. G. (2003). Nilutamide as second line hormone therapy for prostate cancer after androgen ablation fails. *The journal of urology,* **169** (5), 1742-1744.

KAWAMURA, N., et al. (2015). CRISPR/Cas9-mediated gene knockout of NANOG and NANOGP8 decreases the malignant potential of prostate cancer cells. *Oncotarget,* **6** (26), 22361-22374.

KELLER, Patricia J., et al. (2012). *Defining the cellular precursors to human breast cancer.* Washington, D.C. :, Proceedings of the National Academy of Sciences of the United States of America., **109** (8), 2772-2777.

KERR, J. F., WYLLIE, A. H. and CURRIE, A. R. (1972). Apoptosis: a basic biological phenomenon with wide-ranging implications in tissue kinetics. *British journal of cancer,* **26** (4), 239-257.

KHAITAN, D., et al. (2006). Establishment and characterization of multicellular spheroids from a human glioma cell line; Implications for tumor therapy. *Journal of translational medicine,* **4** , 12.

KIM, Su-Hyeong and SINGH, Shivendra V. (2014). Mammary cancer chemoprevention by withaferin A is accompanied by in vivo suppression of self- renewal of cancer stem cells. *Cancer prevention research,* **7** (7), 738-747.

KIM, M., et al. (2002). The multidrug resistance transporter ABCG2 (breast cancer resistance protein 1) effluxes Hoechst 33342 and is overexpressed in hematopoietic stem cells. *Clinical cancer research : An official journal of the american association for cancer research,* **8** (1), 22-28.

KIM, N. W., et al. (1994a). Specific association of human telomerase activity with immortal cells and cancer. *Science (new york, N.Y.),* **266** (5193), 2011-2015.

KIM, N. W., et al. (1994b). Specific association of human telomerase activity with immortal cells and cancer. *Science (new york, N.Y.),* **266** (5193), 2011-2015.

KIM, R., EMI, M. and TANABE, K. (2007). Cancer immunoediting from immune surveillance to immune escape. *Immunology,* **121** (1), 1-14.

KINZLER, K. W. and VOGELSTEIN, B. (1997). Cancer-susceptibility genes. Gatekeepers and caretakers. *Nature,* **386** (6627), 761, 763.

KISCHKEL, F. C., et al. (1995). Cytotoxicity-dependent APO-1 (Fas/CD95)-associated proteins form a death-inducing signaling complex (DISC) with the receptor. *The EMBO journal,* **14** (22), 5579-5588.

KNIGHT, Eleanor and PRZYBORSKI, Stefan (2015). *Advances in 3D cell culture technologies enabling tissue- like structures to be created in vitro.* J.Anat., **227** (6), 746-756.

KNUDSON, A. G.,Jr (1971). Mutation and cancer: statistical study of retinoblastoma. *Proceedings of the national academy of sciences of the united states of america,* **68** (4), 820-823.

KOH, Cheryl M., et al. (2010). MYC and Prostate Cancer. *Genes & cancer,* **1** (6), 617.

KONG, Dejuan, et al. (2010). Epithelial to mesenchymal transition is mechanistically linked with stem cell signatures in prostate cancer cells. *PloS one,* **5** (8), e12445.

KRAMER, A., MAIER, B. and BARTEK, J. (2011). Centrosome clustering and chromosomal (in)stability: a matter of life and death. *Molecular oncology,* **5** (4), 324-335.

KRISTIANSEN, G., et al. (2002). CD24 is expressed in ovarian cancer and is a new independent prognostic marker of patient survival. *The american journal of pathology,* **161** (4), 1215-1221.

KRISTIANSEN, G., et al. (2003). CD24 expression is a new prognostic marker in breast cancer. *Clinical cancer research : An official journal of the american association for cancer research,* **9** (13), 4906-4913.

KUROSAKA, K., et al. (2003). Silent cleanup of very early apoptotic cells by macrophages. *Journal of immunology (baltimore, md.: 1950),* **171** (9), 4672-4679.

LABRIE, F., et al. (1984). Simultaneous administration of pure antiandrogens, a combination necessary for the use of luteinizing hormone- releasing hormone agonists in the treatment of prostate cancer. *Proceedings of the national academy of sciences of the united states of america,* **81** (12), 3861.

LAGADEC, C., et al. (2014). Tumor cells with low proteasome subunit expression predict overall survival in head and neck cancer patients. *BMC cancer,* **14** , 152-2407-14-152.

LAI, Ming-Chih, CHANG, Chiao-May and SUN, H. S. (2016). Hypoxia Induces Autophagy through Translational Up-Regulation of Lysosomal Proteins in Human Colon Cancer Cells. *PloS one,* **11** (4), e0153627.

LAIHO, M., et al. (1990). Growth inhibition by TGF-beta linked to suppression of retinoblastoma protein phosphorylation. *Cell,* **62** (1), 175-185.

LAJTHA, L. G., OLIVER, R. and ELLIS, F. (1954). Incorporation of 32P and adenine 14C into DNA by human bone marrow cells in vitro. *British journal of cancer,* **8** (2), 367-379.

LANE, D. P. (1992). Cancer. p53, guardian of the genome. *Nature,* **358** (6381), 15-16.

LAPIDOT, T', et al. (1994). *A cell initiating human acute myeloid leukaemia after transplantation into SCID mice.* London] :, Nature, **367** 17.

LARSON, B. (2015). 3D Cell Culture: A Review of Current Techniques.

LEE, Kuen Yong and MOONEY, David J. (2011). Alginate: Properties and biomedical applications. *Progress in polymer science,* .

LEES, Ja, et al. (1993). The retinoblastoma protein binds to a family of E2F transcription factors. *Molecular and cellular biology,* **13** (12), 7813-7825.

LEI, S., et al. (1995). Overexpression of HER2/neu oncogene in pancreatic cancer correlates with shortened survival. *International journal of pancreatology : Official journal of the international association of pancreatology,* **17** (1), 15-21.

LEMMON, Mark A. and SCHLESSINGER, Joseph (2010). Cell signaling by receptor tyrosine kinases. *Cell,* **141** (7), 1117-1134.

LESLIE, N. R. and DOWNES, C. P. (2004). PTEN function: how normal cells control it and tumour cells lose it. *The biochemical journal,* **382** (Pt 1), 1-11.

LEVINE, A. J. (1997). P53, the Cellular Gatekeeper for Growth and Division. *Cell,* **88** (3), 323-331.

LEVITT, J. M., et al. (2006). Intrinsic fluorescence and redox changes associated with apoptosis of primary human epithelial cells. *Journal of biomedical optics,* **11** (6), 064012.

LI, Hangwen, et al. (2008). PC3 human prostate carcinoma cell holoclones contain self-renewing tumor-initiating cells. *Cancer research,* **68** (6), 1820-1825.

LI, J., et al. (1997). PTEN, a putative protein tyrosine phosphatase gene mutated in human brain, breast, and prostate cancer. *Science (new york, N.Y.),* **275** (5308), 1943-1947.

LI, L., CHEN, Y. and GIBSON, S. B. (2013a). Starvation-induced autophagy is regulated by mitochondrial reactive oxygen species leading to AMPK activation. *Cellular signalling,* **25** (1), 50-65.

LI, Lin, CHEN, Yongqiang and GIBSON, Spencer B. (2013b). Starvation- induced autophagy is regulated by mitochondrial reactive oxygen species leading to AMPK activation. *Cellular signalling,* **25** (1), 50-65.

LI, Nan, et al. (2013). The effect of electrostatic microencapsulation process on biological properties of tumour cells. *Journal of microencapsulation, 2013,* **30; Vol.30** (6; 6), 530; 530-537; 537.

LIANG, D., et al. (2012). The hypoxic microenvironment upgrades stem-like properties of ovarian cancer cells. *BMC cancer,* **12** , 201-2407-12-201.

LIANG, Jiyong, et al. (2002). PKB/ Akt phosphorylates p27, impairs nuclear import of p27 and opposes p27- mediated G1 arrest. *Nature medicine,* **8** (10), 1153.

LIM, J. and THIERY, J. P. (2012). Epithelial-mesenchymal transitions: insights from development. *Development (cambridge, england),* **139** (19), 3471-3486.

LIMONTA, P., MONTAGNANI MARELLI, M. and MORETTI, R. M. (2001). LHRH analogues as anticancer agents: pituitary and extrapituitary sites of action. *Expert opinion on investigational drugs,* **10** (4), 709-720.

LIN, Cheng-Wei, et al. (2012). Epithelial cell adhesion molecule regulates tumor initiation and tumorigenesis via activating reprogramming factors and epithelial-mesenchymal transition gene expression in colon cancer. *The journal of biological chemistry,* **287** (47), 39449.

LIN, E. Y., et al. (2001). Colony-stimulating factor 1 promotes progression of mammary tumors to malignancy. *The journal of experimental medicine,* **193** (6), 727-740.

LIN, Hui-Kuan, et al. (2002). Proteasome activity is required for androgen receptor transcriptional activity via regulation of androgen receptor nuclear translocation and interaction with coregulators in prostate cancer cells. *The journal of biological chemistry,* **277** (39), 36570.

LIN, T., et al. (2005). p53 induces differentiation of mouse embryonic stem cells by suppressing Nanog expression. *Nature cell biology,* **7** (2), 165-171.

LIN, Ting, DING, Yan-Qing and LI, Jian-Ming (2012). Overexpression of Nanog protein is associated with poor prognosis in gastric adenocarcinoma. *Medical oncology (northwood, london, england),* **29** (2), 878-885.

LIPSCOMB, TH, et al. (2007). Function and clinical application of embryonic gene nanog in cancer. *HAEMATOLOGICA-THE HEMATOLOGY JOURNAL,* **92** , 15-16.

LITVINOV, I. V., et al. (2006). Low-calcium serum-free defined medium selects for growth of normal prostatic epithelial stem cells. *Cancer research,* **66** (17), 8598-8607.

LIU, B., et al. (2014a). Nanog1 in NTERA-2 and recombinant NanogP8 from somatic cancer cells adopt multiple protein conformations and migrate at multiple M.W species. *PloS one,* **9** (3), e90615.

LIU, D. and SY, M. S. (1997). Phorbol myristate acetate stimulates the dimerization of CD44 involving a cysteine in the transmembrane domain. *Journal of immunology (baltimore, md.: 1950),* **159** (6), 2702-2711.

LIU, Hong-Li, LIU, Shi-Jun and CHEN, Qi-Yuan (2012). Excess molar enthalpies for ternary mixtures of (methanol or ethanol + water + tributyl phosphate) at T = 298.15 K. *Journal of thermal analysis and calorimetry; an international forum for thermal studies,* **107** (2), 837-841.

LIU, Y., et al. (1995). Hypoxia regulates vascular endothelial growth factor gene expression in endothelial cells. Identification of a 5' enhancer. *Circulation research,* **77** (3), 638-643.

LIU, Y., et al. (2014b). Tumor-associated macrophages promote tumor cell proliferation in nasopharyngeal NK/T-cell lymphoma. *International journal of clinical and experimental pathology,* **7** (9), 5429-5435.

LOCKE, Matthew, et al. (2005). Retention of intrinsic stem cell hierarchies in carcinoma-derived cell lines. *Cancer research,* **65** (19), 8944-8950.

LOCKSLEY, R. M., KILLEEN, N. and LENARDO, M. J. (2001). The TNF and TNF receptor superfamilies: integrating mammalian biology. *Cell,* **104** (4), 487-501.

LOEB, L. A., LOEB, K. R. and ANDERSON, J. P. (2003). Multiple mutations and cancer. *Proceedings of the national academy of sciences of the united states of america,* **100** (3), 776-781.

LOEB, L. A., SPRINGGATE, C. F. and BATTULA, N. (1974). Errors in DNA replication as a basis of malignant changes. *Cancer research,* **34** (9), 2311-2321.

LOEB, Lawrence A. (2011). Human cancers express mutator phenotypes: origin, consequences and targeting. *Nature reviews cancer,* **11** (6), 450.

LOH, Y. H., et al. (2006). The Oct4 and Nanog transcription network regulates pluripotency in mouse embryonic stem cells. *Nature genetics,* **38** (4), 431-440.

LOMBAERTS, M., et al. (2006). E-cadherin transcriptional downregulation by promoter methylation but not mutation is related to epithelial-to-mesenchymal transition in breast cancer cell lines. *British journal of cancer,* **94** (5), 661-671.

LORDA-DIEZ, C. I., et al. (2015). Apoptosis during embryonic tissue remodeling is accompanied by cell senescence. *Aging,* .

LORENZO, Petra Isabel and SAATCIOGLU, Fahri (2008). Inhibition of Apoptosis in Prostate Cancer Cells by Androgens Is Mediated through Downregulation of c- Jun N-terminal Kinase Activation. *Neoplasia,* **10** (5), 418-428.

LUNDBERG, A. S. and WEINBERG, R. A. (1998). Functional inactivation of the retinoblastoma protein requires sequential modification by at least two distinct cyclin-cdk complexes. *Molecular and cellular biology,* **18** (2), 753.

M, A. Davies and SAMUELS, Y. (2010). Analysis of the genome to personalize therapy for melanoma. *Oncogene,* **29** (41), 5545.

MA, Irene and ALLAN, Alison L. (2011). The Role of Human Aldehyde Dehydrogenase in Normal and Cancer Stem Cells. *Stem cell reviews and reports,* **7** (2), 292-306.

MA, S., et al. (2010). miR-130b Promotes CD133(+) liver tumor-initiating cell growth and self-renewal via tumor protein 53-induced nuclear protein 1. *Cell stem cell,* **7** (6), 694-707.

MACHEDA, M. L., ROGERS, S. and BEST, J. D. (2005). Molecular and cellular regulation of glucose transporter (GLUT) proteins in cancer. *Journal of cellular physiology,* **202** (3), 654-662.

MAKKI, J. (2015). Diversity of Breast Carcinoma: Histological Subtypes and Clinical Relevance. *Clinical medicine insights.pathology,* **8** , 23-31.

MANI, Sendurai A., et al. (2008). The epithelial-mesenchymal transition generates cells with properties of stem cells. *Cell,* **133** (4), 704-715.

MANOOCHEHRI, M., et al. (2014). Down-regulation of BAX gene during carcinogenesis and acquisition of resistance to 5-FU in colorectal cancer. *Pathology oncology research : POR,* **20** (2), 301-307.

MANUEL IGLESIAS, J., et al. (2013). Mammosphere formation in breast carcinoma cell lines depends upon expression of E-cadherin. *PloS one,* **8** (10), e77281.

MATHIEU, J., et al. (2011). HIF induces human embryonic stem cell markers in cancer cells. *Cancer research,* **71** (13), 4640-4652.

MCCLINTOCK, B. (1941). The Stability of Broken Ends of Chromosomes in Zea Mays. *Genetics,* **26** (2), 234-282.

MCCLINTOCK, B. (1942). The Fusion of Broken Ends of Chromosomes Following Nuclear Fusion. *Proceedings of the national academy of sciences of the united states of america,* **28** (11), 458-463.

MCLEOD, David G. (2003). Hormonal therapy: historical perspective to future directions. *Urology,* **61** (2), 3-7.

MEEKER, A. K. (2006). Telomeres and telomerase in prostatic intraepithelial neoplasia and prostate cancer biology. *Urologic oncology,* **24** (2), 122-130.

MENG, HM, et al. (2010). Overexpression of nanog predicts tumor progression and poor prognosis in colorectal cancer. *CANCER BIOLOGY & THERAPY,* **9** (4), 295-302.

MEYER, M. J., et al. (2009). Dynamic regulation of CD24 and the invasive, CD44posCD24neg phenotype in breast cancer cell lines. *Breast cancer research : BCR,* **11** (6), R82.

MEYERS, F. J., et al. (1998). Very frequent p53 mutations in metastatic prostate carcinoma and in matched primary tumors. *Cancer,* **83** (12), 2534-2539.

MIKI, Y., et al. (1994). A strong candidate for the breast and ovarian cancer susceptibility gene BRCA1. *Science (new york, N.Y.),* **266** (5182), 66-71.

MILLER, K. D., et al. (2005). Randomized phase III trial of capecitabine compared with bevacizumab plus capecitabine in patients with previously treated metastatic breast cancer. *Journal of clinical oncology : Official journal of the american society of clinical oncology,* **23** (4), 792-799.

MINGUZZI, Sandro, et al. (2002). Cytotoxic withanolides from Acnistus arborescens. *Phytochemistry,* **59** (6), 635-641.

MITSUI, K., et al. (2003). The homeoprotein Nanog is required for maintenance of pluripotency in mouse epiblast and ES cells. *Cell,* **113** (5), 631-642.

MIZUSHIMA, Noboru (2007). *Autophagy: process and function.* Genes Dev., **21** (22), 2861-2873.

MOITRA, Karobi (2015). Overcoming Multidrug Resistance in Cancer Stem Cells. *BioMed research international,* **2015** .

MOLYNEUX, G., et al. (2010). BRCA1 basal-like breast cancers originate from luminal epithelial progenitors and not from basal stem cells. *Cell stem cell,* **7** (3), 403-417.

MONTGOMERY, R. B., et al. (2008). Maintenance of intratumoral androgens in metastatic prostate cancer: a mechanism for castration-resistant tumor growth. *Cancer research,* **68** (11), 4447.

MOORE, Nathan and LYLE, Stephen (2011). Quiescent, Slow- Cycling Stem Cell Populations in Cancer: A Review of the Evidence and Discussion of Significance. *Journal of oncology,* **2011** .

MORENO, S. and NURSE, P. (1994). Regulation of progression through the G1 phase of the cell cycle by the rum1+ gene. *Nature,* **367** (6460), 236-242.

MORGAN, D. O. (1997). Cyclin-dependent kinases: engines, clocks, and microprocessors. *Annual review of cell and developmental biology,* **13** , 261-291.

MORSE, David L., et al. (2005). Docetaxel induces cell death through mitotic catastrophe in human breast cancer cells. *Molecular cancer therapeutics,* **4** (10), 1495-1504.

MUELLER-KLIESER, W., FREYER, J. P. and SUTHERLAND, R. M. (1986). Influence of glucose and oxygen supply conditions on the oxygenation of multicellular spheroids. *British journal of cancer,* **53** (3), 345-353.

MULLER, H' J. (1938). The Remaking of Chromosomes. *Collecting net,* **13** , 181-198.

MULLIN, Nicholas P., et al. (2008). The pluripotency rheostat Nanog functions as a dimer. *The biochemical journal,* **411** (2), 227-231.

MUNAKATA, K., et al. (2016). Cancer stem-like properties in colorectal cancer cells with low proteasome activity. *Clinical cancer research : An official journal of the american association for cancer research,* .

MUNROE, D. G., et al. (1988). Loss of a highly conserved domain on p53 as a result of gene deletion during Friend virus-induced erythroleukemia. *Oncogene,* **2** (6), 621-624.

MURDOCH, C., et al. (2008). The role of myeloid cells in the promotion of tumour angiogenesis. *Nature reviews.cancer,* **8** (8), 618-631.

MURILLO, H., et al. (2001). Role of PI3K signaling in survival and progression of LNCaP prostate cancer cells to the androgen- refractory state. *Clinical cancer research; clin.cancer res.,* **7** (11), 3775S-3775S.

MUSACCHIO, Andrea and SALMON, Edward D. (2007). *The spindle-assembly checkpoint in space and time.* England :, Nature reviews., **8** (5), 379-393.

MUTSKOV, V. and FELSENFELD, G. (2004). Silencing of transgene transcription precedes methylation of promoter DNA and histone H3 lysine 9. *The EMBO journal,* **23** (1), 138-149.

MUZIO, G., et al. (2012). Aldehyde dehydrogenases and cell proliferation. *Free radical biology & medicine,* **52** (4), 735-746.

NAGLE, R. B., et al. (1986). Characterization of breast carcinomas by two monoclonal antibodies distinguishing myoepithelial from luminal epithelial cells. *The journal of histochemistry and cytochemistry : Official journal of the histochemistry society,* **34** (7), 869-881.

NAOR, D., SIONOV, R. V. and ISH-SHALOM, D. (1997). CD44: structure, function, and association with the malignant process. *Advances in cancer research,* **71** , 241-319.

NICHOLS, J., et al. (1998). Formation of pluripotent stem cells in the mammalian embryo depends on the POU transcription factor Oct4. *Cell,* **95** (3), 379-391.

NICHOLSON, R. I., GEE, J. M. and HARPER, M. E. (2001). EGFR and cancer prognosis. *European journal of cancer (oxford, england : 1990),* **37 Suppl 4** , S9-15.

NIGRO, J. M., et al. (1989). Mutations in the p53 gene occur in diverse human tumour types. *Nature,* **342** (6250), 705-708.

NING, Y. and LENZ, HJ (2012). Targeting IL-8 in colorectal cancer. *EXPERT OPINION ON THERAPEUTIC TARGETS,* **16** (5), 491-497.

NISHI, M., et al. (2014). Induction of cells with cancer stem cell properties from nontumorigenic human mammary epithelial cells by defined reprogramming factors. *Oncogene,* **33** (5), 643-652.

NISHIKAWA, Y., et al. (2015). Withaferin A induces cell death selectively in androgen-independent prostate cancer cells but not in normal fibroblast cells. *PLoS ONE,* **10** (7).

NIU, C. S., et al. (2011). Expression of NANOG in human gliomas and its relationship with undifferentiated glioma cells. *Oncology reports,* **26** (3), 593-601.

NORBURY, C. and NURSE, P. (1992). Animal cell cycles and their control. *Annual review of biochemistry,* **61** , 441-470.

NURSE, P. (1990). Universal control mechanism regulating onset of M-phase. *Nature,* **344** (6266), 503-508.

ODOUX, C., et al. (2008). A stochastic model for cancer stem cell origin in metastatic colon cancer. *Cancer research,* **68** (17), 6932-6941.

OH, William K. (2002). The evolving role of estrogen therapy in prostate cancer. *Clinical prostate cancer,* **1** (2), 81.

OKTEM, G., et al. (2013). Expressionprofiling of stem cell signaling alters with spheroid formation in CD133(high)/CD44(high) prostate cancer stem cells. *Cancer research; cancer res.,* **73** (8).

OLSSON, E., et al. (2011). CD44 isoforms are heterogeneously expressed in breast cancer and correlate with tumor subtypes and cancer stem cell markers. *BMC cancer,* **11** , 418-2407-11-418.

ONDER, T. T., et al. (2008). Loss of E-cadherin promotes metastasis via multiple downstream transcriptional pathways. *Cancer research,* **68** (10), 3645-3654.

PACKER, J. R. and MAITLAND, N. J. (2016). The molecular and cellular origin of human prostate cancer. *Biochimica et biophysica acta,* **1863** (6 Pt A), 1238-1260.

PAN, J., et al. (2010). 26S proteasome activity is down-regulated in lung cancer stem-like cells propagated in vitro. *PloS one,* **5** (10), e13298.

PANG, X., et al. (2015). IL-8 inhibits the apoptosis of MCF-7 human breast cancer cells by up-regulating Bcl-2 and down-regulating caspase-3. *Xi bao yu fen zi mian yi xue za zhi = chinese journal of cellular and molecular immunology,* **31** (3), 307-311.

PARDEE, A. B. (1974). A restriction point for control of normal animal cell proliferation. *Proceedings of the national academy of sciences of the united states of america,* **71** (4), 1286-1290.

PARK, S. Y., et al. (2010). Heterogeneity for stem cell-related markers according to tumor subtype and histologic stage in breast cancer. *Clinical cancer research : An official journal of the american association for cancer research,* **16** (3), 876-887.

PARK, Y. M., et al. (2016). Role of cancer stem cell in radioresistant head and neck cancer. *Auris, nasus, larynx,* **43** (5), 556-561.

PATRAWALA, L., et al. (2006). Highly purified CD44+ prostate cancer cells from xenograft human tumors are enriched in tumorigenic and metastatic progenitor cells. *Oncogene,* **25** (12), 1696-1708.

PAULOVICH, A. G., TOCZYSKI, D. P. and HARTWELL, L. H. (1997). When checkpoints fail. *Cell,* **88** (3), 315-321.

PAVLETICH, N. P. (1999). Mechanisms of cyclin-dependent kinase regulation: structures of Cdks, their cyclin activators, and Cip and INK4 inhibitors. *Journal of molecular biology,* **287** (5), 821-828.

PECINA-SLAUS, N. (2003). Tumor suppressor gene E-cadherin and its role in normal and malignant cells. *Cancer cell international,* **3** (1), 17.

PEIRIS-PAGES, M., et al. (2010). Balance of pro- versus anti-angiogenic splice isoforms of vascular endothelial growth factor as a regulator of neuroblastoma growth. *The journal of pathology,* **222** (2), 138-147.

PERTEGA-GOMES, N., et al. (2015). A glycolytic phenotype is associated with prostate cancer progression and aggressiveness: a role for monocarboxylate transporters as metabolic targets for therapy. *The journal of pathology,* **236** (4), 517-530.

PETRUZZELLI, R., et al. (2014). HIF-2alpha regulates NANOG expression in human embryonic stem cells following hypoxia and reoxygenation through the interaction with an Oct-Sox cis regulatory element. *PloS one,* **9** (10), e108309.

PEZARO, Carmel J., MUKHERJI, Deborah and DE BONO, Johann S. (2012). Abiraterone acetate: redefining hormone treatment for advanced prostate cancer. *Drug discovery today,* **17** (5-6), 221-226.

PHILLIPS, Tiffany M., MCBRIDE, William H. and PAJONK, Frank (2006). The response of CD24(-/ low)/ CD44+ breast cancer- initiating cells to radiation. *Journal of the national cancer institute,* **98** (24), 1777.

PIAO, L. S., et al. (2012). CD133+ liver cancer stem cells modulate radioresistance in human hepatocellular carcinoma. *Cancer letters,* **315** (2), 129-137.

PIESTUN, D., et al. (2006). Nanog transforms NIH3T3 cells and targets cell-type restricted genes. *Biochemical and biophysical research communications,* **343** (1), 279-285.

PIETENPOL, J. A., et al. (1990). Transforming growth factor beta 1 suppression of c-myc gene transcription: role in inhibition of keratinocyte proliferation. *Proceedings of the national academy of sciences of the united states of america,* **87** (10), 3758-3762.

PONTA, Helmut, SHERMAN, Larry and HERRLICH, Peter A. (2003). CD44: From adhesion molecules to signalling regulators. *Nature reviews molecular cell biology,* **4** (1), 33.

PORTILLO-LARA, R. and ALVAREZ, M. M. (2015). Enrichment of the Cancer Stem Phenotype in Sphere Cultures of Prostate Cancer Cell Lines Occurs through Activation of Developmental Pathways Mediated by the Transcriptional Regulator DeltaNp63alpha. *PloS one,* **10** (6), e0130118.

QI, Lisha, et al. (2012). *Dickkopf-1 inhibits epithelial-mesenchymal transition of colon cancer cells and contributes to colon cancer suppression.* England, WILEY-BLACKWELL. Cancer Science, **103** (4), 828-835.

QIAO, S. P., et al. (2016). An alginate-based platform for cancer stem cell research. *Acta biomaterialia,* **37** , 83-92.

QIN, H., et al. (2007). Regulation of apoptosis and differentiation by p53 in human embryonic stem cells. *The journal of biological chemistry,* **282** (8), 5842-5852.

QUINTANA, E., et al. (2008). Efficient tumour formation by single human melanoma cells. *Nature,* **456** (7222), 593-598.

RAMIS-CONDE, I., et al. (2009). Multi-scale modelling of cancer cell intravasation: the role of cadherins in metastasis. *Physical biology,* **6** (1), 016008-3975/6/1/016008.

RAO, W., et al. (2014). Enhanced enrichment of prostate cancer stem-like cells with miniaturized 3D culture in liquid core-hydrogel shell microcapsules. *Biomaterials,* **35** (27), 7762-7773.

REHMAN, Y. and ROSENBERG, Je (2012). *Abiraterone acetate: oral androgen biosynthesis inhibitor for treatment of castration-resistant prostate cancer.* Drug Design Development And Therapy; Drug Des.Dev.Ther., **6** 13-18.

REN, F., SHENG, Wq and DU, X. (2013). *CD133: A cancer stem cells marker, is used in colorectal cancers.* World Journal Of Gastroenterology; World J.Gastroenterol., **19** (17), 2603-2611.

REYES-REYES, E., et al. (2013). Physangulidine A, a withanolide from Physalis angulata, perturbs the cell cycle and induces cell death by apoptosis in prostate cancer cells. *Journal of natural products,* **76** (1), 2-7.

RICARDO, Sara, et al. (2011). Breast cancer stem cell markers CD44, CD24 and ALDH1: expression distribution within intrinsic molecular subtype. *Journal of clinical pathology,* **64** (11), 937-946.

RICHARDSON, G. D., et al. (2004). CD133, a novel marker for human prostatic epithelial stem cells. *Journal of cell science,* **117** (Pt 16), 3539-3545.

RIEDER, C. L., et al. (1995). The checkpoint delaying anaphase in response to chromosome monoorientation is mediated by an inhibitory signal produced by unattached kinetochores. *The journal of cell biology,* **130** (4), 941-948.

RIORDAN, J. R., et al. (1985). Amplification of P-glycoprotein genes in multidrug-resistant mammalian cell lines. *Nature,* **316** (6031), 817-819.

RODDA, David J., et al. (2005). Transcriptional regulation of nanog by OCT4 and SOX2. *The journal of biological chemistry,* **280** (26), 24731-24737.

RODENHUIS, S. and SLEBOS, R. J. (1992). Clinical significance of ras oncogene activation in human lung cancer. *Cancer research,* **52** (9 Suppl), 2665s-2669s.

ROSANÒ, Laura, et al. (2006). Endothelin-1 is required during epithelial to mesenchymal transition in ovarian cancer progression. *Experimental biology and medicine (maywood, N.J.),* **231** (6), 1128-1131.

ROWEHL, R. A., et al. (2014). Establishment of highly tumorigenic human colorectal cancer cell line (CR4) with properties of putative cancer stem cells. *PloS one,* **9** (6), e99091.

ROY, Ram V., et al. (2013). Withaferin a, a steroidal lactone from withania somnifera, induces mitotic catastrophe and growth arrest in prostate cancer cells. *Journal of natural products,* **76** (10), 1909-1915.

RUBIN GRANDIS, J., et al. (1998). Levels of TGF-alpha and EGFR protein in head and neck squamous cell carcinoma and patient survival. *Journal of the national cancer institute,* **90** (11), 824-832.

RUBIO-MOSCARDO, F., et al. (2005). Characterization of 8p21.3 chromosomal deletions in B-cell lymphoma: TRAIL-R1 and TRAIL-R2 as candidate dosage-dependent tumor suppressor genes. *Blood,* **106** (9), 3214-3222.

RUDOLPH, K. L., et al. (2001). Telomere dysfunction and evolution of intestinal carcinoma in mice and humans. *Nature genetics,* **28** (2), 155-159.

RUSSO, J. and RUSSO, I. H. (2004). Development of the human breast. *Maturitas,* **49** (1), 2-15.

SAELENS, Xavier, et al. (2004). Toxic proteins released from mitochondria in cell death. *Oncogene,* **23** (16), 2861.

SAKIYAMA-ELBERT, S. and HUBBELL, J. (2001). Functional biomaterials: Design of novel biomaterials. *Annual review of materials research,* **31** , 183.

SAMMAR, M., et al. (1994). Heat-stable antigen (CD24) as ligand for mouse P-selectin. *International immunology,* **6** (7), 1027-1036.

SANTISTEBAN, M., et al. (2009). Immune-induced epithelial to mesenchymal transition in vivo generates breast cancer stem cells. *Cancer research,* **69** (7), 2887-2895.

SAXENA, Parmita, et al. (2012). PSA regulates androgen receptor expression in prostate cancer cells. *Prostate,* **72** (7), 769-776.

SBI (2016). Pluripotenct reporters, Lentivirus-based reporters of pluripotency. *Https://Www.systembio.com/stem-cell-research/pluripotency-reporters/overview,* .

SCAFFIDI, Paola and MISTELI, Tom (2011). In vitro generation of human cells with cancer stem cell properties. *Nature cell biology,* **13** (9), 1051.

SCHALLY, A. V. (1999). Luteinizing hormone- releasing hormone analogs: their impact on the control of tumorigenesis. *Peptides,* **20** (10), 1247.

SCHARENBERG, C. W., HARKEY, M. A. and TOROK-STORB, B. (2002). The ABCG2 transporter is an efficient Hoechst 33342 efflux pump and is preferentially expressed by immature human hematopoietic progenitors. *Blood,* **99** (2), 507-512.

SCHIMMER, A. D. (2004). Inhibitor of apoptosis proteins: translating basic knowledge into clinical practice. *Cancer research,* **64** (20), 7183-7190.

SCHOPPMANN, S. F., et al. (2002). Tumor-associated macrophages express lymphatic endothelial growth factors and are related to peritumoral lymphangiogenesis. *The american journal of pathology,* **161** (3), 947-956.

SCHRECENGOST, R. and KNUDSEN, K. E. (2013). Molecular pathogenesis and progression of prostate cancer. *Seminars in oncology,* **40** (3), 244-258.

SCHWAB, L. P., et al. (2012). Hypoxia-inducible factor 1alpha promotes primary tumor growth and tumor-initiating cell activity in breast cancer. *Breast cancer research : BCR,* **14** (1), R6.

SCHWEIZER, Michael T. and ANTONARAKIS, Emmanuel S. (2012). Abiraterone and other novel androgen-directed strategies for the treatment of prostate cancer: A new era of hormonal therapies is born. *Therapeutic advances in urology,* **4** (4), 167-178.

SCREATON, G. R., et al. (1992). Genomic structure of DNA encoding the lymphocyte homing receptor CD44 reveals at least 12 alternatively spliced exons. *Proceedings of the national academy of sciences of the united states of america,* **89** (24), 12160-12164.

SENTMAN, C. L., et al. (1991). Bcl-2 Inhibits Multiple Forms of Apoptosis but Not Negative Selection in Thymocytes. *Cell,* **67** (5), 879-888.

SERRANO, M., et al. (1997). Oncogenic ras provokes premature cell senescence associated with accumulation of p53 and p16INK4a. *Cell,* **88** (5), 593-602.

SHAN, J., et al. (2012). Nanog regulates self-renewal of cancer stem cells through the insulin-like growth factor pathway in human hepatocellular carcinoma. *Hepatology (baltimore, md.),* **56** (3), 1004-1014.

SHARMA, S., KELLY, T. K. and JONES, P. A. (2010). Epigenetics in cancer. *Carcinogenesis,* **31** (1), 27-36.

SHENG, X., et al. (2013). Isolation and enrichment of PC-3 prostate cancer stem-like cells using MACS and serum-free medium. *Oncology letters,* **5** (3), 787-792.

SHERIDAN, Carol, et al. (2006). CD44 + / CD24 - Breast cancer cells exhibit enhanced invase properties: An early step necessary for metastasis. *Breast cancer research,* **8** (5).

SHERR, Charles J. (2004). Principles of Tumor Suppression. *Cell,* **116** (2), 235-246.

SHIMIZU, S., et al. (1996). Induction of apoptosis as well as necrosis by hypoxia and predominant prevention of apoptosis by Bcl-2 and Bcl-XL. *Cancer research,* **56** (9), 2161.

SHINTANI, Y., et al. (2008). Collagen I promotes epithelial-to-mesenchymal transition in lung cancer cells via transforming growth factor-beta signaling. *American journal of respiratory cell and molecular biology,* **38** (1), 95-104.

SHIRAKIHARA, T., SAITOH, M. and MIYAZONO, K. (2007). Differential regulation of epithelial and mesenchymal markers by deltaEF1 proteins in epithelial mesenchymal transition induced by TGF-beta. *Molecular biology of the cell,* **18** (9), 3533-3544.

SHIRURE, V. S., et al. (2015). CD44 variant isoforms expressed by breast cancer cells are functional E-selectin ligands under flow conditions. *American journal of physiology.cell physiology,* **308** (1), C68-78.

SHOOK, D. and KELLER, R. (2003). Mechanisms, mechanics and function of epithelial-mesenchymal transitions in early development. *Mechanisms of development,* **120** (11), 1351-1383.

SILVERSTEIN, M. J., et al. (1995). Prognostic classification of breast ductal carcinoma-in-situ. *Lancet (london, england),* **345** (8958), 1154-1157.

SINGH, Amritpal, et al. (2010). - *Withanolides: Phytoconstituents with significant pharmacological activities.* - Int J Green Pharm, **- 4** (- 4), - 229-- 237.

SLADEK, N. E. (2003). Human aldehyde dehydrogenases: potential pathological, pharmacological, and toxicological impact. *Journal of biochemical and molecular toxicology,* **17** (1), 7-23.

SLAMON, Dennis J., et al. (1989). Studies of the HER- 2- neu proto- oncogene in human breast and ovarian cancer. *Science,* **244** (4905), 707.

SLAMON, Dennis J., et al. (2001). Use of chemotherapy plus a monoclonal antibody against HER2 for metastatic breast cancer that overexpresses HER2. *The new england journal of medicine,* **344** (11), 783-92.

SLAMON, Dennis, et al. (1987). Human Breast Cancer: Correlation of Relapse and Survival with Amplification of the HER- 2/ neu Oncogene. *Science,* **235** (4785), 177.

SLEE, E. A., ADRAIN, C. and MARTIN, S. J. (2001). Executioner caspase- 3, -6, and -7 perform distinct, non- redundant roles during the demolition phase of apoptosis. *The journal of biological chemistry,* **276** (10), 7320.

SLINGERLAND, J. and PAGANO, M. (2000). Regulation of the cdk inhibitor p27 and its deregulation in cancer. *Journal of cellular physiology,* **183** (1), 10-17.

SMITH, S. C., et al. (2006). The metastasis-associated gene CD24 is regulated by Ral GTPase and is a mediator of cell proliferation and survival in human cancer. *Cancer research,* **66** (4), 1917-1922.

SMITH, S. M. and CAI, L. (2012). Cell specific CD44 expression in breast cancer requires the interaction of AP-1 and NFkappaB with a novel cis-element. *PloS one,* **7** (11), e50867.

SONVEAUX, P., et al. (2008). Targeting lactate-fueled respiration selectively kills hypoxic tumor cells in mice. *The journal of clinical investigation,* **118** (12), 3930-3942.

SPORN, M. B. and ROBERTS, A. B. (1985). Autocrine growth factors and cancer. *Nature,* **313** (6005), 745-747.

SPRENGER, C. C. and PLYMATE, S. R. (2014). The link between androgen receptor splice variants and castration-resistant prostate cancer. *Hormones & cancer,* **5** (4), 207-217.

SRIVASTAVA, S., et al. (1990). Germ-line transmission of a mutated p53 gene in a cancer-prone family with Li-Fraumeni syndrome. *Nature,* **348** (6303), 747-749.

STEINER, M. S., et al. (2000). p16/MTS1/INK4A suppresses prostate cancer by both pRb dependent and independent pathways. *Oncogene,* **19** (10), 1297-1306.

STRAUSSMAN, Ravid, et al. (2012). Tumour micro- environment elicits innate resistance to RAF inhibitors through HGF secretion. *Nature,* **487** (7408), 500.

SUN, Chun, et al. (2013a). NANOG promotes liver cancer cell invasion by inducing epithelialamesenchymal transition through NODAL/SMAD3 signaling pathway. *International journal of biochemistry and cell biology,* **45** (6), 1099-1108.

SUN, Hongmei, et al. (2013b). CD44+/CD24- breast cancer cells isolated from MCF-7 cultures exhibit enhanced angiogenic properties. *Clinical & translational oncology : Official publication of the federation of spanish oncology societies and of the national cancer institute of mexico,* **15** (1), 46-54.

SZIC, Katarzyna, et al. (2014). Pharmacological Levels of Withaferin A (Withania somnifera) Trigger Clinically Relevant Anticancer Effects Specific to Triple Negative Breast Cancer Cells. *PLoS one,* **9** (2), e87850.

T, L. Yuan and L, C. Cantley (2008). PI3K pathway alterations in cancer: variations on a theme. *Oncogene,* **27** (41), 5497.

TAI, S., et al. (2011). PC3 Is a Cell Line Characteristic of Prostatic Small Cell Carcinoma. *Prostate; prostate,* **71** (15), 1668-1679.

TAICHMAN, N. S., et al. (1998). Vascular endothelial growth factor in normal human salivary glands and saliva: a possible role in the maintenance of mucosal homeostasis. *Laboratory investigation; a journal of technical methods and pathology,* **78** (7), 869-875.

TAKAHASHI, Kazutoshi and YAMANAKA, Shinya (2006). Induction of Pluripotent Stem Cells from Mouse Embryonic and Adult Fibroblast Cultures by Defined Factors. *Cell,* **126** (4), 663-676.

TANOOKA, H. (2004). X chromosome inactivation-mediated cellular mosaicism for the study of the monoclonal origin and recurrence of mouse tumors: a review. *Cytogenetic and genome research,* **104** (1-4), 320-324.

TAPLIN, Mary-Ellen, et al. (1995). Mutation of the androgen- receptor gene in metastatic androgen- independent prostate cancer. *The new england journal of medicine,* **332** (21), 1393.

TENG, M. W., et al. (2015). From mice to humans: developments in cancer immunoediting. *The journal of clinical investigation,* **125** (9), 3338-3346.

TENG, M. W., et al. (2008). Immune-mediated dormancy: an equilibrium with cancer. *Journal of leukocyte biology,* **84** (4), 988-993.

TESH, Vl (2010). *Induction of apoptosis by Shiga toxins.* Future Microbiology; Future Microbiol., **5** (3), 431-453.

THAIPARAMBIL, Jose T., et al. (2011). Withaferin A inhibits breast cancer invasion and metastasis at sub- cytotoxic doses by inducing vimentin disassembly and serine 56 phosphorylation. *International journal of cancer,* **129** (11), 2744-2755.

The Leuprodile Study Group (1984). Leuprolide versus diethylstilbestrol for metastatic prostate cancer. The Leuprolide Study Group. *The new england journal of medicine,* **311** (20), 1281-1286.

THOMA, C. R., et al. (2014). 3D cell culture systems modeling tumor growth determinants in cancer target discovery. *Advanced drug delivery reviews,* **69-70** , 29-41.

THOMAS, Carson H., et al. (2002). Engineering gene expression and protein synthesis by modulation of nuclear shape.(Abstract). *Proceedings of the national academy of sciences of the united states,* **99** (4), 1972.

THOMAS, J. E., et al. (1997). Induction of phosphorylation on BRCA1 during the cell cycle and after DNA damage. *Cell growth & differentiation : The molecular biology journal of the american association for cancer research,* **8** (7), 801-809.

THOMPSON, Erik W., NEWGREEN, Donald F. and TARIN, David (2005). Carcinoma invasion and metastasis: a role for epithelial-mesenchymal transition? *Cancer research,* **65** (14), 5991-5995.

TINKER-KULBERG, Rachel and MORGAN, David O. (1999). Pds1 and Esp1 control both anaphase and mitotic exit in normal cells and after DNA damage.(Statistical Data Included). *Genes & development,* **13** (15), 1936.

TOMLINS, Scott A., et al. (2005). Recurrent fusion of TMPRSS2 and ETS transcription factor genes in prostate cancer. *Science (new york, N.Y.),* **310** (5748), 644.

TONINI, G., et al. (2013). New molecular insights in tobacco-induced lung cancer. *Future oncology (london, england),* **9** (5), 649-655.

TRACHTENBERG, J., et al. (2002). A phase 3, multicenter, open label, randomized study of abarelix versus leuprolide plus daily antiandrogen in men with prostate cancer. *The journal of urology,* **167** (4), 1670-1674.

TSENG, Chun-Hsien, et al. (2011). Sema3E/plexin-D1 mediated epithelial-to-mesenchymal transition in ovarian endometrioid cancer. *PloS one,* **6** (4), e19396.

TSUNODA, T., et al. (2001). Upregulated expression of angiogenesis genes and down regulation of cell cycle genes in human colorectal cancer tissue determined by cDNA macroarray. *Anticancer research,* **21** (1A), 137-143.

TU, W. H., et al. (2003). The loss of TGF-beta signaling promotes prostate cancer metastasis. *Neoplasia (new york, N.Y.),* **5** (3), 267-277.

TURNER, Nicholas and GROSE, Richard (2010). Fibroblast growth factor signalling: from development to cancer. *Nature reviews cancer,* **10** (2), 116.

TWARD, A. D., et al. (2007). Distinct pathways of genomic progression to benign and malignant tumors of the liver. *Proceedings of the national academy of sciences of the united states of america,* **104** (37), 14771-14776.

UCHINO, Keita, et al. (2012). Human Nanog pseudogene8 promotes the proliferation of gastrointestinal cancer cells. *Experimental cell research,* **318** (15), 1799-1807.

VAJDIC, C. M. and VAN LEEUWEN, M. T. (2009). Cancer incidence and risk factors after solid organ transplantation. *International journal of cancer,* **125** (8), 1747-1754.

VALASTYAN, S. and WEINBERG, R. A. (2011). Tumor metastasis: molecular insights and evolving paradigms. *Cell,* **147** (2), 275-292.

VAN DE RIJN, M., et al. (2002). Expression of cytokeratins 17 and 5 identifies a group of breast carcinomas with poor clinical outcome. *The american journal of pathology,* **161** (6), 1991-1996.

VAN LOO, G., et al. (2002). The role of mitochondrial factors in apoptosis: a Russian roulette with more than one bullet. *Cell death and differentiation,* **9** (10), 1031-1042.

VAN WEEREN,P.C., et al. (1998). Essential role for protein kinase B (PKB) in insulin-induced glycogen synthase kinase 3 inactivation. Characterization of dominant-negative mutant of PKB. *The journal of biological chemistry,* **273** (21), 13150.

VARKARIS, A., et al. (2011). The role of HGF/c-Met signaling in prostate cancer progression and c-Met inhibitors in clinical trials. *Expert opinion on investigational drugs,* **20** (12), 1677-1684.

VASILIOU, Vasilis, VASILIOU, Konstandinos and NEBERT, Daniel W. (2009). Human ATP-binding cassette (ABC) transporter family. *Human genomics,* **3** (3), 281-290.

VAUGHAN, Roger A., et al. (2013). Tumor necrosis factor alpha induces Warburg- like metabolism and is reversed by anti-inflammatory curcumin in breast epithelial cells. *International journal of cancer,* **133** (10), 2504-2510.

VAUX, D. L., CORY, S. and ADAMS, J. M. (1988). Bcl-2 gene promotes haemopoietic cell survival and cooperates with c-myc to immortalize pre-B cells. *Nature,* **335** (6189), 440-442.

VERGANI, L., GRATTAROLA, M. and NICOLINI, C. (2004). Modifications of chromatin structure and gene expression following induced alterations of cellular shape. *The international journal of biochemistry & cell biology,* **36** (8), 1447-1461.

VERGARA, Daniele, et al. (2010). Epithelial–mesenchymal transition in ovarian cancer. *Cancer letters,* **291** (1), 59-66.

VERKAIK, N. S., et al. (1999). Down-regulation of CD44 expression in human prostatic carcinoma cell lines is correlated with DNA hypermethylation. *International journal of cancer,* **80** (3), 439-443.

VERMEULEN, K., VAN BOCKSTAELE, D. R. and BERNEMAN, Z. N. (2003). The cell cycle: a review of regulation, deregulation and therapeutic targets in cancer. *Cell proliferation,* **36** (3), 131-149.

VESELY, M. D. and SCHREIBER, R. D. (2013). Cancer immunoediting: antigens, mechanisms, and implications to cancer immunotherapy. *Annals of the new york academy of sciences,* **1284** , 1-5.

VLASHI, E., et al. (2013). Targeted elimination of breast cancer cells with low proteasome activity is sufficient for tumor regression. *Breast cancer research and treatment,* **141** (2), 197-203.

VOGELSTEIN, B. and KINZLER, K. W. (2004). Cancer genes and the pathways they control. *Nature medicine,* **10** (8), 789-799.

WAJANT, H. (2002). The Fas signaling pathway: more than a paradigm. *Science (new york, N.Y.),* **296** (5573), 1635-1636.

WALSH, John G., et al. (2008). Executioner caspase- 3 and caspase- 7 are functionally distinct proteases. *Proceedings of the national academy of sciences of the united states of america,* **105** (35), 12815.

WANG, Hui-Chun, et al. (2012a). Withanolides- Induced Breast Cancer Cell Death Is Correlated with Their Ability to Inhibit Heat Protein 90 (Withanolides Inhibit Heat Protein 90). *PLoS ONE,* **7** (5), e37764.

WANG, Jianlong, LEVASSEUR, Dana N. and ORKIN, Stuart H. (2008). Requirement of Nanog dimerization for stem cell self-renewal and pluripotency. *Proceedings of the national academy of sciences of the united states of america,* **105** (17), 6326-6331.

WANG, Lei, et al. (2013a). Enrichment of prostate cancer stem- like cells from human prostate cancer cell lines by culture in serum- free medium and chemoradiotherapy. *International journal of biological sciences,* **9** (5), 472-479.

WANG, M. L., CHIOU, S. H. and WU, C. W. (2013). Targeting cancer stem cells: emerging role of Nanog transcription factor. *OncoTargets and therapy,* **6** , 1207-1220.

WANG, Rong, et al. (2014a). Comparison of mammosphere formation from breast cancer cell lines and primary breast tumors. *Journal of thoracic disease,* **6** (6), 829-837.

WANG, S., et al. (2013b). Enrichment of prostate cancer stem cells from primary prostate cancer cultures of biopsy samples. *International journal of clinical and experimental pathology,* **7** (1), 184-193.

WANG, Z., et al. (2012b). Distinct lineage specification roles for NANOG, OCT4, and SOX2 in human embryonic stem cells. *Cell stem cell,* **10** (4), 440-454.

WANG, Z. A., et al. (2014b). Luminal cells are favored as the cell of origin for prostate cancer. *Cell reports,* **8** (5), 1339-1346.

WARBURG, O. (1956a). On respiratory impairment in cancer cells. *Science (new york, N.Y.),* **124** (3215), 269-270.

WARBURG, O. (1956b). On the origin of cancer cells. *Science (new york, N.Y.),* **123** (3191), 309-314.

WEG-REMERS, S., et al. (2001). *Regulation of alternative pre-mRNA splicing by the ERK MAP-kinase pathway.* London :, The EMBO journal, **20** (15), 4194-4203.

WEI, W., et al. (2012). Relationship of CD44(+)CD24(-/low) breast cancer stem cells and axillary lymph node metastasis. *JOURNAL OF TRANSLATIONAL MEDICINE,* **10** .

WEINBERG, R. A. (1995). The retinoblastoma protein and cell cycle control. *Cell,* **81** (3), 323-330.

WEN, X., et al. (2012). Caspase-mediated programmed cell death pathways as potential therapeutic targets in cancer. *Cell proliferation,* **45** (3), 217.

WETZELS, R. H., et al. (1991). Basal cell-specific and hyperproliferation-related keratins in human breast cancer. *The american journal of pathology,* **138** (3), 751-763.

WILLIAMS, K., et al. (2013). CD44 integrates signaling in normal stem cell, cancer stem cell and (pre)metastatic niches. *Experimental biology and medicine (maywood, N.J.),* **238** (3), 324-338.

WINDUS, L. C., et al. (2012). In vivo biomarker expression patterns are preserved in 3D cultures of Prostate Cancer. *Experimental cell research,* **318** (19), 2507-2519.

WITSCH, E., SELA, M. and YARDEN, Y. (2010). *Roles for Growth Factors in Cancer Progression.* Physiology; Physiology, **25** (2), 85-101.

WONG, K. K. and DEPINHO, R. A. (2003). Walking the telomere plank into cancer. *Journal of the national cancer institute,* **95** (16), 1184-1186.

WRIGHT, W. E. and SHAY, J. W. (2005). Telomere biology in aging and cancer. *Journal of the american geriatrics society,* **53** (9 Suppl), S292-4.

WU, Aibing, et al. (2013). Aldehyde dehydrogenase 1, a functional marker for identifying cancer stem cells in human nasopharyngeal carcinoma. *Cancer letters,* **330** (2), 181-189.

WU, Szu-Yuan, et al. (2014). Ionizing radiation induces autophagy in human oral squamous cell carcinoma. *Journal of B.U.ON.: Official journal of the balkan union of oncology,* **19** (1), 137.

XIANG, Lisha, et al. (2014). Hypoxia- inducible factor 1 mediates TAZ expression and nuclear localization to induce the breast cancer stem cell phenotype. *Oncotarget,* **5** (24), 12509.

XIE, Daxing, et al. (2010). Role of DAB2IP in modulating epithelial-to-mesenchymal transition and prostate cancer metastasis. *Proceedings of the national academy of sciences of the united states of america,* **107** (6), 2485-2490.

XU, Jian, LAMOUILLE, Samy and DERYNCK, Rik (2009). TGF-beta-induced epithelial to mesenchymal transition. *Cell research,* **19** (2), 156-172.

XU, Xiao-Xi, et al. (2014). Enrichment of cancer stem cell- like cells by culture in alginate gel beads. *Journal of biotechnology,* **177** , 1-12.

XU, Ya-Ming, et al. (2015). Discovery of Potent 17β-Hydroxywithanolides for Castration- Resistant Prostate Cancer by High- Throughput Screening of a Natural Products Library for Androgen- Induced Gene Expression Inhibitors. *Journal of medicinal chemistry,* **58** (17), 6984.

XUE, G., et al. (2015). Reprogramming mediated radio-resistance of 3D-grown cancer cells. *Journal of radiation research,* **56** (4), 656-662.

YANAGAWA, Y., et al. (1995). The transcriptional regulation of human aldehyde dehydrogenase I gene. The structural and functional analysis of the promoter. *The journal of biological chemistry,* **270** (29), 17521-17527.

YANG, Huanjie, SHI, Guoqing and DOU, Qping (2007). The Tumor Proteasome Is a Primary Target for the Natural Anticancer Compound Withaferin A Isolated from " Indian Winter Cherry". *Molecular pharmacology,* **71** (2), 426-437.

YANG, K., HITOMI, M. and STACEY, D. W. (2006). Variations in cyclin D1 levels through the cell cycle determine the proliferative fate of a cell. *Cell division,* **1** , 32.

YIN, A. H., et al. (1997). AC133, a novel marker for human hematopoietic stem and progenitor cells. *Blood,* **90** (12), 5002-5012.

YOO, Y. D., et al. (1999). TGF-beta-induced cell-cycle arrest through the p21(WAF1/CIP1)-G1 cyclin/Cdks-p130 pathway in gastric-carcinoma cells. *International journal of cancer,* **83** (4), 512-517.

YOSHIDA, A., et al. (1998). Human aldehyde dehydrogenase gene family. *European journal of biochemistry / FEBS,* **251** (3), 549-557.

YOSHIDA, K. and MIKI, Y. (2004). Role of BRCA1 and BRCA2 as regulators of DNA repair, transcription, and cell cycle in response to DNA damage. *Cancer science,* **95** (11), 866-871.

YU, Cheng-Chia, et al. (2011). MicroRNA let-7a represses chemoresistance and tumourigenicity in head and neck cancer via stem-like properties ablation. *Oral oncology,* **47** (3), 202-210.

YU, M., et al. (2014). Inactivation of TGF-beta signaling and loss of PTEN cooperate to induce colon cancer in vivo. *Oncogene,* **33** (12), 1538-1547.

YU, Y., et al. (2002). AC133-2, a novel isoform of human AC133 stem cell antigen. *The journal of biological chemistry,* **277** (23), 20711-20716.

ZAEHRES, Holm, et al. (2005). High-Efficiency RNA Interference in Human Embryonic Stem Cells. *Stem cells,* **23** (3), 299-305.

ZARKOWSKA, T. and MITTNACHT, S. (1997). Differential phosphorylation of the retinoblastoma protein by G sub(1)/ S cyclin- dependent kinases. *Journal of biological chemistry,* **272** (19), 12738-12746.

ZHANG, C., et al. (2016). Hypoxia induces the breast cancer stem cell phenotype by HIF-dependent and ALKBH5-mediated m6A-demethylation of NANOG mRNA. *Proceedings of the national academy of sciences of the united states of america,* **113** (14), E2047-56.

ZHANG, Jingyu, et al. (2005). Expression of Nanog gene promotes NIH3T3 cell proliferation. *Biochemical and biophysical research communications,* **338** (2), 1098-1102.

ZHANG, Jingyu, et al. (2006). NANOGP8 is a retrogene expressed in cancers. *FEBS journal,* **273** (8), 1723-1730.

ZHANG, S. S., et al. (2012). CD133(+)CXCR4(+) colon cancer cells exhibit metastatic potential and predict poor prognosis of patients. *BMC medicine,* **10** , 85-7015-10-85.

ZHANG, X., et al. (1999). Telomere shortening and apoptosis in telomerase-inhibited human tumor cells. *Genes & development,* **13** (18), 2388-2399.

ZHANG, Xuan, et al. (2011). Down- regulation of estrogen receptor- alpha and rearranged during transfection tyrosine kinase is associated with withaferin a- induced apoptosis in MCF- 7 breast cancer cells. *BMC complementary and alternative medicine,* **11** (1), 84.

ZHANG, Yingpei and HERMAN, Brian (2002). Ageing and apoptosis. *Mechanisms of ageing and development,* **123** (4), 245-260.

ZHAO, S., et al. (2012). Activation of Akt/GSK-3beta/beta-catenin signaling pathway is involved in survival of neurons after traumatic brain injury in rats. *Neurological research,* **34** (4), 400-407.

ZHOU, Xi, et al. (2011). Expression of the stem cell marker Nanog in human endometrial adenocarcinoma. *International journal of gynecological pathology : Official journal of the international society of gynecological pathologists,* **30** (3), 262-270.